Histone H3 variants and chaperones in Arabidopsis thaliana heterochromatin dynamics

Matthias Benoit

CLERMONT UNIVERSITÉ
N° D.U. : 2497 - N° D'ORDRE : 642

Année 2014

ÉCOLE DOCTORALE
DES SCIENCES DE LA VIE, SANTÉ, AGRONOMIE, ENVIRONNEMENT

Thèse

Présentée à l'Université Blaise Pascal
pour l'obtention du grade de

DOCTEUR D'UNIVERSITÉ
Spécialité : Physiologie et Génétique Moléculaires

Soutenue le 17 Octobre 2014

Matthias BENOIT

HISTONE H3 VARIANTS AND CHAPERONES IN *ARABIDOPSIS THALIANA* HETEROCHROMATIN DYNAMICS

Présidente :	Dr. Chantal VAURY, GReD, Clermont-Ferrand
Rapporteurs :	Dr. Cristel CARLES, LPCV, Grenoble
	Dr. Elaine DUNLEAVY, CCB, Galway
	Dr. Ortrun MITTELSTEN SCHEID, GMI, Vienne
Directrice de thèse :	Dr. Aline PROBST, Université Blaise Pascal, Aubière

Génétique, Reproduction & Développement
UMR CNRS 6293 - Clermont Université - INSERM U1103
24, avenue des Landais 63177 Aubière Cedex

CLERMONT UNIVERSITÉ
N° D.U. : 2497 - N° D'ORDRE : 642

Année 2014

ÉCOLE DOCTORALE
DES SCIENCES DE LA VIE, SANTÉ, AGRONOMIE, ENVIRONNEMENT

Thèse

Présentée à l'Université Blaise Pascal
pour l'obtention du grade de

DOCTEUR D'UNIVERSITÉ
Spécialité : Physiologie et Génétique Moléculaires

Soutenue le 17 Octobre 2014

Matthias BENOIT

HISTONE H3 VARIANTS AND CHAPERONES IN *ARABIDOPSIS THALIANA* HETEROCHROMATIN DYNAMICS

Présidente :	Dr. Chantal VAURY, GReD, Clermont-Ferrand
Rapporteurs :	Dr. Cristel CARLES, LPCV, Grenoble
	Dr. Elaine DUNLEAVY, CCB, Galway
	Dr. Ortrun MITTELSTEN SCHEID, GMI, Vienne
Directrice de thèse :	Dr. Aline PROBST, Université Blaise Pascal, Aubière

Génétique, Reproduction & Développement
UMR CNRS 6293 - Clermont Université - INSERM U1103
24, avenue des Landais 63177 Aubière Cedex

Cette thèse n’aurait pas été possible sans vous, alors un grand merci :

A Mesdames Cristel Carles, Elaine Dunleavy et Ortrun Mittelsten Scheid d’être venues des quatre coins de France et d’Europe pour évaluer ce travail, et à Chantal Vaury d’avoir presidé ce jury de thèse exclusivement féminin,

A Aline, la Chef, pour tout ce que tu m’as apporté durant ces quatre années. Merci de m’avoir donné ma chance et de m’avoir laissé t’accompagner dans cette aventure qui a commencé en terrasse d’un café Place de Jaude. Merci pour ton investissement, tes conseils et tes corrections sur la thèse même après deux heures du matin. Merci de ton optimisme quand le mien baissait. Merci de ta patience quand je laissais trainer mes plantes en serre. Tu as été et tu continueras à être un exemple pour moi,

A Sylvette, pour m’avoir accueilli à BIOMOVE et lancé dans le grand bain, pour ton aide et ton regard bienveillant sur le petit thésard que j’étais. Et pour Buda !

A Marie-Claude, ma maman du labo, d’avoir pris soin de moi pendant ces 4 années, à peigner des girafes (un peu), éplucher des cotylédons (beaucoup), papoter au café (beaucoup beaucoup) et à se raconter les hauts et les bas de nos vies. Les derniers mois sans toi au labo étaient déjà bien trop longs, tu vas me manquer,

A Chantal, d’avoir partagé bien plus que la moitié de ton bureau et d’avoir supporté mon coté bordélique (tiens où est ma clé USB ?!). J’espère que mon futur voisin de bureau sera aussi cool que toi !

A Céline, pour m’avoir énormément aidé et conseillé sur la fin de thèse. Merci de m’avoir transmis (ne serait-ce qu’un peu !) de ta rigueur et de ton ouverture d’esprit. Je ne mangerai plus de lentilles de la même façon,

A Sam pour ta joie et bonne humeur, ton aide sans faille, le style prof romantique et les soirées au Nirvana,

A Manu pour les enseignements partagés ensemble, les anecdotes sur Toulouse et tes chemisettes,

A Sylviane pour ton aide et ta gentillesse, ainsi que les western et les cookies,

A Sylvie pour m’avoir guidé lors de mes premiers pas comme enseignant et d’avoir accepté d’écouter Nova pendant quatre ans dans le labo 3, et cela sans broncher !

A Christophe pour ton pragmatisme et ton optimisme, ainsi que de m’avoir soutenu aussi bien pour la thèse que pour le monitorat,

A Benjamin et Ortrun de m’avoir fait profiter de leur expertise et gentillesse lors des comités de thèse. Merci à Ortrun et Jasmin pour l’accueil chaleureux reçu à Vienne,

A Marie-No pour le ménage. A Thierry pour le debrief rugby du week-end,

A Simon et ODI pour la triplette squash / picon bière / Baraka,

A Maryse et Marie-Jo, pour mes commandes et mes envois TOUJOURS hyper-urgents et hyper-importants,

A Leti, Angeles et Sébich pour leur bonne humeur et la bière de fin de journée (et ta chemise Sébich !),

A Isa pour l’enseignement et les (nombreuses !) discussions plus ou moins sérieuses sur les post-docs et l’avenir en général,

Aux copains de PCE et du PIAF pour les repas pizzas, bagels, food trucks, apéros …

A Margaux et Pierre, pour la relève,

A Elodie, dit Mich’, d’avoir été la vieille thésarde et de m’avoir fait l’historique du labo à mon arrivée. Merci pour les discussions venant de la paillasse de derrière et des répliques de la Cité de la Peur,

A Heïdi pour le confort visuel et le Ricard de 16 heures. See you in Cambridge,

Aux copains dispatchés dans toute la France pour les moments de décompression (week-ends, restos, concerts, matchs …) et de vous être déplacés pour la soutenance !

Aux copains thésards de l'équipe :

A Axel, mon jumeau maléfique,

A Lauriane, ma jeune padawan chocolatphile,

A Mélanie, ma Mad'moizelle,

Merci d'avoir été les compagnons du quotidien dans les bons moments et ceux plus difficiles. Un joyeux mélange de licornes et de petits poneys, de pauses thé/café/Rugbynistère, de débrief ciné, de petites bouffes sympas, de croustilles, de listes de ménage arrangées, de repas de midi salvateurs … !

A Lili et Valen pour leur soutien et amour sans faille,

A mes oncles, tantes, cousins, cousines, à travers toute la France,

A mon filleul que j'aime de tout mon cœur,

A mes grands-parents,

A mes parents et mon frère, pour leur soutien et amour indéfectible, ainsi que pour m'avoir encouragé si tôt à ouvrir mon esprit et découvrir le monde,

A Emilie de partager tout cela avec moi, de me pousser à aller toujours plus loin et de m'accompagner sur ce chemin pas toujours facile. Et puis au pire on s'aime.

Abstract

To understand how histones H3 are handled and how histone dynamics impact higher-order chromatin organization such as chromocenter formation in Arabidopsis, a comprehensive analysis of the different histone chaperone complexes is required. We identified and characterized the different subunits of the Arabidopsis HIR complex. AtHIRA is the central subunit and its loss affects non-nucleosomal histone levels, reduces nucleosomal occupancy not only at euchromatic but also at heterochromatic targets and alleviates transcriptional gene silencing. While the HIR complex-mediated histone deposition is dispensable for higher-order organization of Arabidopsis heterochromatin, I show that CAF-1 plays a central role in chromocenter formation. During post-germination development in cotyledons when centromeric and pericentromeric repeats cluster progressively into chromocenter structures, these repetitive elements but not euchromatic loci become enriched in H3.1 in a CAF-1-dependent manner. This enrichment, together with the appropriate setting of repressive histone post-translational marks, contributes to chromocenter formation, identifying chromatin assembly by CAF-1 as driving force in formation and maintenance of genome structure. Finally, while absence of HIR or CAF-1 complexes sustains viability, only the simultaneous loss of both severely impairs nucleosomal occupancy and plant development, suggesting a limited functional compensation between the different histone chaperone complexes and plasticity in histone variant interaction and deposition in plants.

Keywords: Heterochromatin dynamics, chromocenter, histone H3, histone chaperone, *Arabidopsis thaliana*

Afin d'étudier la prise en charge des histones H3 jusqu'à l'ADN et pour comprendre l'influence de leur dynamique dans l'organisation d'ordre supérieur de la chromatine, une analyse des chaperonnes d'histones a été menée. Nous avons identifié et caractérisé les sous-unités du complexe HIR, impliqué dans l'assemblage de la chromatine réplication-indépendante chez Arabidopsis. La perte d'AtHIRA, la sous-unité centrale du complexe, affecte le niveau d'histone soluble, l'occupation nucléosomale des régions euchromatiniennes et héterochromatiniennes ainsi que la mise sous silence transcriptionnel des séquences d'ADN répétées. Alors que le complexe HIR ne participe pas à l'organisation d'ordre supérieur de la chromatine, j'ai montré que CAF-1, impliqué dans l'assemblage de la chromatine au cours de la réplication, joue un rôle central dans la formation des chromocentres. Lors du développement post-germinatif des cotylédons, les séquences d'ADN répétées centromériques et péricentromériques se concentrent dans les chromocentres et s'enrichissent en histone H3.1 de manière CAF-1 dépendante. Cet enrichissement, associé à des modifications post-traductionnelles d'histones associées à un état répressif de la transcription, participe à la formation des chromocentres et met en évidence l'importance de l'assemblage de la chromatine par CAF-1 dans la structure et le maintien du génome. Alors que la perte individuelle de HIR ou de CAF-1 n'affecte pas la viabilité, l'absence des deux complexes altère fortement l'occupation nucléosomale et le développement des plantes. Ceci suggère que la compensation fonctionnelle entre ces complexes de chaperonnes ainsi que la plasticité des voies de dépôt des histones restent limitées.

Mots-clés: Dynamique de l'heterochromatine, chromocentre, histone H3, chaperonne d'histone, *Arabidopsis thaliana*

Table of contents

Abbreviations

AGO4: Argonaute 4

ASF1: Anti-Silencing Factor 1

ATP: Adenosine Triphosphate

ATRX: Alpha Thalassemia/mental Retardation X-linked syndrome

ATXR: Arabidopsis Trithorax-Related protein

BAC: Bacterial Artificial Chromosome

BLAST: Basic Local Alignment Search Tool

Bp: Base pair

CAC: Chromatin Assembly Complex

CAF-1: Chromatin Assembly Factor-1

CBN: Cabin

cDNA: Complementary DNA

CENH3: Centromeric Histone H3

CENP-A: Centromere Protein A

ChIP: Chromatin Immunoprecipitation

ChIP-Seq: Chromatin Immunoprecipitation-Sequencing

CLF: Curly Leaf

cM: Centimorgan

CMT: Chromomethylase

Dag: Days after germination

DAPI: 4',6'-diamidino-2-phenylindole

DAXX: Death domain-associated protein

DCL3: Dicer-Like 3

DDM1: Decrease in DNA Methylation 1

DLP: DAXX-Like Protein

DME: Demeter

DML: Demeter-Like

DNA: Deoxyribonucleic Acid

DNMT: DNA (cytosine-5)-Methyltransferase

DRM2: Domains Rearranged Methyltransferase 2

DRS: Direct RNA Sequencing

DSB: Double-Strand Break

DUO1: Duo Pollen 1

E2F: Elongation Factor 2

FAS: Fasciata

FISH: Fluorescent *In Situ* Hybridization

FITC: Fluorescein Isothiocyanate

GABI: Genomanalyse im Biologischen System Pflanze

gDNA: Genomic DNA

GUS: β-Glucoronidase

HIR: Histone Regulator

HIRA: Histone Regulator A

HP1: Heterochromatin Protein 1

HPT: Hygromycin Phosphotransferase

HTR: Histone Three Related

HXK1: Hexokinase 1

H3K9: Histone 3 lysine 9

H3K27: Histone 3 lysine 27

IDN2: Involved in De Novo 2

Kb: Kilobase

kDa: Kilodalton

KYP: Kryptonite

LHP1: Like-HP1

lncRNA : Long non-coding RNA

LSH: Lymphoid-Specific Helicase

LTR: Long Terminal Repeat

Mb: Megabase

MEA: Medea

MEF2: Myocyte Enhancer Factor 2

MET1: Methyltransferase 1

miRNA: microRNA

M-MLV: Moloney Murine Leukemia Virus

MOM1: Morpheus' Molecule 1

MORC: Microrchidia

MSI1: Multicopy Suppressor of Ira 1

NASC: Nottingham Arabidopsis Stock Centre

NCN: Nuclein

NOR: Nucleolus Organizer Region

NRPE1: Nuclear RNA Polymerase E1

Nt: Nucleotide

OCS: Octopine Synthase

PCNA: Proliferating Cell Nuclear Antigen

PCR: Polymerase Chain Reaction

PHD: Plant Homeodomain

Pol IV: RNA Polymerase IV

PRC: Polycomb Repressive Complex

RdDM: RNA-directed DNA Methylation

RDR2: RNA-Dependent RNA polymerase 2

RHF: Relative Heterochromatin Fraction

ROS1: Repressor Of Silencing 1

rDNA: Ribosomal DNA

RNA: Ribonucleic Acid

RNAi: Ribonucleic Acid interference

RNAPII: RNA Polymerase II

rRNA: Ribosomal RNA

RT-qPCR: Reverse Transcription-quantitative Polymerase Chain Reaction

SAHF: Senescence-Associated Heterochromatin Foci

SAIL: Syngenta Arabidopsis Insertion Library

SD: Standard Deviation

SEM: Standard Error of the Mean

SDS-PAGE: Sodium Dodecyl Sulfate-Polyacrylamide Gel Electrophoresis

SHH1: Sawadee Homeodomain Homolog 1

SIN3: SWI-independent 3

siRNA: Small interfering RNA

SPT5L: Suppressor of Ty insertion 5-Like

sRNA: small RNA

SUMO: Small Ubiquitin-like Modifier

SU(VAR)3-9: Suppressor of Variegation 3-9

SUVH: Su(var)3-9 Homologue

SWI/SNF2: Switch/Sucrose Non Fermentable 2

TAIR: The Arabidopsis Information Resource

T-DNA: Transfer-DNA

TPR: Tetratricopeptide Repeat

TSI: Transcriptionally Silent Information

TSS: Transcription Start Site

TTS: Transcription Termination Site

UBC28: Ubiquitin-conjugating Enzyme 28

UBN1: Ubinuclein1

UEV1C: Ubiquitin-conjugating Enzyme E2 Variant 1C

UHRF1: Ubiquitin-like containing PHD and RING Finger domains 1

UTR: Untranslated Region

UV: Ultraviolet

VIM1: Variant In Methylation 1

WISC: Wisconsin

WMD: Web MicroRNA Designer

WT: Wild Type

XNP: ATRX homolog X-linked Nuclear Protein

4C: Circularized Chromosome Conformation Capture

5mC: 5-methylcytosine

List of illustrations

State of the art

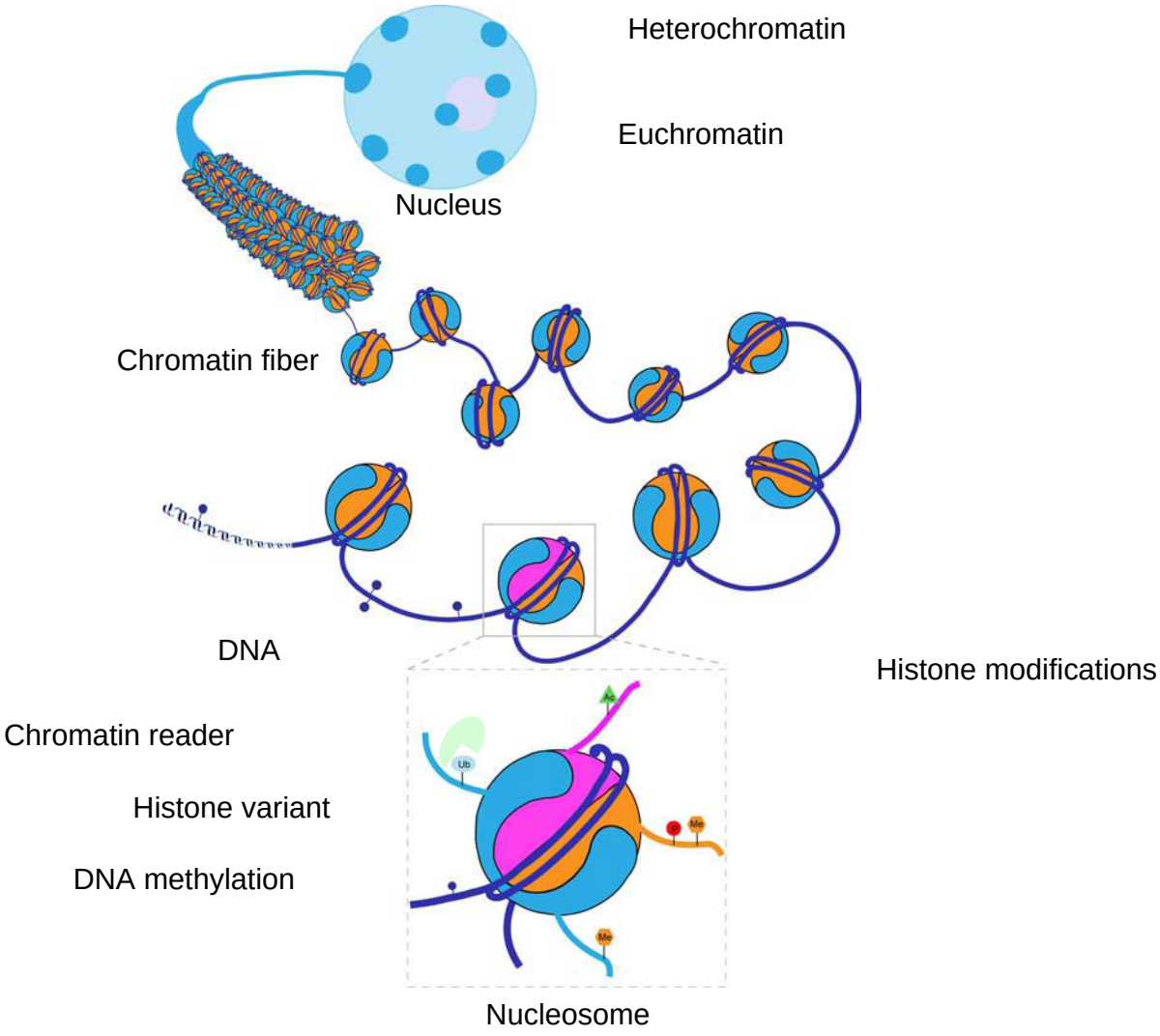

***Figure 1*: Epigenetic information is chromatin-based.**

In the eukaryotic nucleus, DNA is organized together with histones forming the basic subunit of chromatin, the nucleosome, in which 146 bp of DNA wrap around a histone tetramere of H3-H4 and two H2A-H2B dimers. Candidates for key players in epigenetic inheritance are situated at different levels of chromatin and include DNA and histone modifications, histone variants, non-histone chromatin proteins that bind directly to DNA or histone modifications, and higher-order organization as well as spatial organization of a given locus within the nucleus. Histones can be post-translationally modified e.g. by acetylation, phosphorylation, methylation and each mark constitutes a signal red alone or in combination with other modifications on the same or neighbouring histones as the 'histone code'. The presence of histone variants, in particular H3 and H2A variants adds further complexity to the epigenetic information (adapted from Probst et al., 2009).

1. Organization of eukaryotic genomes in chromatin

Individual cells of an organism comprise identical DNA content, but development and differentiation require specific gene expression patterns regulated in a time- and tissue-specific manner. How an organism controls the transcription of a given locus during development is therefore a key question. Besides specific sets of transcription factors and signaling cascades responding to environmental cues, epigenetic information, defined as mitotically heritable changes in gene expression that occur without alterations in DNA sequence (Riggs et al., 1996), is integrated at the chromatin level and is of critical importance regarding these questions.

Indeed, in eukaryotic organisms the genetic information encoded by the bulky linear DNA is tightly organized in a nucleoprotein structure called chromatin. Chromatin packages DNA to fit the small compartment of the cell nucleus, but also regulates DNA accessibility. The nucleosome is the basic subunit of chromatin and consists in DNA wrapped around histone proteins (Luger et al., 1997). Accessibility of the transcriptional machinery to DNA is determined by the levels of packaging based on electrostatic interactions between DNA and histones. Nucleosome features therefore directly impact accessibility of the nuclear machinery to the underlying DNA sequence, thus affecting fundamental DNA-based processes such as gene transcription, DNA replication and repair (Probst et al., 2009). Following this idea, chromatin appears as a potential framework for gene expression program maintenance and inheritance. Epigenetic information is essentially chromatin-based and includes covalent modifications at the level of DNA, histones, non-histone chromatin binding proteins, non-coding RNA and histone variants (Probst et al., 2009). Moreover, local properties of chromatin also have consequences on the higher-order nuclear organization and thus can influence the positioning of genes and entire chromosomes within the nucleus (Lieberman-Aiden et al., 2009; Saez-Vasquez and Gadal, 2010) (***Figure 1***). Therefore, epigenetic information carried by chromatin provides a form of memory critical for the maintenance of genome function, including both developmental gene expression patterns and the propagation of essential architectural features of the genome, such as chromosome positioning and definition of telomeres and centromeres (Probst et al., 2009).

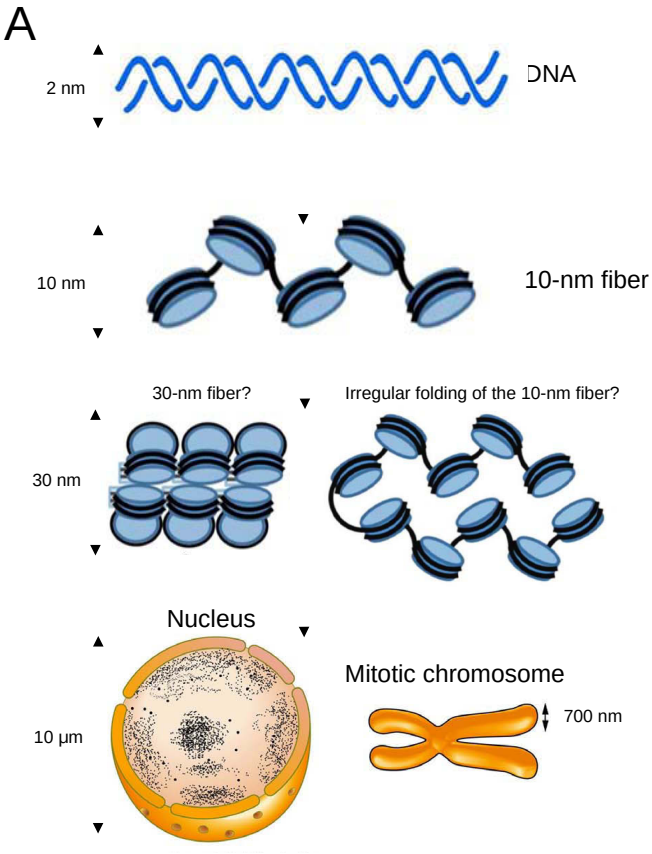

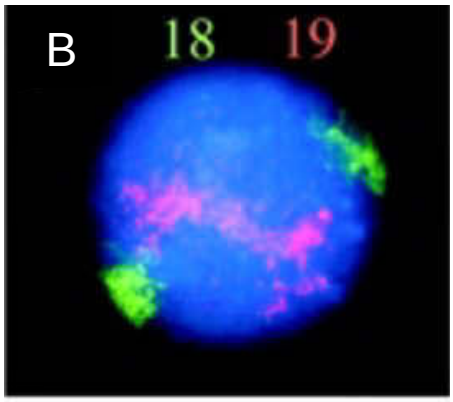

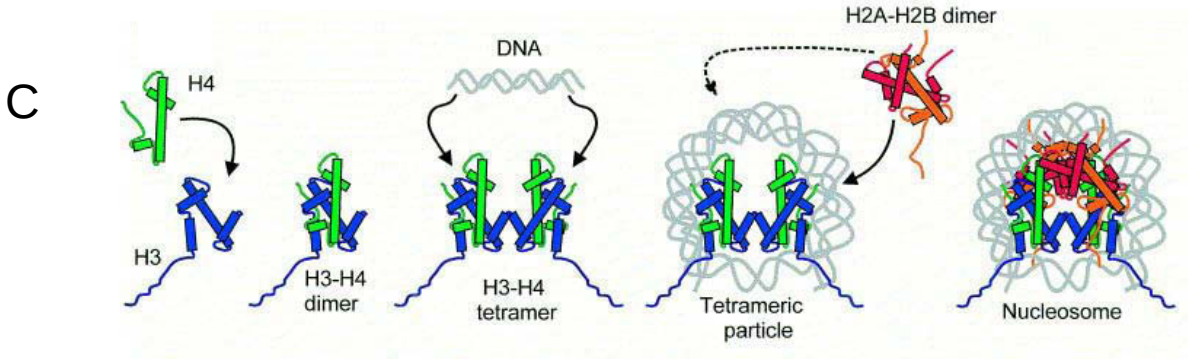

***Figure 2*: Different levels of chromatin compaction.**

A. The 2 nm-long DNA molecule is wrapped around a core histone octamer and forms a 10-nm "beads-on-a-string" fiber. The 10-nm fiber has long been assumed to fold into a 30-nm fiber that could be organized in a one-start helical solenoid model or in a two-start helix conformation (not shown). Recent data argue instead for the presence *in vivo* of an irregularly folded 10-nm fiber. These intermediate chromatin structures subsequently participate in the higher-order chromatin organization of interphase nuclei or mitotic chromosomes (adapted from Maeshima et al., 2010 and Volle and Dalal., 2014).
B. Higher levels of chromatin folding exemplified by the distinct chromosomal territories occupied by human chromosomes 18 (green) and 19 (red) in the nuclear volume during interphase. Chromosomes 18 and 19 are revealed by fluorescent *in situ* hybridization in human primary lymphocytes (from Croft et al., 1999).
C. The nucleosome core particle consists of 146 bp of DNA wrapped in a ¾ superhelical turn around a histone octamer. The histone octamer consists of two molecules each of histone H2A, H2B, H3 and H4 with their N-terminal tails protruding from the globular domains (from Morales et al., 2001). First a H3-H4 dimer, then a tetramer is formed that associates with DNA to form a tetrameric particle and two H2A-H2B dimers complete the nucleosome core particle.

1.1. Functional significance of chromatin

We distinguish four major levels of chromatin organization (***Figure 2A***): (i) the nucleosome, where DNA is tightly wrapped around the histone core; (ii) the 10-nm beads-on-a-string nucleosomal array (iii) the 30-nm fiber, with an estimated linear compaction of 100-200 kb/μm; (iv) higher folding levels, which position the chromatin fiber within a chromosome territory and allow the elevated compaction of metaphase chromosomes (***Figure 2B***). The general picture of chromatin is a polymer of nucleosomes, each of which is formed by an octamer of the core histones H2A, H2B, H3 and H4, around which a 146-bp DNA helix is wrapped 1.7 times in a left-handed superhelical fashion (Luger et al., 1997) (***Figure 2C***). The core histones are structurally defined by two distinct conserved motifs: the histone fold domain and the unstructured N-terminal and C-terminal histone tails that protrude from the globular part. The histone fold domain participates in interactions between core histones through three α-helices (α1, α2, and α3) connected by short loops (Arents and Moudrianakis, 1995). Histones are highly basic proteins, since their amino acid sequence is lysine- and argenine-rich, which tightly interact with the acidic phosphate groups of the DNA forming fourteen non-covalent histone-DNA contact points within the nucleosome (Luger et al., 1997). The nucleosome core assembly is achieved by the initial heterodimerization of H3/H4 followed by dimerization to form a $(H3–H4)^2$ tetramer (Eickbush and Moudrianakis, 1978), initiating first contacts with DNA (Luger, 2001). Dimers of H2A/H2B then bind to the $(H3–H4)^2$ tetramer creating new histone/DNA contact points and facilitate DNA wrapping around the histone octamer to form the nucleosome core complex (Hayes et al., 1990, 1991; Luger, 2001).

The beads-on-a-string model consists of a linear array of nucleosomes stabilized by the binding of linker histone H1 to linker DNA (Thomas, 1999; Maeshima et al., 2014) (***Figure 2A***). The 20-60 bp of linker DNA between nucleosomes is critical for the spatial orientation of the nucleosomal array and fixes the distance between adjacent nucleosomes (Grigoryev et al., 2009; Arya et al., 2010). This tightly controlled architecture establishes the 10-nm beads-on-a-string structure, which is a basis for further compaction of the chromatin fiber (Horn and Peterson, 2002; Mohd-Sarip and Verrijzer, 2004; Yelagandula et al., 2014). Existence of chromatin in form of a 30-nm fiber remains controversial due to

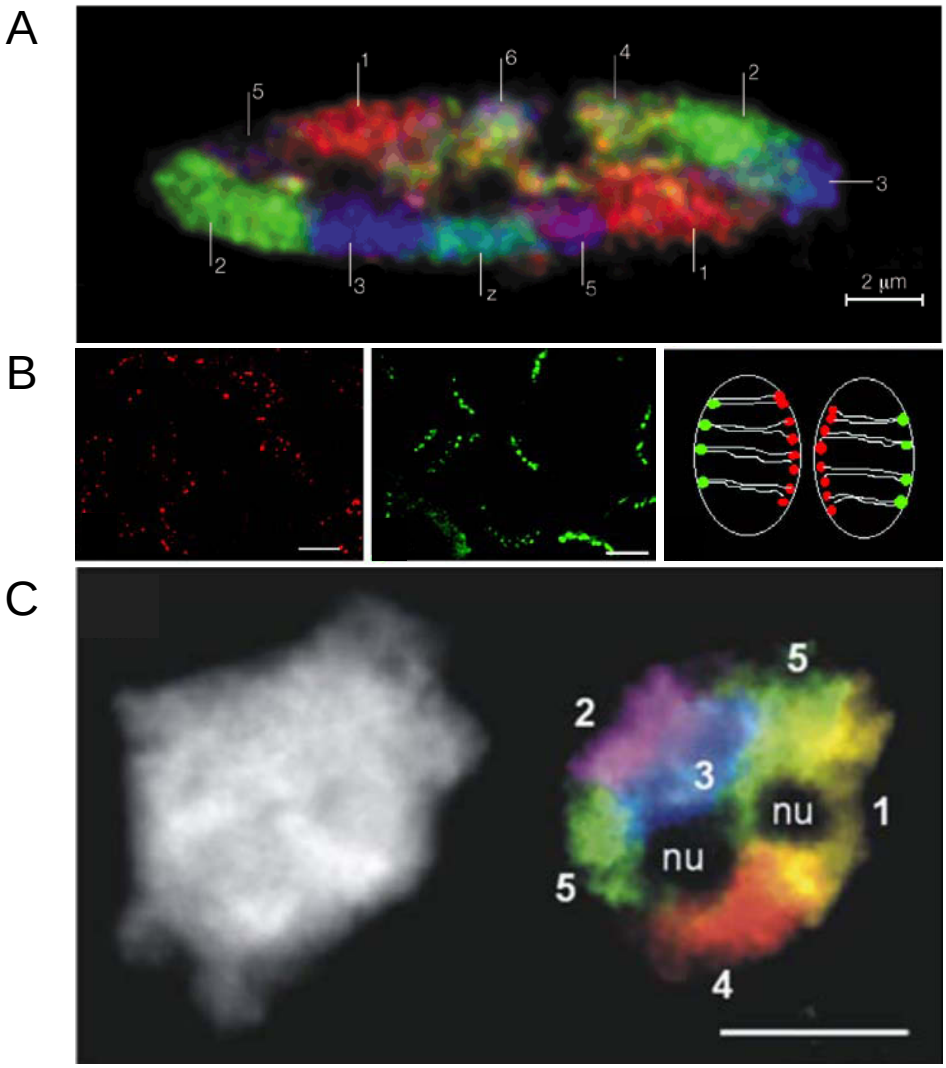

***Figure 3*: Chromatin arrangement in interphase nuclei.**

A. Chromosome painting on a chicken fibroblast nucleus reveals chromosomes organized within exclusive chromosome territories (from Cremer and Cremer, 2001).
B. Interphase chromosomes of wheat meristematic root nuclei display Rabl configuration. Telomeres (in red) and centromeres (in green) are found at opposite poles of the interphase nucleus. Scale bars: 10 µm (from Santos and Shaw, 2004).
C. Chromosomes organize in distinct territories in *Arabidopsis thaliana.* DAPI-stained 4C leaf nucleus (left) and multi-color chromosome painting of individual Arabidopsis chromosome arms (right). Nucleoli (nu) and repetitive DNA sequences are unstained. Scale bar: 5 µm (from Pecinka et al., 2004).

structural complexity (Robinson and Rhodes, 2006; Maeshima et al., 2010; Joti et al., 2012). The 30-nm fiber is currently hypothesized following two models (Wu et al., 2007; Fransz and de Jong, 2011). The one-start helix (solenoid model) displays a linear arrangement and interactions between neighboring nucleosomes, while the two-start helix (zigzag model) exhibits repetitive units of nucleosomes that alternate into an irregular 3D zigzag architecture. However, some recent evidences suggest that *in vivo,* the 30-nm chromatin fiber could be preferentially replaced by irregularly folded 10-nm fibers participating in further organization of particular high-order chromatin domains within the nuclear volume (Maeshima et al., 2014; Volle and Dalal, 2014; Yelagandula et al., 2014).

Higher levels of folding locate the chromatin fiber within the 3D volume of the nucleus. The spatial organization of the chromosomes is not random and is mediated by many factors such as chromosome length, DNA sequence, changing gene activity during cell growth and differentiation, local or global chromatin context, nuclear volume or external stimuli. Within the nucleus, each chromosome preferentially occupies a proper subdomain called chromosome territory (***Figure 3***). Interestingly, gene-rich chromosomes are preferentially found in a central position (Croft et al., 1999; Kozubek et al., 2002; Chambeyron and Bickmore, 2004; Scheuermann et al., 2004), while gene-poor chromosomes tend to localize at the nuclear periphery, which is thought to form a transcriptionally repressive microenvironment (Croft et al., 1999; Boyle et al., 2001; Cremer and Cremer, 2001, 2010). However this organization is not universal since particularly highly-expressed genes have been described close to the nuclear periphery (Brown et al., 2006; Küpper et al., 2007). In mammals and plants, transcription leads to chromatin decondensation and looping out from the chromosome territory. Whether the distribution of chromosome territories is conserved through mitosis remains controversial (Gerlich et al., 2003; Kalmárová et al., 2008; Cremer and Cremer, 2010; Ishii and Houben, 2014). In Arabidopsis, chromosome territories location within the nucleus can be transmitted in a transient mirror-symmetrical pattern through mitosis (Berr and Schubert, 2007). Inside each chromosome territory, the centromere and the telomeres are arranged in a specific manner. Centromeric chromatin is mostly located at the periphery, near the nuclear membrane, whereas disposition of telomeric regions varies between species. In human cells, centromeres are partly localized to the nuclear periphery depending the cell cycle phase (Solovei et al., 2004). Plants with large genomes such as wheat and

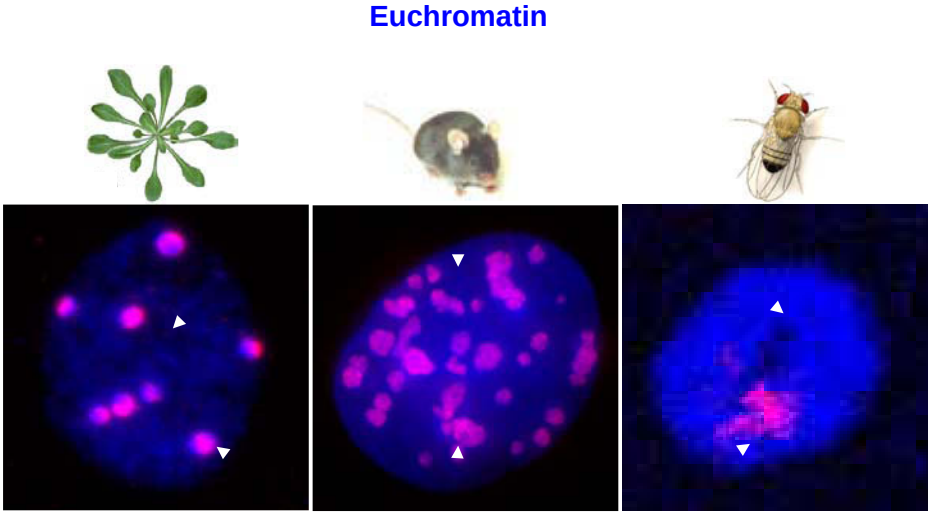

***Figure 4*: Euchromatin and heterochromatin are two distinct chromatin states in eukaryotes.**

Two distinct forms of chromatin exist in eukaryotic genomes: on the one hand euchromatin, stained here in blue by DAPI in nuclei from Arabidopsis leaf tissue, mouse fibroblasts and Drosophila salivary glands, is relatively decondensed and includes chromatin domains with transcription-permissive features. On the other hand, heterochromatin remains condensed throughout the whole cell cycle and forms at repetitive sequences and transposable elements – here visible in pink by DNA fluorescence *in situ* hybridization of repetitive sequences (adapted from Probst et al., 2003. Pictures of mouse and Drosophila courtesy of A. Probst and E. Brasset).

close relatives, as well as the budding yeast *Saccharomyces cerevisiae* exhibit a Rabl organization, where centromeres cluster at the spindle pole body, facing telomeres found in perinuclear foci on the opposite side of the nucleus. In *Arabidopsis thaliana*, the centromeres are located at the nuclear periphery (Fang and Spector, 2005), while telomeres cluster at the periphery of the nucleolus (Fransz et al., 2002; Probst et al., 2003).

1.2. Heterochromatin is a specialized chromatin subdomain

1.2.1. Structure of heterochromatin

Local modifications of the nucleosome structure and chromatin fiber organization translate in the formation of two major chromatin states in eukaryotes, visible in cytological preparations after coloration by DNA stains (***Figure 4***). The less compact euchromatin includes mainly genes and promotes a transcriptionally permissive environment. Densely packaged heterochromatin instead forms mostly at repetitive sequences and transposable elements, rendering them largely inaccessible to RNA polymerases by adopting a “closed” chromatin conformation. Heterochromatin thereby contributes to the control of potentially deleterious DNA elements and organizes repetitive DNA sequences at both centromeres and telomeres. Historically, heterochromatin has been cytologically defined in moss as chromosomal regions or chromosomes that remain intensely stained during the whole cell cycle, in contrast to the lightly stained euchromatin that decondenses at interphase (Heitz, 1928). This distinction was initially established by light microscopy using chromatin-staining dyes such as acetocarmine and then validated by other cytological techniques, such as Fluorescent *In Situ* Hybridization (FISH). The definition of heterochromatin has been enriched afterwards by molecular, biochemical and structural features together with the finding that heterochromatin contains abundant tandem-repeated DNA, wrapped around densely arranged nucleosomes relatively insensitive to DNase I (Chodavarapu et al., 2010; Shu et al., 2012, 2013), enriched in heavily methylated DNA and histones H3 methylated at lysine in position 9 (H3K9) and 27 (H3K27), thus promoting transcriptional repression, and subjected to late-replication (Karpen and Allshire, 1997; Hennig,

1999; Henikoff, 2000; Chodavarapu et al., 2010; Almouzni and Probst, 2011; Shu et al., 2012). In most eukaryotic species, centromeric, pericentromeric and telomeric regions contain a high density of repetitive DNA sequences such as clusters of satellite sequences and transposons, and are principal candidates for heterochromatin formation (Martens et al., 2005; Schueler and Sullivan, 2006; Blasco, 2007; Slotkin and Martienssen, 2007; Schoeftner and Blasco, 2009). Centromeric and pericentromeric heterochromatin are required for correct chromosome segregation (Peters et al., 2001; Lippman and Martienssen, 2004; Dunleavy et al., 2005; Kanellopoulou et al., 2005; Pidoux and Allshire, 2005; Folco et al., 2008), and intra- and inter-chromosomal association of heterochromatin domains has been shown to be an important factor in the higher-order organization of chromosomes since it promotes the formation of specialized heterochromatin domains such as chromocenters in mouse (Guenatri et al., 2004) and Arabidopsis (Fransz et al., 2002). Chromocenters are conspicuous heterochromatin clusters containing most of the repetitive DNA content of the genome (Fransz et al., 2002; Guenatri et al., 2004).

In mouse *Mus musculus domesticus*, pericentromeres and centromeres consist of two types of repetitive DNA sequences spanning around 3.5% of the genome: the AT-rich major satellite repeats (6 Mb of 234 bp units) and the minor satellite repeats (600 kb of 123 bp units) respectively, localizing to the tip of the acrocentric chromosomes (Vissel and Choo, 1989; Choo, 1997; Lehnertz et al., 2003). *In situ* hybridization on metaphase chromosomes has shown that minor satellite sequences constitute the centromeric part, while major satellite repeats locate pericentromerically (Wong and Rattner, 1988; Joseph et al., 1989; Kuznetsova et al., 2006). Pericentromeres cluster to form chromocenters in interphase (Hsu et al., 1971; Guenatri et al., 2004). Chromocenter organization is found in most of the somatic mouse cells, but the levels of clustering and the spatial location of the chromocenters in the nucleus differ between cell types (Guenatri et al., 2004; Terranova et al., 2005; Solovei et al., 2009). At the molecular level, chromocenters are characterized by repressive epigenetic marks including DNA methylation, repressive post-translational modifications and strong enrichment in Heterochromatin Protein 1 (HP1) (Jeppesen et al., 1992; Peters et al., 2001; Lehnertz et al., 2003). The centromeric domain promotes kinetochore formation and the pericentromeric domain has been proposed to play a role in sister chromatid cohesion and proper

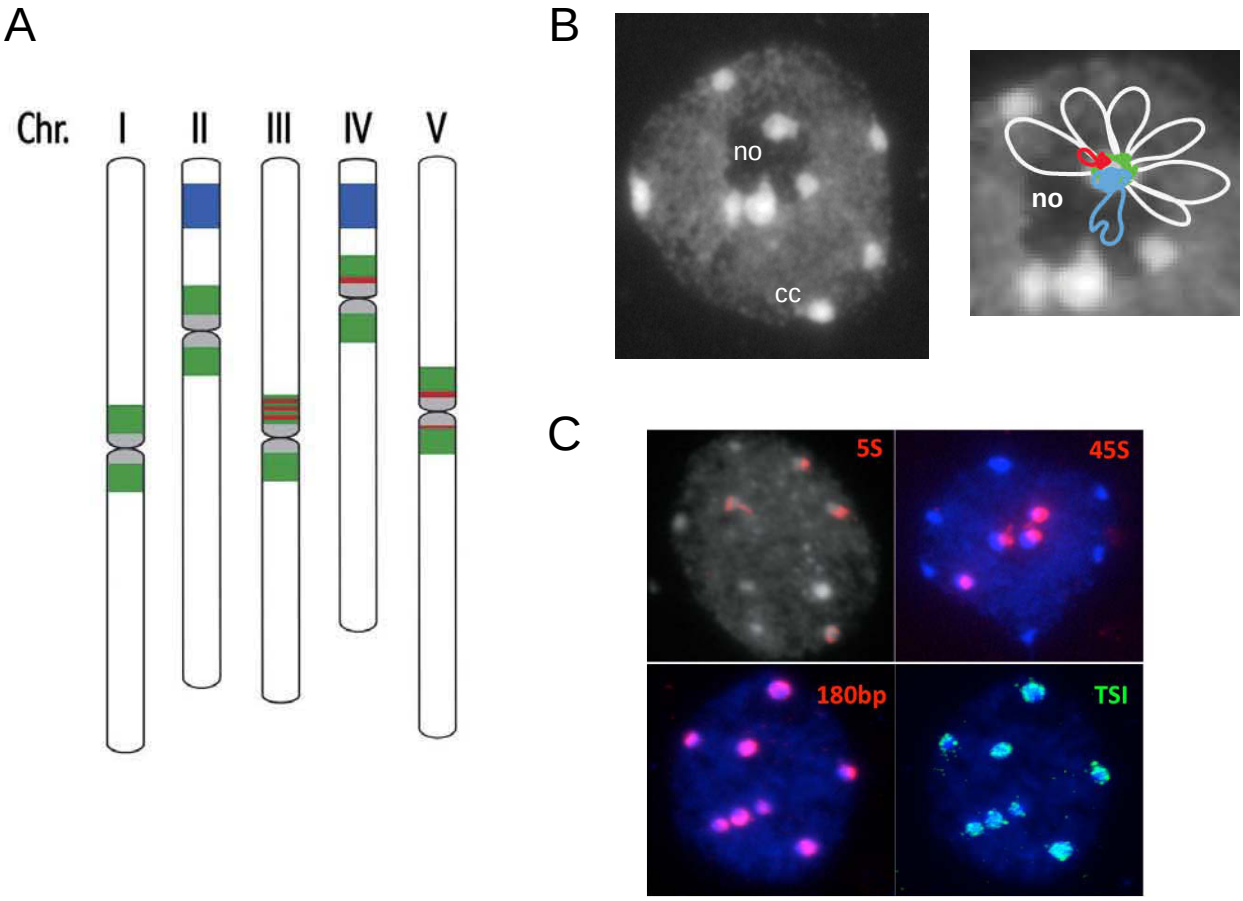

Figure 5*: Heterochromatin is organized in chromocenters in *Arabidopsis thaliana.

A. Schematic representation of the five Arabidopsis chromosomes (2n = 10) in the Columbia accession. Chromosome II and IV carry the 45S rDNA loci (Nucleolus Organizer Regions, NOR, blue). The 5S rDNA loci (red) are present on chromosomes III, IV and V, in close proximity to centromeric repeats (180 bp repeats, gray) and inside the pericentromeric domains (green) (from Benoit et al., 2013).
B. Left: Spread of an Arabidopsis leaf mesophyll nucleus stained with DAPI. Note the euchromatin in light gray and the nine brightly stained chromocenters (cc). The nucleolus (no) appears as a DAPI-unstained region. Scale bar: 5 µm. Right: Model of an Arabidopsis chromocenter of chromosome IV adjacent to the nucleolus (no). The chromocenter of chromosome IV comprises the 45S (blue), 5S (red), centromeric (light gray) and pericentromeric (green) repeats from which euchromatic loops (white) emanate (adapted from Fransz et al., 2002). Parts of the ribosomal DNA repeats which are actively transcribed are represented as 45S rDNA sequences (blue) that loop out from the chromocenter into the nucleolus (Probst et al., 2004) and 5S rDNA (red) loops within the euchromatin compartment (Mathieu et al., 2003) respectively.
C. Clustering of repetitive sequences in chromocenters revealed by FISH. Different repetitive sequences (5S, 45S, 180 bp, and Transcriptionally Silent Information (TSI) repeats) are revealed by DNA FISH (adapted from Douet et al., 2008 and Probst et al., 2003).

chromosome segregation (Guenatri et al., 2004). Indeed, mice lacking both the methylation at H3 lysine 9 (H3K9me) and HP1 at major satellites show chromosome missegregation (Peters et al., 2001; Lippman and Martienssen, 2004; Dunleavy et al., 2005; Kanellopoulou et al., 2005). The centromere region of the fruit fly *Drosophila melanogaster* displays a tripartite organization (Miklos and Cotsell, 1990), with the core domain consisting in gene-poor highly repetitive DNA and the flanking segments, observable only in polytene chromosomes, forms at middle repetitive DNA, interspersed with domains containing high density of genes (Eberl et al., 1993; Lohe et al., 1993). These heterochromatin domains are enriched in H3K9me2/3 and HP1 (Roy et al., 2010; Kharchenko et al., 2011; Riddle et al., 2011).

In Arabidopsis, heterochromatin is essentially composed of repetitive sequences and transposable elements, including the centromeric 180 bp repeats and interspersed pericentromeric repeats, as well as silenced 45S and 5S rRNA genes (Kumekawa et al., 2000; Nagaki et al., 2003; Benoit et al., 2013) (***Figure 5A***). The centromeres of *Arabidopsis thaliana* have been genetically mapped (Copenhaver et al., 1999; Heslop-Harrison et al., 1999). The centromere core is depleted from genes while silent and low-density genes (<1 per 100 kb compared to euchromatin with 1 gene per 5 kb) are found in pericentromeric regions (Kumekawa et al., 2000; The Arabidopsis Genome Initiative, 2000; Haupt et al., 2001; Hosouchi et al., 2002; Hall et al., 2003), together with various types of repetitive DNA elements, including transposons, retrotransposons and telomere-like repeats, were identified in the pericentromeric region (Richards, 1991; The Arabidopsis Genome Initiative, 2000). The organization of the Arabidopsis centromeric region translates in two domains: the centromere core, containing the functional centromere/kinetochore complex and consisting mainly in 180 bp repeats, and the flanking pericentromeric domains. Each Arabidopsis centromere core contains several megabases (near 20,000 copies spanning about 1.3 to 2.1 Mb) (Haupt et al., 2001) of the 180 bp repeat (Copenhaver et al., 1999; Kumekawa et al., 2000; Hosouchi et al., 2002; Hall et al., 2003), organized into long tandem arrays (The Arabidopsis Genome Initiative, 2000). In addition, a 398 bp fragment of the Athila2 Long Terminal Repeat (LTR) called 106B was discovered as associated with the 180 bp centromeric repeats (Thompson et al., 1996; Slotkin, 2010). The 106B repeat is interspersed as single copies within long stretches of 180 bp repeats. The centromere core region is flanked by pericentromeric heterochromatin domains that contain many transposons,

retrotransposons and telomere-like repeats (Richards, 1991; The Arabidopsis Genome Initiative, 2000). The Athila family of LTR retrotransposons (approximately 500 copies) (Pélissier et al., 1996) and TSI (Transcriptionally Silent Information) repeats constitute most of the genomic content of pericentromeric heterochromatin regions of Arabidopsis chromosomes. TSI repeats exhibit sequence homology with the 3' terminal part of the Athila retrotransposon (Steimer et al., 2000; Slotkin, 2010). Contrary to Drosophila, chromosome-specific repeats have not yet been identified in Arabidopsis except for the ribosomal gene clusters (Cloix et al., 2000). The genome of *Arabidopsis thaliana* encodes approximately 1000 copies of 5S rRNA genes, which are arranged as tandem arrays in several loci located in the pericentromeric heterochromatin of chromosomes 3, 4 and 5 in the Columbia accession (Campell et al., 1992; Layat et al., 2012b; Benoit et al., 2013) (***Figure 5A***). 5S rRNA gene transcription has been found only at the array located on chromosome 4 and at the large locus on chromosome 5, while 5S rRNA genes from chromosome 3 and from the small locus on chromosome 5 are transcriptionally silent (Cloix et al., 2002, 2003; Layat et al., 2012b). Interestingly, at active 5S rDNA loci only the most distal copies are expressed while units close from to centromere remain largely silenced and display increasing levels of mutations (The Arabidopsis Genome Initiative, 2000; Cloix et al., 2002; Vaillant et al., 2008). Upon developmental cues, some of the low-mutated silent units can revert and become transcribed to ensure appropriate amount of 5S rRNA. In Arabidopsis, the 45S rRNA genes are located at the tips of the short arms of chromosomes 2 and 4, in domains called Nucleolar Organizer Regions (NOR). The 570 to 750 copies of 45S rRNA genes are organized in tandem arrays (Copenhaver et al., 1995; Copenhaver and Pikaard, 1996; Layat et al., 2012b). Similar to the 5S rRNA genes, only a fraction of the 45S rRNA gene units are transcribed but the extent of this fraction can be dynamically modified during development (Pontvianne et al., 2010).

Centromeric and pericentromeric heterochromatin clusters with silenced 45S and 5S rDNA arrays of the same chromosome in a chromocenter (Fransz et al., 2002; Fransz and de Jong, 2011) (***Figure 5B***). In 4′,6′-diamidino-2-phenylindole (DAPI)-stained interphase nuclei, these chromocenters appear as 6-10 intensely stained chromatin foci (Fransz et al., 2002; Dittmer et al., 2007). Immunolocalization studies confirmed the enrichment in repressive chromatin marks, such as high levels of DNA methylation, H3K9me2 and H3K27me1 (Soppe et al., 2002; Probst et al.,

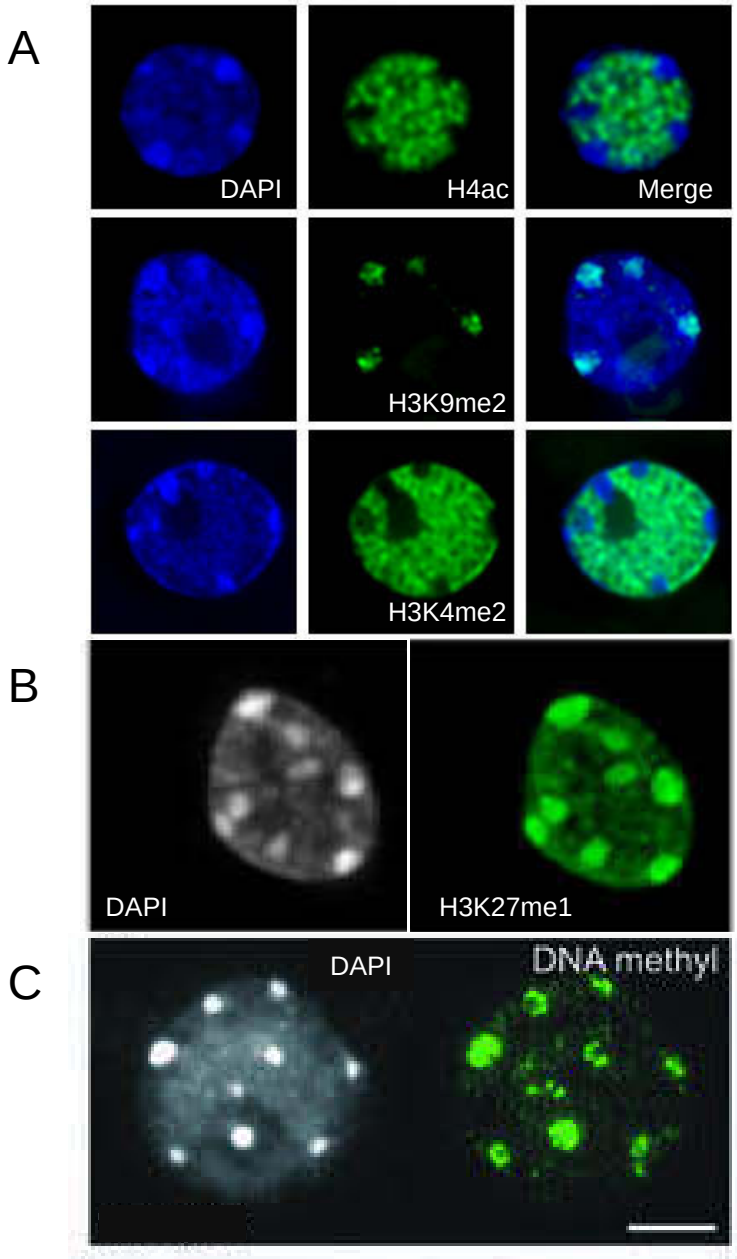

***Figure 6*: Chromocenters are enriched in repressive chromatin marks.**

A. Immunolocalization of H4ac (top), H3K9me2 (middle) and H3K4me2 (bottom) in interphase nuclei isolated from young rosette leaves counterstained with DAPI. The repressive H3K9me2 mark colocalizes with heterochromatic chromocenters, while active marks H4ac and H3K4me2 are excluded (from Probst et al., 2003).
B. Immunodetection of H3K27me1 in interphase nuclei from young rosette leaves counterstained with DAPI. As a repressive histone post-translational modification, the H3K27me1 immunosignal is found colocalizing with chromocenters but is also present in euchromatin (from Mathieu et al., 2005).
C. Immunolocalization of DNA methylation with a 5mC specific antibody on interphase nuclear spreads from young rosette leaves counterstained with DAPI. The DNA methylation immunosignal concentrates in chromocenters. Scale bar: 5 µm (from Soppe et al., 2002).

2003; Mathieu et al., 2005) (***Figure 6***). The model emitted by Fransz and collaborators, based on FISH analysis in interphase nuclei, suggests that gene-rich euchromatin loops visualized using gene-rich Bacterial Artificial Chromosomes (BAC) as probes emanate from the chromocenters, thus defining chromosome territories (Fransz et al., 2002; Pecinka et al., 2004) (***Figure 5B***). Such an organization is important for proper compartmentalization and transcriptional silencing of repetitive DNA, meanwhile allowing efficient transcription of genes located in the euchromatic loops. Cytological observations were further confirmed by testing intra- and inter-chromosomal interactions using a 4C assay, revealing that heterochromatic repetitive sequences, including the ones dispersed along the chromosome arms, interact preferentially with each other thus generating specific and well-defined chromatin landscapes (Grob et al., 2013).

1.2.2. Heterochromatin is actively defined by epigenetic mechanisms

A defining feature of heterochromatin is that its transcriptionally repressed state and highly condensed structure self-perpetuates during the cell cycle in a region-specific manner (Probst et al., 2009). During S phase, epigenetic marks are diluted as a consequence of DNA replication. Therefore, sophisticated mechanisms that exploit the mutual reinforcement of DNA and histone modifications are required to ensure inheritance of chromatin marks and maintenance of heterochromatin in its specific higher-order structure (Probst et al., 2009).

1.2.2.1. DNA methylation

Cytosine residues are methylated in a wide diversity of organisms, including plants, mammals and Neurospora, while very low DNA methylation levels are present in yeast, Drosophila or *Caenorhabditis elegans* (Simpson et al., 1986; Lyko et al., 1999; Tang et al., 2012). DNA methylation has been shown since long to be critical for development in plants and mammals, involved in transcriptional gene silencing, imprinting and X-chromosome inactivation. Methylation acts in many ways and is

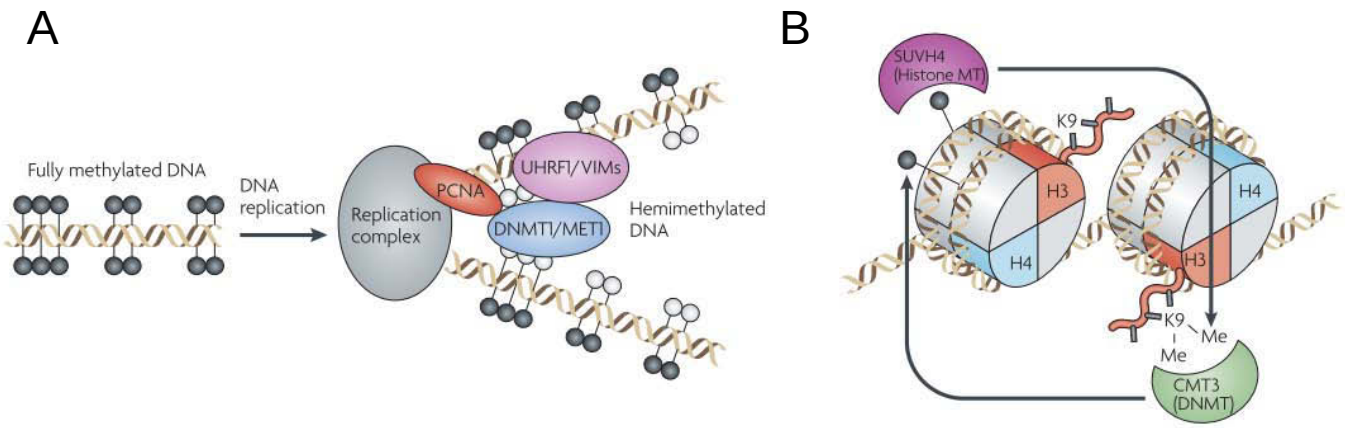

***Figure 7*: Model of CG and CHG methylation maintenance.**

A. Model of CG methylation maintenance during DNA replication. DNMT1 is targeted to the replication fork *via* interaction with UHRF1, specifically binding hemimethylated DNA, and PCNA. Following recruitment, DNMT1 fully reestablishes methylation patterns. In *Arabidopsis thaliana*, DNMT1 and UHRF1 orthologs, respectively MET1 and VIM, are involved in a similar manner in CG methylation maintenance (from Law and Jacobsen, 2010).
B. Model of CHG methylation maintenance in plants by a self-reinforcing loop between DNA and histone methylation. The DNA methyltransferase CMT3 establishes CHG methylation, which is recognized by SUVH4 histone methyltransferase. SUVH4 in turn dimethylates H3K9. This modification is then recognized by the chromodomain of CMT3 allowing maintenance of CHG methylation (from Law and Jacobsen, 2010).

susceptible to block binding of transcription factors, thus preventing transcription, or it can interact with chromatin modifiers that modify the neighbouring histones and enhancing transcriptional silencing. DNA methylation can occur in three different nucleotide sequence contexts: CG, CHG and CHH (H = C, T or A). CG methylation is observed widely in plants and mammals, while CHG as well as CHH are preferentially found in Arabidopsis. Cytosine methylation (5mC) is predominantly present at highly repetitive DNA, including centromeric and pericentromeric repeats, rDNA arrays and transposable elements (***Figure 6C***), where it often coexists with H3K9me2 and H3K27me1 (***Figure 6AB***), but also in the body of 30% of genes, many of which are characterized by moderate expression levels (Zhang et al., 2006; Zilberman et al., 2007; Vaughn et al., 2007; Bernatavichute et al., 2008; Cokus et al., 2008; Lister et al., 2008). Interestingly, while gene bodies contain mainly CG methylation (Cokus et al., 2008), CHG methylation is linked to centromeric and pericentromeric regions enriched in H3K9me2 (Bernatavichute et al., 2008), while CHH is a hallmark of long transposable elements (Zemach et al., 2013; Cavrak et al., 2014). CHH methylation establishment and maintenance rely on the production of small interfering RNA (siRNA) and the RNA-directed DNA methylation (RdDM) pathway.

1.2.2.1.1. Maintenance

In both mammals and plants, maintenance of CG methylation is achieved by a specific DNA methyltransferase associated to a co-factor that senses hemi-methylated DNA at the replication fork and by interaction with PCNA (Proliferating Cell Nuclear Antigen). In Arabidopsis, this is achieved by MET1 (DNA METHYLTRANSFERASE 1) and VIM1 (VARIATION IN METHYLATION 1) activity and in mammals, by DNMT1 (DNA cytosine-5-Methyltransferase 1) and UHRF1 (Ubiquitin-like containing PHD and RING Finger domains 1) (Law and Jacobsen, 2010) (***Figure 7A***). Moreover, the *de novo* DNA methyltransferases DNMT3A and DNMT3B are also involved in the maintenance of CG methylation patterns at some loci (Chen et al., 2003). Mutant alleles of *MET1* display an important decrease in CG methylation levels, but also CHG and CHH, at centromeric repeats (Saze et al., 2003). Concomitantly, H3K9me2 is redistributed from the chromocenters, suggesting

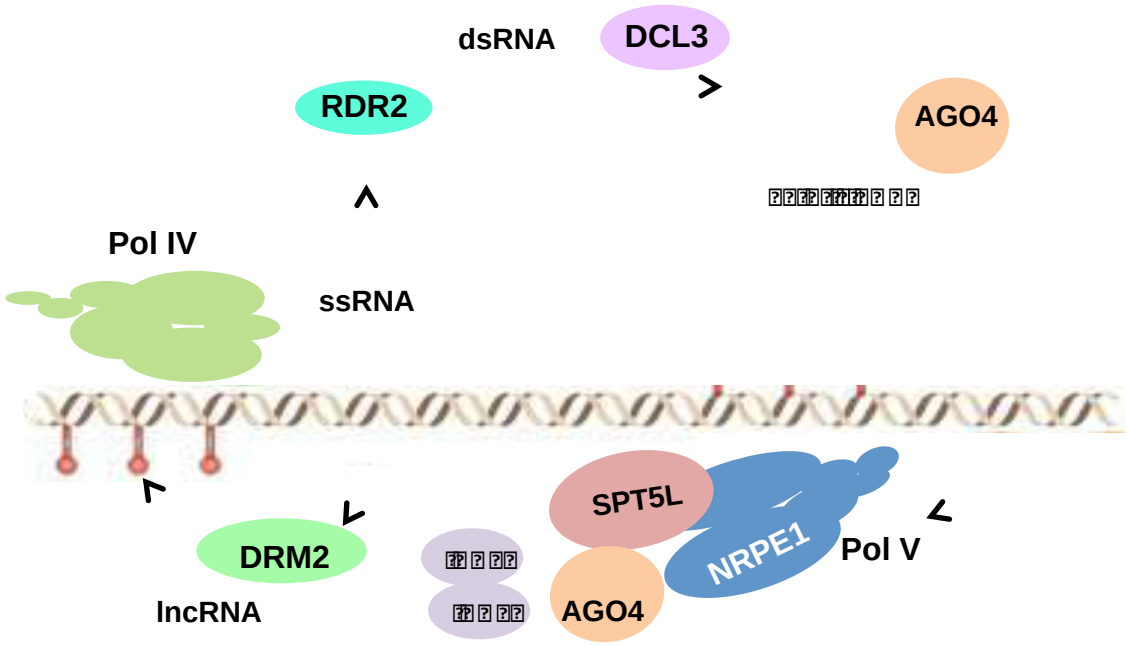

***Figure 8*: RNA-directed DNA methylation pathway.**

RNA-directed DNA Methylation (RdDM) necessitates the synthesis of single-stranded RNA (ssRNA), produced from the repetitive and transposon-rich DNA domains to be silenced by the plant-specific DNA-dependent RNA polymerase Pol IV. These transcripts are then processed by RDR2 for synthesis of double-strand RNA (dsRNA). After fragmentation in 24-nt long sequences by DCL3 the siRNA are loaded in AGO4 for transport to the sequence of origin where they are thought to recognize scaffold RNA originating from Pol V activity. Interaction between 24-nt siRNA and lncRNA is the basis for further recruitment of DRM2, the main DNA methyltransferase involved in RdDM, for methylation of the DNA domain (figure courtesy of M. Thomas).

a fundamental role of CG methylation for H3K9me2 setting at chromocenters (Tariq et al., 2003; Mathieu et al., 2005).

DNA methylation in the CHG context is found widely in Arabidopsis and other plant genomes. Histone methylation by the KYP (KRYPTONITE) / SUVH4 (SUPPRESSOR OF VARIEGATION 3-9 HOMOLOGUE 4) methyltransferase together with the plant-specific DNA methyltransferase CMT3 (CHROMOMETHYLASE 3) sustain a feed-forward loop that maintains CHG methylation (Lindroth et al., 2001; Jackson et al., 2002; Johnson et al., 2007; Feng et al., 2010) (***Figure 7B***). Depletion of CMT3 leads to genome-wide decrease in CHG context methylation (Lindroth et al., 2004). CMT3 recognizes H3K9me2, which colocalizes with H3K27me1/2 at CMT3-controlled loci, suggesting that CMT3 recruitment relies on the combination of both marks (Lindroth et al., 2004; Du et al., 2012; Law et al., 2013).

CHH methylation is driven by two distinct pathways: one is the RdDM pathway that involves siRNA originating from repeats and transposon-rich heterochromatin domains and participates in the control of transcriptional gene silencing by targeting DNA methylation to the sequences to be suppressed (Lippman et al., 2004; Lippman and Martienssen, 2004) (***Figure 8***). 24-nt-long siRNA are produced from heterochromatic repeats and transposable elements. The siRNA synthesis is achieved by the plant-specific DNA-dependent RNA polymerase Pol IV, which produces single-stranded RNA from repetitive regions (Herr et al., 2005; Onodera et al., 2005; Sidorenko et al., 2009; Havecker et al., 2010). Pol IV transcripts are then converted into double-strand RNA by RNA-Dependent RNA polymerase 2 (RDR2) and subsequently cut in 24-nt-long sequences by DICER-LIKE3 (DCL3) (Xie et al., 2004). These 24-nt siRNA are then loaded in AGO4 (Argonaute 4) complexes which target the siRNA to the locus of origin by sequence homology (Chan et al., 2004; Qi et al., 2006; Ye et al., 2012) where they hybridize to genomic DNA or scaffold RNA (Wierzbicki et al., 2009). Scaffold RNA molecules are long non-coding RNA (lncRNA) produced independently from siRNA by Pol V (Wierzbicki et al., 2008, 2012). Complementarity between 24-nt siRNA and scaffold RNA is thought to help the recruitment of DNA methyltransferases, notably DRM2 (DOMAINS REARRANGED METHYLTRANSFERASE 2 – homolog of DNMT3) (Naumann et al., 2011), but the precise mechanism remains poorly characterized. siRNA-mediated heterochromatin

formation is found in many other eukaryotes, including fission yeast, Drosophila and mammals (Hall et al., 2002; Volpe et al., 2002; Verdel et al., 2004).

The second pathway involves CHROMOMETHYLASE 2 (CMT2), methyltransferase maintaining both CHG and CHH. Indeed, *drm1 drm2 cmt2* triple mutants loose all methylation in the CHH context (Stroud et al., 2014). Interestingly, DRM2 activity is thought to be promoted through the recruitment of Pol IV by the binding of methylated histone binding protein SHH1 to H3K9me1, H3K9me2 and H3K9me3, as observed for CMT3. While CMT3 exhibits no preference in binding affinity towards the number of methyl groups at H3K9, CMT2 interacts preferentially with H3K9me2 (Stroud et al., 2014). Together, these data suggest that DRM2, CMT2 and CMT3 control non-CG methylation in plants, and establish a self-reinforcing loop together with H3K9 methylation. Both CHG and CHH methylation also exist at low levels in mammalian embryonic stem cells where they are probably mediated by DNMT3A and DNMT3B (Ramsahoye et al., 2000; Chen et al., 2003; Lister et al., 2009).

The combination of genome-wide DNA methylation patterns with global nucleosome positioning maps revealed that DNA methylation deposition is influenced by nucleosome positioning in Arabidopsis (Chodavarapu et al., 2010). Consistently, DNA methyltransferases preferentially target nucleosome-bound DNA. The same observation has been described for human nucleosomal DNA, suggesting that DNA methylation and nucleosomal occupancy are tightly linked (Chodavarapu et al., 2010).

1.2.2.1.2. Demethylation

Removal of methylated cytosines occurs during epigenome reprogramming. In plants, four bifunctional helix-hairpin-helix DNA glycosylases and AP lysases are found. DME (DEMETER), DML2 (DEMETER-LIKE 2), DML3 (DEMETER-LIKE 3) and ROS1 (REPRESSOR OF SILENCING 1) excise methylated cytosines. The remaining 1-nt gap is then filled by a new unmethylated cytosine by a still unknown DNA ligase (Zhu, 2009). DML2, DML3 and ROS1 activities are mainly found in vegetative tissues and target hundreds of genes throughout the genome (Penterman et al., 2007; Yu et al., 2013). In the mammalian embryo, *de novo* DNA methylation of

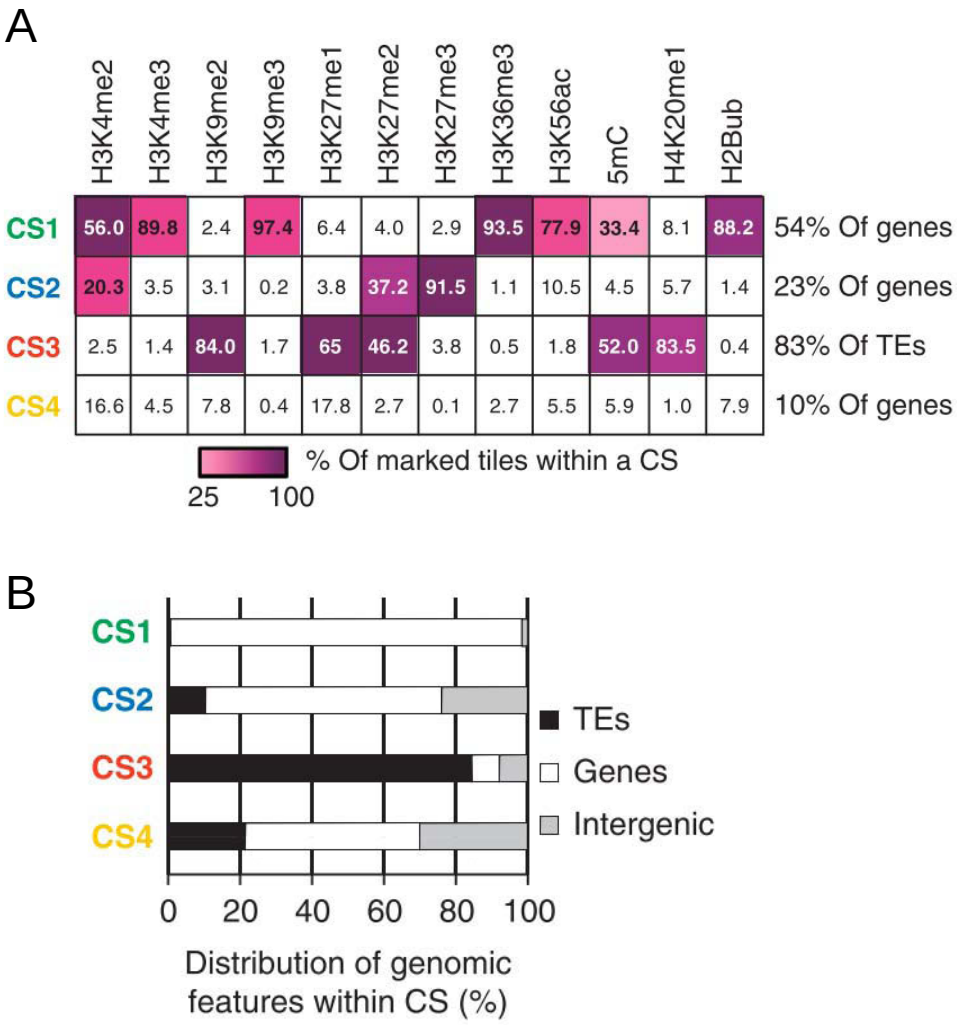

***Figure 9*: At least four different chromatin states can be defined in Arabidopsis based on their enrichment in histone post-translational marks.**

A. The genome-wide distribution of the twelve chromatin marks analyzed defines four main chromatin states based upon heat map values ranging from 25% (light purple) to 100% (dark purple) (from Roudier et al., 2011).
B. The four chromatin states defined display different relative proportion of genomic features. While active marks-associated chromatin state 1 (CS1) and CS2 contain mostly genes, CS3 covers most of the transposable elements, which is coherent with its strong bias towards repressive mark enrichment. CS4 shows no particular enrichment in any of the studied chromatin marks and contains mainly genomic regions outside of genes and transposable elements (modified from Roudier et al., 2011).

the inner cell mass following massive demethylation is critical to drive the identity and stability of embryonic lineages, whereas the placenta remains mainly unmethylated (Law and Jacobsen, 2010; Seisenberger et al., 2013). In plants, genome-wide demethylation occurs during plant reproduction in the companion cells of the sperm and egg cells (Ibarra et al., 2012) and then during post-fertilization seed development (Gehring et al., 2009; Hsieh et al., 2009). At this stage the nutrient tissue, the endosperm, undergoes genome-wide demethylation in contrast to the embryo (Hsieh et al., 2009). This phenomenon is of particular importance for early embryogenesis by the establishment of maternal imprinted gene expression patterns (Pillot et al., 2010; Autran et al., 2011; Raissig et al., 2011). As a conclusion, DNA methylation reprogramming is important to establish epigenetic patterns of embryonic and extra-embryonic lineages.

1.2.2.2. Histone post-translational marks associated with heterochromatin

Histone tail domains are preferential targets for many and diverse post-translational modifications such as acetylation, methylation, and phosphorylation (Kouzarides, 2007). Such modifications can influence the biochemical properties of the nucleosome as well as its stability and interactions with remodeling factors (Zheng and Hayes, 2003), thus participating in the regulation of genome activity (Davie and Chadee, 1998) and higher-order chromatin architecture (Dorigo et al., 2003). Genome-wide studies argue for the role of epigenetic marks such as DNA methylation, histone post-translational modifications and chromatin binding proteins in establishing functional chromatin landscapes and defining euchromatin and heterochromatin (Filion et al., 2010; Roudier et al., 2011; Sequeira-Mendes et al., 2014) (***Figure 9***). Consequently, while transcribed regions of the genome bear marks permissive for transcription such as H3K4me2/3 and H4 acetylation (***Figure 6A***), repetitive sequences contained in chromocenters are enriched in histone marks involved in transcriptional repression such as H3K9 and H3K27 methylation (Soppe et al., 2002; Jasencakova et al., 2003; Probst et al., 2003; Lindroth et al., 2004; Mathieu et al., 2005; Naumann et al., 2005) (***Figure 6AB***).

1.2.2.2.1. H3K9me2/3

In eukaryotes, H3K9 methylation is a hallmark of heterochromatic repeats. Methylation of this lysine residue, which can be mono-, di- or trimethylated, is a characteristic of transcriptional silencing. In mammals, modified H3 histones H3K9m3, catalyzed by histone methyltransferases Suv39h, are associated with pericentromeric heterochromatin (Peters et al., 2001; Lehnertz et al., 2003). H3K9me3 is recognized by HP1 *via* its chromodomain (Bannister et al., 2001). Furthermore, HP1 has the ability to recruit Suv39h which allows setting of new HP1-binding sites, thereby forming a self-reinforcing loop (Maison and Almouzni, 2004; Krouwels et al., 2005). This is the basis for further recruitment of H4K20 histone methyltransferases and DNA methyltransferases (Fuks et al., 2003; Schotta et al., 2004; Karachentsev et al., 2005). Pericentromeric heterochromatin of knockout mice for Suv39h methyltransferases lacks H3K9me3 and HP1. These mice display genomic instability and impaired viability revealing the role of this histone post-translational mark in mammalian development (Maison et al., 2002; Guenatri et al., 2004). Suv39h homologs have been shown in many organisms to play roles in heterochromatin formation and gene silencing. A few examples include Cryptic Loci Regulator 4 (Clr4) in yeast (*Schizosaccharomyces pombe*) and SU(VAR)3-9 proteins in Drosophila (Nakayama et al., 2001; Schotta et al., 2002).

In Arabidopsis, contrary to other eukaryotes, only H3K9m2 is enriched in heterochromatin. Several histone methyltransferases such as SUVH4, SUVH5 and SUVH6 are responsible for H3K9m2 deposition (Jackson et al., 2002; Ebbs et al., 2005; Ebbs and Bender, 2006). Genome-wide analysis by Chromatin Immunoprecipitation (ChIP) in Arabidopsis showed that H3K9me2 is highly enriched at pericentromeric heterochromatin in large and continuous blocks, but can also be found punctually at euchromatic repeats and transposons (Bernatavichute et al., 2008; Roudier et al., 2011). The Arabidopsis ortholog of HP1, LIKE HETEROCHROMATIN PROTEIN 1 (LHP1), does not bind H3K9me2 as its counterpart in yeast and mammals. Instead, it binds H3K27me3 *in vitro* through its chromodomain and is associated genome-wide with H3K27me3 (Gaudin et al., 2001; Libault et al., 2005; Turck et al., 2007). Instead, Arabidopsis H3K9me2 can be recognized by the maintenance DNA methyltransferase for CHG sites CMT3, which also contains a chromodomain (Lindroth et al., 2004; Du et al., 2012). The

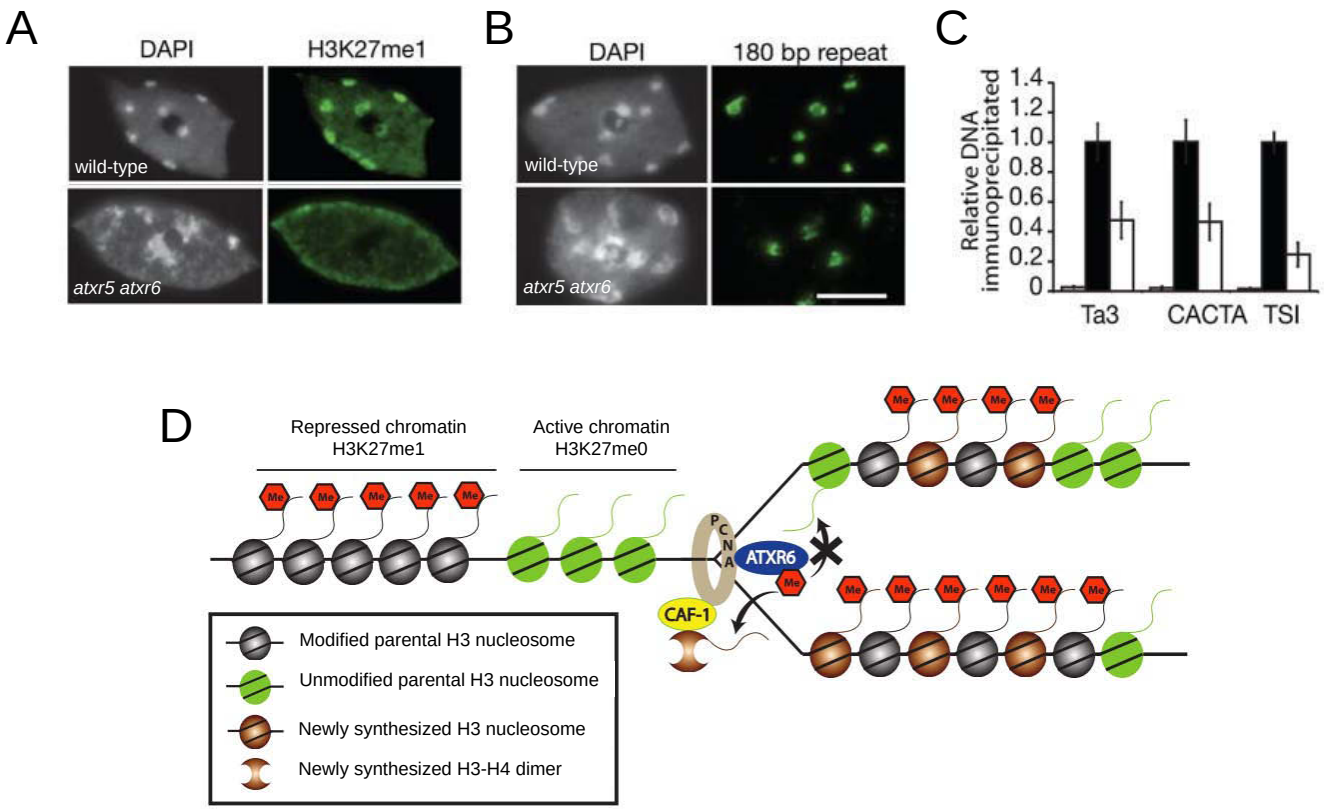

***Figure 10*: Arabidopsis *atxr5 atxr6* mutants display defects in heterochromatin organization and transcriptional silencing.**

A. Immunodetection of H3K27me1 (green) in interphase nuclei from either wild type (WT) or *atxr5 atxr6* leaves. DNA is counterstained with DAPI (grey). Most of *atxr5 atxr6* nuclei display chromocenter decondensation and show no H3K27me1 staining at residual chromocenters (from Jacob et al., 2009).
B. FISH on spread interphase nuclei with probes detecting 180 bp centromeric repeats in WT and *atxr5 atxr6* plants. DNA is counterstained with DAPI (grey). The centromeric repeats display mild dispersion from the chromocenters in *atxr5 atxr6.* Scale bar: 5 µm (from Jacob et al., 2009).
C. ChIP assay showing relative H3K27me1 enrichment at repetitive sequences. Relative enrichment of H3K27me1 at Ta3, CACTA and TSI is lower in *atxr5 atxr6* mutants (white bars) compared to WT (black bars). Grey bars represent no-antibody controls (from Jacob et al., 2009).
D. Model for the role of ATXR5 and ATXR6 in the maintenance of H3K27me1 during DNA replication in Arabidopsis. ATXR5 and ATXR6 participate in the mitotic inheritance and distribution of H3K27me1 in Arabidopsis. Following recruitment to the replication fork during S phase through their interaction with PCNA, they specifically monomethylate K27 at newly incorporated H3 to ensure maintenance of chromatin states (modified from Jacob et al., 2014).

maintenance of H3K9me2 and CHG methylation in heterochromatin is achieved by a self-reinforcing loop between SUVH4 and CMT3. In mammals, the histone H3K9 monomethyltransferase SetDB1 (SET domain bifurcated-1) and the K9 dimethylase G9a interact with PCNA and are recruited to the replication fork (Estève et al., 2006; Loyola et al., 2006, 2009). In *Schizosaccharomyces pombe*, transcription of centromeric chromatin during S phase is essential for preservation of H3K9 methylation by means of a mechanism involving RNA, the HP1 homologue Swi6, the methyltransferase Clr4 and the RNA-induced transcriptional silencing complex (Volpe et al., 2002; Volpe and Martienssen, 2011).

1.2.2.2.2. H3K27me1

H3K27me1 is a silencing mark described in plant and mammals as DNA methylation- and H3K9me2-independent (Ebert et al., 2004; Mathieu et al., 2005). H3K27me1 was first identified in mouse at heterochromatic major and minor satellite repeats (Peters et al., 2001). In Arabidopsis, immunolocalization and genome-wide ChIP-seq data have revealed enrichment of H3K27me1 in centromeric and pericentromeric heterochromatin (Lindroth et al., 2004; Jacob et al., 2009; Roudier et al., 2011) (***Figure 10AB***). H3K27me1 deposition at chromocenters is mediated by the H3K27 monomethyltransferases ARABIDOPSIS TRITHORAX-RELATED PROTEIN 5 (ATXR5) and ATXR6 in Arabidopsis (Jacob et al., 2009, 2010, 2014) (***Figure 10AB***). Maintenance of the H3K27me1 mark is achieved through the interaction of the plant homeodomain (PHD) of both ATXR5 and ATXR6 proteins with PCNA at the DNA replication fork (***Figure 10D***).

atxr5 atxr6 mutants show pleiotropic effects on plant development, significant decondensation of chromocenters and alleviation of transcriptional silencing of a wide variety of repetitive sequences including TSI and transposable elements (e.g. Ta3, CACTA) (Jacob et al., 2009) (***Figure 10C***). Moreover, the simultaneous mutation of both *ATXR5* and *ATXR6* allows re-replication of reactivated transposons and repetitive elements normally associated with high levels of H3K27me1 pointing to a positive correlation between repetitive sequences transcriptional reactivation and over-replication (Jacob et al., 2010).

1.2.2.3. Chromatin remodeling factors

1.2.2.3.1. DDM1

DDM1 (DECREASE IN DNA METHYLATION 1), known as LSH in mice, is an important chromatin remodeling factor involved in DNA and histone methylation and required for transcriptional silencing at repeats and transposable elements. This Switch/Sucrose Non Fermentable 2 (SWI/SNF2)-like ATP-dependent chromatin remodeler was historically found through a genetic screen for defects in genomic 5mC levels in Arabidopsis mutants (Jeddeloh et al., 1999). DDM1 participates in the control of silent centromeric and pericentromeric repeats and transposable elements through maintenance of CG and non-CG methylation (Jeddeloh et al., 1999; Zemach et al., 2013). Recently, Zemach and collaborators have shown that DDM1 controls DNA methylation at chromatin regions highly enriched in the linker histone H1 (Zemach et al., 2013). They suggest that accessibility of the DNA methyltransferases to repeats and transposable elements necessitates the remodeling of H1-containing heterochromatin by DDM1. Their conclusions are based on the observation that *h1* single mutants show increased DNA methylation in heterochromatin, while the double *h1 ddm1* mutant restores normal levels of DNA methylation. Plants defective in DDM1 exhibit loss of DNA methylation, H3K9me2 and 24-nt siRNA targeting 180 bp centromeric repeats and transposable elements (Gendrel et al., 2002; Lippman et al., 2004; Lippman and Martienssen, 2004; May et al., 2005), resulting in transcriptional reactivation of silent repeats. The *ddm1-5* mutant, which lacks detectable levels of DDM1 transcripts, displays a severe chromatin phenotype in which pericentromeric heterochromatin, including the 180 bp centromeric repeats, exhibit reduced DNA methylation levels and is decondensed from chromocenters (Mittelsten Scheid et al., 2002; Probst et al., 2003; May et al., 2005). Taken together, these data indicate the important role of the chromatin remodeler DDM1 in the formation and maintenance of heterochromatin domains in plants.

1.2.2.3.2. MOM1

MORPHEUS' MOLECULE 1 (MOM1) is a component of the transcriptional silencing system operating in heterochromatin specific for the plant kingdom (Amedeo et al., 2000; Steimer et al., 2000; Mittelsten Scheid et al., 2002; Probst et al., 2003). The *mom1* mutant results in transcriptional activation of pericentromeric repetitive sequences such as TSI or silent 5S rRNA genes (Mathieu et al., 2003; Tariq et al., 2003; Mathieu et al., 2005; Habu et al., 2006; Vaillant et al., 2006), without any effect on DNA methylation or histone marks (Amedeo et al., 2000; Numa et al., 2010). Transcriptional gene silencing activity of MOM1 is driven by its Conserved MOM1 Motif 2 (CMM2) (Caikovski et al., 2008). However, compared to the *ddm1* mutant, mutation in the *MOM1* gene does not lead to chromocenter decondensation and heterochromatin architecture preserves wild-type morphology (Soppe et al., 2002; Probst et al., 2003).

1.2.2.3.3. MORC

Members of the conserved microrchidia (MORC) adenosine triphosphatase (ATPase) family have been described as regulator of heterochromatin silencing and structure in eukaryotes. The Arabidopsis genome encodes seven MORC paralogs, among which AtMORC1 and AtMORC6 have been characterized as mediators of transcriptional silencing of repetitive DNA and maintain heterochromatin superstructure. The *atmorc1* and *atmorc6* mutants display derepression of pericentromeric regions and transposable elements but surprisingly do not affect DNA methylation, histone methylation and siRNA levels. While this pattern resembles the one in *mom1* mutants, *mom1 morc6* double mutants show synergistic release of silencing suggesting that they operate in different pathways (Moissiard et al., 2012, 2014). In the nucleus, AtMORC1 and AtMORC6 proteins are found in small nuclear foci not within but at the immediate periphery of chromocenters and plants lacking both paralogs exhibit decondensed chromocenters, consistent with an active role in the maintenance of heterochromatin compaction (Moissiard et al., 2012, 2014). AtMORC1 and AtMORC6 appear as a novel layer of control of heterochromatin

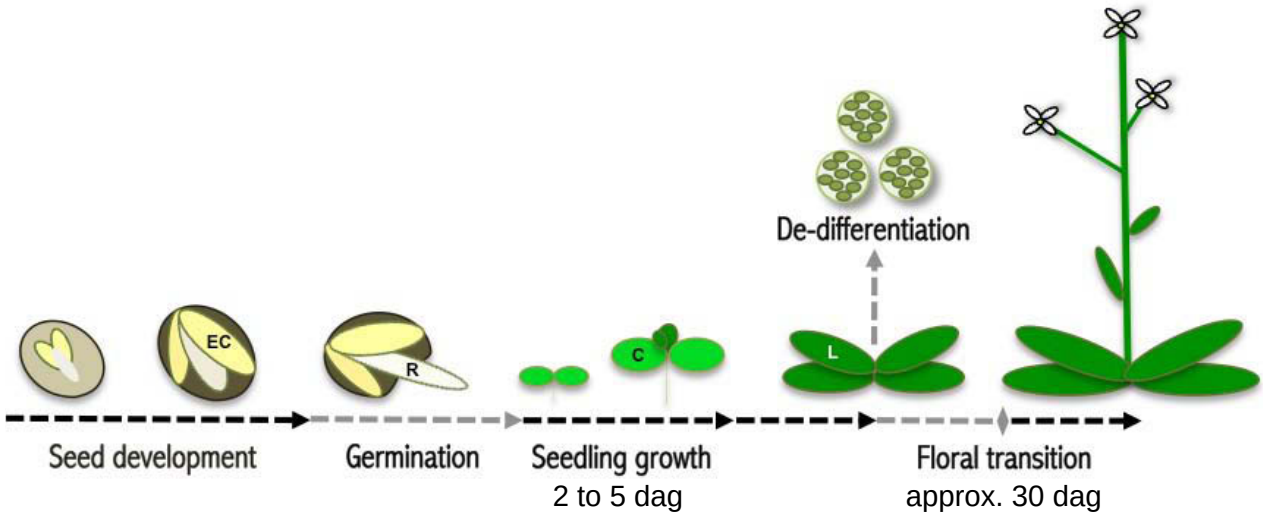

***Figure 11*: Overview of developmental phase transitions involving important chromatin dynamics in *Arabidopsis thaliana*.**

Large-scale chromatin dynamics take place in embryonic cotyledons (EC, yellow) during seed development and germination, in cotyledons (C, light green) during seedling growth from 2 to 5 days after germination (dag) and in leaves (L, dark green) upon de-differentiation into protoplasts or during the floral transition. Developmental transitions associated with heterochromatin decondensation are marked with gray, those implicating predominantly heterochromatin condensation with black arrows. The radicle (R) is shown in white in the developing and germinating seed (from Benoit et al., 2013).

silencing and heterochromatin compaction but the precise way of action remains to be deciphered.

1.3. Dynamics of heterochromatin during developmental phase transitions in Arabidopsis

To ensure successful reproduction, annual plants need to finely tune their major developmental phase switches such as germination and flowering according to environmental stimuli. The transition from a developmental phase to the next requires changes in the spatial and temporal patterns of gene expression. Many signaling cascades and receptors have been described (Amasino, 2010; Huijser and Schmid, 2011), as well as specific sets of genes undergoing selective transcriptional activation or repression through different developmental phase changes (Schmid et al., 2003; Holdsworth et al., 2008). Transcriptional reprogramming of these genes involves active modification of their chromatin structure (Exner and Hennig, 2008; Adrian et al., 2009; He, 2009; Jarillo et al., 2009; Wollmann and Berger, 2012). Interestingly, studies in the model plant *Arabidopsis thaliana* revealed certain environmental conditions and developmental transitions not only to locally affect chromatin structure of the genes undergoing activation or repression but to profoundly impact higher-order chromatin organization (***Figure 11***).

1.3.1. Heterochromatin remodeling during floral transition and dedifferentiation

Floral transition occurs when the plant is exposed to favorable photoperiod and temperature conditions. Flowering is initiated involving the reprogramming of gene expression patterns specific for vegetative to those for reproductive growth (Liu et al., 2009; Huijser and Schmid, 2011). This transition requires external and endogenous signals transmitted to the apical meristem, the meristematic tissue at the tip of the plant shoot, which then undertakes fate change. During reproductive phase transition, chromatin of leaves undergo global reorganization, illustrated by decondensation of chromocenters observed 4 days before emergence of the floral

stem (Tessadori et al., 2007b). A strong decompaction of repetitive sequences from chromocenters was measured (Tessadori et al., 2007b). This reduction resulted essentially from the dispersion of pericentromeric repeats and 5S rDNA, while centromeric 180 bp repeats and 45S rDNA arrays stayed highly condensed (Tessadori et al., 2007b). Therefore, the different repeats of the Arabidopsis genome are unequally affected by the chromatin remodeling during floral transition (Tessadori et al., 2007b). Then, the chromocenters reform once the elongation of the floral stem achieved, endorsing the reversibility of global heterochromatin decondensation processes.

Decondensation of heterochromatin was also described by other authors (Tessadori et al., 2007a; Koukalova et al., 2005; Zhao et al., 2001; Ondrej et al., 2009) associated to dedifferentiation of Arabidopsis, cucumber and tobacco leaf cells into protoplasts which are cells devoid of cell walls. Indeed, during the dedifferentiation of Arabidopsis cells, the heterochromatin fraction of the nucleus decreases, associated with a reduced number of chromocenters revealed by DAPI (Tessadori et al., 2007a). FISH analysis showed that pericentromeric repeats, 5S rRNA genes and even the centromeric 180 bp repeats were excluded from the remaining chromocenter structures, while the only partially condensed 45S rDNA sequences were retained within the chromocenters. This decondensation occurs rapidly but could be partially reversed during further protoplast culturing (Tessadori et al., 2007a). Importantly, floral transition-associated heterochromatin decondensation seems not to involve major changes in methylation since repetitive sequences remain highly DNA methylated. Only the nuclear distribution of 5mC, cytologically revealed by an antibody recognizing methylated cytosines, mirrors the decondensation of the repeats and appears dispersed in the nucleus (Tessadori et al., 2007b). However, dynamics of other repressive marks classically associated with chromocenters such as H3K9me2 or H3K27me1 have not been tested during floral transition. Concomitantly after dedifferentiation in protoplasts, nuclear 5mC signals are redistributed, while Southern blots revealed that DNA methylation at repetitive sequences was globally unaltered. In parallel, no difference in the level of the repressive histone modification H3K9me2 was observed (Tessadori et al., 2007a). Other studies however revealed subtle localized changes in DNA methylation levels at an Athila retrotransposon (Avivi et al., 2004). Whether the transcriptional silencing of heterochromatic sequences is affected during floral transition and dedifferentiation

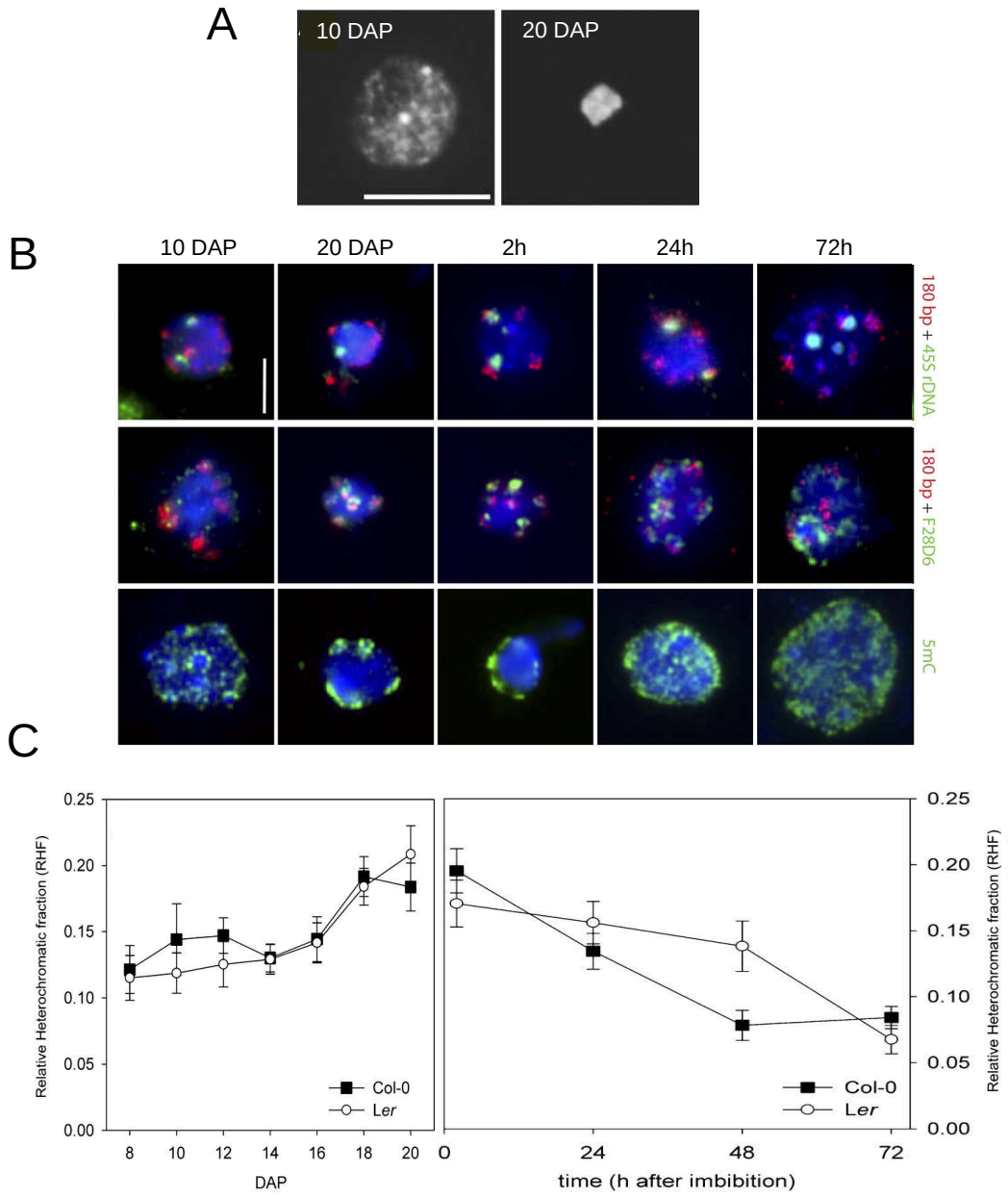

***Figure 12*: Heterochromatin dynamics in embryonic cotyledons during seed development and germination.**

A. Chromatin organization and nuclear size change in embryonic cotyledons during seed maturation. Representative DAPI-stained embryonic cotyledon nuclei at 10 days (left) and 20 days (right) after pollination (DAP). Scale bar: 10 µm (from Van Zanten et al., 2011).
B. Cytogenetic analysis of embryonic cotyledon nuclei during seed maturation, imbibition, and germination reveals large-scale chromatin dynamics. FISH with specific probes of 180 bp repeats (red, top and middle), 45S rDNA repeats (green, top) and a BAC (F28D6) (green, middle) containing pericentromeric repeats, as well as immunodetection of 5mC (green, bottom) during seed maturation (10 and 20 DAP) and germination (2h, 24h, and 72h after imbibition). DNA is counterstained with DAPI (blue). Scale bar: 5 µm (modified from Van Zanten et al., 2011).
C. RHF measured during seed maturation (left), imbibition and germination (right) in Col-0 (black squares) and Ler (white circles) ecotypes. The RHF increases during seed maturation prior to a dramatic decrease at imbibition and germination (from Van Zanten et al., 2011).

has not been widely studied and was limited to Athila (Avivi *et al.*, 2004) and a repetitive transgenic locus (Tessadori et al., 2007b) which do not undergo transcriptional silencing release.

1.3.1.1. Heterochromatin dynamics in cotyledons

In addition to the chromatin dynamics occurring in mature leaf tissues, major changes in heterochromatin organization have also been observed in Arabidopsis cotyledons (Mathieu et al., 2003; Douet et al., 2008; van Zanten et al., 2011). Cotyledons are the first aerial tissues to emerge at germination. They are formed during embryogenesis and then expand after germination, become photosynthetic, and are maintained throughout the vegetative life of the plant (Chandler, 2008).

1.3.1.1.1. Heterochromatin dynamics during seed development

Seed development is initiated at fertilization and can be divided in three phases: a phase of embryogenesis, followed by the maturation of the seed and finally the acquisition of dormancy and desiccation tolerance. As discussed before for other developmental phase transitions, major changes in the transcriptional program associated with chromatin reorganization occur in embryonic cotyledons during seed maturation (van Zanten et al., 2011, 2012). Pollination is the starting point of seed development in a process that requires twenty days in Arabidopsis. The embryo is completely formed at day 8-10 after pollination, and seed maturation occurs afterwards (Van Zanten et al., 2011). Van Zanten and collaborators demonstrated that embryonic cotyledon nuclei at 8 days after pollination exhibit heterochromatin compaction similar to mature leaf nuclei (van Zanten et al., 2010). Chromatin condensates further during seed maturation, and compaction reaches maximum levels in the dry seed. Concomitantly, a reduction in nuclear size was seen but nuclear size and chromatin compaction, since displaying different dynamics were suggested to be independent phenomena (***Figure 12A***). Distribution of centromeric, pericentromeric, and 45S rDNA sequences in cotyledons during seed development were assessed by FISH which revealed clustering of repetitive sequences in

chromocenters in dry seeds (van Zanten et al., 2011) (***Figure 12B***). While 180 bp repeats and 45S rDNA were always found organized into chromocenters, pericentromeric domains cluster progressively through seed maturation. This is associated with changes in the patterns of nuclear 5mC distribution from early to late seed maturation, mirroring the localization of pericentromeric sequences. From dispersion at 8 and 10 days after pollination, pericentromeric repeats and 5mC signals match with chromocenters in dry seeds. To quantify compaction of chromatin into chromocenters, the relative heterochromatin fraction (RHF), which is defined by the area and fluorescence intensities of the chromocenters relative to the area and fluorescence intensity of the entire nucleus (Soppe et al., 2002) was used. While most phase transitions are associated with transient chromatin decondensation, the transition from embryo to dry seed involves increased chromatin compaction (van Zanten et al., 2011), likely because chromatin features in mature seed contribute to maintain chromatin in a transcriptionally inert stage, and to protect the underlying DNA from desiccation (***Figure 12BC***). Indeed, consistently with the negative correlation between chromatin compaction and gene expression (Tessadori et al., 2004; Exner and Hennig, 2008; Fransz and de Jong, 2011), transcription in mature seeds is very low. Upon germination, the nuclear volume increases and heterochromatin expands followed by important changes in the transcriptome (Holdsworth et al., 2008).

1.3.1.1.2. Heterochromatin dynamics during germination and seedling growth

Under favorable environmental conditions, the seed exits dormancy and initiates germination. During seed imbibition and the following germination process, heterochromatin strongly decondenses in embryonic cotyledon nuclei (van Zanten et al., 2011). FISH experiments revealed that centromeric and pericentromeric sequences disperse during the transition from dry seed to seedling, concomitantly with changes in the distribution of 5mC signals on nuclear spreads (van Zanten et al., 2011) (***Figure 12B***). Accordingly, studies from our laboratory showed reduced chromocenters size and the presence of small pre-chromocenters in cotyledon nuclei of Arabidopsis after germination (Mathieu et al., 2003; Douet et al., 2008).

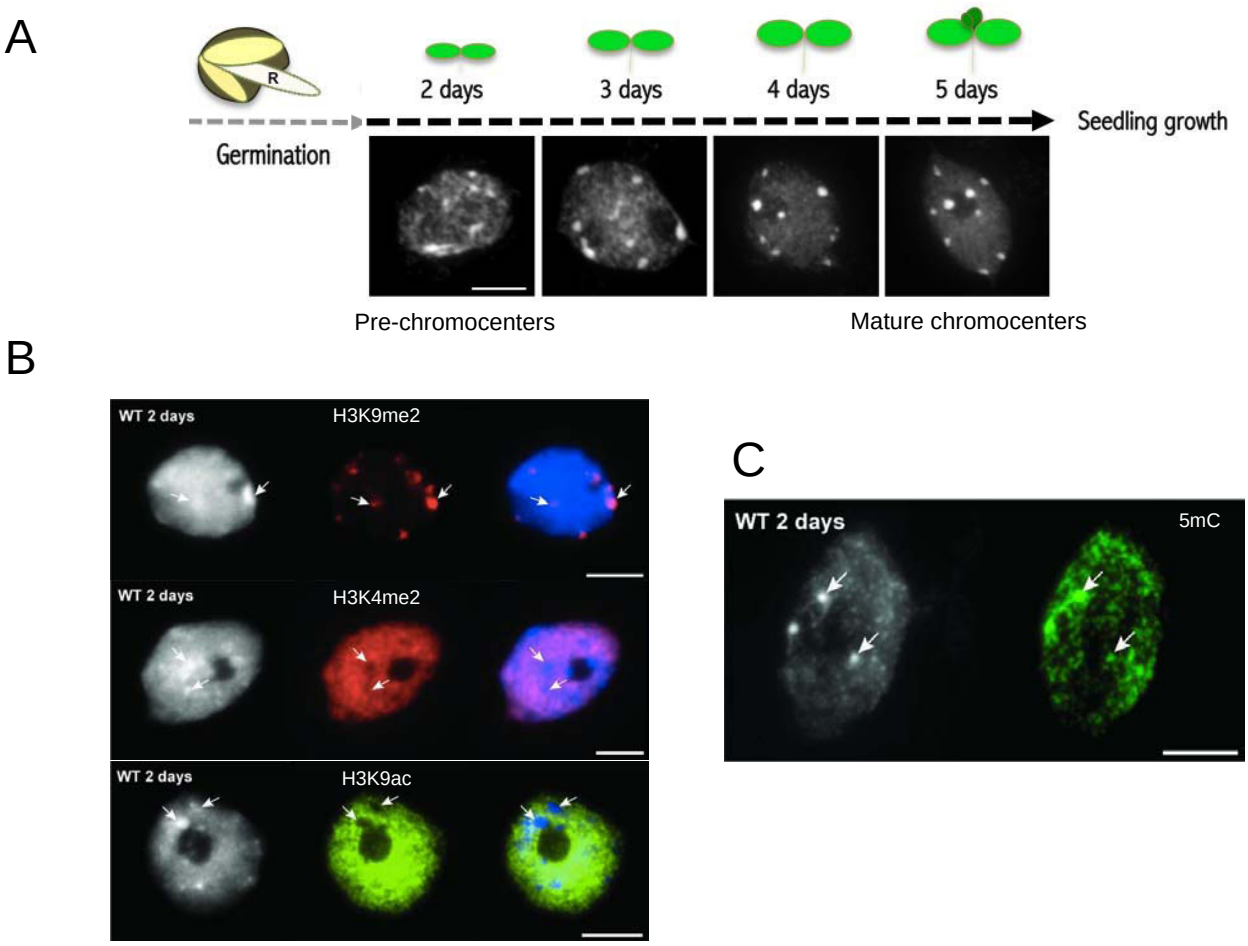

***Figure 13*: Repressive chromatin marks localize to pre-chromocenters.**

A. Chromocenters form progressively between 2 and 5 dag in cotyledons. Representative DAPI-stained nuclei display small pre-chromocenters only in cotyledons at 2 dag. The pre-chromocenters progressively organize through the first days of post-germination development to reach a mature-like chromocenter shape in 5 dag nuclei. Scale bar: 5 µm (modified from Benoit et al., 2013).
B. Immunolocalization of chromatin modifications in cotyledon nuclei at 2 dag. Histone H3K9me2 immunosignals (red, top) localize preferentially to pre-chromocenters, while H3K4me2 (red, middle) and H3K9ac (green, bottom) immunosignals are enriched in euchromatin and excluded from heterochromatin. DNA is counterstained with DAPI (left), immunosignals (middle), and the merge of both (right) are shown. Arrows indicate pre-chromocenters. Scale bars: 5 µm (from Mathieu et al., 2003).
C. Immunolocalization of 5mC in cotyledon nuclei at 2 dag. 5mC signals are dispersed throughout the nucleus, but show enrichment at pre-chromocenters. DAPI staining (left) and immunosignals (right, green) are shown. Arrows indicate pre-chromocenters. Scale bar: 5 µm (from Mathieu et al., 2003).

Consequently, heterochromatin in embryonic cotyledons undergoes decondensation when the dry seed, in which chromatin is highly condensed and nuclear size reduced, initiates germination (***Figure 12C***).

After seed germination, which is associated with heterochromatin decompaction, the cotyledons start to expand and the seedling undergoes the transition from heterotrophic to photoautotrophic growth. During seedling growth a chromocenter organization similar to mature leaf tissues is progressively established: at 2 days after germination (dag) in cotyledon nuclei, poorly-condensed pre-chromocenters that are much smaller than chromocenters of mature leaf nuclei were monitored by DAPI staining (Mathieu et al., 2003; Douet et al., 2008) (***Figure 13A***). Heterochromatin then organizes progressively and mature-shaped chromocenters are detectable at 4 dag in cotyledon nuclei, in a range similar to those observed for mature leaf nuclei (***Figure 13A***). The dynamics of two chromatin marks classically associated with heterochromatin have been tested by immunofluorescence between 2 and 5 dag in cotyledon nuclei (Mathieu et al., 2003) (***Figure 13BC***). Surprisingly, it appeared that both 5mC and H3K9me2 already colocalized at 2 dag pre-chromocenters and remained tightly associated with heterochromatin all along the maturation process while active H3K4me2 and H3K9ac were excluded (***Figure 13BC***). However, beyond cytologically defined condensed heterochromatin structures, little is known concerning local features of centromeric and pericentromeric heterochromatic repeats and how these impact the chromatin fiber folding and ultimately higher-order structures.

During the developmental time window situated between 2 and 5 dag in cotyledon nuclei, the dynamics of a particular repetitive DNA family, the 5S rDNA, has been studied extensively in the laboratory both at the level of chromatin organization and transcription pattern (Mathieu et al., 2003; Douet et al., 2008; Layat et al., 2012a). The 5S rDNA repeat arrays are localized in the pericentromeric regions of chromosome 3, 4 and 5 in the Columbia ecotype and undergo large-scale reorganization between 2 and 5 dag in cotyledon nuclei (Douet et al., 2008). At 2 dag, despite the detection of small pre-chromocenters and dispersion of 45S rDNA repeats (Pontvianne et al., 2010; van Zanten et al., 2011), 5S rDNA loci exhibit precocious condensation and co-localize with the pre-chromocenters (***Figure 14A***). At 3 dag, 5S rDNA arrays undergo sudden decondensation and adopt a mature organization in which part of the 5S rDNA locus forms loop structures (***Figure 14B***).

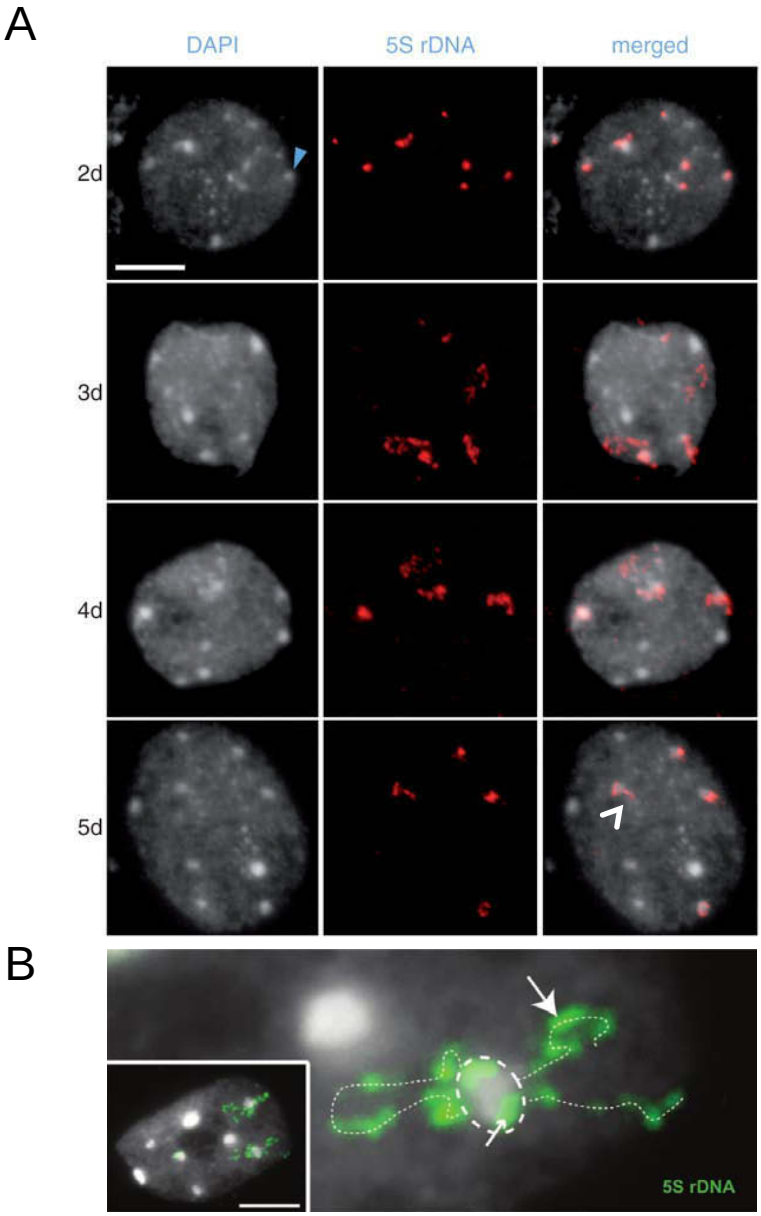

***Figure 14*: 5S rDNA chromatin organization is dynamic during early post-germination development in cotyledons.**

A. FISH labeling of 5S rDNA repeats (red, middle), DAPI staining (left) and merge (right) of cotyledon nuclei at 2 to 5 dag. 5S rDNA decondenses between 2 and 3 dag in cotyledons, prior to subsequent re-condensation and establishment of a mature organization with small 5S rDNA loops. The blue arrow points to a pre-chromocenter. The white arrow shows a 5S rDNA loop. Scale bar: 5 µm (from Douet et al., 2008).

B. 5S rDNA loops (white lines) emanate from a chromocenter (circled) revealed by FISH with a 5S rDNA probe (green) on 3-week-old plants. Inset: whole nuclei with 5S rDNA loops. Fraction of the 5S rDNA probe hybridizes to the chromocenter (small arrow), and the other localizes within euchromatin loops (large arrow). Scale bar: 5 µm (from Mathieu et al., 2003).

These 5SrDNA repeats in the loops are thought to constitute the transcriptionally active fraction, while the repressed ones are considered to remain condensed in the core of the chromocenter (Mathieu et al., 2003; Douet et al., 2008) (***Figure 14B***). Being sequences to be expressed within a silent heterochromatic environment, the 5S rRNA genes are susceptible to present specific epigenetic features in order to preserve efficient transcription during heterochromatin remodeling.

In contrast to the chromatin decondensation during floral transition that seems not to implicate important changes in DNA methylation (Tessadori et al., 2007b), 5S rDNA repeats gain symmetric (CG, CHG) (Mathieu et al., 2003) and loose asymmetric (CHH) DNA methylation. CHH demethylation of 5S rDNA repeats during seedling growth requires the DNA demethylase ROS1 (Douet et al., 2008). ROS1 is also required for 5S rDNA decondensation, suggesting a link between DNA methylation reprogramming and chromatin reorganization of ribosomal arrays in this context.

In addition, the same study (Douet et al., 2008) reported that 5S rDNA chromatin fails to recondense at 4 and 5 dag in mutants of a common subunit of RNA polymerases Pol IV and Pol V. These plant-specific polymerases are involved in RdDM at heterochromatic targets (Herr et al., 2005; Kanno et al., 2005; Pontier et al., 2005; Zhang et al., 2007). These data highlight the importance of a proper setting of chromatin marks for heterochromatin dynamics to achieve proper organization of 5S rRNA genes in Arabidopsis. The important chromatin reorganization observed for the 5S rDNA loci opened the possibility to investigate the link between chromatin dynamics and transcriptional regulation at these developmental stages. The dynamics by which other repetitive sequences acquire a mature organization and to what extend the organization and composition of the chromatin fiber changes during early seedling development has not been addressed to date.

1.3.1.2. Environment-induced heterochromatin dynamics

Plants are sessile organisms, and have therefore to cope with varying environmental conditions such as temperature stress. Adaptation through modification of gene expression patterns permits survival and reproduction and involves changes in chromatin organization and chromatin marks. Recent studies

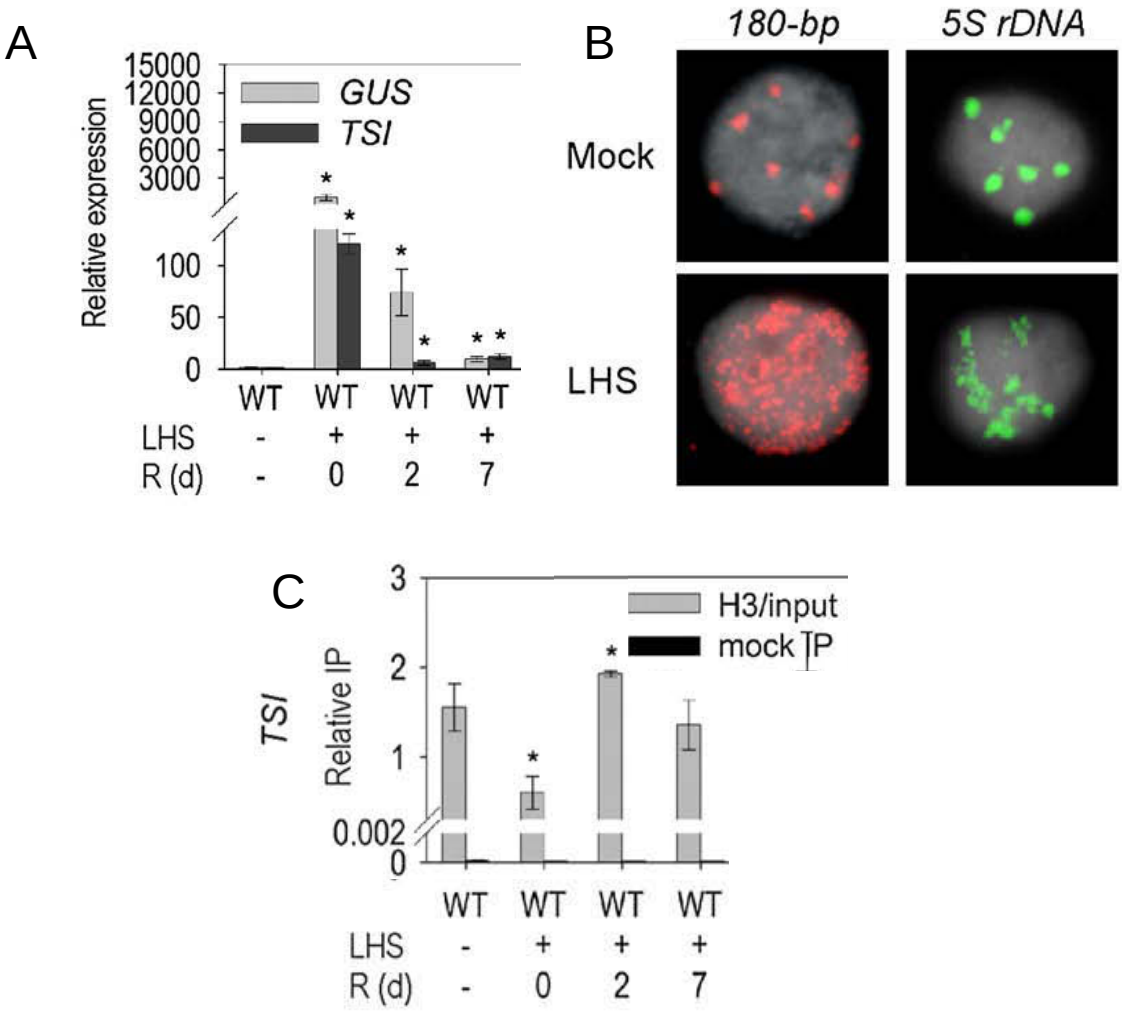

***Figure 15*: Prolonged high temperature stress results in heterochromatin disorganization and release of transcriptional silencing.**

A. Long heat stress (LHS) induces alleviation of transcriptional gene silencing at repetitive sequences, which is progressively reinstalled during recovery at standard growth temperatures. Relative expression of GUS (grey) and TSI (black) assessed by quantitative RT-PCR on 3-week-old plantlets of line L5 after heat stress. LHS = 30 h at 37°C, R(d) = recovery time in days (from Pecinka et al., 2010).
B. FISH staining reveals 180 bp (red, left) and 5S rDNA (green, right) on nuclei isolated from control plants and plants subjected to LHS reveals a loss of heterochromatin compaction induced by LHS (from Pecinka et al., 2010).
C. Nucleosome occupancy is affected upon heat stress. Original levels are resumed within a few days following application of the stress. Relative immunoprecipitation of histone H3 assessed by ChIP (grey) on 3-week-old plantlets after heat stress. Bars corresponding to no-antibody control (mock) are in black (from Pecinka et al., 2010).

have shown that a prolonged high temperature stress results in important changes in the plants' transcriptome including a genome-wide alleviation of silencing of many repetitive elements in pericentromeric and centromeric heterochromatin, including tandem repeat 180 bp satellite sequences, 5S ribosomal DNA arrays, 106B interspersed repeats and transposable elements (Lang-Mladek et al., 2010; Pecinka et al., 2010; Tittel-Elmer et al., 2010; Ito et al., 2011; Barah et al., 2013; Iwasaki and Paszkowski, 2014) (***Figure 15A***). Transcriptional reactivation of silent transgenes also takes place suggesting that the response to heat stress results from changes of local epigenetic features rather than to depend on the DNA sequences of the different elements (Pecinka et al., 2010; Tittel-Elmer et al., 2010). Transcriptional silencing is rapidly re-established upon return to classical growth temperatures (***Figure 15A***). Surprisingly, the heat-induced alleviation of transcriptional silencing is not associated with changes in DNA methylation or H3 methylation levels at K9 and K27, classically linked to silencing (Pecinka et al., 2010; Tittel-Elmer et al., 2010). Senescence, DNA repair, and heat stress signaling are also not involved in this process (Pecinka et al., 2010). Moreover, re-establishment of silencing after heat stress treatments is not altered in Arabidopsis mutants involved in *de novo* DNA methylation or H3K9me deposition (Tittel-Elmer et al., 2010). Many plants impaired in chromatin modifiers, including members of the RdDM pathway, revealed identical levels of transcription induction and similar kinetics of resilencing after heat stress (Kanno et al., 2004; Tittel-Elmer et al., 2010). This suggests that transcriptional reactivation of heterochromatin upon heat stress is independent of major repressive chromatin marks and characterized chromatin modifiers. However, heat stress affects chromocenter organization. FISH analysis of 180 bp and 5S rDNA repeats revealed significant dispersion from chromocenters in interphase nuclei of leaves subjected to heat stress (Lang-Mladek et al., 2010; Pecinka et al., 2010; Tittel-Elmer et al., 2010; Ito et al., 2011; Barah et al., 2013) (***Figure 15B***). These higher-order heterochromatin structure defects are long-lasting since visible for up to one week of recovery and persisting beyond re-establishment of transcriptional silencing. This global modification of heterochromatin correlates with local modifications of the chromatin fiber structure as nucleosome occupancy is strongly altered upon heat stress (Pecinka et al., 2010) (***Figure 15C***). The initial level of nucleosome occupancy is then restored during post-stress recovery. These dynamics of nucleosome occupancy are not restricted to sequences undergoing transcriptional reactivation but

are found genome-wide. Initial observations support an implication of chromatin assembly and disassembly in nucleosomal dynamics. Indeed, there are evidences for a role of chromatin assembly in recovery of transcriptional gene silencing and nucleosome occupancy, but the nature of the histones involved, their source and the exact implication of the different histone deposition machineries remain to be elucidated.

2. Biology of histone H3

Structural and biochemical features of chromatin are influenced by the characteristics of nucleosomes, with increasing evidence accounting for a master role of core histone proteins (Zlatanova et al., 2009). Histones H2A, H2B, H3 and H4 are highly conserved proteins due to their role in structuring the nucleosome core. From an inert single wrapping unit, nucleosomes have emerged nowadays as carrier of epigenetic marks. The emergence of histone variants supports the idea that intrinsic features of the nucleosome contribute to chromatin regulation. Interestingly, variant versions are found for all core histones with the exception of H4 (Talbert and Henikoff, 2010). Most of the time, variant counterparts exhibit few amino acid substitutions, but some histone variants such as macroH2A differ by large protein domains from their canonical counterparts. These changes often have singular consequences on assembly and genomic localization of the histone variant and modify the structural and biochemical features of nucleosomes, and consequently their stability, which may translate in an open or closed chromatin state. For example, histone variant H2A.Z is mainly associated to transcriptionally poised chromatin (Jin et al., 2009; Thakar et al., 2009), while nucleosomes containing macroH2A are most stable and are susceptible to promote a repressive chromatin state (Chakravarthy and Luger, 2006). Moreover, some histone variants are associated with important cellular processes, exemplified by the critical role of the phosphorylated form of H2A.X in DNA repair (Rogakou et al., 1998). From a gene expression point of view, histone-encoding genes can be expressed in a replication-dependent or replication-independent manner, and ubiquitously or in a tissue-specific fashion (Schümperli, 1986). Replication-dependent histones are the predominant group of histones and their expression peak in S phase of the cell cycle, when newly replicated DNA has to

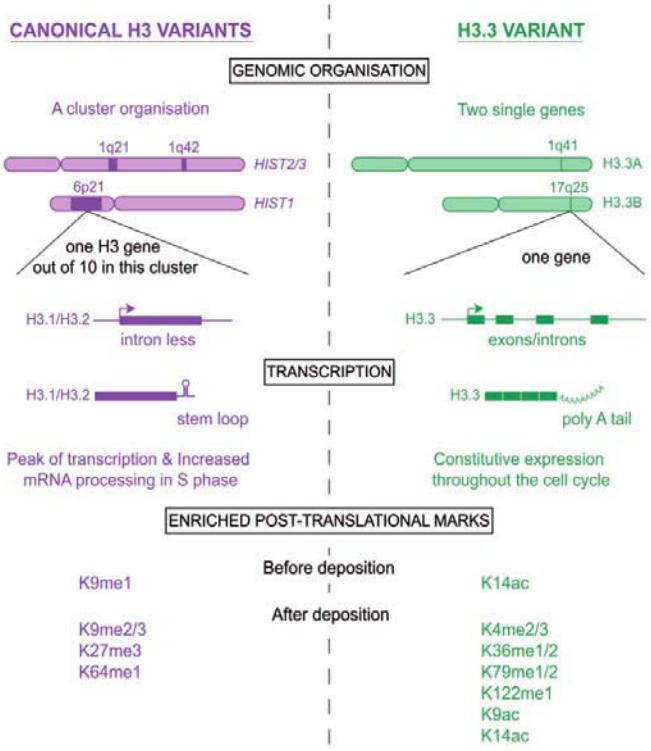

***Figure 16*: Human canonical histone H3.1/H3.2 compared to replacement variant H3.3.**

Comparison of the canonical H3 variants (H3.1 and H3.2) features (purple) with the replacement variant H3.3 (green) in mammals. Canonical histone genes are organized in tandem within gene clusters, lack introns and corresponding transcripts display a stem loop, facilitating transcription and processing in S phase. In contrast, the genes encoding H3.3 are polyadenylated and expressed throughout the cell cycle. H3.1/H3.2 and H3.3 are differentially modified by post-translational marks before and after assembly in chromatin (modified from Szenker et al., 2011).

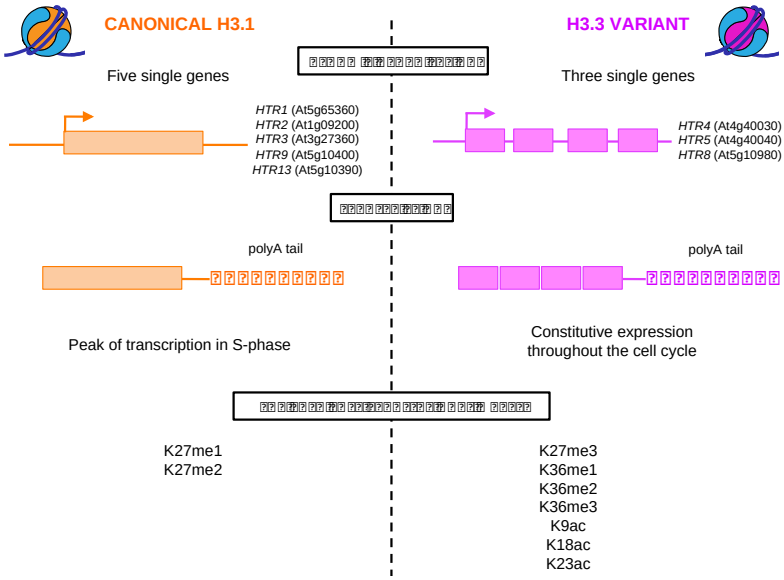

***Figure 17*: Summary of distinct features discriminating the canonical histone H3.1 from the replacement variant H3.3 in *Arabidopsis thaliana*.**

Arabidopsis H3.1 is encoded by five single intron-less genes producing polyadenylated transcripts mainly in S phase (Okada et al., 2005). Arabidopsis H3.3 is encoded by three genes bearing introns and which are constitutively transcribed in polyadenylated transcripts all along the cell cycle. H3.1 and H3.3 are found to carry distinct post-translational marks in chromatin (Johnson et al., 2004).

be organized into chromatin (Franklin and Zweidler, 1977; Ahmad and Henikoff, 2002a; Szenker et al., 2011). These histones (H2A, H2B, H3 and H4) are considered as the canonical histones (Zweidler, 1984). In contrast, the replication-independent histones are not expressed exclusively during S phase, but throughout the cell cycle and are widely defined as replacement histones (Ahmad and Henikoff, 2002b; Elsaesser et al., 2010; Szenker et al., 2011).

When considering histones as carrier of epigenetic and therefore heritable marks, histone H3 can be considered as a central player. Not only the H3-H4 dimers have slow exchange rates compared to H2A-H2B dimers (Zweidler, 1984; Jackson, 1990; Brooks and Jackson, 1994; Kimura and Cook, 2001), but H3 carries an important variety of post-translational modifications and, in contrast to H4, occurs in several variants in eukaryotes as distant as humans, flies or plants. The number of histone H3 genes varies between organisms: yeast encodes three histone H3 genes, Drosophila four genes, *Caenorhabditis elegans* twenty-four genes and mouse fifty-seven genes (Okada et al., 2005; Nakano et al., 2011). In most organisms, the replicative histones H3.1/H3.2 (Ahmad and Henikoff, 2002a; Marzluff et al., 2002; Loyola and Almouzni, 2007; Szenker et al., 2011), the replacement variant H3.3 (Ahmad and Henikoff, 2002b; Loyola and Almouzni, 2007; Szenker et al., 2011), the centromere-specific CENH3 variant (Allshire and Karpen, 2008; Talbert and Henikoff, 2010) and tissue-specific H3 variants can be distinguished.

2.1. Canonical H3.1

2.1.1. Gene organization and expression

Synthesis of the canonical H3.1 is tightly coupled to DNA replication. Indeed, H3.1 expression peaks exclusively in early S phase and is tightly linked to the need to reassemble chromatin at the neo-synthesized DNA following passage of the replication fork (Franklin and Zweidler, 1977; Ahmad and Henikoff, 2002a; Marzluff et al., 2002; Loyola and Almouzni, 2007; Szenker et al., 2011). In mammals and Drosophila, H3.1-encoding genes are intron-less and organized in tandem multicopy clusters (***Figure 16***). Transcription of these H3.1 gene arrays produces non-polyadenylated mRNA with a stem-loop structure (***Figure 16***). The recognition of the

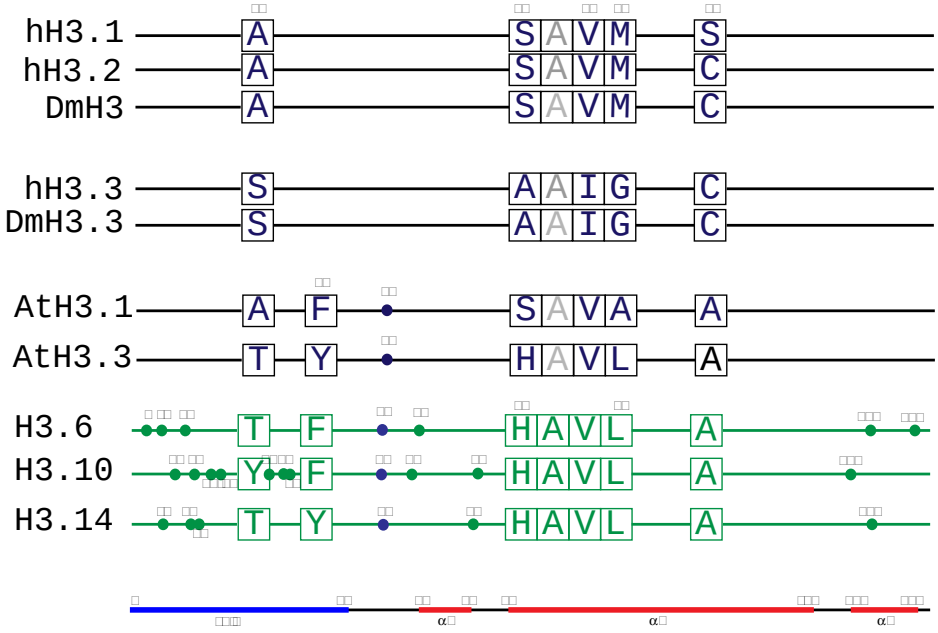

***Figure 18*: Schematic representation of amino acid sequence of canonical and variant histone H3.**

Amino acids in squares differ between the canonical histone H3.1/H3.2 and the replacement H3.3 variant in different species. Amino acids in squares are highlighted to illustrate important differences. Colored dots present amino acid changes in the Arabidopsis (At) sequence compared to the human (h)/Drosophila (Dm) sequence. H3.6, H3.10 and H3.14 are H3.3-like proteins. The tail region as well as α-helices in the globular histone domain is indicated below. While in mammals, amino acid differences between H3.2 and H3.3 are restricted to position 31, 87, 89 and 90, only two amino acid differences concern the globular region (87 and 90) in Arabidopsis, two other localize to the tail region (31 and 41). In addition to the position, distinct amino acid changes distinguish H3.1/H3.2 and H3.3 in animals and plants (adapted from Elsaesser et al., 2010).

stem-loop binding protein together with the U7 small nuclear RNA to the 3' end of the histone mRNA participates in mRNA stability and tightly regulates its translation (Marzluff et al., 2002; Dominski and Marzluff, 2007). Together, these features allow an important production of canonical H3.1 histones at early S phase, ensuring ample supply for chromatin reassembly of the neo-replicated DNA at the replication fork. Canonical H3.1 can also be incorporated in a DNA synthesis-dependent manner at sites of DNA repair after UV lesion and other genome integrity impairment (Polo et al., 2006; Adam et al., 2013).

Bioformatical BLASTX analysis revealed the presence of fifteen histone genes in the Arabidopsis genome (Okada et al., 2005). Five of them show the highly conserved replicative H3.1-encoding sequence: *HTR1* (At5g65360), *HTR2* (At1g09200), *HTR3* (At3g27360), *HTR9* (At5g10400) and *HTR13* (At5g10390) (Okada et al., 2005; Ingouff and Berger, 2010; Ingouff et al., 2010; Talbert et al., 2012). As observed for their animal counterparts Arabidopsis H3.1 genes are intron-less, but are not organized in clusters. Instead, two of them, *HTR9* and *HTR13* are organized in tandem, likely arising from a duplication, while the others are dispersed throughout the genome (Okada et al., 2005) (***Figure 17***). Moreover, H3.1 transcripts are polyadenylated (Wu et al., 1989), and it has been described that induction of H3.1 gene expression occurs mainly at the transcriptional level and is linked to initiation of DNA replication (Reichheld et al., 1995, 1998). In parallel, H3.1 synthesis tightly follows DNA synthesis and is managed at the post-transcriptional and possibly translational level, before rapid degradation of remaining H3.1 transcripts are upon S phase completion (Reichheld et al., 1998).

2.1.2. Protein structure

In term of amino acid sequence, Arabidopsis H3.1 differs from mammalian and Drosophila canonical H3 by four residues at positions 41, 53, 90 and 96 (***Figure 18***). A large-scale expression analysis experiment in Arabidopsis synchronous cell suspensions allowed the monitoring of histone gene expression during cell-cycle progression (Menges et al., 2003). H3.1-encoding genes were found expressed in early S phase. This has been further supported by Affymetrix chip data showing that H3.1 genes are highly expressed in actively dividing tissues (Okada et al., 2005).

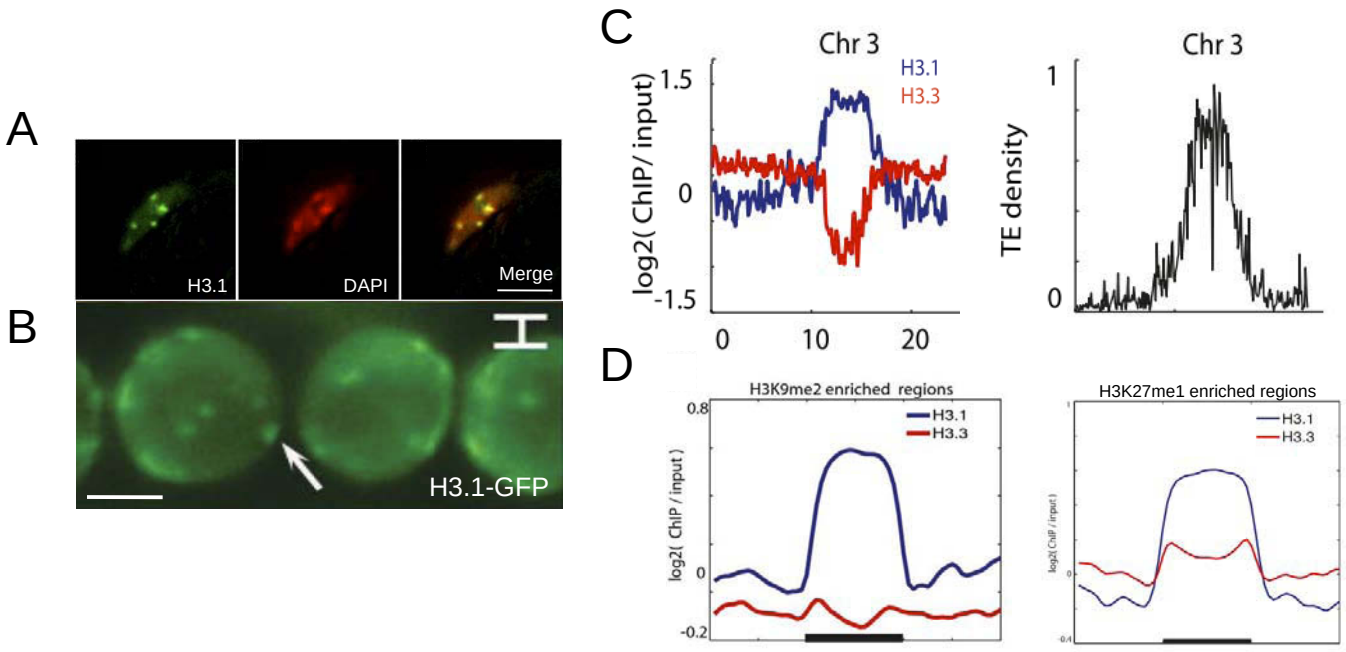

***Figure 19*: Arabidopsis histone H3.1 shows specific localization in the genome.**

A. H3.1 is found genome-wide and particularly enriched at chromocenters. Left: H3.1/HTR1-GFP in a nucleus of a leaf epidermal cell. Middle: DAPI-stained leaf epidermal cell nucleus reveals the position of chromocenters. Right: Merge of both. Scale bar: 10 µm (from Shi et al., 2011).
B. H3.1/HTR2-GFP in a nucleus of a root cell. The white arrow points to a chromocenter. Scale bar: 5 µm (from Ingouff et al., 2010).
C. H3.1 and H3.3 display distinct genomic distribution. Enrichment of H3.1 and H3.3 relative to input genomic DNA at chromosome 3 obtained by ChIP-seq (left). Plot showing transposable element density indicates location of pericentromeric heterochromatin (right). H3.1 occupancy at centromeric and pericentromeric heterochromatin is important in comparison to euchromatic chromosome arms (from Stroud et al., 2012).
D. H3.1 distribution correlates with enrichment in repressive post-translational marks. Distribution of H3.1 and H3.3 over H3K9me2 (left) and H3K27me1 (right) enriched regions (from Stroud et al., 2012).

However the *cis*-acting element OCT motif, participating in proliferation-coupled and S phase-specific gene expression regulation, has been found only in the promoter of *HTR2* and *HTR9* (Meshi et al., 2000). This suggests other regulatory mechanisms such as the lack of introns (Seiler-Tuyns and Paterson, 1986; Okada et al., 2005) may contribute to the expression timing of these genes.

2.1.3. Genomic localization

First evidences for plant H3.1 subnuclear localization in Arabidopsis were obtained by the observation of H3.1 fused to a fluorescent protein (Ingouff et al., 2010). These studies showed that H3.1 is found in the whole chromatin and is enriched in chromocenters (***Figure 19AB***). This is in agreement with incorporation throughout the genome during replication and selective maintenance at silenced areas, including centromeric and pericentromeric heterochromatin. Genome-wide studies gave a more precise view on H3.1 distribution (Stroud et al., 2012; Wollmann et al., 2012; Vaquero-Sedas and Vega-Palas, 2013; Sequeira-Mendes et al., 2014) (***Figure 19C***). Interestingly, the pattern of H3.1 enrichment at genes revealed an anti-correlation between H3.1 occupancy and transcriptional activity. Consistently, H3.1 levels are high over centromeric and pericentromeric transposable elements, suggesting that H3.1 is tightly associated with heterochromatin (***Figure 19C***). This study also stated a positive correlation between H3.1 enrichment and DNA methylation in all sequence contexts. Another evidence for H3.1 association with silent genes was given by the observation that H3K9me2- and H3K27me3-rich regions contain canonical H3.1 (***Figure 19D***). These sites also show globally higher nucleosome occupancy, suggesting that regions enriched in H3.1 tend to display a closed chromatin conformation, densely packed with nucleosomes carrying repressive histone marks, isolating the underlying DNA from the transcriptional machinery and thus setting transcriptional silencing.

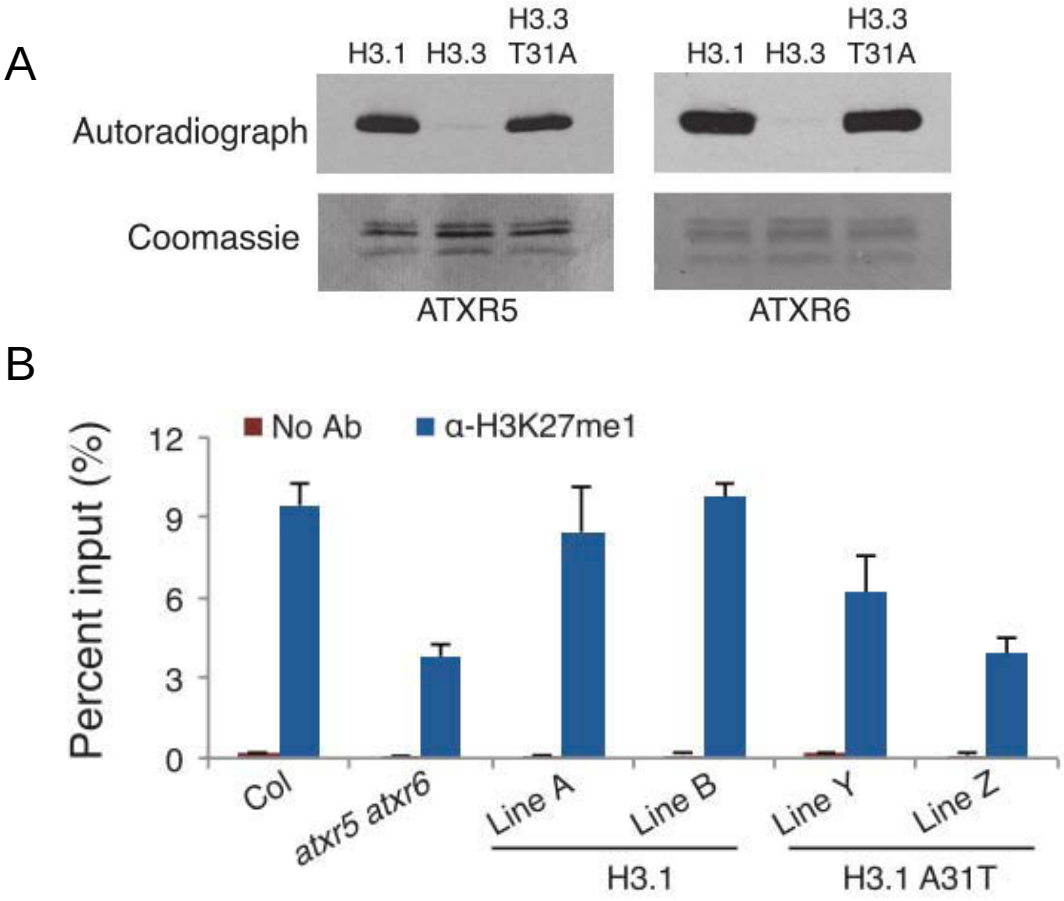

***Figure 20*: H3.1 is preferentially monomethylated at K27 by ATXR5 and ATXR6.**

A. H3.1 monomethylation by ATXR5 and ATXR6 as revealed by *in vitro* histone lysine methyltransferase assays using chromatin containing H3.1, H3.3, or mutagenized H3.3 T31A. A31 of H3.1 is critical for correct H3K27me1 deposition *in vitro* (from Jacob et al., 2014).
B. H3K27me1 enrichment at TSI repeats is reduced *in vivo* in *atxr5 atxr6* double mutants and plants expressing a mutated version of H3.1 (A31T) as revealed by ChIP (from Jacob et al., 2014).

2.1.4. Histone post-translational modifications

Initial analyses of H3 variant enrichment in specific histone post-translational marks were done on *Medicago sativa* total acid-extracted material, mostly consisting of nucleosomal histone content (Waterborg, 1990). This approach, further confirmed by other methods, has shown that H3.1 is widely associated with repressive marks and show relative depletion of active acetylation mark (Waterborg, 1990). This analysis has then been performed in mammals (Benson et al., 2006; Hake and Allis, 2006; Hake et al., 2006; Loyola et al., 2006; Loyola and Almouzni, 2007) (***Figure 16***), Drosophila (McKittrick et al., 2004) and Arabidopsis (Johnson et al., 2004) (***Figure 17***). The first characterization of histone H3 N-terminal modifications in Arabidopsis using mass spectrometry by Johnson and collaborators reported H3.1 depletion in active transcription marks and preferential enrichment in marks associated with transcriptional silencing (Johnson et al., 2004) (***Figure 17***). In this study, around 80% of H3.1 are modified with silencing-related H3K27 methylation marks (60% H3K27me1, 16% H3K27me2 and 5% H3K27me3), associated with null or low level of active marks (H3K9ac, H3K14ac, H3K36me). A similar pattern has also been observed in mammals (Hake et al., 2006; Loyola et al., 2006) (***Figure 16***), Drosophila (McKittrick et al., 2004) and *Medicago sativa* (Waterborg, 1990). Surprisingly, no particular evidence for a preferential methylation of H3.1K9 has been found, suggesting that the H3K9 methyltransferases can act independently of the histone variant type (Jacob et al., 2014). The methyltransferases ATXR5 and ATXR6 have been described as the major H3K27me1 methyltransferases responsible for deposition of this mark in heterochromatin (Jacob et al., 2009, 2010, 2014). By histone lysine methyltransferase assays, Jacob and collaborators showed *in vitro* that the ATXR5 and ATXR6 activities are preferentially directed to H3.1-containing nucleosomes (Jacob et al., 2014) (***Figure 20***). ATXR5 reads the H3.1-specific S31 and any other residue at position 31, such as H3.3 T31, inhibits ATXR5 and ATXR6 activity *in vivo* (***Figure 20***). H3.1-specific activity was not found *in vitro* for other H3K27 methyltransferases, such as Polycomb Repressive Complex 2 (PRC2) complexes MEDEA (MEA) and CURLY LEAF (CLF), which catalyze H3K27me3 (Jacob et al., 2014). In summary, the canonical histone H3.1 is enriched in modifications associated with transcriptional silencing and shows a strong bias towards K27me1 modification by the ATXR5 and ATXR6 methyltransferases.

2.2. Replacement variant H3.3

2.2.1. Gene organization and expression

Replacement histone variant H3.3 was originally identified as a product of histone genes whose synthesis occurs outside of S phase (Zweidler, 1984). Synthesis of the replication-independent variant H3.3 occurs not only in S phase but throughout the cell cycle in contrast to the canonical H3.1 (Ahmad and Henikoff, 2002b; Loyola and Almouzni, 2007; Szenker et al., 2011). In mouse, human and Drosophila, replacement histones H3.3 are encoded by two single genes, *H3.3A* and *H3.3B* (Wellman et al., 1987; López-Fernández et al., 1997) (***Figure 16***). Contrary to their canonical counterparts, they possess introns and are polyadenylated. Both genes encode identical H3.3 proteins, but have distinct untranslated regions (Szenker et al., 2011) (***Figure 16***).

In Arabidopsis, H3.3 is encoded by three genes: *HTR4* (At4g40030), *HTR5* (At4g40040) and *HTR8* (At5g10980) (Okada et al., 2005; Ingouff and Berger, 2010) (***Figure 17***). As observed in other eukaryotes, all Arabidopsis H3.3 genes possess introns (Okada et al., 2005; Ingouff and Berger, 2010) (***Figure 17***). Expression analysis of H3.3 genes in Arabidopsis synchronous cell suspensions suggested that H3.3 gene expression is constitutive throughout the cell cycle and does not peak in S phase in contrast to H3.1 (Menges et al., 2003). The combination of endogenous H3.3 promoters together with introns in the 5' untranslated regions (5' UTR) is critical for driving H3.3 gene expression throughout the cell cycle (Chaubet-Gigot et al., 2001).

2.2.2. Protein structure

Remarkably, the replacement variant H3.3 is one of the most conserved proteins in the eukaryotic kingdom, since H3.3 proteins are thought to be the ancestors of the H3.1 histones (Wells et al., 1987). In mammals and Drosophila, four amino acid substitutions discriminate H3.3 (S31-A87-I89-G90) from H3.1 (A31-S87-V89-M90) (***Figure 18***). Interestingly, residues at positions 87, 89 and 90 are located in the $\alpha 2$ helix of the histone fold domain, which drives arrangement in the

nucleosome core particle. In Drosophila, amino acid substitution S87-V89-M90 from H3.1 towards the A87-I89-G90 residues of H3.3 results in DNA synthesis-independent incorporation of H3.1 (Ahmad and Henikoff, 2002b). This suggests that the nature of amino acids at positions 87, 89 and 90 is responsible for the replication-dependent or independent histone deposition. In Arabidopsis, amino acids at position 31, 41, 87, and 90 discriminate H3.1 from H3.3, but involve a different set of amino acids. H3.3 T31-Y41-H87-L90 differs from H3.1 A31-F41-S87-A90 (***Figure 18***). Comparison of H3.3 and H3.1 protein sequences, including the plant-specific substitution at position 41 of the N-terminal tail (Okada et al., 2005), suggest that H3 variants evolved independently in plants and animals. Amino acid at position 31 and 41 are sufficient to determine the time- and region-specific deposition of the histone variant since H87 is critical for the correct deposition of H3.3 at the transcriptionally active rDNA arrays (Shi et al., 2011). Furthermore, the N-terminal histone tail residues T31 and Y41 are required for H3.3 removal from the rDNA loci when nucleolar transcription stops. In summary, the small number of amino acid changes in H3.3 *versus* H3.1 variants together with their distinct expression patterns is thought to drive their respective dynamics of incorporation into chromatin. Moreover, this may lead to unique local chromatin structures, and ultimately, specific biological functions such as gene transcription or transcriptional silencing.

2.2.3. Genomic localization

H3.3 distribution along the genome has been increasingly studied for the last few years. First analysis using immunofluorescence assays targeting either tag- or fluorophore-H3.3 fusion in Drosophila Kc cells have shown dispersion in euchromatin, no particular enrichment in heterochromatin and high concentration at nucleolar rDNA foci (Ahmad and Henikoff, 2002b). In plants, the use of H3.3-GFP proteins in root nuclei showed no particular enrichment in chromocenters and wide distribution in euchromatin (Ingouff et al., 2010; Shi et al., 2011) (***Figure 21AB***). Chromatin immunoprecipitation together with high-resolution genome mapping has provided a detailed genome-wide localization profile of H3.3 in mammals, Drosophila and Arabidopsis. In both mammals and Drosophila, sites of gene expression are associated with H3.3 enrichment, together with high levels of RNA Polymerase II

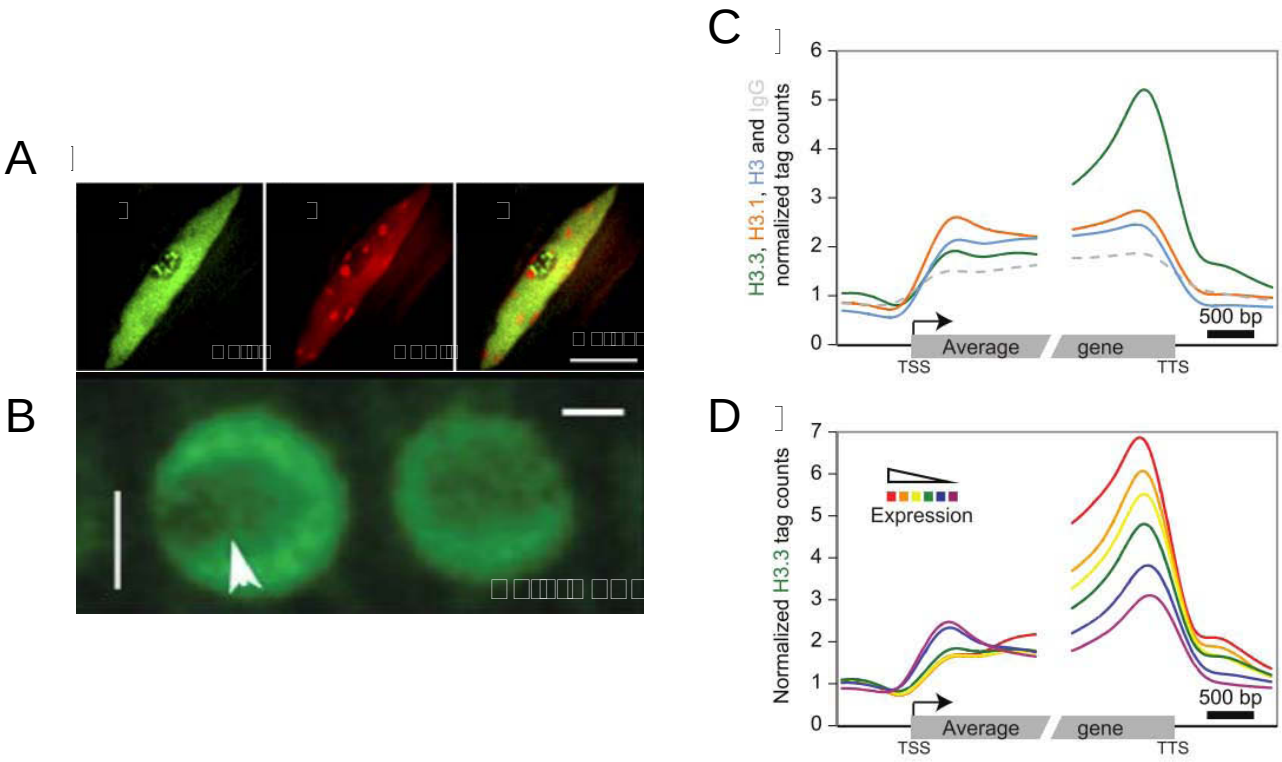

***Figure 21*: Arabidopsis histone H3.3 variant shows specific localization in the genome.**

A. H3.3 is widely found in euchromatin and is not particularly enriched at chromocenters. Left: H3.3/ HTR4-GFP in a nucleus of a leaf epidermal cell. Middle: DAPI-stained leaf epidermal cell nucleus reveals the position of chromocenters. Left: Merge of both. Note the enrichment of H3.3 at the NOR. Scale bar: 10 µm (from Shi et al., 2011).
B. H3.3/HTR5-GFP in a nucleus of a root cell. The arrowhead shows the nucleolus. Scale bar: 5 µm (from Ingouff et al., 2010).
C. H3.3 enrichment is biased towards the 3' end of genes. H3.3 occupancy (green), H3.1 (orange), H3 (blue) and IgG (dashed grey) data obtained by ChIP-seq plotted over gene bodies of Arabidopsis protein-coding genes (from Wollman et al., 2012).
D. H3.3 enrichment over protein-coding genes grouped according to their expression levels reveals positive correlation between expression level and H3.3 enrichment (from Wollman et al., 2012).

(RNAPII). H3.3 is found at transcription start sites (TSS), gene bodies and transcription termination sites (TTS) of genes. In Drosophila, H3.3 is particularly enriched in 5′ of genes (Mito et al., 2005), while H3.3 enrichment was observed in 3′ in mammals and plants (Goldberg et al., 2010; Wollmann et al., 2012; Shu et al., 2014) (***Figure 21C***), suggesting that H3.3 deposition at genes could be intimately linked to chromatin remodeling during transcription. The H3.3 enrichment profile over genes correlates with expression, since H3.3 occupancy in 3' of genes is positively correlated with the level of gene transcription (***Figure 21D***). Nucleosomes containing H3.3 have been described particularly instable compared to nucleosomes with H3.1, thus facilitating removal of nucleosomes and maintenance of an open chromatin during transcription (Henikoff et al., 2004; Jin and Felsenfeld, 2007). Concomitantly, H3.3 nucleosome replacement occurs mostly at transcribed regions of genes and at promoters (Mito et al., 2005; Jin et al., 2009; Ooi et al., 2010). Furthermore, promoters are enriched in H3.3 as well, which might be important for the activity of *cis*-regulatory elements. Interestingly, nucleosomes containing both H3.3 and the histone variant H2A.Z are found at nucleosome-free regions of active promoters and other regulatory regions in the human genome (Jin et al., 2009). H3.3 has also been found to accumulate together with H3.1 at origins of DNA replication in order to maintain high level of nucleosome occupancy at these sites (Deal et al., 2010; MacAlpine et al., 2010; Stroud et al., 2012). This suggests that a certain crosstalk exists between histone variants to establish and maintain specific local chromatin landscapes.

H3.3 incorporation is however not limited to euchromatic regions of the genome since H3.3 has also been detected at transcriptionally inactive genes and pericentromeric heterochromatin in mammals (Szenker et al., 2011; Filipescu et al., 2013). H3.3 localization at telomeres has been described in mouse embryonic cells where it mediates repression of telomeric repeats (Goldberg et al., 2010; Lewis et al., 2010). Accumulation of H3.3 in pericentromeric heterochromatin has been observed in mouse embryos, ES cells and embryonic fibroblasts as well as in human HeLa cells (Hake et al., 2006; Drané et al., 2010; Santenard et al., 2010; Akiyama et al., 2011). During mammalian meiotic sex chromosome inactivation, the transcriptional silencing of the X and Y chromosomes that occurs during the meiotic phase of spermatogenesis, H3.3 accumulates at the silent XY body (Turner, 2007; van der Heijden et al., 2007). Interestingly, Kraushaar and collaborators have analyzed

histone H3.3 turnover at the genome-wide level by studying epitope-tagged H3.3 enrichment at different time points after induction in mammalian cells (Kraushaar et al., 2013). They showed that H3.3 turnover was different depending on the region of the genome. Enhancers, promoters and gene bodies display high rates of H3.3 nucleosome turnover, together with active marks (H3K4me3, H3K9ac and RNAPII enrichment). Heterochromatin is associated with a slow or negligent turnover of H3.3 at telomeres and pericentromeric regions, respectively. This suggests that the genomic context of H3.3 deposition is of high importance and might suggest different biological significance of H3.3 occupancy at these regions. Indeed, rapid turnover of H3.3 at genes suggests a role in initiation and transcriptional elongation, while H3.3 that present a slow turnover within telomeric and centromeric repeats are susceptible to contribute to stabilization of heterochromatin structure, transcriptional silencing and maintenance of genome stability.

Genome-wide distribution of H3.3 is dynamically modified during development in order to respond to stage- or cell-specific chromatin remodeling associated with modification of gene expression patterns (Tagami et al., 2004; Mito et al., 2005; Goldberg et al., 2010; Stroud et al., 2012; Wollmann et al., 2012). In both mice and Drosophila, functional copies of *H3.3A* and *H3.3B* genes are required for fertility (Hödl and Basler, 2009; Sakai et al., 2009; Tang et al., 2013). Heterozygous *H3.3B* male mice display impaired spermiogenesis (Tang et al., 2013). In female mice, H3.3 enrichment is visible in euchromatin during oocyte maturation (Akiyama et al., 2011). Depletion of H3.3 in the Drosophila male germline leads to meiotic chromosome missegregation and defective post-meiotic genome remodeling (Sakai et al., 2009). At fertilization in Drosophila, decondensation of the paternal genome occurs concomitantly with a global deposition of maternal H3.3 replacing protamines before the first round of DNA replication (Loppin et al., 2005; Bonnefoy et al., 2007; Orsi et al., 2009, 2013). In mice, *de novo* heterochromatin formation in the male pronucleus is associated with a transient H3.3 enrichment. H3.3 is found in both euchromatin and heterochromatin until compartmentalization to euchromatin only at late preimplantation stages (Santenard et al., 2010; Akiyama et al., 2011). Interestingly, mutation of H3.3K27 but not H3.1K27 provokes aberrant transcription of pericentromeric repeats and defective chromosome segregation (Santenard et al., 2010). In *Xenopus laevis*, high H3.3 expression is required for correct gastrulation (Szenker et al., 2012; Lim et al., 2013).

The genome-wide analysis of H3.3 localization in Arabidopsis has given new insights in the function of this replacement variant in plants (Stroud et al., 2012; Wollmann et al., 2012; Sequeira-Mendes et al., 2014; Vaquero-Sedas and Vega-Palas, 2013; Shu et al., 2014). H3.3 is positively correlated with gene expression and gene length and thus associated with transcribed genes. Plant H3.3 enrichment is high at the 3' end of genes, peaking immediately upstream of the TTS (Stroud et al., 2012; Wollmann et al., 2012; Shu et al., 2014). Consistent with this observation, H3.3 accumulation is associated with epigenetic marks permissive for transcription such as H3K4me1, CG gene body methylation, ubiquitinated H2B and RNAPII occupancy. Arabidopsis H3.3 levels decreased over the centromere compared to the chromosome arms, and low H3.3 enrichment associates with centromeres and transposable elements compared to H3.1 (Stroud et al., 2012; Wollmann et al., 2012; Vaquero-Sedas and Vega-Palas, 2013; Shu et al., 2014). Meanwhile, telomeres are enriched in H3.3 compared to centromeric regions (Stroud et al., 2012; Wollmann et al., 2012; Vaquero-Sedas and Vega-Palas, 2013). While a general pattern of H3.3 localization emerges, plant and animal H3.3 localization also exhibit differences: H3.3 enrichment at *cis*-regulatory elements and repressed genes is not obvious in plants contrary to mammals and Drosophila. Altogether these data suggest similar trends and convergent evolution of the regulatory functions of H3.3 in plants and animals.

2.2.4. Histone post-translational modifications

Initial analysis of histone post-translational marks associated with H3.3 in *Medicago sativa* showed an initial two-fold enrichment in acetylation compared to H3.1 (Waterborg, 1990). Consistent with its localization in euchromatic regions of the genome, H3.3 is enriched in transcriptionally permissive marks K4 and K36 methylation, and K9, K18 and K23 acetylation in mammals (Benson et al., 2006; Hake and Allis, 2006; Hake et al., 2006; Loyola et al., 2006; Loyola and Almouzni, 2007) (***Figure 16***), Drosophila (McKittrick et al., 2004) and Arabidopsis (Johnson et al., 2004). Consistent with its relative depletion from pericentromeric heterochromatin, a clear anti-correlation between H3.3 and H3K9me2 levels over centromeres has been revealed in Arabidopsis (Stroud et al., 2012; Wollmann et al., 2012). H3.3K27 is poorly mono- or dimethylated in contrast to promoters of genes

enriched in H3K27me3 and submitted to strong developmental regulation by Polycomb group proteins (Shu et al., 2014). Moreover in mammals, the histone post-translational marks already present in non-nucleosomal H3.3 differs significantly from those on non-nucleosomal H3.1. Notably, H3.3 pre-modifications H3K9me2, H3K9ac and H3K14ac suggest the establishment of an open chromatin structure while pre-deposition H3.1 modified by H3K9me1 could be a basis for heterochromatinization by further H3K9me3 synthesis by the histone methyltransferase Suv39h (Loyola et al., 2006) (***Figure 16***).

2.3. H3.3-like

Additional H3 variants have been described in many organisms. They are considered as H3.3-like proteins since they display amino acid substitutions commonly found in variant H3.3 at positions 31, 41, 87 and 90. Their synthesis is independent from the cell cycle phase and most of them are expressed in a tissue-specific and / or developmental stage-specific manner (López-Fernández et al., 1997; Malik and Henikoff, 2003; Tachiwana et al., 2008; Talbert et al., 2012). In Arabidopsis, the H3.3-like variant family is defined as such: absent or degenerated N-terminal region of the protein, H3.3 residues at positions 31, 41, 87, and 90 and absence of introns. High degeneration of protein sequences is associated with pseudogenization in animals (Wellman et al., 1987; Wells et al., 1987) and in Arabidopsis (Okada et al., 2005). Indeed, *HTR7* (At1g75610) lacks a part of the N-terminal region and RT-PCR analysis revealed absence of transcription, as observed for *HTR15* (At5g12910) (Okada et al., 2005). *HTR11* (At5g65350) is expressed following a read-through transcript together with *HTR1* (At5g65360), with coding regions separated by only 273 nucleotides. However, since this transcript bears an intron overlapping from the 3' UTR of *HTR1* to the N-terminal coding region of *HTR11*, the latter is also suspected to produce a non-functional protein.

Based on these features, only Arabidopsis H3.6, H3.10 and H3.14 variants have been classified as histone H3.3-like family members and are likely to be expressed. The H3.10 variant, encoded by *HTR10* (At1g19890) accumulates in sperm cells (Okada et al., 2005; Ingouff et al., 2007, 2010). Its expression is under control of the DUO1 transcription factor which is specific for the sperm cell lineage

(Brownfield et al., 2009). The enrichment of H3.10 has been suggested to contribute to the male gamete-specific gene expression program. H3.10 may also have a role in organizing the highly condensed chromatin structure in sperm cells (Okada et al., 2005). Surprisingly, diminution of H3.10 activity in a T-DNA insertion mutant did not lead to aberrant vegetative growth or altered fertility (Okada et al., 2005). H3.14, encoded by *HTR14* (At1g75600), is expressed only in both the vegetative cell nucleus and the central cell and but not in the mature egg cell (Ingouff et al., 2007, 2010). Expression of *HTR6* (At1g13370) encoding H3.6 has not been detected in vegetative or reproductive tissues but only in cell suspensions where its transcription varies in a cell cycle dependent manner (Menges et al., 2003). However, *HTR6* and *HTR14* gene transcription are concomitantly upregulated in plants lacking the replication-dependent chromatin assembly pathway and upon heat stress. These genes are therefore potentially co-regulated and might have similar roles (Schönrock et al., 2006; Exner et al., 2008; Tittel-Elmer et al., 2010; Probst et al., unpublished results).

2.4. CENH3

CENH3 histone variants are specifically deposited in centromeric chromatin (Yoda et al., 2000; Ahmad and Henikoff, 2002a; Blower et al., 2002). While H3 is one of the most conserved proteins within the eukaryotic proteome, CENH3 is rapidly evolving, displaying high divergence in amino acid sequence and N-terminal tail length between species (Malik and Henikoff, 2001; Cooper and Henikoff, 2004; Talbert et al., 2002). CENP-A was the first centromeric H3 variant identified in humans (Palmer et al., 1987, 1991). Studies of chromatin fibers showed that the building blocks of CENH3-containing nucleosomes are linearly interspersed with H3.1-containing and H3.3-containing domains creating functional centromeres (Sullivan and Karpen, 2004; Dunleavy et al., 2011). CENP-A deposition is cell cycle-regulated and was first thought to take place in G2 phase, supported by the observation that treatment by the DNA replication inhibitor aphidicolin does not block CENP-A assembly. Concomitantly with CENP-A protein levels peaking in late G2 phase (Shelby et al., 1997, 2000), a SNAP tag approach showed that the deposition of new CENP-A at centromeres is restricted to telophase–early G1 phase in

H3 family	*Gene*	ID
H3.1	*HTR1*	At5g65360
	HTR2	At1g09200
	HTR3	At3g27360
	HTR7	At1g75610
	HTR9	At5g10400
	HTR11	At5g65350
	HTR13	At5g10390
H3.3	*HTR4*	At4g40030
	HTR5	At4g40040
	HTR8	At5g10980
H3.3-like	*HTR6*	At1g13370
	HTR10	At1g19890
	HTR14	At1g75600
CenH3	*HTR12*	At1g01370

***Table 1*: H3-encoding genes in Arabidopsis.**

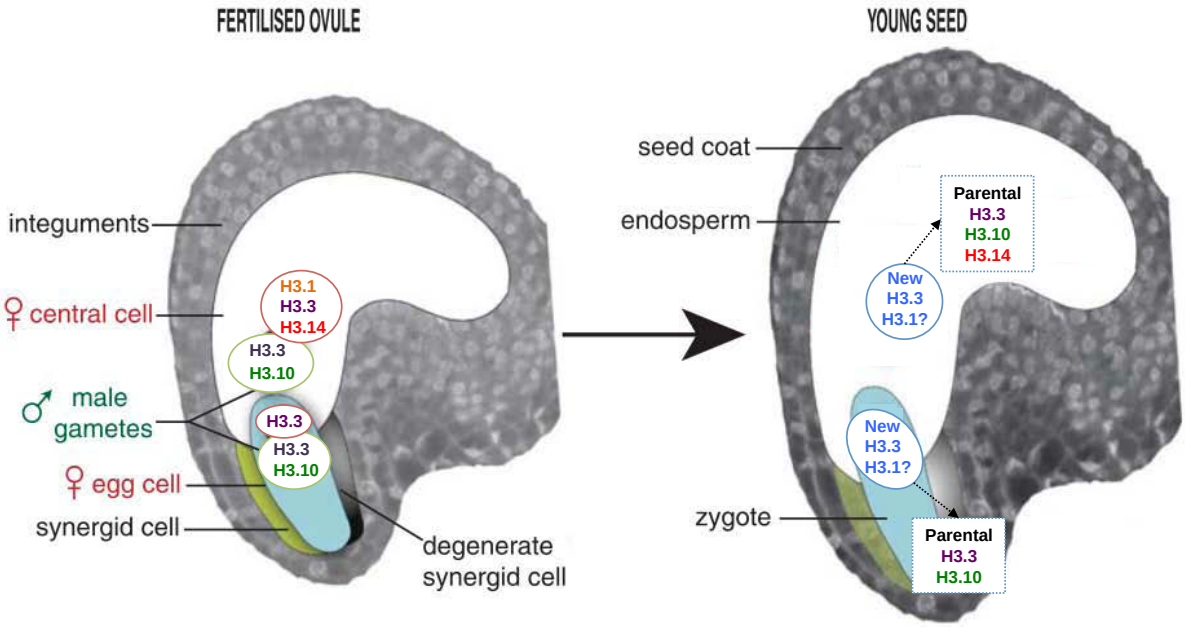

***Figure 22*: Histone H3 variant dynamics at fertilization in Arabidopsis.**

Schematic dynamics of the parental H3 variants at fertilization in Arabidopsis. H3.3 and H3.10 accumulate in the sperm nuclei, while the central cell nucleus contains H3.1, H3.3 and H3.14, and the egg cell nucleus exhibits H3.3. Upon fertilization of the egg cell by a sperm cell, parental H3.3 and H3.10 are rapidly removed from the zygote before the first round of replication and actively replaced by newly synthesized H3.3. The fertilization of the central cell by the second sperm cell initiates endosperm development. Here, parental H3.3, H3.10 and H3.14 are thought to be removed by dilution through DNA replication (modified from Ingouff et al., 2010).

mammalian cells (Jansen et al., 2007). CenH3 has been described in all eukaryotic models (Henikoff et al., 2001; Sullivan et al., 2001). First evidence of a plant centromeric H3 variant arose from works on Arabidopsis and maize (Talbert et al., 2002; Zhong et al., 2002). Arabidopsis CENH3, encoded by the single *HTR12* gene, appears drastically divergent from other H3 variants, in particular in its N-terminal domain. CENH3 localizes at the 180 bp repeats centromeric region and has been identified as a major player in kinetochore establishment and chromosome segregation during mitosis and meiosis (Ingouff et al., 2010).

Arabidopsis H3-encoding genes are listed in ***Table 1***.

2.5. Histone dynamics in Arabidopsis development

In Arabidopsis, H3 dynamics are particularly obvious during gamete formation and fertilization. The male gametophyte is the pollen and consists of three cells: two sperm cells associated to an accessory vegetative cell that delivers the sperm cells to the female gametes. The embryo sac is the female gametophyte that contains the egg cell and the central cell (Rudall, 2006; Rudall and Bateman, 2007). Interestingly, gametophytic nuclei display different chromatin features with particular differences in histone variant content. In the male gametophyte, sperm cell nuclei have compact chromatin compared to the vegetative cell nucleus. The sperm cells present high levels of H3.3 encoded by *HTR5*, as well as the expression of the sperm-specific H3.10 (***Figure 22***). At the same time, H3.1 and CENH3 are not detected (Okada et al., 2005; Ingouff et al., 2007, 2010). In addition, chromatin of the vegetative cell is more relaxed than the sperm nuclei, and presents a different H3 repertoire with the presence of H3.3 encoded by both *HTR5* and *HTR8*, together with H3.14 and enrichment in permissive histone post-translational modifications (Okada et al., 2005; Ingouff et al., 2007, 2010). Histone variant composition between the female gametes appears different as well. The egg cell possesses only the *HTR5*-encoded H3.3, also observed in the sperm cells, *HTR8*-encoded H3.3 being lost during maturation and without any detectable H3.1 proteins despite a few transcripts (Ingouff et al., 2010) (***Figure 22***). The central cell exhibits *HTR8*-encoded H3.3 together with the H3.3-like variant H3.14 and the presence of *HTR3*-encoded H3.1 (***Figure 22***). Based on these

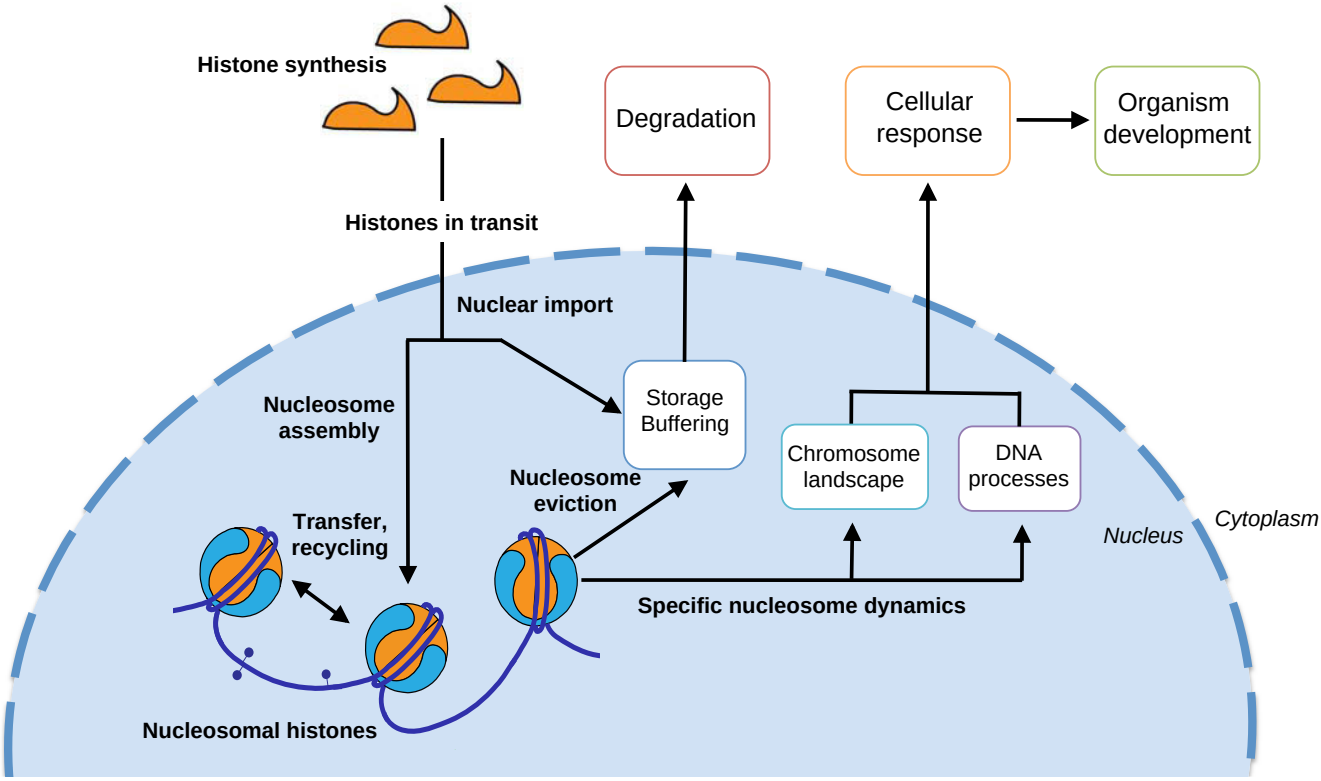

***Figure 23*: Histone chaperones are critical players in histone dynamics and participate in several DNA metabolic processes.**

All along their cellular life, histones are found associated to a network of escorting chaperones controlling their nuclear transport, buffering, recycling, degradation, assembly, and dynamics at chromatin. These processes are fundamental for correct genome activity and cellular functions, affecting ultimately the development of the whole organism (adapted from Gurard-Levin et al., 2014).

observations, the gametes can be distinguished from their respective companion cells based on their H3 variant content.

Double fertilization occurs between sperm cells and female gametes. The fertilized egg develops into the embryo, while the fertilized central cell generates the extra-embryonic nurturing endosperm tissue (Talbert et al., 2002; Zhong et al., 2002). The zygote chromatin is progressively depleted from paternal and maternal H3 variants. At 8 hours after fertilization, *de novo* synthesis of H3.3 and CENH3 occurs, followed by *de novo* synthesis of canonical H3 at the two-cell embryo stage, restoring the somatic H3 variant repertoire (Lermontova et al., 2006; Ingouff et al., 2010; Lermontova et al., 2011; Ravi et al., 2011) (***Figure 22***). This implies that H3 variants are not carrier of transgenerational inheritable information in this process since parental H3 variants are immediately removed upon fertilization. However, some histones could still be retained at specific loci or regulatory regions at levels not detectable with fluorescent protein fusions.

3. Biological significance of histone chaperone networks

The dynamics of H3 variants are finely tuned *in vivo* by a set of histone chaperones, controlling their nuclear transport, storage, recycling, degradation, assembly, and dynamics in chromatin (***Figure 23***). Histone chaperones are defined as escort proteins that associate with soluble histones to control their supply and incorporation into chromatin (De Koning et al., 2007). Histone chaperones contribute to the localization of a dedicated variant to particular sites of the genome.

3.1. Chromatin Assembly Factor-1 (CAF-1)

3.1.1. Composition

CAF-1 (Chromatin Assembly Factor-1) is a heterotrimeric complex found highly conserved in eukaryotes. Termed Chromatin Assembly Complex (CAC) in yeast, it is composed of three subunits (Cac1, Cac2 and Cac3) (Kaufman et al., 1997), while mammalian Chromatin Assembly Factor-1 (CAF-1) is constituted by the

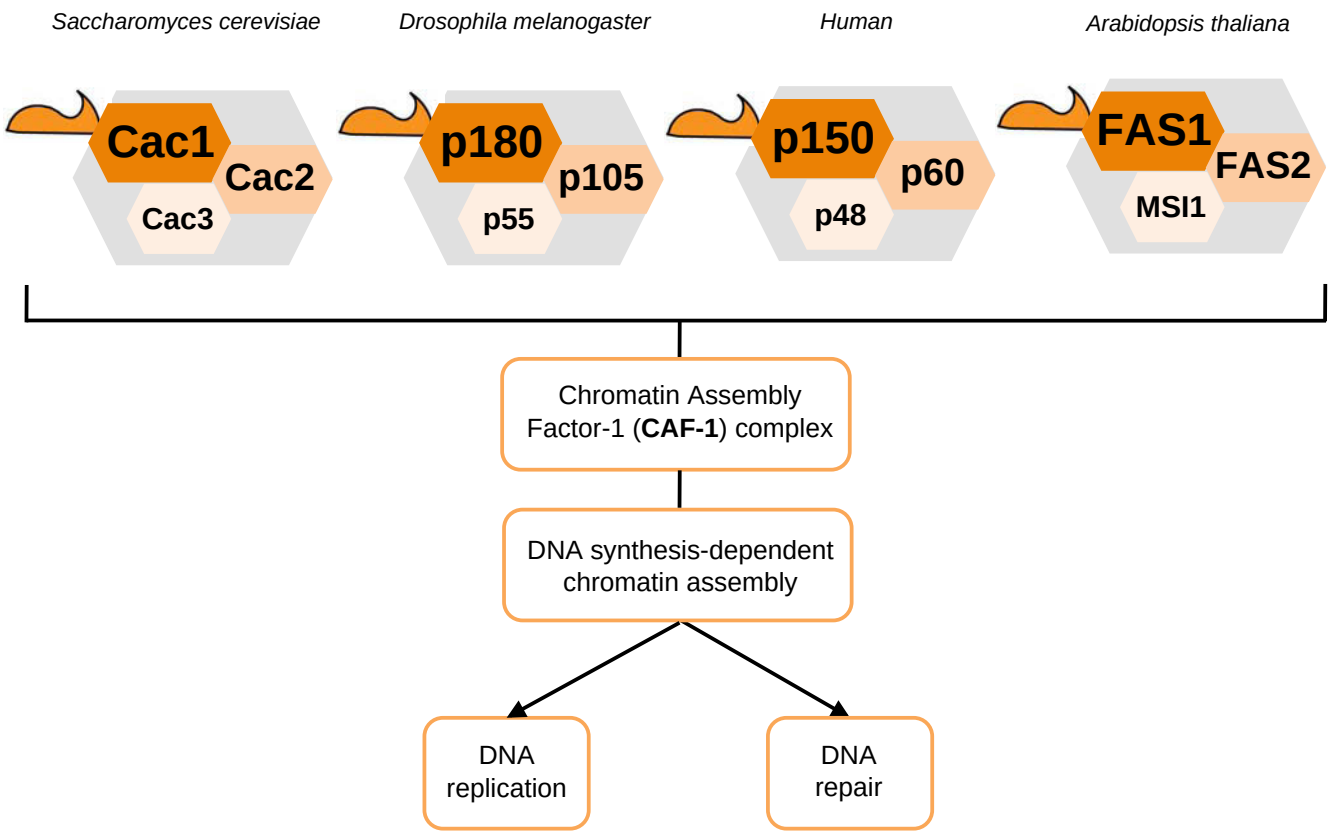

***Figure 24*: Chromatin Assembly Factor-1 chaperone complex.**

CAF-1 (Chromatin Assembly Factor-1) is a heterotrimeric complex found highly conserved in eukaryotes. In *Saccharomyces cerevisiae*, the CAF-1 complex is composed of Chromatin Assembly Complex1 (Cac1), Cac2 and Cac3, which are the large, middle and small subunit respectively. The Drosophila CAF-1 complex comprises the p180, p105 and p55 subunits. The human CAF-1 complex consists of the large p150, middle p60 and small p48 subunits. Finally, the Arabidopsis CAF-1 complex is composed of FASCIATA1 (FAS1), FASCIATA2 (FAS2) and MULTICOPY SUPRESSOR OF IRA1 (MSI1) subunits. CAF-1 function involves DNA synthesis-dependent chromatin assembly during DNA replication and repair.

p150, p60 and p48 subunits (Stillman and Smith, 1989; Kaufman et al., 1995; Verreault et al., 1996). Arabidopsis orthologs of the large p150, middle p60 and small p48 subunits are termed FASCIATA1 (FAS1), FASCIATA2 (FAS2) and MULTICOPY SUPPRESSOR OF IRA1 (MSI1), respectively (Leyser and Furner, 1992; Kaya et al., 2001; Hennig, 2003) (***Figure 24***).

Direct interaction between human CAF-1 and histone H3-H4 dimers is mediated by the acidic domain of the large p150 subunit (Kaufman et al., 1995; Ramirez-Parra and Gutierrez, 2007b). The p150 subunit also mediates association with PCNA at the replication fork, targeting CAF-1 to replication- and repair-coupled chromatin assembly sites (Ridgway and Almouzni, 2000). Both the middle subunit (p60/Cac2/FAS2) and the small subunit (p48/Cac3/MSI1) bear WD40 repeats mediating protein-protein interactions, notably with histone deacetylases (Martínez-Balbás et al., 1998; Vermaak et al., 1999). The smallest subunit also participates in other complexes and interacts with other cell cycle-regulating proteins such as Retinoblastoma (Qian and Lee, 1995; Nicolas et al., 2001; Ausín et al., 2004) and E2F components (Gutierrez, 2005), with Polycomb group proteins (Czermin et al., 2002; Kuzmichev et al., 2002; Köhler et al., 2003) and components of the flowering time control pathway in Arabidopsis (Bouveret et al., 2006).

In Arabidopsis, transcription of the large subunit-encoding gene *FAS1* is cell cycle regulated. Coherent with a role of CAF-1 in chromatin assembly during DNA replication, *FAS1* expression peaks in S phase (Kaya et al., 2001). Sequence analysis of the promoter region of *FAS1*, but also of *FAS2* and *MSI*, showed presence of binding sites for the E2F transcription factors. Binding of E2F proteins to the promoter as been shown *in vitro* and *in vivo* by electrophoretic mobility shift assays and ChIP respectively (Ramirez-Parra and Gutierrez, 2007a, 2007b). Overexpression of E2F increases *FAS1* transcription while overexpressing the E2F repressor causes decrease in *FAS1* expression, suggesting that E2F is a key regulator of *FAS1* transcription. Expression patterns of *FAS1* have been assessed using a reporter construct expressing the β-glucuronidase gene under the control of the *FAS1* promoter and revealing a correlation between *FAS1* expression and highly proliferative tissues (Ramirez-Parra and Gutierrez, 2007a). However, available microarray data from synchronized cell cultures suggested that neither *FAS2* nor *MSI1* expression peak during S phase despite presence of E2F binding sites within their promoter regions (Menges et al., 2003). This view has recently been challenged

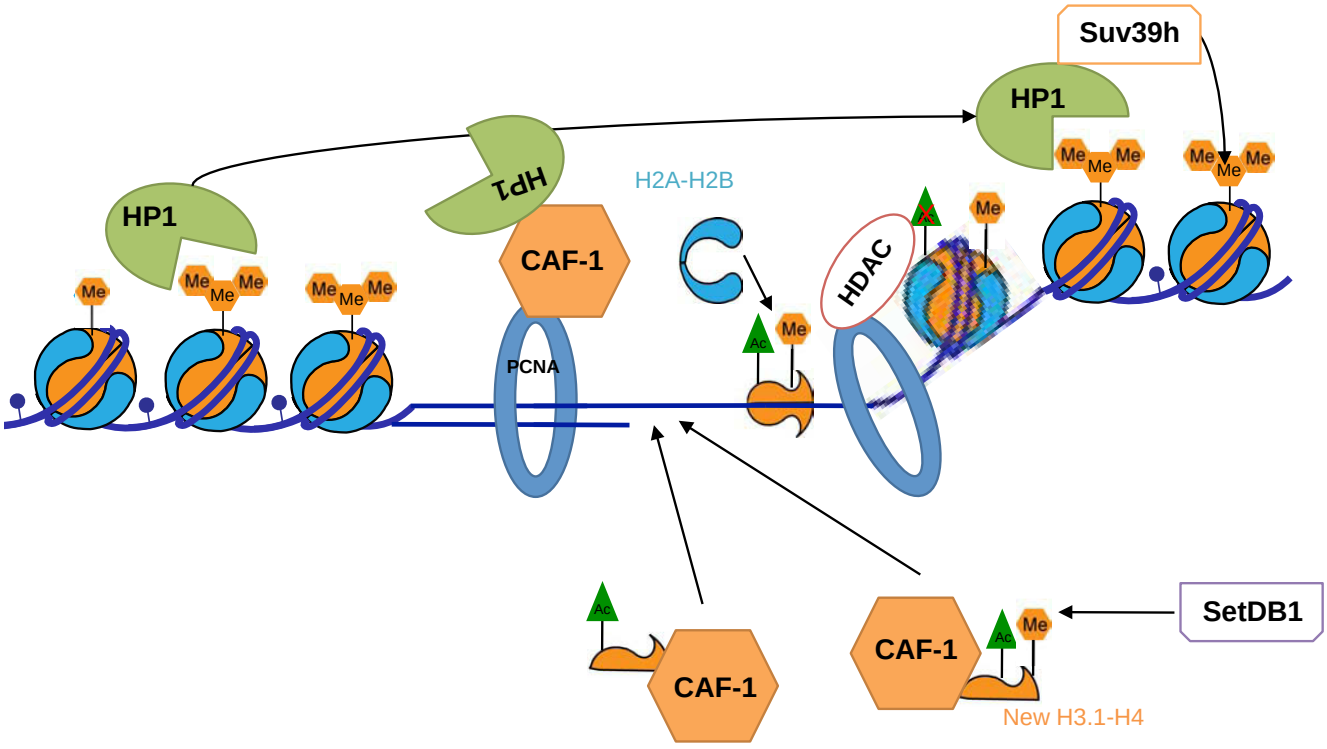

***Figure 25*: Interaction between CAF-1 and the replication machinery tightly links DNA replication and maintenance of chromatin states.**

CAF-1 is recruited *via* PCNA to the replication fork where it participates actively in the maintenance of chromatin states and nucleosome assembly. Histones H3 in the CAF-1 complex can be monomethylated at position K9 by SetDB1 prior to deposition (Loyola et al., 2009). CAF-1 is also involved in the transfer of HP1 ahead of the replication fork to newly assembled chromatin (Quivy et al., 2008). HP1 further helps recruitment of the Suv39h methyltransferase for subsequent H3K9me3 methylation of new monomethylated H3 deposited by CAF-1 (adapted from Almouzni et al., 2011).

by mRNA sequencing data (www.cyclebase.org) (Gauthier et al., 2010; Wollmann et al., 2012) showing that *FAS2* transcription is higher in dividing *versus* non-dividing tissues.

3.1.2. Functions

DNA replication in eukaryotes necessitates coordinated nucleosome disassembly and subsequent re-packaging of the newly synthesized strand in nucleosomes. CAF-1 is the master player in replication-coupled nucleosome assembly and its activity has been shown in a wide variety of organisms, including mammals, Drosophila, Xenopus, yeast and *Arabidopsis thaliana* (***Figure 24***). First evidences for such a role has been provided *in vitro* by Smith and collaborators, showing that CAF-1 mediates assembly of nucleosomes through deposition of H3-H4 onto newly newly-replicated DNA in human cell extracts (Stillman and Smith, 1989; Shibahara and Stillman, 1999). *In vivo*, CAF-1 deposits H3-H4 preferentially onto replicating DNA. Consistently, CAF-1 is localized at replication foci during S phase and is also found at DNA damage-associated PCNA foci (Gaillard et al., 1996). Interaction between CAF-1 and the replication machinery tightly links DNA replication and chromatin assembly events, presenting CAF-1 as a DNA replication-dependent histone chaperone (***Figure 25***). Human CAF-1 is found in a high specificity complex with the replicative H3.1 and H4 (Tagami et al., 2004). In sharp contrast, CAF-1 is not found associated with the replacement histone variant H3.3.

Furthermore, CAF-1 displays interactions with many chromatin-interacting proteins such as HP1 (Murzina et al., 1999; Quivy et al., 2004), the H3K9-specific histone methyltransferase SetDB1, and the small H3-H4 histone chaperone Anti-Silencing Function 1 (ASF1) (Mello et al., 2002; Tamburini et al., 2006) (***Figure 25***). At the replication fork, CAF-1 participates in the propagation of H3K9 methylation by interacting with SetDB1 to facilitate K9 methylation of new H3 prior to deposition onto newly synthesized DNA (Reese et al., 2003; Sarraf and Stancheva, 2004). Moreover, CAF-1 participates in HP1 dynamics by removing HP1 upon replication fork progression and replacing it back afterwards (Murzina et al., 1999; Quivy et al., 2008) (***Figure 25***). This suggests that CAF-1 is actively involved in maintenance and establishment of chromatin features at the replication fork.

In addition to its role in chromatin assembly at the replication fork, CAF-1 nucleosome assembly activity has also been studied in the context of DNA repair. *In vitro* experiments demonstrated that epitope-tagged H3.1 are actively loaded by CAF-1 onto DNA after UV damage (Polo et al., 2006). In human cells, CAF-1-dependent nucleosome assembly using newly synthesized tagged-H3.1 has been described *in vivo* at sites of DSB and UV-induced damage (Polo et al., 2006). CAF-1 is targeted to the sites of DNA damage through its interaction with PCNA, establishing a molecular link between DNA synthesis and chromatin assembly in both replication and repair processes (Martini et al., 1998; Moggs et al., 2000; Green and Almouzni, 2003). This highlights the fact that CAF-1-mediated H3.1 deposition, which is mainly restricted to S phase, can also be found outside of S phase and is critical for restoration of chromatin integrity after DNA repair.

Loss of the CAF-1 complex results in a wide variety of consequences in eukaryotes. Knockdown of CAF-1 in human cell cultures leads to slower DNA replication and accumulation of cells in early and mid S phase due to checkpoint activation (Krude, 1999; Hoek and Stillman, 2003; Ye et al., 2003; Nabatiyan and Krude, 2004; Sanematsu et al., 2006). In mice, embryos lacking the large p150 subunit of CAF-1 arrest development at the 16-cell stage with severe alterations in heterochromatin organization (Houlard et al., 2006). Moreover, knockdown of p150 promotes aberrant heterochromatin formation and H3 variant distribution after fertilization (Akiyama et al., 2011). In Xenopus, expression of a dominant negative form of CAF-1 provokes developmental arrest before gastrulation (Quivy et al., 2001), and downregulation of p150 alters gastrulation at a later stage (Szenker et al., 2012). Concomitantly, Drosophila CAF-1 mutants die during larval stages (Klapholz et al., 2009). In yeast, CAC mutants display chromosomal rearrangements (Myung et al., 2003) and aberrant chromatin assembly (Adkins and Tyler, 2004). This is translated by an alleviation of transcriptional silencing at mating-type loci (Osley and Lycan, 1987; Enomoto and Berman, 1998; Kaufman et al., 1998) and telomeres (Monson et al., 1997) together with increased UV sensitivity (Kaufman et al., 1995). In *Caenorhabditis elegans*, CAF-1-dependent chromatin assembly is required for normal neuronal bilateral asymmetry (Nakano et al., 2011).

In contrast to Drosophila and mammals, Arabidopsis mutants lacking either the FAS1 or the FAS2 subunit are viable, despite pleiotropic morphological defects, aberrant meristem organization, phyllotaxy, leaf structure and trichome branching

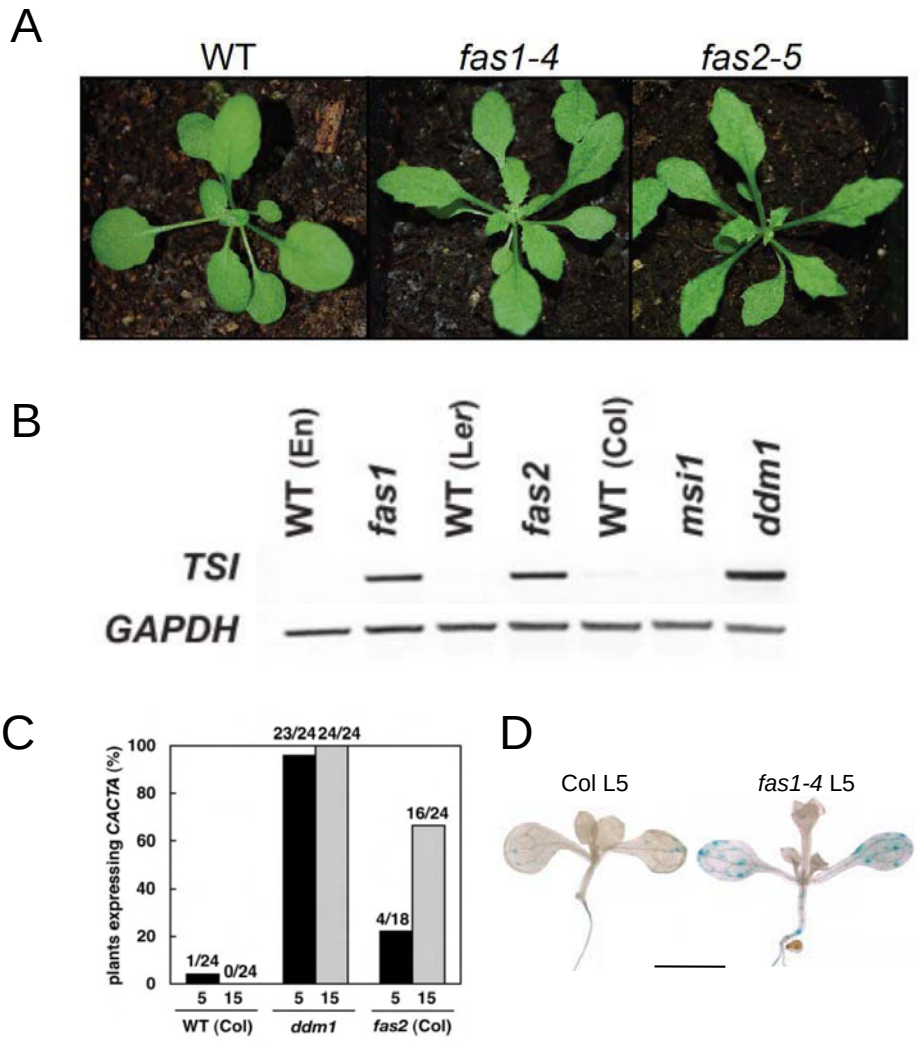

***Figure 26*: Effects of loss of CAF-1 on plant development and maintenance of heterochromatin silencing.**

A. Representative 25-day-old plantlets of WT, *fas1-4* and *fas2-5* mutants grown on soil (from Duc, Benoit et al., submitted).
B. Transcriptional silencing of TSI pericentromeric repeats is alleviated in *fas* mutants. RT-PCR detection of TSI transcripts in WT, *fas1, fas2* and *ddm1* (from Schönrock et al., 2006). *ddm1* is a well described mutant impaired in transcriptional gene silencing of repetitive sequences (Probst et al., 2003).
C. Transcriptional silencing of the CACTA transposon is alleviated in *fas* mutants. The percentage of plants showing CACTA transcripts in either 5-day-old (black) or 15-day-old (grey) WT, *ddm1 and fas2* seedlings are plotted (from Ono et al., 2006).
D. Release of repression of the transcriptionally silent GUS locus in *fas1* mutants. Fourteen-day-old WT (left) and *fas1-4* (right) plants carrying the GUS locus from the L5 line. Blue staining on the tissue reveals transcriptional silencing release of the GUS transgene. Scale bar: 5 mm (Bassler and Benoit, unpublished results).

(Kaya et al., 2001; Endo et al., 2006; Exner et al., 2006; Kirik et al., 2006; Schönrock et al., 2006; Exner et al., 2008) (***Figure 26A***). Defects in meristem identity in *fas* mutants were the first clue arguing for a role of CAF-1 in maintenance of correct genome activity in plants. Consistent with a role in DNA replication-dependent chromatin assembly, many studies addressed the role of CAF-1 in maintenance of transcriptional gene silencing and chromatin structure (Takeda et al., 2004; Exner et al., 2006; Ono et al., 2006; Schönrock et al., 2006). *fas1* and *fas2* mutants show weak alleviation of transcriptional silencing of endogenous repeats such as TSI together with the reactivation of some transposable elements and of a GUS transgene subjected to silencing (Ono et al., 2006; Schönrock et al., 2006) (***Figure 26BCD***).

Cytological analysis of *fas1* and *fas2* mutant nuclei revealed a decrease in heterochromatin fraction (Schönrock et al., 2006) (***Figure 27A***). Concomitantly, DNase I hypersensitivity of chromatin from mature *fas1* leaf nuclei indicates a lower nucleosome density and a global decondensation of chromatin in CAF-1 mutants (Kirik et al., 2006). H3-ChIP experiments (Pecinka et al., 2010) further indicated a role for CAF-1 in establishing and maintaining correct nucleosome occupancy in mature tissues. While *fas1* mutants display a mildly reduced nucleosomal enrichment at steady state, resilencing and histone deposition at activated elements in response to heat stress is delayed in comparison to the wild type. Nucleosome occupancy further decreases in this mutant upon heat stress, and the initial level is not recovered efficiently even 7 days after treatment. This suggests that CAF-1-dependent histone reloading is important for efficient establishment and further restoration of nucleosomal density and silencing in heterochromatin after heat stress (Pecinka et al., 2010).

MSI1 mutations are lethal since this subunit is involved in other chromatin modifying complexes. However nuclei of plants with reduced MSI1 levels also show a lower heterochromatin amount and an impaired recruitment of repetitive DNA sequences to chromocenters (Hennig, 2003). Surprisingly, DNA methylation levels of the repetitive sequences undergoing transcriptional reactivation and relocalization remain largely unaffected in CAF-1 mutants. In parallel, the heterochromatic histone mark H3K9me2 remains globally enriched at chromocenters of *fas1* nuclei (Kirik et al., 2006; Ono et al., 2006; Schönrock et al., 2006) (***Figure 27B***). These observations argue strongly for a role of CAF-1 in heterochromatin formation, but highlight as well

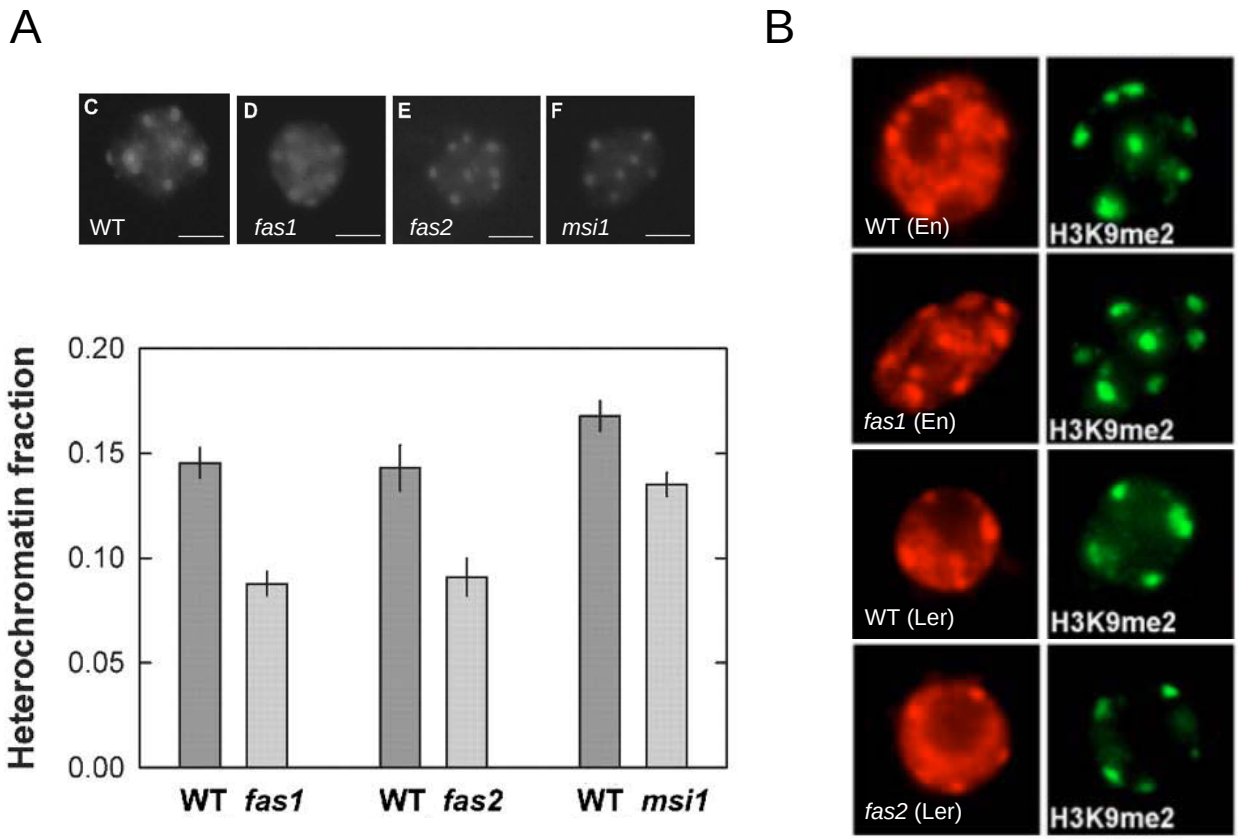

***Figure 27*: CAF-1 is required for heterochromatin compaction.**

A. CAF-1 mutants display a reduced heterochromatin fraction. Representative DAPI-stained nuclei of either *fas1-1* (En), *fas2-1* (Ler) or *msi1-as* (Col) (top) and their corresponding WT. Scale bars: 5 µm. The heterochromatin fraction in nuclei was quantified from DAPI-stained nuclear spreads (bottom) (from Schönrock et al., 2006).
B. H3K9me2 remains globally unaffected at chromocenters in CAF-1 mutants. Immunosignals of H3K9me2 (green, right) reveal enrichment in chromocenters in WT, *fas1* and *fas2* mutants. DNA is counterstained with DAPI (red, left) (adapted from Schönrock et al., 2006).

the complex molecular link between transcriptional silencing mechanisms and heterochromatin organization in the nucleus.

Endoreplication is a particular process in which the genome undergoes sequential rounds of DNA replication without a subsequent mitosis step, thus increasing nuclear DNA content. This phenomenon is of particular importance in plant cell differentiation and organogenesis since endoreplication favors cell expansion, cell differentiation and metabolic activity (Kondorosi et al., 2000; Edgar and Orr-Weaver, 2001; Larkins et al., 2001). Being a master regulator of DNA synthesis-coupled chromatin assembly, lack of CAF-1 may cause DNA damage and genome instability, stopping cell proliferation and ultimately leading to a premature switch to endoreplication which translates in shorter hypocotyls (Exner et al., 2006), reduction in leaf epidermal cell numbers, and increased cell size (Exner et al., 2006; Ramirez-Parra and Gutierrez, 2007a). Furthermore, plants lacking CAF-1 display hypersensitivity to DNA damage. *fas1* mutant plants show a basal increase in DNA double-strand break levels and higher somatic homologous recombination frequency (Endo et al., 2006; Kirik et al., 2006). This leads to the activation of the G2 DNA damage checkpoint, susceptible to promote endoreplication. Together, these observations argue for genome instability in plants lacking CAF-1, as a direct consequence of impaired chromatin assembly.

3.2. Histone Regulator (HIR) complex

3.2.1. Composition

The Histone Regulator (HIR) multimeric complex was first identified in the budding yeast *Saccharomyces cerevisiae* where it consists of the four subunits Hir1, Hir2, Hir3 and Hpc2, and functions as repressor of histone gene expression outside S phase (Osley and Lycan, 1987) (***Figure 28***). The importance of HIR is evident by its evolutionary conservation, and it has been described in diverse organisms. The ortholog of Hir1 and Hir2 is HIRA in Drosophila and mammals (***Figure 28***). In humans, UBINUCLEIN1 (UBN1) and the hypothetical protein FLJ25778 (also termed UBINUCLEIN2) are the orthologs of yeast Hpc2 (***Figure 28***). UBINUCLEIN1 is a ubiquitously expressed nuclear protein that binds to various transcription factors,

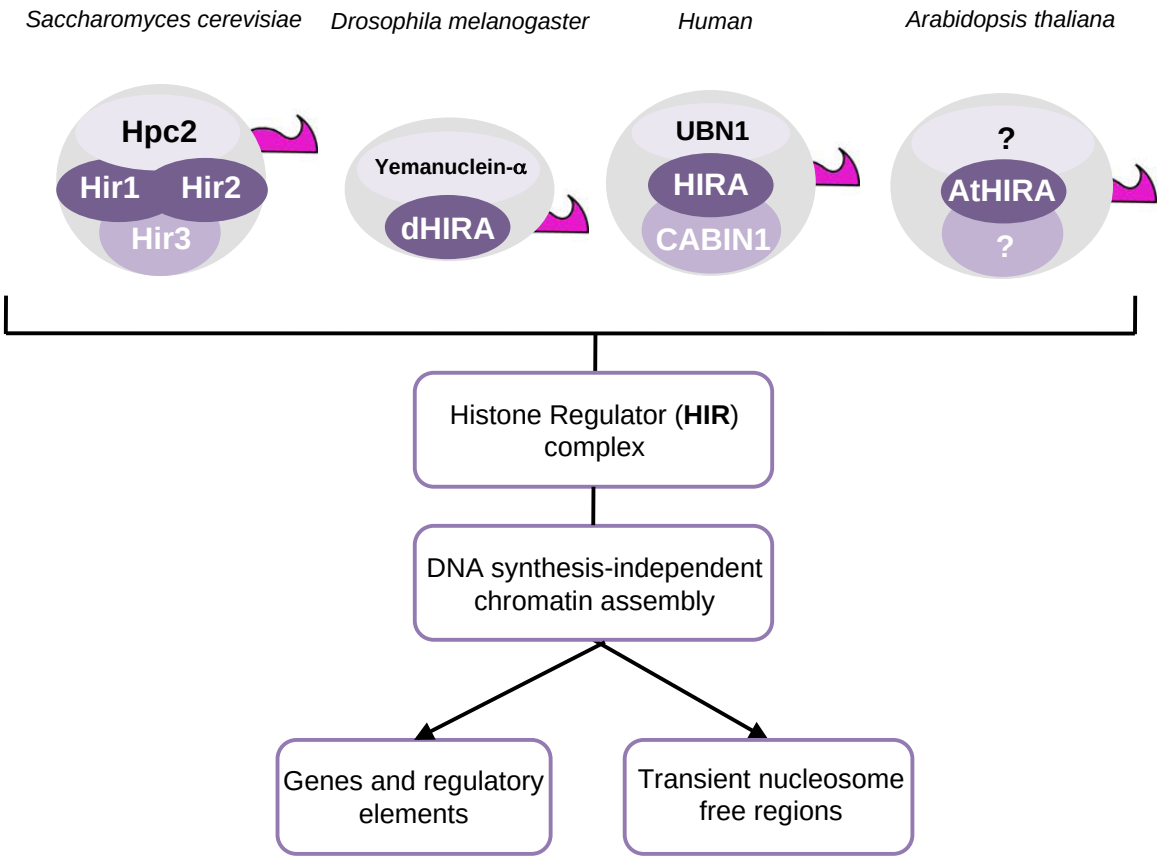

***Figure 28*: Histone Regulator chaperone complex.**

HIR (Histone Regulator) chaperone is a multimeric complex first characterized in *Saccharomyces cerevisiae* where it consists of four subunits Hir1, Hir2, Hir3 and Hpc2. The Drosophila HIR complex consists of the proteins dHIRA and Yemanuclein-α. The human HIR complex is composed of the proteins HIRA, Ubinuclein1 and Cabin1. The HIR complex remains largely uncharacterized in *Arabidopsis thaliana* since only AtHIRA has been described. HIR functions involve DNA synthesis-independent chromatin assembly, required for chromatin remodeling at different genomic regions (adapted from Amin et al., 2012).

including EB1 and c-jun (Aho et al., 2000). Finally, Calcineurin-binding protein 1 (CABIN1) is the ortholog of Hir3. CABIN1 has been identified as a repressor of the transcription factor MEF2, which is activated by calcium signaling causing apoptosis in T-cells (Sun et al., 1998) (***Figure 28***). Activation of calcium signaling leads to dissociation of CABIN1 from MEF2, as a result of the binding of active calmodulin to CABIN1 (Youn et al., 1999). CABIN1 functions as a co-repressor of transcription by interacting with Sin3 and associated histone deacetylases (Balaji et al., 2009). All HIR subunits co-purify with epitope-tagged H3.3 or HIRA (Tagami et al., 2004; Drané et al., 2010; Ray-Gallet et al., 2011). HIRA seems to be central to the complex, as it mediates the binding to UBN1 *via* its N-terminal WD40 repeats (Balaji et al., 2009) and to CABIN1 *via* its Hira domain (Yang et al., 2011). HIRA further interacts with the small chaperone ASF1 through its conserved B domain (Tang et al., 2006). Moreover, all HIR complex members have the ability to interact directly with DNA (Ye et al., 2003; Ray-Gallet et al., 2011).

3.2.2. Functions

Evolutionary conservation of the HIR complex reveals its functional importance. HIR complex activity has been found in several organisms including budding yeast, fission yeast, Drosophila, Xenopus, fish, chicken, mice and human. HIRA remains the member the best described in the literature so far. Its specific ability to deposit H3-H4 was demonstrated *in vitro*. Experiments using *Xenopus laevis* egg extract showed the H3 chaperone activity of HIRA in the DNA synthesis-independent nucleosome assembly pathway (Ray-Gallet et al., 2002). While the study of the human complexes mediating nucleosome assembly showed that CAF-1 specifically interacts with H3.1, H3.3 was found to interact with HIRA (Tagami et al., 2004). Genome-wide deposition of H3.3 by HIRA has been extensively studied and showed that HIRA deposits H3.3 preferentially at promoters, gene bodies, and regulatory elements at which DNA is transiently free of nucleosomes due to transcription or remodeling (Loyola and Almouzni, 2007; Goldberg et al., 2010; Ray-Gallet et al., 2011; Schneiderman et al., 2012). Despite GFP-tagged HIRA localization to telomeres and pericentromeres (Wong et al., 2009), H3.3 specific

deposition at these sites is HIRA-independent in mouse embryonic stem cells (Goldberg et al., 2010; Lewis et al., 2010).

As observed for CAF-1, loss of HIRA is lethal in mammals, the embryo showing gastrulation defects and early embryonic lethality (Roberts et al., 2002). HIRA depletion in mouse embryonic stem cells causes reduced genome-wide H3.3 deposition (Goldberg et al., 2010) and downregulation of HIRA in Xenopus embryos causes gastrulation defects (Szenker et al., 2012). In contrast, Drosophila HIRA is not necessary for viability (Bonnefoy et al., 2007). Surprisingly, HIRA mutants do not show global H3.3 deposition defects in Drosophila embryos or adult cells, suggesting that other chaperones accomplish H3.3 nucleosome assembly in its absence (Loppin et al., 2005; Bonnefoy et al., 2007). HIRA and Yemanuclein-α, the Drosophila ortholog of UBINUCLEIN (Loppin et al., 2005; Bonnefoy et al., 2007; Orsi et al., 2013) are in contrast absolutely required for chromatin assembly and H3.3 deposition during sperm nucleus decondensation after fertilization (Loppin et al., 2005; Bonnefoy et al., 2007; Nakayama et al., 2007). In humans, CABIN1, UBN1 and UBN2 co-immunoprecipitate with H3.3 and HIRA, showing that the yeast HIR complex is conserved between organisms (Tagami et al., 2004; Balaji et al., 2009; Banumathy et al., 2009; Rai and Adams, 2012), implying that HIRA mediates H3.3 nucleosome assembly in a chaperone complex.

How much plants depend on HIRA for normal development, and how histones are assembled outside S phase in plants remain unclear and under debate. On the one hand, an ortholog of the metazoan HIRA protein, encoded by *AtHIRA* (At3g44530), was identified in Arabidopsis and its knockout was reported to be embryo lethal (Phelps-Durr et al., 2005). In addition, AtHIRA co-suppression lines displayed defects in developing leaves, which are thought to originate from defective silencing of the class I KNOX homeobox genes (Phelps-Durr et al., 2005; Guo et al., 2008). On the other hand, a loss-of-function mutant caused by another independent T-DNA insertion displayed no defects during vegetative growth or sexual reproduction (Ingouff et al., 2010). Taken together, the function of AtHIRA and the molecular consequences of its loss in Arabidopsis remain contradictory and it is therefore of particular interest to characterize the role of AtHIRA and the HIR complex in plant development and genome regulation.

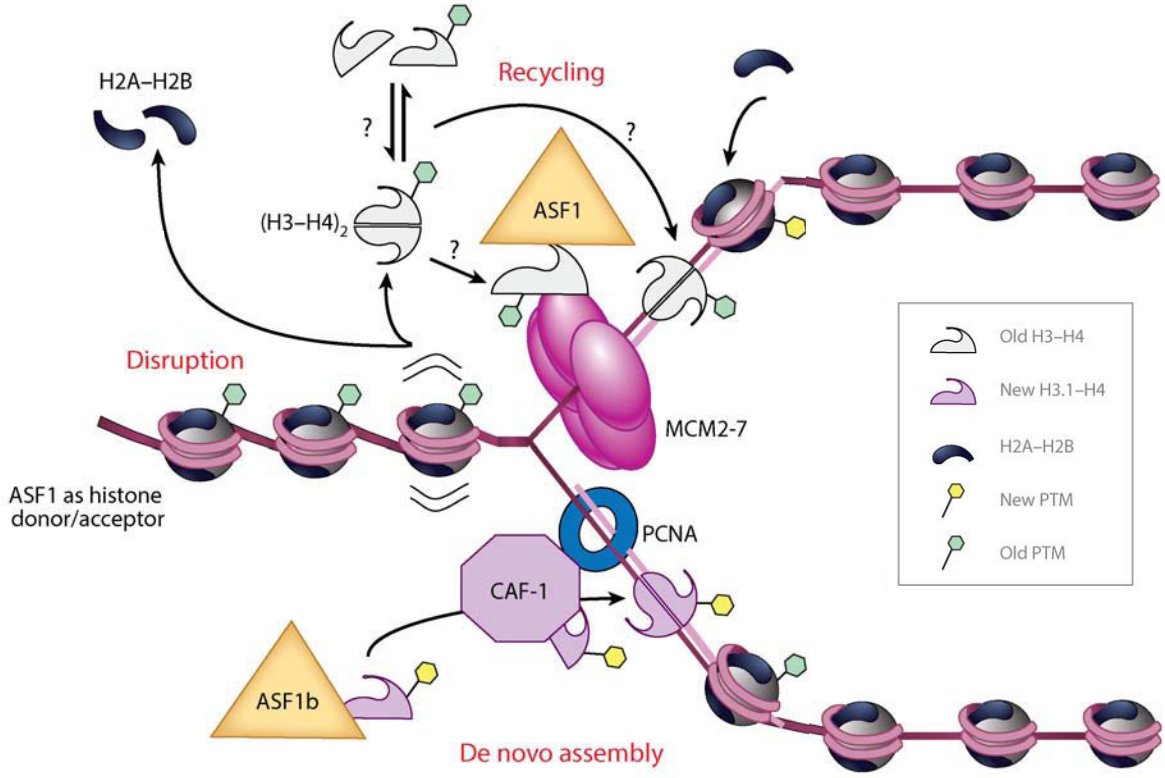

***Figure 29*: ASF1 is actively involved in maintenance of chromatin states during DNA replication.**

ASF1 participates in the transfer of parental H3-H4 from nucleosomes disrupted ahead of the replication fork to the new DNA strand to re-assemble nucleosomes. Evicted H3–H4 tetramers may proceed through a transient dimeric state to allow ASF1 binding. During recycling, ASF1 is targeted to the replication fork through the interaction between MCM2-7 helicases, and histones. During *de novo* chromatin assembly upon the passage of the replication fork, ASF1 transfers newly synthesized H3.1–H4 dimers to CAF-1 for incorporation. PTM = Post-translational modification (modified from Gurard-Levin et al., 2014).

3.3. Other histone H3.3 chaperones

In addition to the HIR complex, H3.3 is also found associated in assembly complexes with the Death domain-associated protein (DAXX) and the Alpha-thalassemia/mental retardation X-linked syndrome protein (ATRX), belonging to the SNF2-like ATP dependent chromatin remodeling factor family (Salomoni and Khelifi, 2006; Drané et al., 2010; Elsässer et al., 2012). DAXX has a H3.3 specific chaperone and chromatin assembly activity (Drané et al., 2010; Lewis et al., 2010) and interacts with ATRX (Xue et al., 2003). Contrary to HIRA, H3.3 deposition at genes and regulatory elements does not require DAXX/ATRX. Instead, DAXX deposits H3.3 at pericentromeric heterochromatin in mouse embryonic fibroblast (Drané et al., 2010) together with ATRX, which localizes to pericentromeric heterochromatin in HeLa cells (McDowell et al., 1999) and to telomeres in murine embryonic stem cells (Goldberg et al., 2010; Lewis et al., 2010). On a developmental point of view, ATRX is required for correct trophoblast development in mice (Garrick et al., 2006) and mice lacking DAXX die during early embryo development (Michaelson et al., 1999). DAXX is further found at the XY body during meiotic sex chromosome inactivation (Rogers et al., 2004). Interestingly, DAXX can bind H3.3 without ATRX, suggesting that ATRX might specify H3.3 targeting to defined and localized chromosome landmarks. Surprisingly, DAXX-deficient cells show association of CAF-1 with H3.3, suggesting that a replication-dependent pathway for H3.3 deposition can be used to bypass the loss of DAXX (Drané et al., 2010). The simultaneous deletion of Drosophila HIRA and XNP, the Drosophila homologue of ATRX causes lethality during larval development (Schneiderman et al., 2012). In summary, HIRA/CABIN1/UBN1 and DAXX/ATRX are two distinct replication-independent H3.3 nucleosome assembly complexes, thought to direct H3.3 deposition at separate chromatin domains.

DEK was initially defined as structurally unique component of metazoan chromatin (Kappes et al., 2001), maintaining heterochromatin structure by enhancing HP1 binding to H3K9me3 (Kappes et al., 2011). Analysis of the DEK-containing complexes in Drosophila and human cells revealed that DEK serves as histone chaperone facilitating H3.3 assembly (Sawatsubashi et al., 2010). Loss of DEK leads to a Su(var) phenotype, suggesting that DEK maintains identity of the heterochromatin / euchromatin boundaries regions (Kappes et al., 2011). Homologous proteins of mammalian DEK are annotated in the Arabidopsis genome.

3.4. Anti-Silencing Function 1 (ASF1)

ASF1 (Anti-Silencing Function 1) has been first described in yeast as alleviating transcriptional silencing of mating-type loci upon overexpression (Le et al., 1997). ASF1 is involved in regulation of transcription in yeast (Adkins and Tyler, 2004; Han et al., 2007; Mousson et al., 2007) and Drosophila (Moshkin et al., 2002; Goodfellow et al., 2007). *In vitro* replication-coupled nucleosome assembly assays described ASF1 as a H3-H4 chaperone facilitating CAF-1-dependent chromatin assembly (Tyler et al., 1999, 2001; Mello et al., 2002). In humans, there are two ASF1 isoforms, ASF1A and ASF1B, sharing 71% amino acid identity. Their highly conserved N-termini interact with the C-terminal helix of histone H3 (Munakata et al., 2000; Mousson et al., 2005; English et al., 2006; Natsume et al., 2007). In the cytoplasm, ASF1 proteins bind newly synthesized H3-H4 dimers and shuttle them to the sites of nucleosome assembly in the nucleus (Groth et al., 2007). ASF1 proteins also buffer the transient overaccumulation of histones as a result of replicational stress (Groth et al., 2005). ASF1 activity during replication can be separated in two distinct pathways. On the one hand, ASF1 provides new H3.1 to CAF-1 through interaction with the p60 subunit for replication-coupled nucleosome assembly downstream of the replication fork (Tyler et al., 1999, 2001; Krawitz et al., 2002; Mello et al., 2002; Groth et al., 2005; Sanematsu et al., 2006; Tang et al., 2006; Jasencakova et al., 2010) (***Figure 29***). On the other hand, ASF1 transfers parental H3-H4 dimers to the new DNA strand during replication fork progression through interaction with the Minichromosome Maintenance (MCM) helicases (Tagami et al., 2004; Groth et al., 2007) (***Figure 29***). These proteins unwind DNA and are critical for accessibility of the chaperones handling histones at the replication fork (Groth et al., 2007; Jasencakova et al., 2010). The expression of ASF1B, but not ASF1A, which is ubiquitously expressed, seems to be linked to the cell cycle since its levels fall about 5-fold upon the exit from the cell cycle (Corpet et al., 2011). Concomitantly, ASF1B is highly expressed in proliferative tissues, such as testes and tumors (Corpet et al., 2011).

In addition to its role facilitating CAF-1-directed H3.1 chromatin assembly, ASF1 co-purifies also with the replacement histone H3.3 (Tagami et al., 2004), and the different members of the HIR complex (Sharp et al., 2001; Green et al., 2005; Zhang et al., 2005; Tang et al., 2006; Malay et al., 2008). While CAF-1 interacts

indifferently with ASF1A and ASF1B, HIR displays preferential interaction with ASF1A. ASF1A interacts with HIRA through the recognition of its conserved N-terminus by the HIRA B domain (Daganzo et al., 2003; Tagami et al., 2004; Zhang et al., 2005). However, binding specificity of HIRA for ASF1A compared to ASF1B is driven by sequences flanking the core interaction domains of both proteins (Tang et al., 2006). This specificity of interaction suggests that ASF1A only is associated with H3.3 replication-independent chromatin assembly (Tang et al., 2006). In fission yeast, the HIRA/Asf1/H3-H4 complex is targeted to heterochromatin by HP1 and mediates, through the histone deacetylase Clr6, large-scale deacetylation of histones (Yamane et al., 2011).

The fact that both HIRA and CAF-1 p60 use similar motifs to bind ASF1 suggests a competition for this chaperone (Tang et al., 2006). In fact, the CAF-1 p60 C-terminus contains B domain–like motifs that resemble those in HIRA and recognize the same region of ASF1A, explaining why these two histone chaperones bind ASF1A in a mutually exclusive manner, as was recently confirmed in vertebrate cells (Tyler et al., 2001; Mello et al., 2002; Green et al., 2005; De Koning et al., 2007; Campos and Reinberg, 2010).

Chicken, Drosophila and human cells lacking simultaneously both ASF1 proteins exhibit stalling in S phase and problems in DNA replication leading to cell death (Groth et al., 2005; Sanematsu et al., 2006; Schulz and Tyler, 2006). Moreover depletion of ASF1 in yeast impairs S phase and provokes aberrant DNA unwinding due to defects in histone supply dynamics during DNA repair-associated chromatin assembly (Franco et al., 2005; Chen et al., 2008). Genome instability and DNA repair defects have been reported in yeast lacking ASF1 (Myung et al., 2003; Prado et al., 2004; Ramey et al., 2004). These defects can be overruled by introduction of human ASF1A, while normal growth and protection from replication stress is rescued by human ASF1B (Tamburini et al., 2005). This is coherent with mice lacking ASF1A showing embryonic lethality (Hartford et al., 2011), while ASF1B mutants are viable (www.informatics.jax.org). This suggests that the two human ASF1 proteins have different functions regarding maintenance of chromatin integrity, possibly related to their specificity in interaction with either CAF-1 or HIR chromatin assembly complexes. Histone deposition by the HIR complex is severely impaired upon loss of interaction with ASF1 (Ray-Gallet et al., 2007). Conversely, deletion of any of the HIR complex subunits disrupts the binding to Asf1 in yeast (Green et al., 2005),

Complex	*Gene*	Gene ID
CAF-1	*FAS1*	At1g65470
	FAS2	At5g64630
	MSI1	At5g58230
HIR	*AtHIRA*	At3g44530
	NCN1	At1g77310
	NCN2	At1g21610
	CBN	At4g32820
	AtASF1A	At1g66740
	AtASF1B	At5g38110

***Table 2*: H3 chaperone-encoding genes characterized in Arabidopsis.**

suggesting that binding activity of Asf1 to the HIR complex is important for chromatin assembly activity. Yeast lacking both Hir1 and Asf1 show decreased deposition of H3 and defects in telomere and mating-type loci silencing, but effects were comparable to those observed in single *asf1* or *hir1* mutants (Sharp et al., 2001). This suggests that both proteins belong to the same nucleosome assembly and transcriptional silencing pathway. Moreover, telomeric silencing is partially maintained in yeast lacking either CAF-1 or displaying a mutated PCNA form with low affinity for CAF-1, but totally alleviated upon Asf1 of Hir1 loss (Sharp et al., 2001), suggesting that CAF-1 and HIR/Asf1 are different yet functionally overlapping heterochromatin maintenance pathways in yeast.

In Arabidopsis, AtASF1A and AtASF1B are encoded by the paralogs *AtASF1A* (At1g66740) and *AtASF1B* (At5g38110) (Zhu et al., 2011). Both AtASF1A and AtASF1B are found in complex with H3, and they are expressed ubiquitously in different plant tissues with high levels of proliferation. Both proteins localize to the cytoplasm and the nucleus. *AtASF1A* and *AtASF1B* genes are targets of the E2F transcription factor; their expression is therefore linked to cell cycle progression. Indeed, based on the data obtained from synchronous Arabidopsis cell cultures (Menges et al., 2003), *AtASF1A* and *AtASF1B* expression peak in S phase. *AtASF1A* and *AtASF1B* transcription have recently been described to increase following UV-B treatment (Lario et al., 2013). The same study also shows that AtASF1A and AtASF1B interact with acetylated N-terminal H3 tails and associated histone acetyltransferases, suggesting that AtASF1A and AtASF1B participate in the regulation of genome structure and activity by modulating histone mark deposition. Furthermore, AtASF1A and AtASF1B participate in transcriptional activation of heat stress responsive *HEAT STRESS FACTOR* and *HEAT STRESS PROTEIN* genes by stimulating H3K56ac enrichment at these loci (Weng et al., 2014). Single mutants of either AtASF1A or AtASF1B show no obvious phenotypic defects, while plants lacking both proteins display impaired plant growth and abnormal vegetative and reproductive organ development (Zhu et al., 2011; Weng et al., 2014). Moreover, *atasf1ab* plants have reduced cell number, S phase delay and reduced endopolyploidy levels (Zhu et al., 2011). Overexpression of S phase checkpoint (G2 to M transition) specific genes was observed in loss-of-function mutants. Absence of both AtASF1A and AtASF1B results in increased levels of DNA damage due to replication fork stalling despite activation of the DNA damage checkpoint and

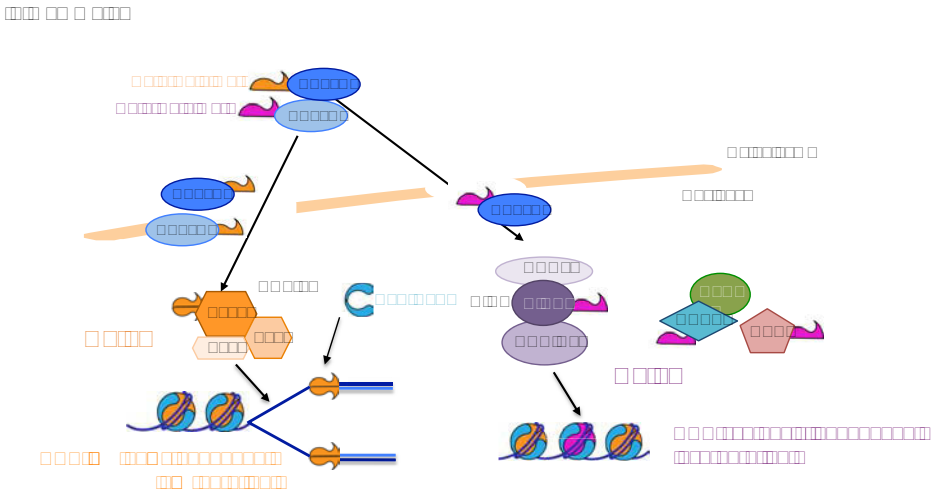

***Figure 30*: Schematic representation of the different histone H3-H4 assembly networks as known in mammals.**

Histone supply, buffering and dynamics are finely tuned *in vivo* by a complex network of histone chaperones. Chaperones direct the assembly of histones to an appropriate genomic region. The small chaperone ASF1 binds histone H3-H4 dimers in the cytoplasm and is involved in their transport into the nucleus. ASF1A and ASF1B hand over H3.1-H4 to CAF-1, which will deposit the canonical H3.1 in a DNA synthesis-dependent manner during replication and repair. In contrast, only ASF1A hands over H3.3-H4 to the HIR complex, which deposits H3.3 in a DNA synthesis-independent manner at genes and regulatory regions. Other H3.3 chaperones such as DEK and DAXX/ATRX deposit H3.3 at other genomic regions such as pericentromeric heterochromatin and telomeres.

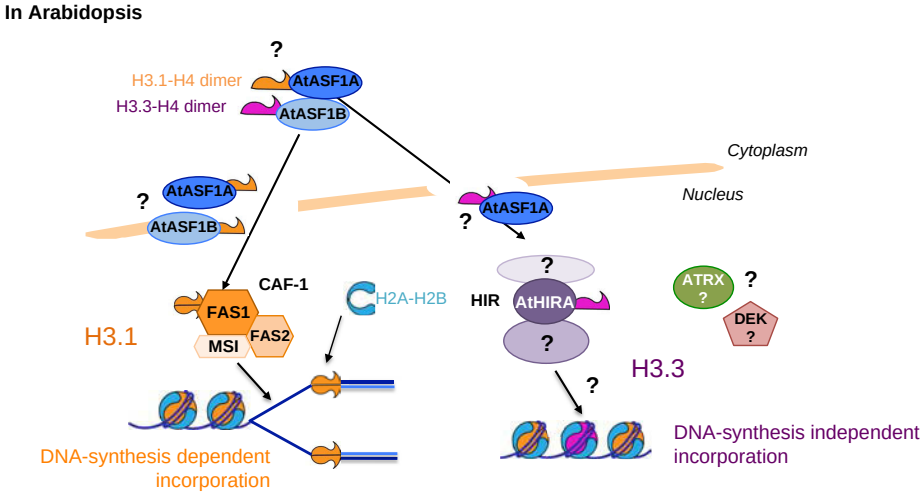

***Figure 31*: Schematic representation of the different histone H3-H4 assembly networks as known in Arabidopsis.**

Contrary to its mammalian counterpart, the histone H3-H4 assembly network remains poorly described in Arabidopsis. The Arabidopsis genome encodes two ASF1 orthologs (Zhu et al., 2011) and the well-described CAF-1 complex (Kaya et al., 2001). The HIR subunit AtHIRA has also been described. Whether other replacement histone chaperone complexes exist and whether the different chaperone complexes show a clear specificity for histone H3 variants as it is the case in mammals remains to be determined.

associated repair genes of the homologous recombination pathway. In addition, plants with decreased levels of both AtASF1A and AtASF1B display reduced DNA damage response after UV-B treatment (Lario et al., 2013). The gene duplication leading to *AtASF1A* and *AtASF1B* in plants appears relatively recent compared to other eukaryotes (Zhu et al., 2011), questioning whether there is subfunctionalization of the different Arabidopsis ASF1 proteins. To date, we have no evidence arguing for a specific binding to canonical or H3 variants or linking the different phenotypes observed in the mutants to a preferential interaction with either CAF-1 or HIR chromatin assembly pathways.

As a summary, histone chaperones are key regulators of all facets of histone metabolism since they finely tune the supply and dynamics of histones for chromatin assembly and disassembly. Correct genomic and timely distribution of canonical and histone variants defines distinct chromatin landscapes that impact directly genome activity, stability, and cell identity (***Figure 30***). Interestingly, these networks are well conserved between species, but remain largely unknown in the plant model Arabidopsis (***Figure 31***).

H3 chaperone-encoding genes characterized in Arabidopsis are listed in ***Table 2***.

Objectives

Establishment of chromocenters compartmentalizes heterochromatin away from the rest of the genome and is thought to contribute to transcriptional repression by creating a high local concentration of silencing factors (Almouzni and Probst, 2011). How the organization of heterochromatin into chromocenters is achieved during development and subsequently maintained is a critical question regarding eukaryotic genome integrity. Since histones are an evolutionary highly conserved set of proteins that play a central role in the functional organization of eukaryotic DNA into chromatin, they are likely candidates to play a role in this process. The plant model Arabidopsis offers a unique system to gain insight into the role of histone dynamics in heterochromatin organization, given that mutants deficient in histone chaperones or chromatin modifiers are viable and that dynamics of higher-order heterochromatin organization in chromocenters can be easily followed cytologically.

This thesis aimed to contribute to our understanding of the mechanisms and the molecular players involved in heterochromatin dynamics. I focused on the role of histone H3 variants as well as the network of their specific histone chaperones. My work is based on the hypothesis that proper chromatin assembly of histone variants and the consecutive setting of specific histone post-translational modifications contributes to the progressive establishment of distinct chromatin features at genes and repetitive sequences and subsequently the formation of specific higher-order structures such as chromocenters. Different mechanisms might be involved in the formation of higher-order structures *versus* their maintenance. It is therefore critical to understand how histones are handled, deposited and modified during different developmental stages as well as to enlighten how the tight interrelationship between histone variants and post-translational modifications contributes to the formation of chromocenters.

This work, requiring the characterization of a repertoire of Arabidopsis mutants for histone H3 variants and chaperones, together with the creation of lines expressing epitope-tagged version of the H3 variants (**Chapter I),** was driven by two objectives: (i) to gain insight into the handling of histone H3 by specific histone chaperones in plants together with the genetic interaction between the different chaperone pathways and the role of histone dynamics in maintenance of chromatin organization (**Chapter II**), and (ii) to understand how chromatin assembly of specific H3 variants and their dedicated set of post-translation modifications contribute to the formation of chromocenters during post-germination development (**Chapter III**).

Results

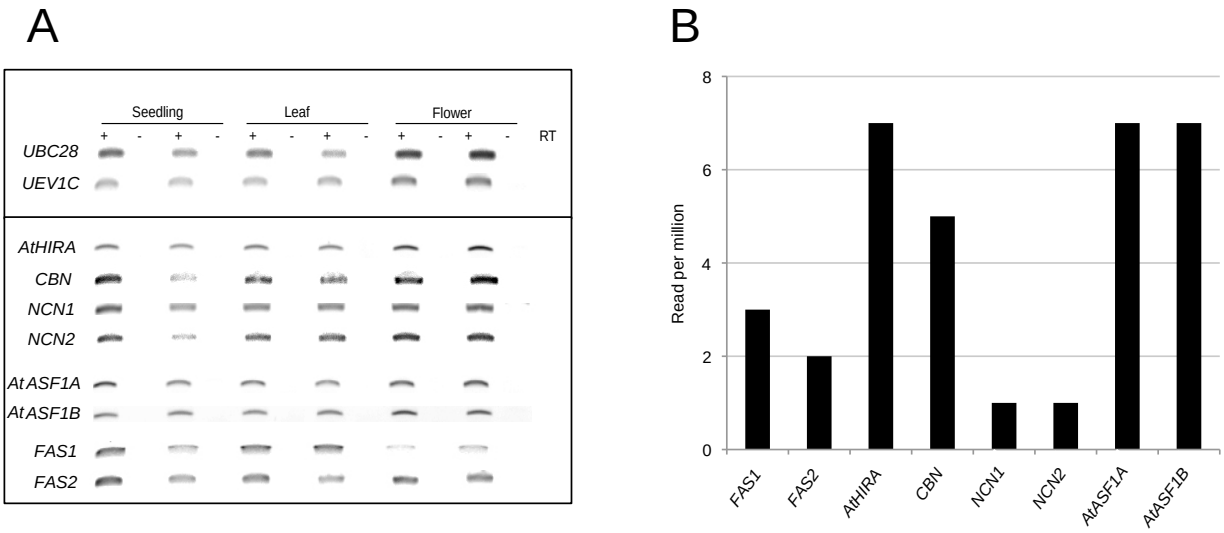

***Figure 32*: H3 chaperone-encoding genes are ubiquitously expressed.**

A. RT-PCR analysis of *AtHIRA*, *CBN*, *NCN1*, *NCN2*, *AtASF1A*, *AtASF1B*, *FAS1* and *FAS2* expression in 10-day-old WT seedlings, rosette leaves and flowers.
B. Transcript levels of *FAS1, FAS2, AtHIRA, CBN, NCN1, NCN2*, *AtASF1A* and *AtASF1B* as determined by Direct RNA Sequencing of RNA from 2-week-old seedlings (from Sherstnev et al., 2012).

Chapter I: Characterization and functional analysis of H3.1, H3.3 and associated histone chaperones in Arabidopsis

1.1. Characterization of Arabidopsis histone H3 chaperones

Histones are important structural components of chromatin and carriers of epigenetic information. Proper handling of histones during their cellular life is therefore required for correct genome function and is ensured by a network of histone chaperones. The role of histone H3 chaperones in chromatin dynamics is so far poorly understood in Arabidopsis and research has focused nearly exclusively on the CAF-1 complex. While the roles of several histone chaperones in other organisms are well described, the function of the plant homologs may not necessarily be conserved and developmental stage-specific roles or different requirements in response to the dynamic need of chromatin reorganization can be expected. To get insights into the Arabidopsis histone H3 chaperone network I first focused on the expression patterns of different genes encoding subunits of the H3 chaperone complexes that were previously identified (*AtASF1A, AtASF1B, FAS1*, *FAS2* and *AtHIRA*). We also identified homologs of the other mammalian and yeast HIR complex subunits by BLAST analysis, which we termed NUCLEIN1 (NCN1), NUCLEIN2 (NCN2) AND CABIN (CBN). I then characterized Arabidopsis mutants for the different chaperone proteins to investigate their implication in chromatin dynamics and maintenance.

1.1.1. Study of expression of H3 chaperone-encoding genes

I first analyzed transcript levels of the different chaperone-encoding genes and tested if some of them display tissue-specific expression patterns (***Figure 32A)***. To do so, I performed reverse transcription on total RNA extracted either from 10-day-

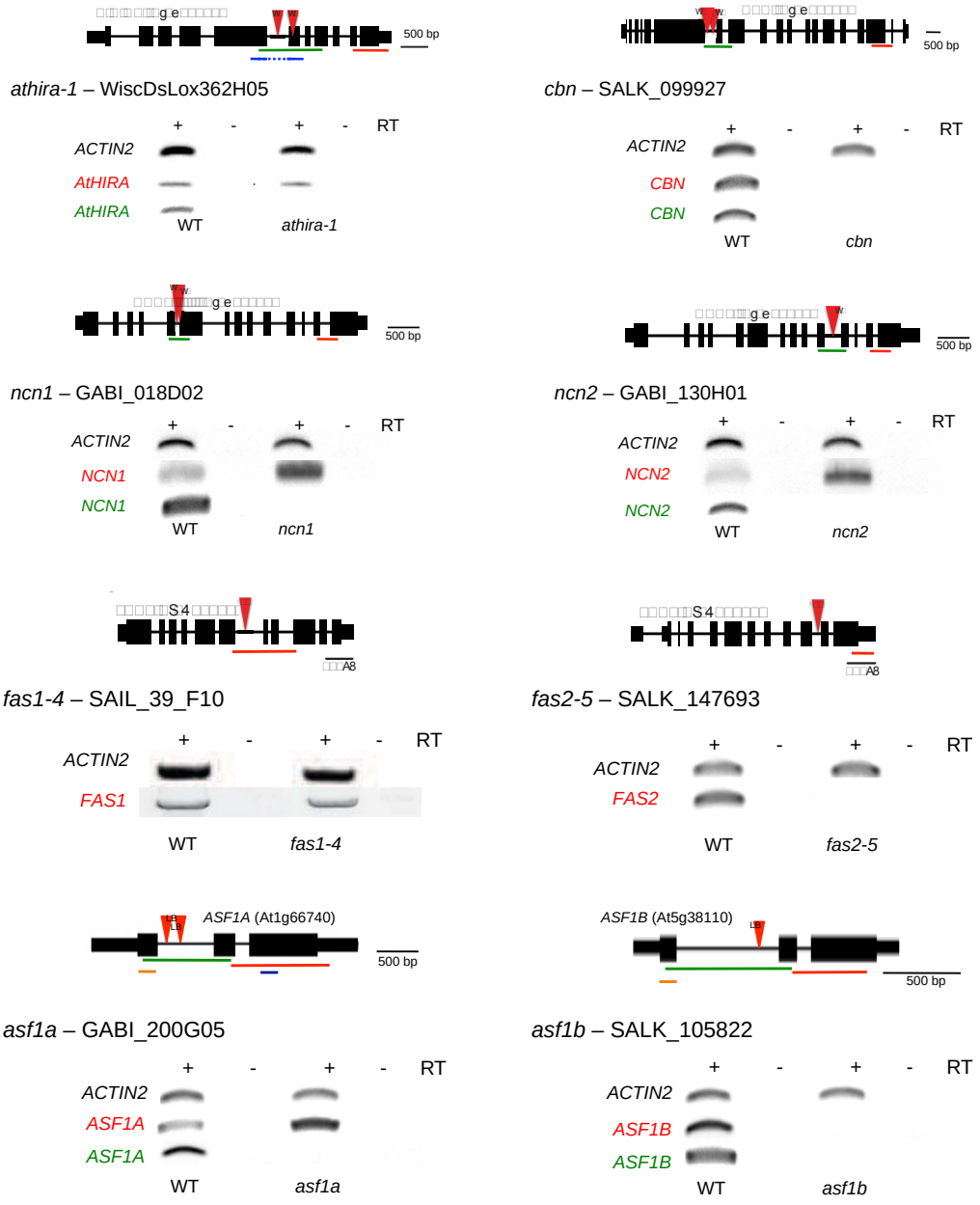

***Figure 33*: Validation of H3 chaperone mutants.**

Structure of H3 chaperone gene loci. Exons are denoted by rectangles, UTR by adjoining narrower rectangles and introns by lines. T-DNA insertions sites are displayed by red triangles. Orientation symbolized by the left border (LB) of the T-DNA. Absence of full-length transcripts is revealed by RT-PCR using primers spanning the T-DNA insertion site (green). Primers located in the 3' region (red) of the transcript reveal partial transcripts in certain mutants. Sequence targeted by an artificial miRNA in *AtHIRA* and *AtASF1A* transcripts is indicated by a blue line. Another single artificial miRNA further targets both *AtASF1A* and *AtASF1B* transcripts (orange).

old seedlings, rosette leaves or flowers. Transcript levels of the different chaperone-encoding genes were determined by semi-quantitative PCR using specific primers (***Table 4*** - Material and Methods). This analysis revealed a ubiquitous expression of all H3 chaperones tested in seedlings, leaves and flowers (***Figure 32A***).

The broad pattern of expression of H3 chaperones was further confirmed by Direct RNA Sequencing (DRS) data of 2-week-old seedlings (Sherstnev et al., 2012), detecting transcripts from HIR members-encoding genes, as well as both CAF-1 subunits FAS1 and FAS2 together with AtASF1A and AtASF1B (***Figure 32B***). Altogether, these data revealed broad expression of H3 chaperone genes.

1.1.2. Analysis of the role of the H3 chaperones *in vivo*

To gain insight into the roles of Arabidopsis H3 chaperones in chromatin establishment and maintenance during plant development, I used Arabidopsis mutant lines for the different H3 chaperone-encoding genes. Two strategies were used: (i) the characterization of available T-DNA insertion lines and (ii) the creation of lines in which selected chaperone transcripts are targeted by specific artificial miRNA (Schwab et al., 2006; Ossowski et al., 2008). I took benefit of the large collection of T-DNA insertion mutant lines available at the European Arabidopsis Stock Center (NASC, http://arabidopsis.info) to test lines displaying T-DNA insertions in genes encoding H3 chaperones. Plants homozygous for the T-DNA insertion within the gene of interest were identified by genotyping using PCR. In order to determine whether the T-DNA insertion affects the transcription of the gene, I performed reverse transcription on total RNA extracted from plants homozygous for the T-DNA insertion in the gene of interest, followed by PCR using primers located either at the 3' end of the transcript or spanning the T-DNA insertion site (***Figure 33***). Both approaches were necessary since, in some cases (*AtASF1A*, *AtHIRA*, *NCN1* and *NCN2*), the primers located in the 3' end detected a transcript, likely a truncated non-functional and aberrant transcript that might originate from promoters contained within the T-DNA, while we showed the absence of full-length transcripts using T-DNA-spanning primers. While it was known that mutants in the genes encoding the two large subunits of the CAF-1 complex were viable, at the beginning of our study we did not know what phenotype to expect for plants missing the small AtASF1

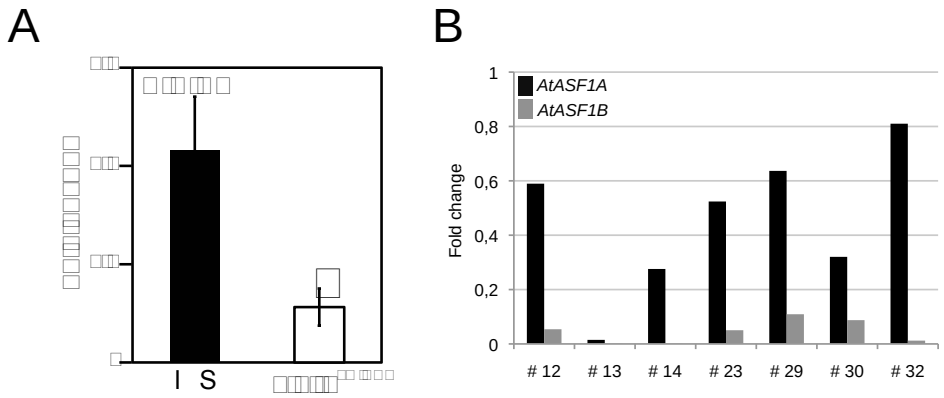

***Figure 34*: Artificial miRNA efficiently interfere with *AtHIRA*, *AtASF1A* and *AtASF1B* transcripts.**

A. RT-qPCR analysis of *AtHIRA* expression in the *athira* amiRNA line. Histograms show mean transcript levels ± SEM obtained for two independent PCR amplifications of three biological replicates. The y-axis shows the fold change relative to WT (WT set to 1) after normalization to *SAND* gene expression.
* p<0.05 ; Student's t-test.
B. Semi-quantitative RT-PCR analysis of *AtASF1A* and *AtASF1B* expression in the amiRNA line targeting simultaneously both *AtASF1A* and *AtASF1B* transcripts. Histograms show transcript levels for *AtASF1A* (black) and *AtASF1B* (grey) from individual *atasf1ab* amiRNA T1 lines identified on the x-axis from one PCR amplification relative to WT (set to 1) after normalization to *ACTIN2* transcript levels.

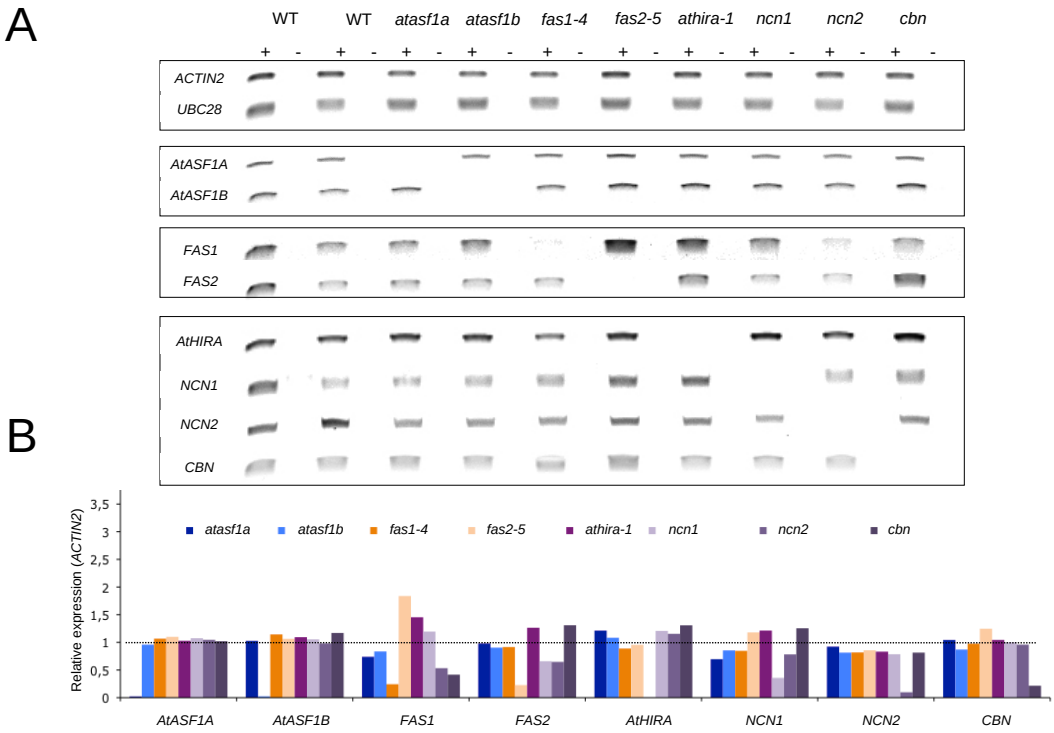

***Figure 35*: Loss of H3 chaperones does not lead to changes in transcription of other chaperone genes.**

A. RT-PCR analysis of *AtASF1A*, *AtASF1B*, *FAS1*, *FAS2, AtHIRA*, *NCN1*, *NCN2* and *CBN* expression in 10-day-old mutant seedlings lacking different H3 chaperones.
B. Quantification of *AtASF1A*, *AtASF1B*, *FAS1*, *FAS2, AtHIRA*, *NCN1*, *NCN2* and *CBN* expression by semi-quantitative RT-PCR relative to *ACTIN2* and *UBC28* in 10-day-old mutant seedlings lacking different H3 chaperones.

chaperones or the HIR complex. Indeed, the simultaneous deletion of both AtASF1A and AtASF1B proteins causes severe developmental phenotypes (Zhu et al., 2011), and a T-DNA insertion in the 5' end of the *AtHIRA* gene was reported to cause lethality (Phelps-Durr et al., 2005). For this reason I led in parallel the generation of lines expressing artificial miRNA targeting the mRNA of *AtHIRA*, *AtASF1A* and *AtASF1B*. This approach has the advantage to recover lines with distinct degrees of transcript interference and allowed me to target simultaneously different members of a multigenic family. Transcription of the artificial miRNA constructs is under control of the strong viral 35S promoter known to drive high and constitutive expression during Arabidopsis development. The level of interference with the target mRNA was monitored by RT-PCR and a significant decrease in transcript levels was observed, as exemplified for *AtHIRA* (***Figure 34A***), *AtASF1A* and *AtASF1B* (***Figure 34B***). The artificial miRNA construct targeting both *AtASF1A* and *AtASF1B* transcripts was found to be more effective on the latter.

In order to check potential compensation of the loss of one chaperone by increased transcription of other chaperone-encoding genes, I tested by semi-quantitative RT-PCR the expression of the different chaperones in plants with T-DNA insertions in the *AtASF1A, AtASF1B, FAS1, FAS2, AtHIRA, NCN1, NCN2* and *CBN* genes (***Figure 35A***). This revealed that the transcript levels of the other H3 chaperones remain broadly unchanged in case of loss of a certain chaperone (***Figure 35B***). Small but biologically significant effects can however be envisaged and would require more precise analysis by quantitative PCR. I further generated double H3 chaperone mutants by crossing single mutant lines. Notably, *atasf1ab*, *athira-1 fas1* and *athira-1 fas2* mutants showed interesting phenotypes and will be characterized further in this manuscript. The exhaustive list of H3 chaperone mutant lines used during this thesis can be found in ***Table 3***.

1.1.3. Functional analysis of histone H3 chaperones and impact on chromatin organization

Heterochromatin organization is highly dynamic during early post-germination development (Mathieu et al., 2003; Douet et al., 2008). After seed germination, which is associated with heterochromatin decompaction, the cotyledons formed during

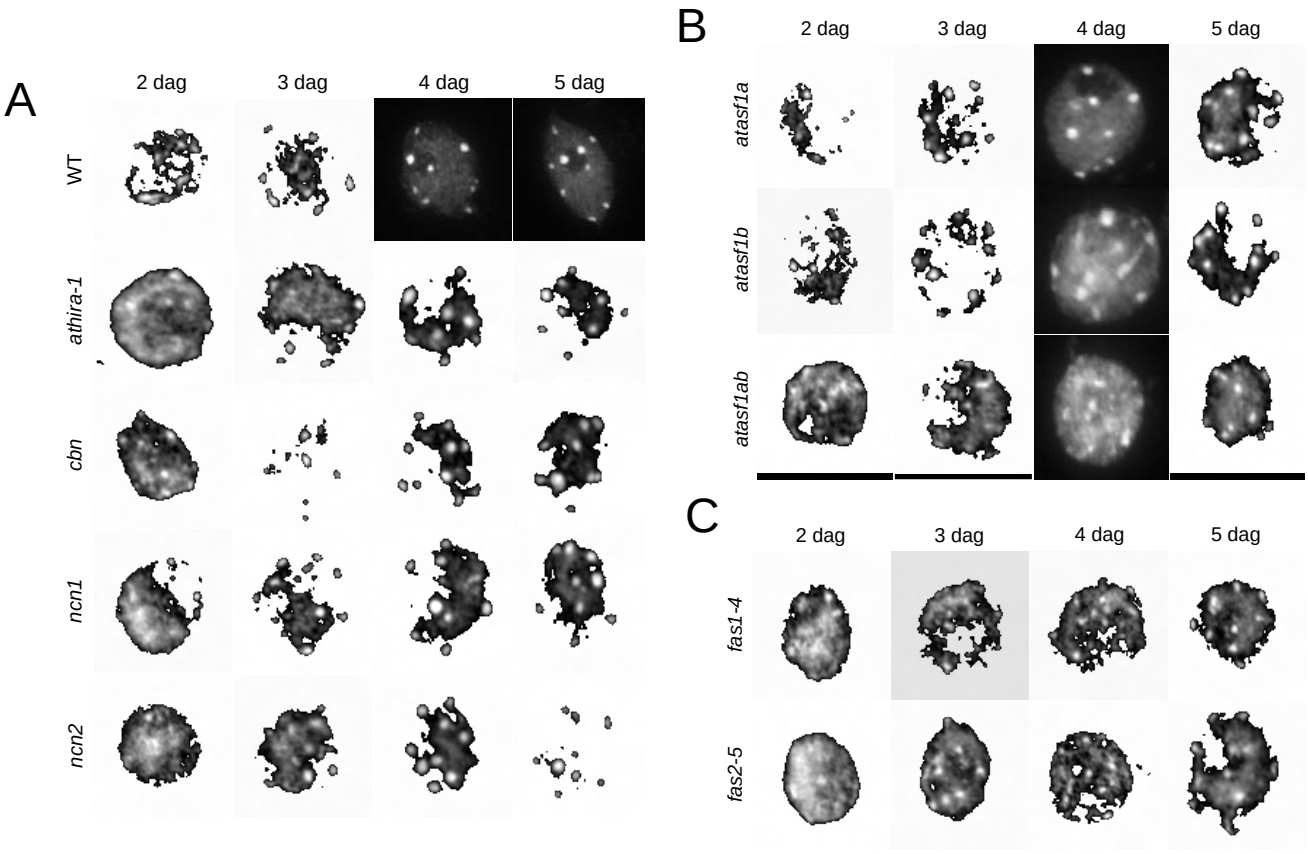

***Figure 36*: Chromocenter formation is impaired in absence of CAF-1, AtASF1A and AtASF1B while loss of HIR members has no effect.**

A. Representative nuclear spreads from WT, *athira-1*, *cbn*, *ncn1* and *ncn2* cotyledons aged 2, 3, 4 and 5 dag. DNA is counterstained with DAPI. Scale bar: 5 µm.
B. Representative nuclear spreads from *atasf1a*, *atasf1b* and *atasf1ab* cotyledons aged 2, 3, 4 and 5 dag. DNA is counterstained with DAPI. Scale bar: 5 µm.
C. Representative nuclear spreads from *fas1-4* and *fas2-5* cotyledons aged 2, 3, 4 and 5 dag. DNA is counterstained with DAPI. Scale bar: 5 µm.

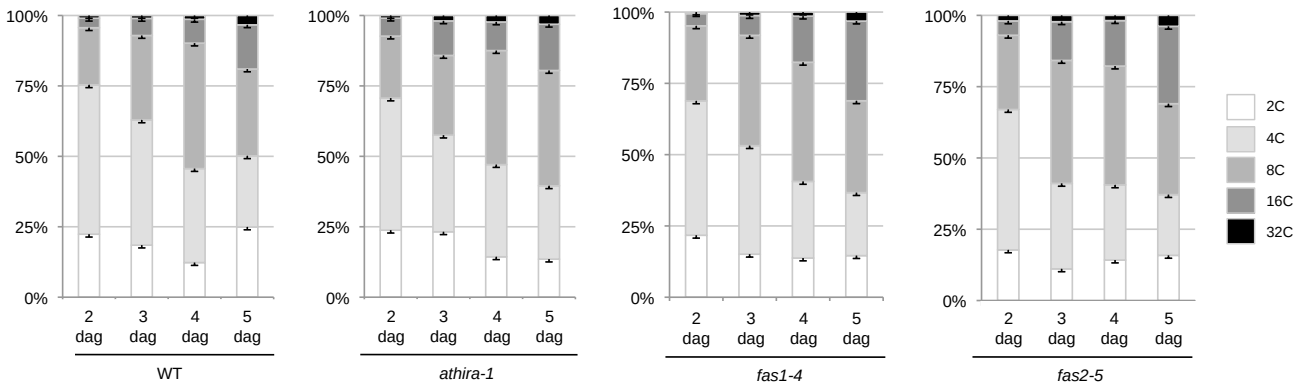

***Figure 37*: Plants lacking CAF-1 display precocious switch to endoreplication and increased polyploid nuclei content.**

Ploidy distribution of WT, *athira-1*, *fas1-4* and *fas2-5* cotyledon nuclei aged 2, 3, 4 and 5 dag. Average values of each nuclear DNA content class ± SD obtained for two independent experiments are presented.

embryogenesis start to expand. Between 2 and 5 dag in cotyledons, heterochromatin clusters progressively in conspicuous chromocenters. I investigated the impact of chromatin assembly on this process. To this aim, I isolated cotyledon nuclei from *fas1*, *fas2*, *athira*, *ncn1*, *ncn2*, *cbn*, *atasf1a*, *atasf1b* and *atasf1ab* mutant plants at 2, 3, 4 and 5 dag. Chromatin organization was revealed by DAPI staining on spread nuclei. This analysis showed that the establishment of chromocenters remained largely unaffected by the loss of HIR complex members (AtHIRA, NCN1, NCN2 and CBN) compared to the WT, exemplified by the detection of nine well-defined chromocenters in cotyledon nuclei at 5 dag (***Figure 36A***). Similarly in single *atasf1a* and *atasf1b* mutants, the kinetics of chromocenter formation is largely maintained (***Figure 36B***). In contrast, nuclei isolated from cotyledons of plants lacking both AtASF1A and AtASF1B showed defects in chromocenter formation, particularly obvious in cotyledon nuclei at 4 and 5 dag (***Figure 36B***). Interestingly, *atasf1ab* chromocenters appeared smaller than the WT even at 5 dag and would require further characterization. In parallel, loss of CAF-1 subunits FAS1 and FAS2 strongly impaired chromocenter establishment (***Figure 36C***). Following this initial observation, I carried out deeper cytological and molecular analysis to understand the involvement of CAF-1 in chromocenter formation. The results are presented in **Chapter II**. It is interesting to note that the pattern of decompaction of chromocenters at 2 dag in cotyledons achieved during germination is similar in the WT and in the different H3 chaperone mutants analyzed, suggesting that chromocenter decondensation upon germination is independent of these chromatin assembly pathways.

The switch from the mitotic cycle to the endocycle is important for cell expansion and cell differentiation in cotyledons (Ramirez-Parra and Gutierrez, 2007a; De Veylder et al., 2011; Edgar et al., 2014). Previous studies have shown a premature switch to the endocycle in *fas* mutants (Ramirez-Parra and Gutierrez, 2007a). I therefore wanted to know to which extent the absence of histone H3 chaperones impacts the transition from the mitotic cycle to the endocycle in cotyledons in my experimental setup. In WT cotyledons at 2 dag, the majority of nuclei are 2C and 4C, with less than 25% of polyploid nuclei. The number of polyploid nuclei increases progressively at 3 dag until 4 and 5 dag where the 8C, 16C and 32C fraction increases up to 50%. Analysis of ploidy levels in *athira* cotyledons from 2 to 5 dag revealed no difference compared to the WT (***Figure 37***). In contrast, plants lacking FAS1 or FAS2 displayed an early switch to the endocycle, exemplified

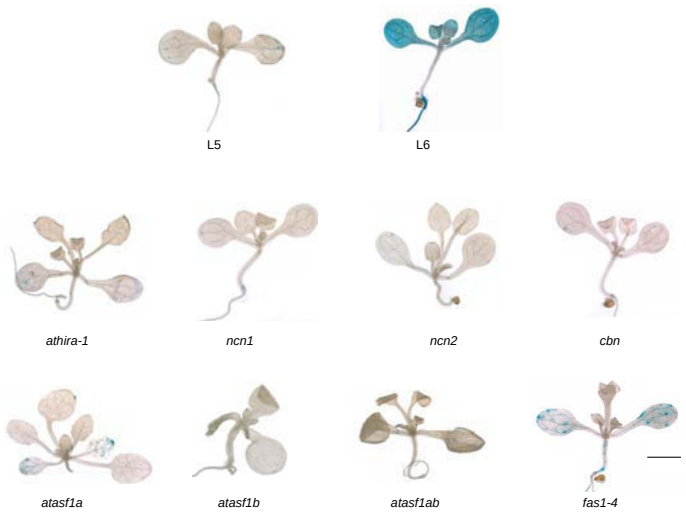

***Figure 38*: Transcriptional gene silencing at the multicopy GUS locus is maintained in all H3 chaperone mutants tested except *fas1-4* mutants.**

Two-week-old plants of WT, *athira-1*, *ncn1*, *ncn2*, *cbn*, *atasf1a*, *atasf1b*, *atasf1ab* and *fas1-4* plants carrying the silent multicopy GUS locus from the L5 line. The L6 line, displaying constitutive expression of the *GUS* gene, is used as positive control. Scale bar: 2 mm.

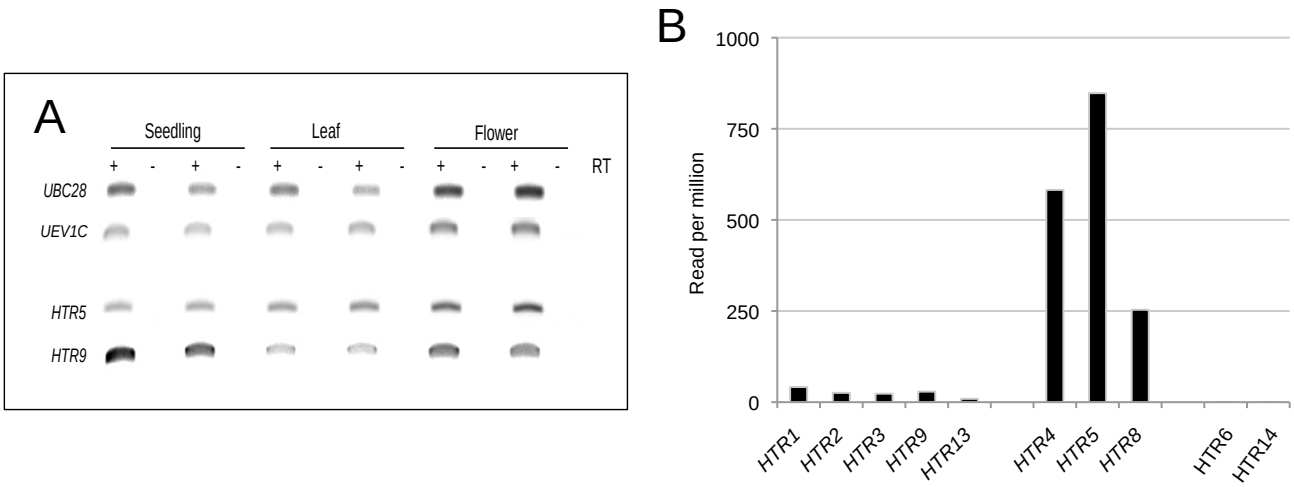

***Figure 39*: H3.1- and H3.3-encoding genes are ubiquitously expressed.**

A. RT-PCR analysis of *HTR9* and *HTR5*, representative H3.1- and H3.3-encoding genes respectively, in 10-day-old WT seedlings, rosette leaves and flowers.
B. Transcripts levels of *HTR1, HTR2, HTR3, HTR9, HTR13, HTR4, HTR5, HTR8*, *HTR6* and *HTR14* as determined by DRS (from Sherstnev et al., 2012).

by the increased percentage of 8C nuclei at 3 dag compared to WT. Such shift in the endocycle progression is further found at 5 dag were both *fas1* and *fas2* cotyledons display a higher number of 16C nuclei compared to WT (***Figure 37***). Consistent with an early switch to endoreplication and cell expansion, *fas1* and *fas2* cotyledons display increased size compared to WT and *athira*. However, the role of CAF-1 in this process is complex and not well understood, but the switch to the endocycle could be the consequence of the resulting DNA damage (Ramirez-Parra and Gutierrez, 2007a). Furthermore, as outcome of its DNA synthesis-dependent chromatin assembly activity, absence of CAF-1 is thought to interfere with correct processing of the replication fork and transmission of epigenetic marks.

I further investigated the capacity of the chaperone mutant plants to maintain transcriptional gene silencing of repetitive sequences in the different plant tissues. To this aim I introduced line L5, which carries a transcriptionally silent GUS transgene under control of a 35S promoter (Elmayan et al., 2005) by crossing into individual chaperone mutant lines. Blue staining revealed by the GUS tissue assay is readout for release of gene silencing. The level and pattern of GUS staining were compared to *fas1* mutant plants, which have previously been reported to release transcriptional silencing at the GUS locus (Ono *et al.,* 2006). This qualitative study revealed that transcriptional silencing of the GUS transgene is mostly unaffected by the loss of the different chaperones exemplified by no or very low staining of plantlets at 10 dag (***Figure 38***). Further analyses on the ability of plants lacking HIR complex members to maintain transcriptional gene silencing are presented in **Chapter II** of this manuscript.

1.2. Characterization of Arabidopsis histone H3 variants

1.2.1. Study of expression of H3 variant-encoding genes

I first checked the expression of H3.1- and H3.3-encoding genes in different plant tissues (***Figure 39A***). RT-PCR analysis showed that *HTR9* and *HTR5*, chosen as representative H3.1- and H3.3-encoding genes respectively, were ubiquitously expressed in the tissues tested. DRS data obtained from 2-week-old seedlings

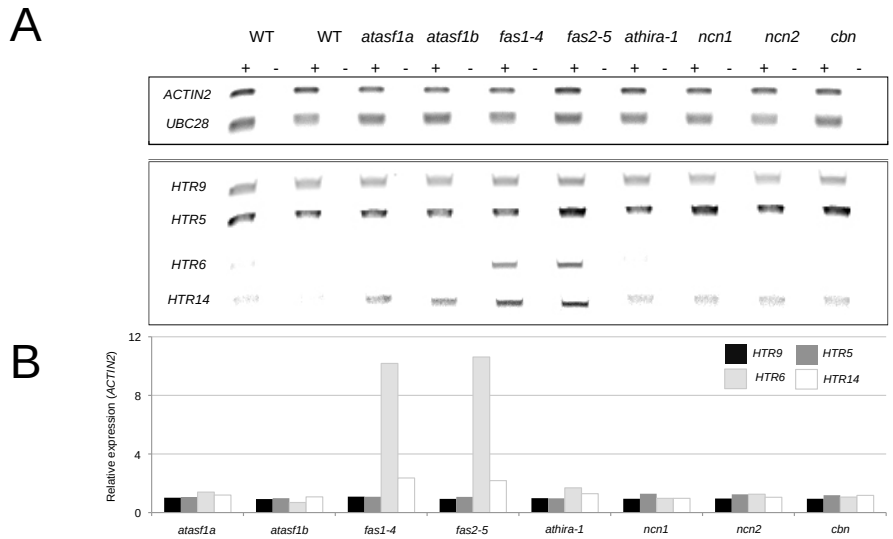

***Figure 40*: H3.1- and H3.3-encoding genes remain unaffected by loss of H3 chaperones, while H3.3-like genes are overexpressed in CAF-1 mutants.**

A. RT-PCR analysis of *HTR9* and *HTR5*, representative H3.1- and H3.3-encoding genes respectively, as well as *HTR6* and *HTR14* encoding H3.3-like histones, in 10-day-old WT and mutant seedlings lacking different H3 chaperones.
B. Quantification of *HTR9*, *HTR5*, *HTR6* and *HTR14* expression in 10-day-old seedlings lacking different H3 chaperones relative to WT (set to 1) and normalized to *ACTIN2* expression.

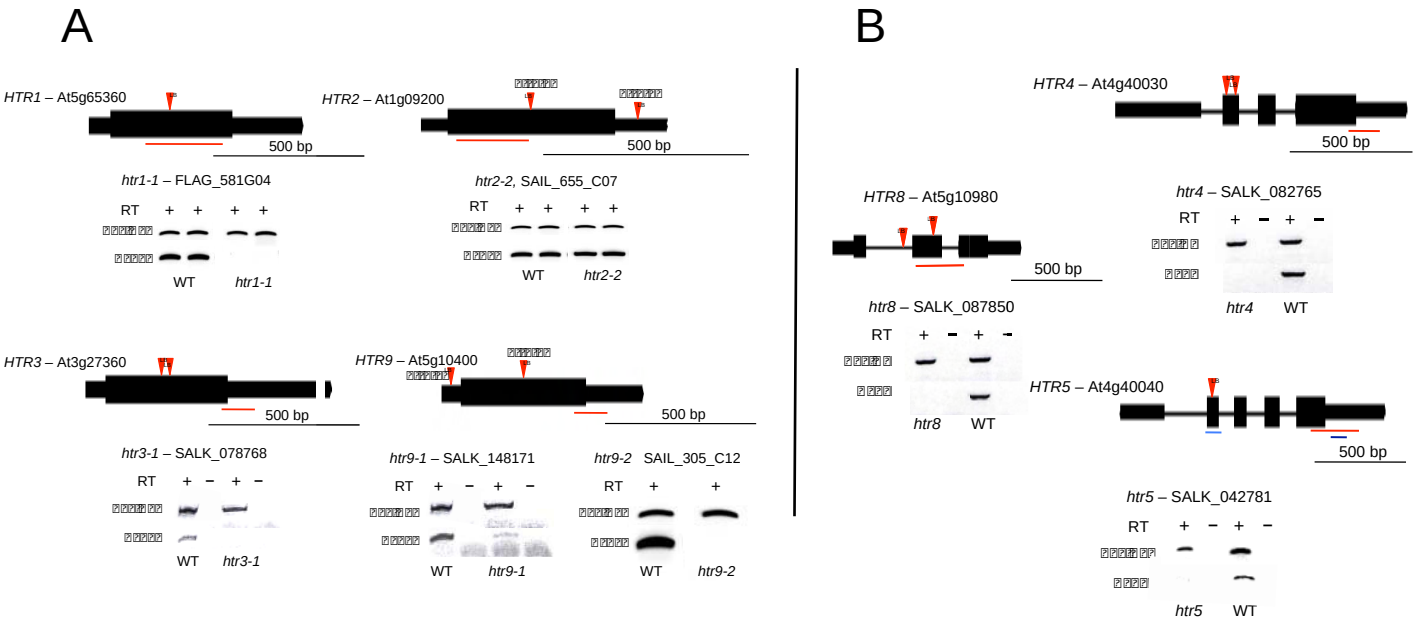

***Figure 41*: Validation of T-DNA insertion mutants for H3.1- and H3.3-encoding genes.**

Structure of H3.1 (A) and H3.3 (B) histone gene loci. Exons are denoted by rectangles, UTR by adjoining narrower rectangles and introns by lines. T-DNA insertions sites are displayed by red triangles. Orientation symbolized by the left border (LB) of the T-DNA. Interference with the full-length transcript is revealed by RT-PCR using primers amplifying the genomic region identified by a red line. *HTR5* transcripts are further independently targeted by two different artificial miRNA (light blue and dark blue).

(Sherstnev et al., 2012) revealed elevated transcript levels for the H3.3-encoding genes *HTR4, HTR5* and *HTR8* compared to the H3.1-encoding genes *HTR1, HTR2, HTR3, HTR9* and *HTR13* (***Figure 39B***). Meanwhile, no transcripts originating from genes encoding H3.6 and H3.14 belonging to the H3.3-like class were detected in this tissue. Based on this experiment, H3.3 genes would be more expressed at this developmental stage than H3.1. More detailed analysis comparing different developmental stages are ongoing to determine whether expression of canonical and H3 variants are dynamic during development.

Since histone assembly is finely tuned *in vivo* by histone chaperones, I wondered if the transcription of histone H3-encoding genes is modified upon loss of histone chaperones. To test this, I checked by semi-quantitative RT-PCR the expression of *HTR9, HTR5, HTR6* and *HTR14* in different chaperone mutant contexts (***Figure 40A***). While *HTR9* and *HTR5* expression remained unchanged despite loss of the chaperones, plants lacking FAS1 and FAS2 exhibit strong increase in *HTR6* expression, and in a lower extent *HTR14* expression (***Figure 40B***). This has been described previously (Schönrock et al., 2006), but it appears here for the first time that loss of FAS1 or FAS2 specifically impacts expression of the H3.3-like genes and not H3.3 variants exemplified by *HTR5*. Origins and consequences of the overexpression of *HTR6* and *HTR14* still remain elusive but may suggest mobilization of a new and CAF-1 independent pathway upon disruption of replication-dependent chromatin assembly. To date, the histone chaperones mediating H3.6 and H3.14 deposition are still unknown.

1.2.2. Generation of plants with reduced levels of canonical and H3 variants

In order to investigate the role of canonical and replacement H3 in chromatin dynamics and gene expression, I generated and characterized mutant plants for either H3.1- or H3.3-coding genes using a combination of T-DNA insertion lines and artificial miRNA constructs. I obtained *htr1-1* and *htr3-1* alleles displaying total abolition of *HTR1* and *HTR3* expression respectively (***Figure 41A***). Meanwhile, *HTR2* expression remained unchanged in *htr2-1* and *htr2-2* mutant alleles with T-DNA insertions in the 5' and 3' UTR respectively (***Figure 41A***). The *htr9-1* allele (two

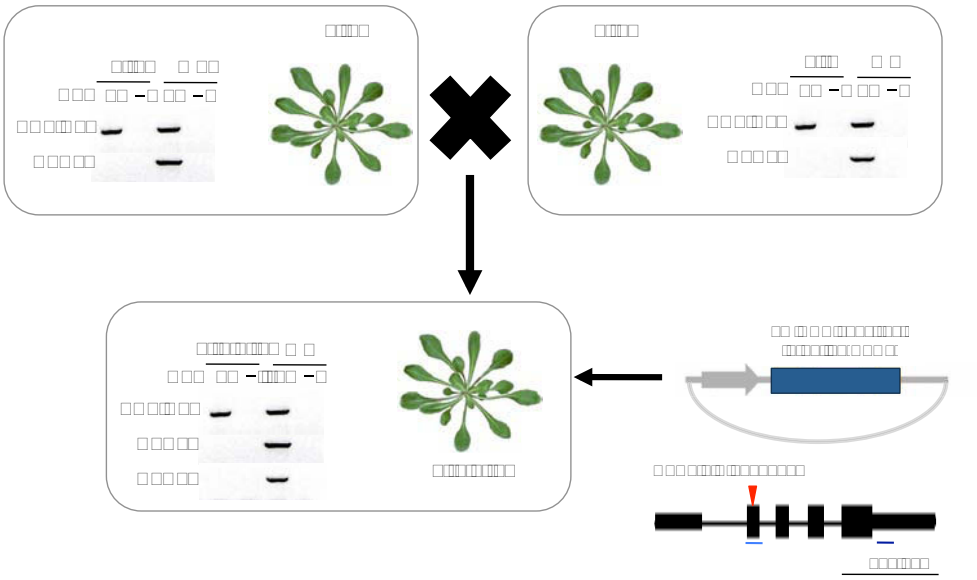

Figure 42: **Triple H3.3 mutants were obtained using a combination of T-DNA insertions and artificial miRNA.**

Plants lacking both *HTR4* and *HTR8* expression obtained by crossing single *htr4* and *htr8* mutants and were transformed with two different artificial miRNA constructs targeting *HTR5* transcripts (at regions revealed by light blue and dark blue lines).

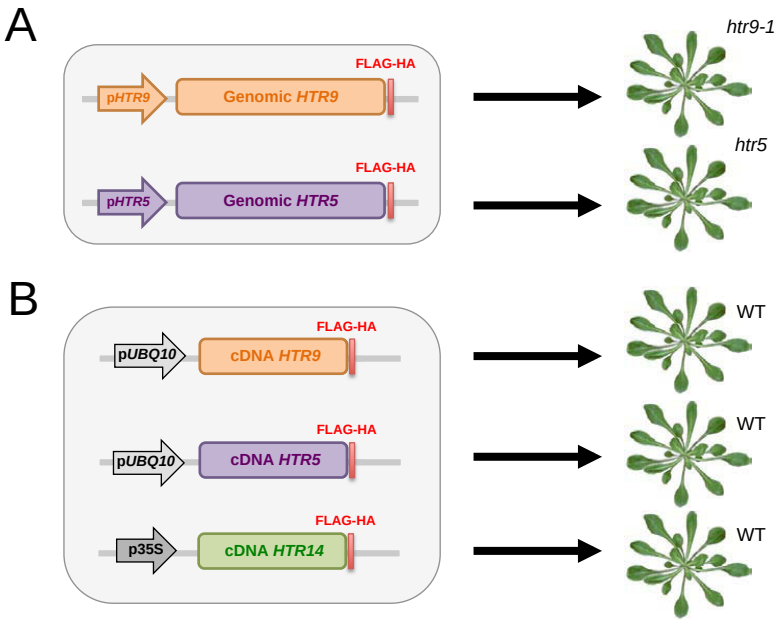

Figure 43: **Transgenes encoding H3.1 and H3.3 proteins fused to a tag were created to follow experimentally H3 dynamics.**

A. Scheme of transgenes containing both the promoter and the coding region of either *HTR9* or *HTR5* fused to a FLAG-HA were transformed in *htr9-1* and *htr5* mutants respectively.
B. Transgenes containing either full-length *HTR9* or *HTR5* cDNA fused to a FLAG-HA and under control of a p*UBQ10* promoter were transformed in WT plants. In parallel, FLAG-HA-fused full-length *HTR14* cDNA controlled by a 35S promoter was transformed in WT plants.

T-DNA insertions, one in the 5' UTR) resulted in a diminution of *HTR9* transcripts of approximately 20%. We therefore later obtained a second allele, *htr9-2*, which contains a single insertion in the exon and abolishes transcription (***Figure 41A***). Double and triple H3.1 mutants were obtained by crossing single mutants and characterization of these mutants is ongoing.

In parallel, I established single, double and triple mutants deficient for different combinations of the three H3.3-encoding genes (*HTR4, HTR5* and *HTR8*). T-DNA insertion lines were available for all three genes and *htr4*, *htr5* and *htr8* mutants displayed complete loss of their respective full-length transcripts (***Figure 41B***), but do not show obvious differences in phenotype. I turned into generating triple H3.3 mutants by crossing single mutants. However, given the physical proximity of *HTR4* (At4g40030) and *HTR5* (At4g40040), double mutants were unlikely to be obtained. I therefore first created double *htr4 htr8* mutants, which have been subsequently transformed with one of the two different artificial miRNA constructs (Ossowski et al., 2008) targeting *HTR5* transcripts (***Figure 42***). Since I expected lethality or severe phenotypes, this approach had the advantage to allow selection by RT-PCR of plants with different degrees of *HTR5* downregulation. The impact of H3.3 deficiency in these triple mutants on general chromatin organization, correct gene expression and maintenance of transcriptional silencing of heterochromatin is currently ongoing. The exhaustive list of H3 mutant lines used during this thesis can be found in ***Table 3***.

1.2.3. Generation of histone tagged lines

To dissect the role of canonical and H3 variants in chromatin organization and genome expression, I wanted to monitor their localization within chromatin together with their dynamics and regulation during their cellular life. Since no antibodies are available discriminating Arabidopsis H3.1 from H3.3, I generated plant lines expressing transgenes encoding H3 proteins fused to an epitope. I used two distinct strategies. On the one hand, I used a genomic fragment containing the promoter and the coding region of a representative H3.1- or H3.3-encoding gene (***Figure 43A***), with the aim to conserve native expression patterns. On the other hand, I used full-length cDNA of H3.1-, H3.3- or H3.14-encoding genes cloned under control of a p*UBQ10* promoter (Grefen et al., 2010) (H3.1 and H3.3) or a strong viral 35S

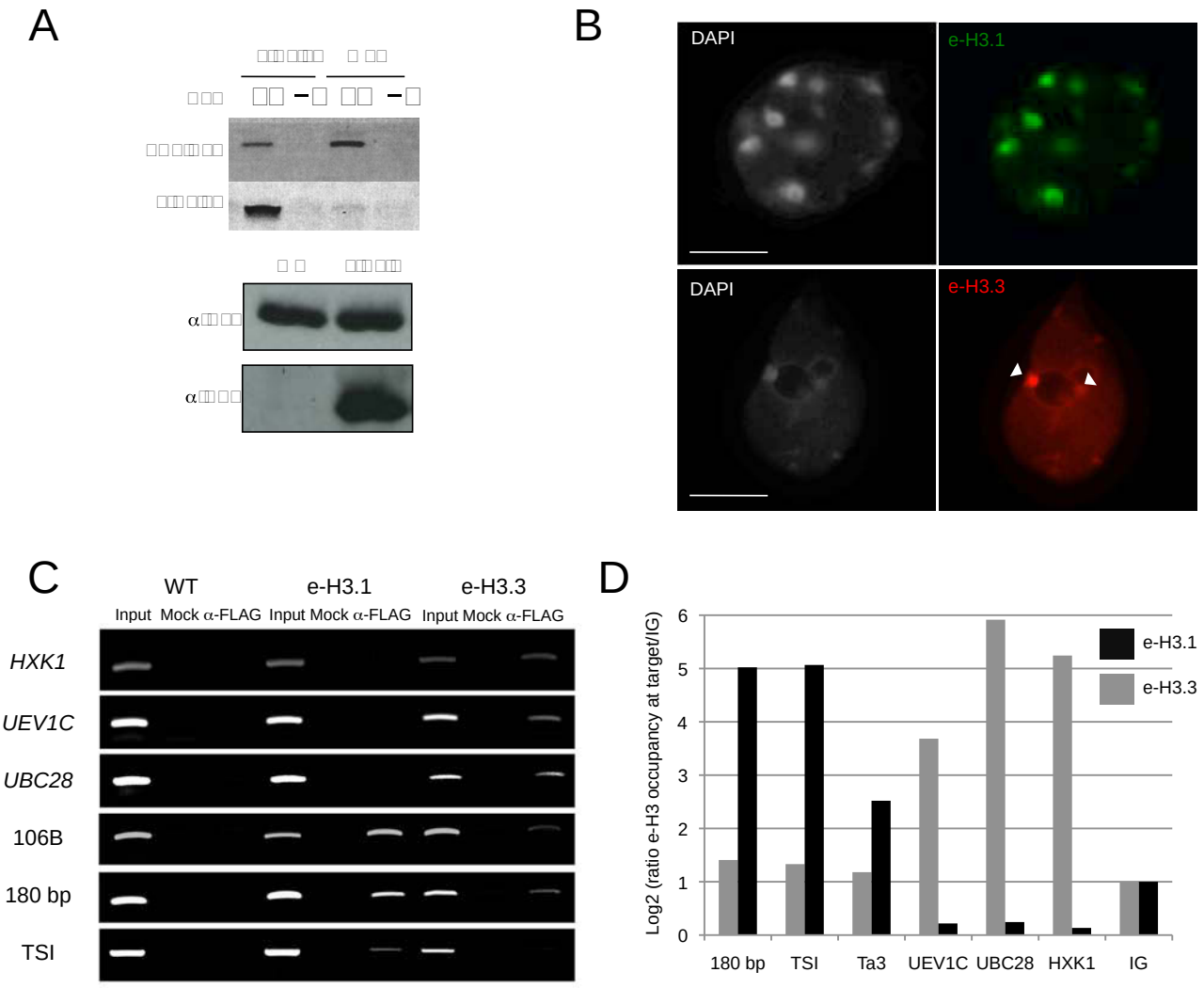

Figure 44: **e-H3.1 and e-H3.3 assembly into chromatin defines distinct genomic regions.**

A. RT-PCR analysis revealing the presence of e-H3.1 fusion transcripts (top). Western blot of nucleosomal histones showing chromatin incorporation of the tagged histone H3.1 variant (bottom).
B. Immunofluorescence staining of 10-day-old cotyledon nuclei of the e-H3.1 line and the e-H3.3 line revealed using an α HA. Scale bars: 5 µm.
C. ChIP experiment in 3-week-old plants expressing either e-H3.1 or e-H3.3 with α-FLAG antibodies reveals enrichment of H3.1 at heterochromatic repeats while H3.3 is preferentially found at euchromatic loci. Immunoprecipitated and input DNA were amplified by PCR.
D. Ratio of e-H3.1 and e-H3.3 occupancy (log2) determined by FLAG-ChIP qPCR relative to input and normalized to levels at an intergenic region (IG) in 10-day-old seedlings at heterochromatic elements (180 bp, TSI and the Ta3 retrotransposon) and euchromatic loci (*HXK1, UBC28* and *UEV1C*). Histograms show mean percentage of 2 independent e-H3.1 lines (black) and 4 independent e-H3.3 lines (grey).

promoter (H3.14) (***Figure 43B***), for ectopic expression of the epitope-tagged histone variant. For the genomic constructs, *HTR9* and *HTR4* were first chosen as representative H3.1 and H3.3 genes respectively regarding their high level of expression in seedlings during early post-germination phase as well as in other tissues (Ingouff et al., 2010 and our data). However, I was unable to amplify a full-length genomic fragment of *HTR4* including its promoter, so I switched towards the amplification and cloning of *HTR5*, which displays similar expression patterns (Ingouff et al., 2010). *HTR9, HTR4* and *HTR14* were used for ectopic expression of H3.1, H3.3 and H3.14 from the cDNA construct respectively. We decided to tag our different H3 histone variants with a FLAG-HA, which has been successfully used to purify histones and histone complexes in mammals (Tagami et al., 2004). The tag was positioned in the structured C-terminal region in order to avoid any perturbation of the N-terminal tail, which is heavily post-translationally modified. The small size of the FLAG-HA tag (2.2 kDa) is susceptible to minimize interference with H3 (≈15 kDa) function and assembly compared to a fluorescent protein tag such as GFP (≈27 kDa). I will refer to those lines in the remaining manuscript as epitope-tagged H3 (e-H3).

Once transformed in appropriate Arabidopsis plants (***Figure 43AB***) and selection of homozygous monolocus insertion of the e-H3-encoding transgenes, I tested the functionality of the constructions. Here I focus on the characterization of the lines expressing either e-H3.1 or e-H3.3 under the control of their respective endogenous promoter. We decided to transform the e-H3.1 construct (*HTR9*) into the *htr9-1* mutant and the e-H3.3 construct (*HTR5*) in the *htr5* mutants with the aim to least affect total H3 or relative H3.1/H3.3 levels in the transgenic lines. I first checked by RT-PCR the transcription of the transgenes using primers specific for the e-H3 fusion transcripts (exemplified in ***Figure 44A*** for e-H3.1). I then confirmed the correct synthesis and chromatin incorporation of the fusion protein by Western blot of nucleosomal histones in 2-week-old leaves (***Figure 44A***). Nuclear distributions of e-H3.1 and e-H3.3 were tested by immunofluorescence on isolated 2-week-old leaf nuclei using an α-HA. While immunosignals of e-H3.1 were found largely colocalized with chromocenters and low in euchromatin, e-H3.3 immunosignals were found in the whole nucleus and enriched in NOR (***Figure 44B***). The distribution of e-H3.1 and e-H3.3 at euchromatic loci (*HXK1*, *UEV1C* and *UBC28*) and heterochromatic repeats

Type	Description	Gene ID	Allele	ID	Ecotype
Histone chaperones	FAS1	At1g65470	*fas1-4*	SAIL_39_F10	Columbia-0
	FAS2	At5g64630	*fas2-5*	SALK_147693	Columbia-0
	AtHIRA	At3g44530	*athira-1*	WiscDsLox362H05	Columbia-2
	NCN1	At1g77310	*ncn1*	GABI_018D02	Columbia-0
	NCN2	At1g21610	*ncn2*	GABI_130H01	Columbia-0
	CBN	At4g32820	*cbn1*	SALK_099927	Columbia-0
	AtASF1A	At1g66740	*asf1a*	GABI_200G05	Columbia-0
	AtASF1B	At5g38110	*asf1b*	SALK_105822	Columbia-0
Histones	HTR1	At5g65360	*htr1-1*	FLAG_581G04	Wassilewskija
	HTR2	At1g09200	*htr2-1*	SALK_022688	Columbia-0
			htr2-2	SAIL_655_C07	Columbia-0
	HTR3	At3g27360	*htr3-1*	SALK_078768	Columbia-0
	HTR4	At4g40030	*htr4*	SALK_082765	Columbia-0
	HTR5	At4g40040	*htr5*	SALK_042781	Columbia-0
	HTR6	At1g13370	*htr6*	GABI_428G03	Columbia-0
	HTR8	At5g10980	*htr8*	SALK_087850	Columbia-0
	HTR9	At5g10400	*htr9-1*	SALK_148171	Columbia-0
			htr9-2	SAIL_305_C12	Columbia-0
Chromatin Modifiers	ATXR5	At5g09790	*atxr5*	SALK_130607	Columbia-0
	ATXR6	At5g24330	*atxr6*	SAIL_240_H01	Columbia-0
	SUVH4	At5g13960	*kyp-6*	SALK_041474	Columbia-0
	SUVH5	At2g35160	*suvh5-2*	GABI_263C05	Columbia-0
	SUVH6	At2g22740	*suvh6-1*	SAIL_1244_F04	Columbia-0
	MOM1	At1g08060	*mom1-2*	SAIL_610_G01	Columbia-0

***Table 3*: Arabidopsis mutant lines used in this work.**

(106B, 180 bp and TSI) was then analyzed by ChIP performed on 2-week-old leaf material. This analysis revealed enrichment of e-H3.1 at repetitive sequences over euchromatic loci (***Figure 44C***), consistent with the pattern of immunolocalization. Meanwhile, e-H3.3 occupancy was found at both euchromatic and heterochromatic loci with a preferential localization at genes compared to repetitive sequences (***Figure 44C***), in line with the immunolocalization data. The distribution of the e-H3 over the genomic domains has further analyzed for two individual H3.1 and four individual H3.3 lines by FLAG-ChIP qPCR (***Figure 44D***) on the same type of tissue. Here, e-H3.1 and e-H3.3 occupancy at euchromatic and heterochromatic loci are plotted relative to occupancy at an intergenic region (IG - between At2g17670 and At2g17680), revealing enrichment of e-H3.1 in heterochromatin relative to euchromatin. On the contrary, a preferential deposition of e-H3.3 at euchromatic loci was observed, together with reduced but nevertheless significant levels at repetitive sequences. In accordance with recent analysis of the genomic distribution of either Myc- or fluorescent protein-tagged H3.1 (*HTR13*) and H3.3 (*HTR5*) in Arabidopsis (Stroud et al., 2012; Wollmann et al., 2012; Vaquero-Sedas and Vega-Palas, 2013; Sequeira-Mendes et al., 2014; Shu et al., 2014) but also in other organisms (Mito et al., 2005; Goldberg et al., 2010), these data argue for distinct distribution of H3.1 and H3.3 along the genome, with a particular enrichment of H3.1 in heterochromatic and H3.3 in euchromatic regions, respectively. Interestingly, my study reveals significant levels of H3.3 enrichment in heterochromatin, which could be explained by the fact that, contrary to the other studies, e-H3.3 is expressed in an *htr5* mutant background. These e-H3.1 and e-H3.3 lines represent valuable and powerful tools to monitor canonical histone and H3.3 variant enrichment at particular nuclear domains and dynamics during development.

1.2.4. Study of the role of post-translational modifications of the canonical H3.1

To gain further insight into the functional importance of specific post-translational modifications of the canonical histone H3.1 in heterochromatin maintenance and organization during development, I created plants expressing

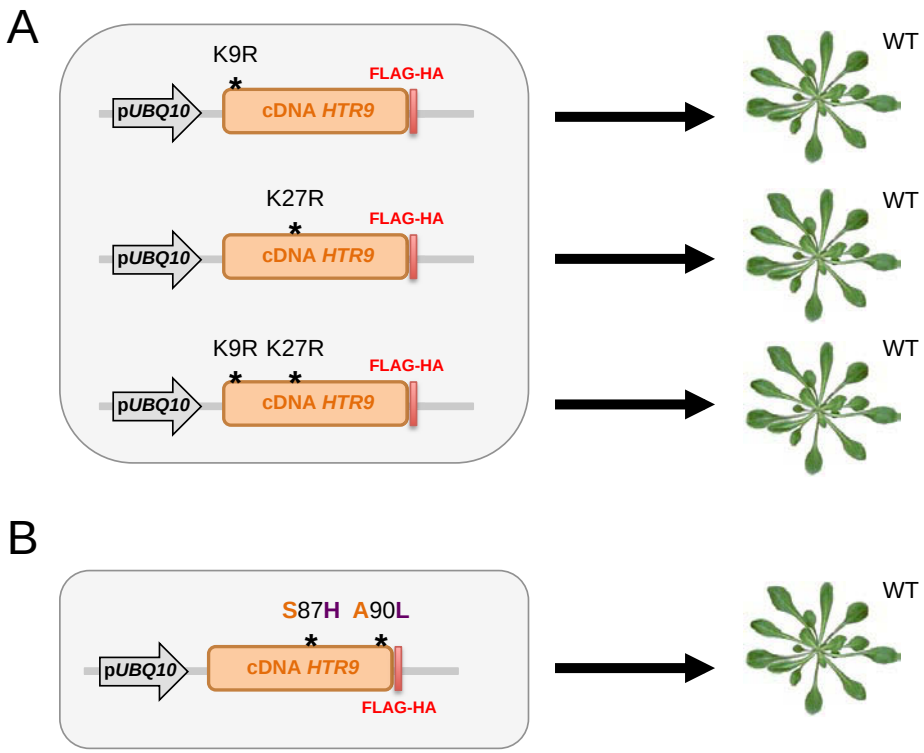

Figure 45: **Plants expressing mutated versions of e-H3.1.**

A. The p*UBQ10*:*HTR9*:FLAG-HA construct was subjected to site-directed mutagenesis to modify lysine 9 (K9) and lysine 27 (K27) residues to argenine (R) prior to transformation.
B. The p*UBQ10*:*HTR9*:FLAG-HA construct was subjected to site-directed mutagenesis to convert serine 87 to histidine and argenine 90 to leucine prior to transformation to create an hybrid H3.1/H3.3 construct.

mutated versions of e-H3.1 carrying single amino acid substitutions in residues subjected to post-translational modifications. We chose to modify residues K9 and K27 on H3.1 as the di- and monomethylation, respectively, at these sites play an important role in heterochromatin organization in Arabidopsis (Mathieu et al., 2005; Naumann et al., 2005; Jacob et al., 2009). Using the full-length cDNA of the H3.1-encoding gene *HTR9* under control of a p*UBQ10* promoter, I performed site-directed mutagenesis modifying the coding sequence so that the lysine at position 9 (K9) and / or at position 27 (K27) is mutated (***Figure 45A***). In order to maintain the global structure and charge of the amino acid chain, polar and positively charged lysine residues in position 9 and 27 were converted to argenine (R) residues, which display very similar biochemical features. The different constructs (*HTR9* K9R, *HTR9* K27R and *HTR9* double K9R/K27R) were transformed in Arabidopsis plants and the transgenes tested for expression and for homozygous monolocus insertion. Potential consequences of such mutations on chromatin organization and dynamics are currently under characterization. I expect that these tools will improve our understanding of the role of the histone post-translational marks H3K9me and H3K27me, on heterochromatin organization and dynamics.

1.2.5. Importance of amino acids at position 87 and 90 for H3 deposition

In Arabidopsis, H3.1 differs from H3.3 in only four single amino acids at position 31, 41, 87 and 90. Nevertheless, H3.1 and H3.3 are differentially distributed along the genome and are deposited by distinct chromatin assembly pathways. The signals that drive specific genomic deposition or depletion of a particular H3 variant were unknown at the beginning of my study. I wanted to investigate whether the two amino acid differences between H3.1 and H3.3 in the core region (positions 87 and 90) are sufficient to account for the distinct patterns of incorporation of H3.1 and H3.3 (Ingouff et al., 2010). To do so, I used the full-length cDNA of the H3.1-encoding gene *HTR9* on which I performed site-directed mutagenesis targeting residues at position 87 and 90. By converting serine 87 to histidine and argenine 90 to leucine, I created a hybrid H3.1 protein displaying an H3.3 signature at positions 87 and 90 (***Figure 45B***). The impact of such mutations on H3.1 genomic deposition and

dynamics is currently evaluated. During the establishment of these lines, Shi and collaborators described that replacement of H3.3 H87 and L90 residues by H3.1 S87 and A90 was sufficient to disrupt proper H3.3 deposition into rDNA arrays in tobacco, while switching of H3.3 T31/Y41 to H3.1 A31/F41 leads to defects in H3.3 nucleosome disassembly at these sites (Shi *et al.*, 2011). Using the hybrid H3.1-encoding line I created it would be thus interesting to test if an H3.1 protein displaying H3.3 H87 and L90 residues is susceptible to be recognized by the H3.3 assembly machinery and deposited at genomic regions usually enriched in H3.3.

As a conclusion of this chapter, I established and validated during my thesis a large repertoire of H3 variants and H3 chaperone mutants, together with plants expressing either wild type or modified epitope-tagged versions of the canonical H3 and H3 variants. These tools allow efficient tracking of H3 dynamics and chromatin assembly and offer new research perspectives in plant histone biology, and are important tools for current and future projects in the laboratory.

Chapter II: The histone chaperone complex HIR controls nucleosome occupancy and transcriptional silencing in plants

Céline Duc, **Matthias Benoit**, Samuel Le Goff, Lauriane Simon, Axel Poulet, Sylviane Cotterell, Christophe Tatout and Aline V. Probst.

Submitted to Plant Journal.

In an attempt to decipher the molecular players involved in the maintenance of chromatin domains such as chromocenters, and genome integrity, we focus on the yet uncharacterized plant HIR chaperone complex. The HIR complex is highly conserved between organisms and is involved in replication-independent chromatin assembly and proper histone handling and dynamics during development in yeast, Drosophila and mammals.

To date evidences for an evolutionary conserved HIR complex in plants are still lacking. In Arabidopsis, only the AtHIRA protein has been identified and its role in chromatin dynamics and genome activity remains elusive. Based on the tools and mutants characterized in **Chapter I**, our manuscript describes the four orthologs of the HIR complex subunits, termed NUCLEIN1 (NCN1), NUCLEIN2 (NCN2) and CABIN (CBN). Using a molecular approach we define the HIR subunit AtHIRA as critical for histone dynamics in Arabidopsis. *athira-1* mutants display limited non-nucleosomal histone pool and decreased nucleosomal occupancy both at euchromatic and heterochromatic loci, resulting in impaired maintenance of transcriptional silencing. Interestingly, while mutants lacking either HIR or CAF-1 chaperone complexes are viable but show reproductive defects, the simultaneous mutation of both complexes leads to severe developmental deficiencies and sterility.

This work describes the conservation of the HIR complex in Arabidopsis and its role in histone dynamics. We show that HIR and CAF-1 complexes are independent histone deposition complexes that however conjointly ensure nucleosome occupancy.

In frame of this research paper, I was involved in the generation and validation of *HIRA, NCN1, NCN2, CBN, FAS1, FAS2* T-DNA mutants. I generated the transgenic line expressing an artificial miRNA directed against AtHIRA. I participated in the crossing of individual HIR complex mutants with each other, with *fas1* and *fas2* mutants and with line L5 carrying the silent GUS transgene, the genotyping of the F2 and subsequent generations and the transcriptional characterization of the progeny. In addition, I established the double *fas1-4 athira-1* mutant and carried out the FISH analysis of centromeric and pericentromeric repeats organization in this mutant.

Abstract

Chromatin organization is essential for coordinated gene expression, genome stability, and inheritance of epigenetic information. Main components of chromatin assembly are specific complexes such as CHROMATIN ASSEMBLY FACTOR 1 (CAF-1) and HISTONE REGULATOR (HIR) that deposit histones in a DNA synthesis-dependent or -independent manner, respectively. Here, we characterize the role of the plant orthologs HISTONE REGULATOR A (HIRA), NUCLEIN (NCN) and CABIN (CBN) constituting the HIR complex, using *Arabidopsis* loss-of-function mutants. We show that loss of AtHIRA affects male gametophytic development, reduces non-nucleosomal histone levels and decreases nucleosome occupancy at both actively transcribed genes and heterochromatic regions. Concomitantly, loss of AtHIRA affects silencing maintenance of pericentromeric repeats and certain transposons, but not the rapid induction of gene expression upon an environmental stimulus. Our genetic analysis based on crosses between mutants deficient in subunits of the CAF-1 and HIR complexes shows that only the simultaneous loss of both, CAF-1 and HIR histone H3 chaperone complexes, impacts plant survival, growth and reproductive development severely. Our results suggest functional compensation between the different histone chaperone complexes in plants and plasticity in histone variant interaction and deposition.

Introduction

Eukaryotic DNA is organized into chromatin. Its basic subunit, the nucleosome, consists of 146 bp of DNA wrapped around a histone octamer that is composed of a $(H3\text{-}H4)_2$ tetramer and two histone H2A-H2B dimers. Chromatin organization profoundly affects accessibility of DNA to the cellular machinery and therefore impacts all cellular processes operating on DNA, such as transcription, replication, repair and recombination. To coordinate these different functions, remodeling of chromatin is required to allow access or exclusion of different factors. Remodeling can encompass movement of nucleosomes along the DNA, but also their disassembly and reassembly, as during the passage of the transcriptional machinery (Petesch and Lis, 2012). These processes are facilitated by factors modulating the stability of the nucleosomes or that of their association with the DNA. Nucleosome stability is affected by covalent modifications of histone proteins and incorporation of different histone variants (Jin and Felsenfeld, 2007). Except histone H4, all histone proteins occur in non-canonical variants that differ in their primary amino acid sequence from the canonical paralogs (Talbert and Henikoff, 2010). These differences range from a few amino acids to large protein domains (Talbert et al., 2012). The canonical histone H3.1 and its variant H3.3, for example, diverge by only four amino acids, but nevertheless are incorporated differently during the cell-cycle and show specific distribution patterns in genomes of mammals and plants (Goldberg et al., 2010; Wollmann et al., 2012; Stroud et al., 2012; Filipescu et al., 2013; Tagami et al., 2004). While nucleosomes with H3.1 are thought to package DNA globally in a DNA synthesis-linked process, the so-called replacement variant H3.3 is preferentially incorporated at enhancers, promoters and gene bodies of actively transcribed genes throughout the cell cycle (Ahmad and Henikoff, 2002; Goldberg et al., 2010; Jin et al., 2009).

The highly basic histone proteins are accompanied from synthesis to chromatin assembly by a network of histone chaperones, thereby preventing uncontrolled interaction with nucleic acids or negatively charged proteins. Histone chaperones were defined as proteins that “associate with histones and stimulate a reaction involving histone transfer without being part of the final product” (De Koning et al., 2007). Consequently, they are involved in all aspects of histone dynamics, such as transport and storage, chromatin assembly, disassembly and parental

histone transfer during DNA replication (Filipescu et al., 2013; Groth et al., 2007; De Koning et al., 2007). In general, histone chaperones can be classified by their preferential binding to either H3-H4 or H2A-H2B subunits. In addition, some chaperones show specificity for particular histone variants and play a crucial role in their chromatin distribution (Tagami et al., 2004; Goldberg et al., 2010; Drané et al., 2010).

While H3 histone variants are assumed to have evolved independently in animals and plants (Ingouff and Berger, 2010), histone chaperones are highly conserved through evolution. The chaperone proteins Anti-Silencing Function 1 (ASF1) bind H3-H4 dimers (Natsume et al., 2007; English et al., 2006) in the cytoplasm and are involved in histone import into the nucleus (Campos et al., 2010). ASF1 then transfers H3-H4 histones to other chaperone complexes involved in nucleosome assembly. In mammals, two distinct pathways control either the deposition of the canonical histone H3.1 or of the variant H3.3. The Chromatin Assembly Factor 1 (CAF-1) consisting of the three subunits p150, p60 and p48 ensures histone deposition in a DNA synthesis-dependent manner during replication and repair (Gaillard et al., 1996; Stillman, 1989). CAF-1 specifically deposits H3.1 (Tagami et al., 2004; Drané et al., 2010) and interacts with ASF1 via its p60 subunit (Tyler and Collins, 2001). Independent of DNA synthesis and throughout the whole cell cycle, histone deposition is promoted by HISTONE REGULATOR A (HIRA), which shows high specificity for the replacement variant H3.3 (Ray-Gallet et al., 2002; Tagami et al., 2004). HIRA depletion results in reduced genome-wide loading of H3.3 (Goldberg et al., 2010; Pchelintsev et al., 2013). In addition, H3.3 is deposited at telomeres and pericentromeric satellites by Death-Associated protein (DAXX) and Alpha-Thalassemia/mental Retardation X-linked syndrome protein (ATRX) (Drané et al., 2010; Goldberg et al., 2010). In mammals, the histone chaperone DEK also contributes to H3.3 deposition (Sawatsubashi et al., 2010). HIRA is part of a multimeric complex termed HIR complex, first identified in *Saccharomyces cerevisiae* where it consists of four subunits (Hir1, Hir2, Hir3 and Hpc2) and functions as repressor of histone genes outside S phase (Osley and Lycan, 1987). Orthologs of Hir1 and Hir2 have then been identified as HIRA in Drosophila and mammals. In humans, the complex further comprises Ubinuclein1 (UBN1) and the hypothetical protein FLJ25778 (also termed Ubinuclein2) as the orthologs of yeast Hpc2, as well as calcineurin-binding protein (CABIN1), the

ortholog of Hir3. All HIR subunits co-purify with epitope tagged H3.3 or HIRA (Tagami et al., 2004; Drané et al., 2010). HIRA seems to be central to the complex, as it mediates the binding to UBN1 via its N-terminal WD40 repeats (Balaji et al., 2009) and to CABIN1 via its Hira domain (Yang et al., 2011). HIRA further interacts with ASF1 through its conserved B domain (Tang et al., 2006). Moreover, all HIR complex members have the ability to directly interact with DNA (Ray-Gallet et al., 2011).

The study of histone chaperone complexes as well as their role for histone dynamics during development has been hampered in higher organisms, as these factors are essential for survival: their absence is lethal at early stages of embryo development. Depletion of CAF-1 subunits in human cell cultures leads to S phase arrest (Ye et al., 2003), and mice embryos deficient in the large subunit of the CAF-1 complex fail to develop beyond early embryonic stages (Houlard et al., 2006). Similarly, mutants of the Drosophila ortholog p180 die during larval development (Klapholz et al., 2009). In Arabidopsis, the CAF-1 complex consists of the subunits FASCIATA1 (FAS1), FASCIATA2 (FAS2) and MULTICOPY SUPPRESSOR OF IRA1 (MSI1) (Kaya et al., 2001). In contrast to vertebrates, Arabidopsis mutants deficient in one of the two large subunits FAS1 or FAS2 are viable, but show pleiotropic morphological abnormalities such as fasciated stems, serrated leaves, meristem alterations or increased trichome branching (Kirik et al., 2006; Exner et al., 2006; Kaya et al., 2001). Consistent with the role in chromatin assembly during DNA replication, CAF-1 mutants fail to maintain repressive chromatin states, as illustrated by weak transcriptional reactivation of normally silent endogenous repetitive sequences and the stochastic reactivation of certain transposable elements (Takeda et al., 2004; Schönrock et al., 2006; Ono et al., 2006). Only mutants in the third subunit MSI1 are lethal, probably due to the participation of this subunit in multiple chromatin modifier and remodeling complexes (Hennig et al., 2005).

Similarly to the CAF-1 knockout, depletion of mammalian HIRA is lethal, since HIRA-knockout mice die during embryonic development (Roberts et al., 2002). Furthermore, down-regulation of HIRA in Xenopus embryos causes gastrulation defects (Szenker et al., 2012), phenotypes that could be explained by the role HIRA plays in transcription (Formosa et al., 2002; Schwartz and Ahmad, 2005; Ray-Gallet et al., 2011). In contrast, Drosophila HIRA is only required for H3.3 deposition in the male pronucleus after fertilization (Loppin et al., 2005), but not for viability (Bonnefoy et al., 2007). Other chaperones, such as ATRX/XNP and DAXX/DLP, are likely to

compensate absence of HIRA in Drosophila (Schneiderman et al., 2012). How much plants depend on HIRA for normal development, and how histones are assembled outside S phase in plants has not been addressed yet. Since an ortholog of the metazoan HIRA protein has previously been identified in Arabidopsis (Phelps-Durr et al., 2005; Ingouff et al., 2010), we decided to study the role of the Arabidopsis HIR complex in histone and chromatin dynamics in plants.

We show here that the Arabidopsis genome encodes four genes orthologous to all HIR subunits that potentially constitute a functional HIR complex. Our molecular analyses identify AtHIRA as an important player for histone dynamics in Arabidopsis. As in case of the CAF-1 mutants, plants lacking the AtHIRA subunit are viable but show developmental defects and are impaired in maintenance of transcriptional silencing. Loss of AtHIRA results in a reduced pool of non-nucleosomal histone H3 and affects nucleosome occupancy not only at euchromatic but also at heterochromatic targets. Simultaneous loss of both CAF-1 and HIR complexes causes severe developmental phenotypes. Surviving plants show important defects in plant growth and reproductive development as well as reduced nucleosome occupancy, without being further affected in maintenance of silencing and heterochromatin organization. We conclude that, in plants, the two evolutionary conserved chromatin assembly complexes CAF-1 and HIR are involved in independent pathways of nucleosomal assembly, but compensate at least partially for one another.

Results

Arabidopsis expresses orthologs of all HIR subunits

To identify candidates for all Arabidopsis genes orthologous to the yeast and mammalian HIR complex subunits, we searched for related protein sequences that are conserved through evolution. A HIRA ortholog of similar length as the mammalian protein had been described earlier (Phelps-Durr et al., 2005; Ingouff et al., 2010; Amin et al., 2011). Using MUSCLE sequence alignments and Interproscan protein prediction, we compared HIRA protein domains between humans, Drosophila and two plant HIRA proteins. The overall protein structure is conserved in plants and also similar to the animal counterparts (50% similarity between human and Arabidopsis HIRA). AtHIRA contains the N-terminal WD40 repeats involved in protein-protein interaction and the C-terminal Hira domain (***Figure 1A***). A detailed protein sequence alignment of the predicted B domain required for binding of human ASF1 shows divergence in the core B domain, but reveals conservation in plants of all critical amino acids of the experimentally defined minimal B domain (***Supplemental Figure 1A***) (Tang et al., 2006). Phylogenetic analysis confirmed that both plant and animal kingdoms share a conserved HIRA protein (***Supplemental Figure 1B***).

Blast searches with the mammalian UBN1 and UBN2 (AAF31755.1 and XP_944191) as baits identified two orthologs in Arabidopsis, which we named AtNUCLEIN1 (NCN1, At1g77310) and AtNUCLEIN2 (NCN2, At1g21610). These two proteins are of similar length, show 59.7% protein sequence identity but are shorter than their human counterparts. As other orthologs, NCN1 and NCN2 proteins contain the evolutionarily conserved approximately 50 aa long motif termed Hpc2-related domain (HRD) (Banumathy et al., 2009) (***Figure 1B*** and ***Supplemental Figure 1C***) as well as the less conserved approximately 30 aa long region termed NHRD (N-terminal to the HRD region) (***Figure 1B*** and ***Supplemental Figure 1D***). In mammals, this domain is necessary and sufficient for interaction with the HIRA WD40 repeats (Tang et al., 2012). NCN1 and NCN2 proteins share another region of similarity with UBN1 and UBN2 called the Ubinuclein middle domain (***Figure 1B***). The phylogenetic tree of NUCLEIN proteins further shows that also other higher plants contain two or more closely related paralogs (***Supplemental Figure 1E***).

In most organisms, the HIR complex includes a third member type, the calcineurin binding protein (CABIN1), characterized by a range of tetratricopeptide (TPR)-like bi-helical repeats, which can form a scaffold for protein-protein interaction (Balaji et al., 2009). BLAST searches with the human CABIN1 protein identified an Arabidopsis ortholog (At4g32820), that we termed AtCABIN (CBN). CBN displays the characteristic TPR repeats but is shorter than the human ortholog (***Figure 1C***). Phylogenetic analysis confirmed that CABIN is found throughout the plant kingdom, some plant genomes encoding two CABIN paralogs (***Supplemental Figure 1F***). All four putative members of the HIR complex identified here localize to the nucleus according to the Gene Ontology terms in TAIR.

To test whether the respective genes are indeed expressed in Arabidopsis, we performed RT-qPCR on 4 week-old WT plants. We confirmed expression of all four genes (***Figure 1D***). We further validated expression of *AtHIRA*, *NCN1, NCN2* and *CBN* by RT-PCR in both dividing and non-dividing tissues (***Supplemental Figure 1G***).

Taken together, these results show that the Arabidopsis genome encodes all essential components of a potentially functional HIR complex, which are expressed in all tested tissues. Conservation of the WD40 repeats, the B and Hira domains suggests that, as in animals, AtHIRA could serve as the scaffold protein for CBN and NCN recruitment and could possibly bind ASF1.

Arabidopsis HIR complex mutants are viable

To gain insight into the biological function of the Arabidopsis HIR complex, we obtained T-DNA insertion mutants for each gene encoding a HIR complex subunit (***Figure 2A-D***). As conflicting results were reported concerning the viability of *AtHIRA* mutants (Phelps-Durr et al., 2005; Ingouff et al., 2010), we acquired four lines with different T-DNA insertions mapping to the *AtHIRA* locus (***Figure 2A***, ***Supplemental Figure 2A***). We determined the exact T-DNA insertion sites by sequencing PCR products obtained with a T-DNA-specific primer and genomic primers surrounding the predicted insertion site (***Figure 2A***, ***Supplemental Figure 2A***). By genotyping, we identified plants homozygous for all mutant alleles except SALK_143806, which lacked any T-DNA insert in seeds from various sources. The insertion in SALK_019573 (also available as homozygous line SALK_019573C) maps to the putative promoter region and contains 2 T-DNA insertions 55 bp apart. The inserts of

GABI_775H03 map to the 5'UTR. The WiscDsLox362H05 allele (Ingouff et al., 2010) contains 2 T-DNA insertions, in the 5th intron and the 6th exon, respectively. RT-PCR and qPCR analysis confirmed that only the WiscDsLox362H05 allele (*athira-1* (Ingouff et al., 2010)), affects *AtHIRA* expression (***Figure 2A***, ***Supplemental Figure 2A-B***). We further generated a transgenic line expressing an artificial microRNA (amiRNA) construct (Schwab et al., 2006) targeting *AtHIRA* transcripts (*athira*^{amiRNA}) and confirmed reduced *AtHIRA* expression levels (***Supplemental Figure 2C***).

Besides *AtHIRA* mutants, we identified T-DNA insertion alleles for *NCN1*, *NCN2* and *CBN* and confirmed the absence of the corresponding full-length transcripts by RT-PCR (***Figure 2B-D***).

Single mutants of the HIR complex subunits display no obvious phenotypic deviation in leaf or silique growth compared to wild-type (WT) plants when grown under standard conditions (***Figure 2E***, ***Supplemental Figure 2D***). In contrast, *fas1-4* and *fas2-5* mutants which are impaired in one of the two larger subunits of the CAF-1 complex show pleiotropic phenotypes including leaves with serrated margins, alteration of silique shape and size as well as a large number of unfertilized ovules (**Supplemental Figure 2D-G**). Therefore, we looked closer at *athira-1* mutant siliques and observed less viable seeds and more unfertilized ovules than in WT (***Figure 2F-G***), but the difference was smaller than in *fas* mutants (***Supplemental Figure 2F-G***). The same phenotype, although less pronounced, was also observed in the *athira*^{amiRNA} line (***Supplemental Figure 2G***). We first confirmed the previously reported (Ingouff et al., 2010) standard Mendelian genetic transmission of the T-DNA mutant allele in the progeny of a self-fertilized *athira-1-1/AtHIRA* plant (21 plants, n=72, $p<0.05$). Then, to determine whether this phenotype results from a male- or a female-specific defect, we carried out reciprocal crosses between *athira-1* mutants and wild type plants. We observed unfertilized ovules and aborted seeds only in crosses in which the pollen was derived from an *athira-1* mutant plant, suggesting predominant defects in male gametogenesis. We therefore investigated male gametophytic development in more detail. In contrast to *fas1-4* and *fas2-5* anthers (***Supplemental Figure 2H***) that are heart-shaped and contain few or no viable pollen, anthers of HIR complex mutants develop rather normally, however a fraction of pollen grains are also non-viable in *athira-1* as revealed by Alexander staining (***Figure 2H***). These data suggest roles for the CAF-1 and HIR complexes in male gametogenesis.

Endoreplication, which involves one or several rounds of DNA replication without nuclear or cell division, is part of regular plant development and leads to polyploidy in somatic cells. Deficiency in histone chaperones can impact endoreplication levels, *e.g*. mutants in the CAF-1 complex switch prematurely to the endocycle and show increased endopolyploidy levels (Ramirez-Parra and Gutierrez, 2007), while the simultaneous loss of the two small H3-H4 chaperone proteins ASF1A and ASF1B leads to reduced endocycle numbers (Zhu et al., 2011). To investigate whether absence of a functional HIR complex member impacts endopolyploidy levels, we carried out flow-cytometry analysis of nuclei from 10 day-old shoot tissues. Whereas *fas2-5* mutant plants show a significantly increased fraction of 8C and 16C nuclei as expected (one and two rounds of endoreplication), endopolyploidy profiles of HIR mutants are not significantly different from WT plants (***Figure 2I***). This suggests that absence of a functional HIR complex does not impact endoreplication.

Thus, single mutants in the Arabidopsis HIR complex are viable and do not reveal altered plant growth, with the exception of plants lacking the AtHIRA subunit that show defects in male reproductive development.

The *athira-1* mutant shows a reduced non-nucleosomal histone pool and altered nucleosome occupancy

In analogy to yeast and animal models, Arabidopsis CAF-1 and HIR complexes are assumed to bind non-nucleosomal histones and coordinate their assembly into nucleosomes. We therefore wanted to investigate whether the mutations would influence the pool of histones in chromatin (nucleosomal) and the pool of free (non-nucleosomal) histones. To recover the non-nucleosomal histone fractions we applied a cell lysis and centrifugation procedure and determined the amount of H3 in *fas1-4* and *athira-1* mutants relative to WT plants by quantitative western blots (***Figure 3A-B***). Both mutants display a reduction of non-nucleosomal H3 levels, suggesting that histone flow and amount of histones available for *de novo* deposition are altered in mutants of both chromatin assembly complexes. Then, we investigated whether the nucleosomal H3 levels are globally affected in *fas1-4* and *hira* mutants. To this aim, we obtained total and nucleosomal histones of the same extracts (see Material and Methods). Using this approach no global reduction in H3

nucleosomal content was observed in either *fas1-4* or *hira* mutants (***Supplemental Figure 3A***).

Then, to compare nucleosome occupancy at specific genomic sites in WT, *fas1-4* and *hira* mutants in a quantitative manner, we used H3-ChIP combined with qPCR. We first analyzed nucleosome occupancy at three constitutively active genes (*UBC28, UEV1C* and *HXK1)* with different expression levels (***Supplemental Figure 3B***). Active genes are generally enriched in H3.3 (Wollmann et al., 2012; Stroud et al., 2012), suggesting that they would be preferential targets for HIRA-mediated H3 deposition. We chose three different amplicons, in the 5', middle and 3' region of each gene (***Figure 3C***). The middle and 3' regions are enriched in H3.3 relative to input in the ChIP-Seq datasets from (Stroud et al., 2012) while neither H3.1 nor H3.3 are particularly enriched in the 5' region (***Supplemental Figure 3C-E***). When we determined H3 enrichment relatively to input at these six distinctive genomic regions in 3 week-old WT and mutant plants grown *in vitro*, we found that, at actively transcribed genes, nucleosome occupancy was unaffected in *fas1-4* mutants. In *athira-1* mutants, however, *UEV1C* and *HXK1* had mildly reduced H3 levels at the middle and 3' regions (***Figure 3C***), but not at the 5' region, revealing a specific role for AtHIRA in H3 deposition at these genic regions.

Since *fas1* mutants were previously shown to have moderately reduced nucleosome occupancy at selected pericentromeric sequences (Pecinka et al., 2010), we also included three heterochromatic repetitive elements (180 bp repeat, 106B centromeric satellites and an endogenous family of transcriptionally repressed repeats called Transcriptionally Silent Information (TSI, (Steimer et al., 2000)), as well as an intergenic region (Pecinka et al., 2010) in our analysis. These heterochromatic regions are globally enriched in H3.1 (Wollmann et al., 2012; Stroud et al., 2012) (Supplemental ***Figure 3F-H***), while neither H3.1 nor H3.3 are particularly enriched at the intergenic region (***Supplemental Figure 3I***). We observed reduced nucleosomal occupancy at 106B and TSI in *fas1-4* mutants (***Figure 3D***) in agreement with previous results (Pecinka et al., 2010). Unexpectedly, we also observed that nucleosome occupancy is reduced in *athira-1* mutants at these two heterochromatic regions and at the intergenic region (***Figure 3D***).

We conclude that loss-of-function of either of the two chromatin-assembly complexes CAF-1 and HIR affects the non-nucleosomal H3 histone pool. Furthermore, loss of AtHIRA impacts nucleosome occupancy at both euchromatic

and heterochromatic regions while loss of CAF-1 mainly affects heterochromatic sequences.

Loss of HIRA interferes with maintenance of transcriptional silencing but not with gene induction upon salt stress

The observed differences in nucleosome occupancy prompted us to investigate the functional consequences of altered histone dynamics in HIR complex mutants. We first analyzed the impact on maintenance of transcriptional silencing in heterochromatin at these three heterochromatic regions (106B, 180 bp and TSI) by ChIP-qPCR. We extracted RNA from 18-day-old soil grown plants and quantified transcript levels by RT-qPCR. As expected, TSI silencing is partially released in *fas1-4.* In agreement with the changes in nucleosomal occupancy, the *athira-1* mutants also show alleviation of TSI silencing (***Figure 4A***), which is not seen in the *cbn*, *ncn1* and *ncn2* mutants. None of the HIR-complex subunit mutants reactivates silencing at 106B, 180 bp or the multicopy p35S::GUS locus in the transgenic line L5 background (Morel et al., 2000) (***Figure 4A*** and ***Supplemental Figure 4A***). To test whether the silencing release in *athira-1* is restricted to TSI sequences or is more general, we analyzed transcript levels of several targets previously reported to be affected in different silencing mutants. We observed alleviation of silencing of the Ta3 retrotransposon and a Mutator-like DNA transposon (Mule, At2g15810) (***Figure 4B***) in *athira-1* compared to WT plants.

Given the suggested function of HIRA in transcription in other species, we wanted to test whether gene transcription is affected in *athira-1* mutants. We first analyzed transcript levels of *UEV1C* and *HXK1*, which show reduced nucleosome occupancy in *athira-1* mutants, but expression levels in WT and *athira-1* mutants were equal (***Supplemental Figure 4B***). We then tested whether loss of a functional HIR complex impacts the plant's capacity to rapidly activate gene expression upon an environmental stimulus. We exposed plants to salt stress and analyzed the expression of four genes previously shown to be induced under these conditions (Zeller et al., 2009). *PP2C* (At3g16800) and *ERF/AP2* (At1g74930) are moderately expressed under normal growth conditions (51 and 54.5 reads per million (RPM), respectively), while MYB41 (At4g28110) and *CBF1* (At4g25490) are not expressed under non-inducing conditions (Zeller et al., 2009; Duc et al., 2013). In WT plants, all four genes are induced after 1 h of exposure to high salt medium, undergoing

changes in transcript levels from 2 fold to several hundred times, depending on the considered gene (***Figure 4C***). The *athira-1* mutant plantlets are not impaired in the rapid transcriptional response and up-regulate salt-responsive genes in a manner similar to WT plants (***Figure 4C***).

Taken together, AtHIRA is implicated in maintenance of transcriptional gene silencing at a selection of endogenous repeat elements and transposons, but is dispensable for rapid gene induction upon salt exposure.

Epistatic relationship between CAF-1 and HIR complexes

To gain further insight into the relative importance of the different members of the HIR complex and to examine the epistatic relationship between CAF-1 and HIR complexes, we crossed *fas1 and fas2* mutants with each mutant (*athira-1*, *ncn1*, *ncn2* or *cbn*) for the different potential HIR complex subunits. We performed segregation analyses in F2 progenies from several independent F1 plants obtained for each of the eight crosses (***Table 1***). We selected plants displaying the serrated leaf margins of homozygous *fas* plants and then determined their genotype for the corresponding HIR-complex mutation. *FAS1, NCN1* and *NCN2* genes are localized on chromosome 1 (~39cM and ~53cM apart from *FAS1*, respectively, ***Supplemental Figure 5A***). The number of *fas1-4 ncn1* and *fas1-4 ncn2* double homozygotes matched the ratio expected for this genetic distance (see Material and Methods); the number of *fas1-4 cbn* double mutants reflects independent segregation as predicted (***Table 1***). None of the double homozygous plants derived from these three crosses exhibited any aggravation of the *fas1-4* growth phenotypes and were fertile (***Figure 5A***). In contrast, significantly less *fas1-4 athira-1* double homozygous mutants were obtained (***Table 1***). The distorted segregation was confirmed by genotyping F2 plants without prior selection of the *fas* phenotype (n= 150, ***Supplemental Table 1A***). The *fas1-4 athira-1* mutants are dwarf and dark-green (***Figure 5B***), have flowers with misshapen carpels and short stamens with aberrant anthers (***Figure 5C***) and do not produce siliques, in agreement with complete male sterility revealed by Alexander staining (***Figure 5D***). No aggravated loss in pollen viability or increase in unfertilized ovules was observed in their heterozygous sister plants (***Supplemental Figure 5B-C***).

We then analyzed the progeny from crosses between *fas2-5* and HIR complex mutants. We obtained *fas2-5 ncn1, fas2-5 ncn2* and *fas2-5 cbn* mutants (***Figure 5E***)

although with reduced frequency (***Table 1***). The *fas2-5 ncn1* and *fas2-5 cbn* double mutants produced siliques, which contained only unfertilized ovules in case of *fas2-5 ncn1* and very little seeds in *fas2-5 cbn* mutants while *fas2-5 ncn2* siliques were similar to WT ones (***Figure 5F***). We therefore looked at anthers from *fas2-5 ncn1* and *fas2-5 cbn* plants, which showed only little viable pollen and in case of the *fas2-5 ncn1* mutants, they were often strongly affected in shape (***Figure 5G***). We could not observe any phenotypic differences between *fas2-5* and *fas2-5 ncn2* plants (***Figure 5E-F***). No *fas2-5 athira-1* double homozygous mutants were observed in the progeny of two independent F1 plants (***Table 1***). Genotyping of additional F2 plants without prior selection of the *fas2* phenotype (***Supplemental Table 1B***) identified two double homozygous mutant plants; their development was however arrested before formation of the first leaves and they died shortly after (***Figure 5E***). Furthermore, *fas2-5 athira-1/HIRA* plants are almost sterile (***Supplemental Figure 5D***) and show little viable pollen (***Supplemental Figure 5E***). We conclude that the simultaneous mutation of CAF-1 and HIR complexes causes strong defects ranging from severe growth and developmental difficulties to lethality.

Taken together, while NCN2 seems to be dispensable for plant survival and reproduction, the simultaneous mutation of FAS2 and the HIR subunits CBN, NCN1 or HIRA causes morphological aberration of increasing severity.

CAF-1 and HIR complexes are involved in independent, but complementary pathways of chromatin assembly

As we anticipated that absence of either FAS1 or FAS2 would render the CAF-1 complex non-functional, we expected similar phenotypes for the two sets of crosses described above. However, all plants carrying the *fas2-5* mutation display more severe defects than those carrying the *fas1-4* mutant allele, suggesting that the latter is not a complete loss-of-function allele. While RT-PCR analysis confirmed the absence of *FAS2* full-length transcripts in *fas2-5* mutants (***Supplemental Figure 6A***), we could detect residual *FAS1* full-length transcripts in *fas1-4* mutants (***Supplemental Figure 6B***, (Ramirez-Parra and Gutierrez, 2007)) but with a 90% decrease compared to the WT level (***Supplemental Figure 6C***). Therefore, *fas1-4 athira-1* plants could still preserve residual CAF-1 activity permitting survival. We also investigated whether other H3 chaperone complexes are differentially expressed in the surviving double mutant plants and analyzed transcript levels of *ASF1A* and

ASF1B by RT-qPCR. We observed a change in the balance of *ASF1* expression: in *fas1-4 athira-1* mutants, *ASF1A* expression is down-regulated while *ASF1B* is up-regulated (***Figure 6A***). Hence, a change in the ASF1A and B protein levels might help adjusting histone flow to the remaining assembly complexes.

The surviving *fas1-4 athira-1* plants offer the unique opportunity to study the molecular consequences of simultaneous mutation of CAF-1 and HIR complexes. To obtain sufficient plant material, we selected double mutants grown on soil by their phenotype from the segregating progeny of *fas1-4/FAS1 athira-1* mother plants (***Supplemental Figure 6D***). Since *fas1-4 athira-1* plants are severely affected in growth and development, we first checked whether heterochromatin organization and silencing are further impaired in the double mutants compared to the single mutants. RT-PCR analysis on 4-week-old soil-grown plants showed that *fas1-4 athira-1* mutants release *TSI*, *Ta3* and *Mule* repression, but not above levels already present in single mutants. In addition, silencing at 106B and 180 bp repeats is not affected (***Figure 6B-C***). Furthermore, Fluorescence *in situ* hybridization revealed that the global organization of 180 bp and TSI repetitive elements into chromocenters is not altered in *fas1-4 athira-1* nuclei (***Supplemental Figure 6E***).

We therefore wondered to what extend histone dynamics and nucleosome occupancy are affected in the surviving *fas1-4 athira-1* plants. As expected from our observations of the respective single mutants, non-nucleosomal H3 histone protein amounts are reduced in *fas1-4 athira-1* plants relative to WT (***Figure 6D-E***). When we assessed nucleosome occupancy by H3-ChIP combined with qPCR on 4-week-old soil-grown plants, we found that nucleosome occupancy was severely reduced at heterochromatic repeats and an intergenic region as well as at the three actively transcribed genes tested and this at most analyzed regions (***Figure 6F-G).***

Taken together, we conclude that if CAF-1 and HIR-mediated assembly pathways are simultaneously impaired, plants fail to maintain nucleosome occupancy in both actively transcribed and transcriptionally repressed genomic regions. Moreover, our data indicate that organization and silencing of repetitive sequences can be maintained despite significant reduction in nucleosome occupancy, suggesting that alternative silencing mechanisms compensate impaired nucleosome assembly and consequently altered nucleosomal content in plants. The aggravated reduction in H3 occupancy in *fas1-4 athira-1* double mutants implies that CAF-1 and

HIR complexes are involved in at least partially independent pathways of chromatin assembly that concomitantly contribute to maintenance of nucleosome occupancy.

Discussion

Proper packaging of DNA into chromatin is essential for genome structure and ensures stability and inheritance of epigenetic information. A particular role in these processes can be assigned to the factors responsible for histone deposition. Indeed, the different chromatin assembly factors as well as other histone chaperones involved in histone transport and storage are highly conserved through evolution.

Distinct contribution of the different members of the HIR complex

In this study, we identified *bona fide* orthologs of the mammalian HIRA, UBINUCLEIN and CABIN1 proteins in the Arabidopsis genome and revealed different levels of importance for the members of the complex. While growth and vegetative development is not affected in single mutants for the different subunits, lack of AtHIRA causes defects in reproductive development. An intriguing hypothesis is that AtHIRA is implicated in histone variant dynamics during male gametogenesis, which necessitates reprogramming of the histone variant repertoire (Ingouff et al., 2007, 2010), to result in the presence of only H3.3 and H3.3-like variants in mature pollen (Ingouff et al., 2010). Regarding the other subunits of the HIR complex, NCN2 is dispensable for plant survival and reproduction in WT or *fas* mutant background, in agreement with the fact that growth or reproduction in the *ncn1 ncn2* double mutant is not impaired beyond that of *ncn1* alone (data not shown). CBN/NCN1 and AtHIRA are less dispensable, in growing order. Given the conservation of the functional domains found in other organisms, HIRA may mediate the interaction with NCN1, CBN and potentially ASF1, and its absence could destabilize the complex. This is the case in yeast where loss of Hir1 or Hir2 reduces Hir3 protein levels (Song et al., 2013) and in mammals, where depletion of HIRA leads to a concomitant decrease in UBN1 and CABIN1 (Ray-Gallet et al., 2011). Our data, however, provide evidence that the Arabidopsis HIR complex is at least still partly functional in the absence of NCN1 or CBN, reflecting mammalian cells where CABIN1 only plays a limited role in H3.3 deposition, followed by UBN1 and finally HIRA, which is crucial for H3.3 incorporation (Ray-Gallet et al., 2011). Furthermore, transcriptional repression of yeast histone genes depends on Hir1 and Hir2, but only partly on Hir3 (Spector et al., 1997; Osley and Lycan, 1987) and the Drosophila HIR complex does not comprise a CABIN ortholog (Amin et al., 2011). An alternative and not exclusive hypothesis is

that AtHIRA also has HIR complex-independent functions. Indeed, genome-wide ChIP-Seq analysis in human cells localized HIRA to several chromosomal positions that are not co-occupied by UBN1 or ASF1 (Pchelintsev et al., 2013). We expect that specific functions of the different Arabidopsis HIR complex subunits might be revealed only under certain growth and environmental conditions, or in particular cell types.

Role of HIRA in nucleosome dynamics

Loss of the AtHIRA subunit results in reduced levels of non-nucleosomal histones, as also observed for CAF-1 mutants. This suggests that absence of histone assembly complexes affects histone flow and might render those histones, which are not readily deposited onto chromatin, prone to degradation. Histone deposition, however, is globally achieved in single mutants for both histone deposition complexes, as the total amount of nucleosomal H3 histones is comparable to that in WT. Analyzing nucleosome occupancy in a locus-specific manner, we found that loss of AtHIRA affects nucleosomal occupancy at certain active genes, and this within the body and 3' ends, regions that were previously shown to be enriched in H3.3 (Stroud et al., 2012). This nucleosome loss at active genes could be explained by failure to restore nucleosomes using H3.3 after passage of the transcriptional machinery. Interestingly, similar to CAF-1, HIRA also impacts H3 occupancy at heterochromatic targets. Despite heterochromatin being not (or very poorly) transcribed and generally considered to have slow histone exchange rates, the presence of H3.3 has been reported in centric and pericentric heterochromatin and telomeres in mouse and human (Drané et al., 2010; Goldberg et al., 2010; Lewis et al., 2010; Wong et al., 2009; Morozov et al., 2012; Dunleavy et al., 2011). It is therefore possible that AtHIRA is implicated in histone deposition at heterochromatic targets, a process that could be particularly important in those cells that undergo neither replication nor endoreplication. Such a requirement for the HIR complex may explain the subtle, but significant transcriptional reactivation of endogenous pericentromeric repeats and transposons observed in *athira-1* mutants and suggest nucleosome occupancy maintenance contributes to transcriptional gene silencing. Interestingly the HIRA orthologs in fission yeast are also involved in transcriptional silencing at pericentromeric heterochromatin (Blackwell and Martin, 2004; Yamane et al., 2011). Further studies, taking the cellular properties of different tissues and developmental

variations into account, should shed further light on cell-specific roles of the HIR complex.

Several lines of evidence link HIRA and deposition of histone replacement variants to transcription control (Ahmad and Henikoff, 2002; Formosa et al., 2002; Sakai et al., 2009; Ray-Gallet et al., 2011; Schneiderman et al., 2012). However, when we analyzed the capacity of HIRA-deficient plants to activate gene transcription in response to salt stress, we found no difference compared to WT, neither for genes with basal expression levels nor for genes silent before induction. Either HIR-mediated histone dynamics or the incorporation of the replacement variant during transcription could be dispensable for proper expression at these sites. The latter is in agreement with observations from both Tetrahymena and Drosophila, which survive and show correct gene expression in absence of the histone variant H3.3 (Hödl and Basler, 2009; Cui et al., 2006) and the lack of strong phenotypes observed in our *athira-1* mutant plants. It is likely that alternative histone chaperone complexes are also implicated in replacement variant deposition. While no DAXX ortholog has been identified in plants (Zhu et al., 2013), Arabidopsis encodes several DEK proteins, and other yet unidentified histone chaperones could play a role in histone variant dynamics.

Functional compensation in histone deposition between CAF-1 and HIR complexes?

The combination of the *fas2-5* mutation with *athira-1* causes post-germination lethality while *fas1-4 athira-1* mutants are viable but sterile. We found remaining full-length transcripts in plants carrying the *fas1-4* allele. The survival of *fas1-4 athira-1* mutants could thus be explained by residual CAF-1 activity, concomitantly with slow growth and potentially a premature switch to endoreplication observed in *fasciata* mutants (Ramirez-Parra and Gutierrez, 2007). In addition, the adaptation of ASF1A/B histone donor function primarily to the CAF-1 complex may help to sustain sufficient nucleosome assembly to permit plant survival.

In *S. cerevisiae*, the loss of silencing at telomeres and mating type loci in *hir* mutants combined with mutants lacking CAF-1 (*cac*) is strongly enhanced over that in *cac* mutants alone (Kaufman et al., 1998; Osley and Lycan, 1987). Maintenance of heterochromatin in the absence of CAF-1 function in yeast therefore requires the HIR complex. However, despite an important reduction in H3 occupancy in the *fas1-4*

athira-1 double mutant, silencing of an endogenous repeat sequence and certain transposons as well as heterochromatin organization is not further affected compared to the single mutants. This is surprising, as appropriate nucleosome assembly is not only required for DNA packaging but also important for propagating epigenetic information. We suggest that the moderate silencing defects observed in *fas1-4 athira-1* mutants are due to a CAF-1 residual function. We interpret this finding by the presence of alternative mechanisms required for gene silencing and heterochromatin maintenance such as DNA methylation, which is of primordial importance in plants in directing histone modifications and silencing (Rigal and Mathieu, 2011) and which is unaffected in *fas* mutants (Schönrock et al., 2006).

The aggravated nucleosomal loss and the accentuated phenotypic defects in *fas1-4 athira-1* double mutants, together with the viability of the respective single mutants, suggest partial functional compensation between the two histone deposition complexes. Hence, we can speculate that the Arabidopsis HIR complex can at least partially compensate a deficiency in replication-coupled histone assembly, potentially by nucleosomal gap-filling mechanisms. Such a mechanism has been proposed in mammals, where in absence of functional CAF-1, the HIR complex recognizes naked DNA stretches remaining after replication via its DNA-binding properties and fills the gaps through H3 deposition (Ray-Gallet et al., 2011). Whether this mechanism occurs in plants remains to be elucidated. Given the only subtle nucleosomal reduction observed in *athira-1* mutants, it could also be envisaged that such compensation works in both directions, allowing also the CAF-1 complex to perform H3.3 incorporation. Interestingly, in mammals, in DAXX- or HIRA-depleted cells, CAF-1 co-purifies with the replacement variant H3.3 (Drané et al., 2010; Lewis et al., 2010).

In conclusion, several lines of evidence support the notion that the Arabidopsis HIR complex functions as a histone chaperone: loss of AtHIRA reduces the pool of non-nucleosomal histone H3, impacts nucleosome occupancy at both active and repressed chromosomal regions and affects transcriptional silencing. In addition, synthetic lethality is observed when *hir* mutants are combined with complete loss-of-function *fas* alleles. Taken together, our results imply an evolutionary conserved mode of action of these two plant histone H3 assembly complexes. Indeed, the presence of Arabidopsis H3.1 and H3.3 variants at, respectively, transcriptionally repressed or active genomic regions is similar to Drosophila and mammals (Mito et

al., 2005; Goldberg et al., 2010; Stroud et al., 2012; Wollmann et al., 2012). This observation may have been unexpected, given that the evolution of functionally divergent H3 variants is thought to have occurred independently between the plant and animal kingdoms. However, the highly conserved function of plant histone chaperone complexes leaves the intriguing possibility that histone chaperones contributed to the functional diversification of the histones they transport and deposit.

Materials and Methods

Plant Material

Mutant *Arabidopsis* lines *fas1-4* (SAIL-662-D10), *fas2-5* (SALK_147693), *athira-1* (WiscDsLox362H05), *ncn1* (GABI_018D02), *ncn2* (GABI_130H01) and *cbn* (SALK_099927) as well as lines SALK_019573, GABI_775H03 and SALK_143806 mapping to the *AtHIRA* locus were obtained from the Nottingham Arabidopsis Stock Center (NASC) and/or were gifts from other laboratories. All mutants are in the Columbia background. The *athira-1* (WiscDsLox362H05) mutant contains two T-DNAs inserted in the 5th intron and the 6th exon, respectively. The SALK_019573 line comprises two T-DNAs localizing to the promoter, and for GABI_775H03, the T-DNA is inserted in the 5'UTR. Line SALK_143806 lacks any T-DNA insertion in the available seed pools. Two T-DNA insertions in tandem were revealed in *ncn1* (GABI_018D02) mutants in the 5th intron, one of them affecting a splice site. One T-DNA insertion was identified in the 10th intron of *ncn2* mutants, while in *cbn* mutants two T-DNAs in tandem were detected in the 6th intron. The *athira*^{amiRNA} line was created by cloning a hairpin construct into pRS300 as described (Schwab et al., 2010). The pRS300 vector was recombined with a destination vector by Gateway technology and WT Columbia plants were transformed with Agrobacterium by the floral dip method. Plants were grown on soil in a growth chamber under 16-h light/8-h dark cycles at 22ºC. For *in vitro* culture, seeds were sterilized in 70% EtOH with 0.05% SDS followed by a wash in 95% EtOH, dried and sown on germination medium containing 0.8% w/v agar, 1% w/v sucrose and half-strength Murashige & Skoog salts (M0255; Duchefa Biochemie, Netherlands). After 2 days of stratification at 4ºC in the dark, plants were grown under 6-h light/8-h dark cycles at 23ºC.

Documentation of phenotypes

Images of dissected siliques and flowers were taken using a Leica binocular and the LAS 3.6 software (Leica Microsystems, Switzerland), with a 0.63x and a 2x magnification, respectively.

Identification of HIR complex components and phylogenetic analysis

To identify Arabidopsis orthologs of the HIR complex subunits, we performed interspecies Blast searches with the mammalian protein sequences. Conserved

motifs for each member of the HIR complex were aligned using the program Muscle (Edgar, 2004) with default settings. Trees were constructed from amino acid sequences of the conserved motifs. Distance analyses used the program PhyML (MEGA 5 package) (Tamura et al., 2011). Distance bootstrap analyses consisted of 1,000 replicates. The following parameters were used: Analysis (Phylogeny Reconstruction), Statistical Method (Maximum Likelihood), Test of Phylogeny (Bootstrap method), Substitution Type (Amino acid), Model/Method (Poisson model), Rates among Sites (Uniform rates), Gaps/Missing Data Treatment (Complete deletion), Tree Inference Options (Nearest-Neighbor-Interchange, Initial Tree for ML, Default - NJ/BioNJ), Branch Swap Filter (Very Strong).

Genotyping

Homozygous plants for the different mutant lines used in this study were identified by PCR amplification with the primers listed in ***Supplemental Table 2***.

Calculation of expected double mutant progenies from crosses between fas1-4 and ncn1 or ncn2 mutants

The *FAS1* and *NCN1* genes have a 39cM distance *i.e.* a 39% recombination frequency. The recombinant gametes of double heterozygote F1 plants (*FAS1*; *NCN1* and *fas1-4*; *ncn1)* are expected with a frequency of 0.39/2. To obtain fertilization by the *fas1-4*; *ncn1* recombinant gametes, the frequency is: (0.39/2) x (0.39/2) = 0.038 *i.e.* 3.8%. Hence, for the 59 genotyped plants, we expected 2 double mutant plants. The genetic distance between *FAS1* and *NCN2* genes is 53cM; therefore these mutant alleles are expected to segregate as unlinked.

Alexander staining

Viability of mature pollen grains was assayed as described in (Alexander, 1969). Anthers from stained flowers were isolated and photographed using a Zeiss Axioplan microscope and the Axiovision 4.2 software (Carl Zeiss Vision GmbH, Le Pecq, France).

Salt treatment

Plantlets grown for 10 days *in vitro* were transferred into liquid MS medium containing 200 mM NaCl. Samples were shock-frozen in liquid nitrogen before treatment and after 1 h of salt exposure.

RNA extraction and RT-PCR

RNA was extracted using Tri-Reagent (Euromedex) according to the manufacturer's instructions. RNA was treated with RQ1 DNase I (Promega) and purified using phenol-chloroform extraction. Reverse transcription was primed either with oligo(dT)15 or with random hexamers using M-MLV reverse transcriptase (Promega). RNA quantity and purity were assessed with the Nanodrop (Thermo Scientific). The resulting cDNAs were used in standard PCR (Promega Flexi) or in quantitative PCR with the LightCycler® 480 SYBR Green I Master kit on the Roche LightCycler® 480. Transcript levels of interest were normalized to *SAND* (Czechowski et al., 2005) using the comparative threshold cycle method.

Fluorescence in situ hybridization

For nuclear spreads, rosette leaves from 4 week-old soil-grown plants were fixed in ethanol-acetic acid (3:1 v/v). FISH was performed essentially as described (Probst et al., 2003). The biotin-labeled 180 bp probe was prepared by PCR with T3 and T7 primers using pBluescript containing two copies of the 180bp repeat as template. Digoxygenin-labeled probes for Transcriptionally Silent Information (TSI) were generated by nick-translation (Roche) using the clones pA2 and pA15 (Steimer et al., 2000). Slides were analyzed with the Zeiss Axio Imager Z.1 microscope. Images were acquired with the Zeiss AxioCam MRm camera system using the Zeiss Axiovision software and processed with ImageJ and Adobe Photoshop.

Ploidy Analysis

Nuclei were prepared using a modified version of the original Galbraith method (Galbraith et al., 1983). Cytometric analysis was carried out using the *Attune*® *Acoustic* Focusing cytometer. For statistical analysis, we performed a Shapiro-Wilk test to confirm that the data are normally distributed, followed by a Bartlett's test to analyze if samples were from populations with equal variances, and finally, a Tukey's HSD (Honest Significant Difference) test was applied in conjunction with an ANOVA

(for the pair-wise comparison of means) to find means that were significantly different from each other.

ChIP analysis

Chromatin of 3 week-old *in vitro* grown plantlets or shoots from 4 week-old soil-grown plants was formaledehyde cross-linked and chromatin immunoprecipitation carried out as previously described (Bowler et al., 2004) with minor modifications: Chromatin was sheared using the Diagenode Bioruptor (10 cycles of 30 s ON and 1.5 min OFF). Protein A-coupled magnetic beads (Diagenode) or Protein A-coupled Dynabeads (Invitrogen) were used instead of Sepharose beads, and the sonicated chromatin was pre-cleared in presence of magnetic beads for 3 h, before immuno-precipitation with the anti-H3 antibody (Abcam, ab1791). Chromatin cross-linking was reversed by heating at 95ºC for 10 min, followed by incubation for 1 h at 43°C in the presence of proteinase K (Roche Diagnostics). Proteinase K was inactivated at 99°C for 10 min. DNA was quantified using qPCR (Roche) and normalized relative to input.

Protein Extraction and Western Analysis

For extracts containing non-nucleosomal histones, 100 mg of WT and mutant plantlets were frozen in liquid nitrogen and ground to a fine powder. Proteins were extracted in 50 mM Tris HCl pH 8, 150 mM NaCl, 10 mM EDTA, 50 mM NaF, 1% NP40, 0.45% desoxycholate, 1% SDS and proteinase inhibitors (Roche). The supernatant of a first centrifugation step (15,000g; 20 min) was centrifuged again with the same parameters and the protein concentration of the second supernatant was quantified using a Bicinchoninic Acid assay (Sigma) with bovine serum albumin as the reference standard. For extracts containing nucleosomal histones, nuclei were prepared from 2 g plant material according to an adapted ChIP-protocol using HONDA buffer (10 mM MgCl2, 0.4 M sucrose, 2.5% Ficoll, 5% Dextran 40, 25 mM Tris-HCl pH=7.4, 5 mM DTT, 0.5 mM PMSF, 1% Protease Inhibitors). Briefly, tissue was ground to powder in liquid nitrogen and re-suspended in HONDA buffer and filtrated; an aliquot was recovered for total extract. After incubation with 0.5% Triton X-100 samples were centrifuged (1,500g; 5 min). Nuclei were washed successively in HONDA buffer with 0.1% Triton X-100 then without Triton X-100 and finally re-suspended in Laemli buffer. SDS–PAGE and Western blots were performed according to standard procedures. Western Blots were probed with the anti-H3

antibody (Abcam, ab1791, 1/5,000). Equal loading of proteins was confirmed with a mouse monoclonal anti-actin antibody (1/1,000; Sigma), Ponceau or Coomassie staining. Primary antibodies were revealed by incubation with a horseradish peroxidase-coupled anti-rabbit secondary antibody (1/25,000) or a horseradish peroxidase-coupled anti-mouse secondary antibody (1/5,000 dilution; Sigma), respectively. Chemiluminescence of the immunoblots were developed using ECL Western blotting detection reagents (GE Healthcare Bio-Sciences, Amersham, www.gelifescience.com). Densitometric analysis of the immunoreactive protein bands obtained in Western blots was performed on non-saturated signals using Multi Gauge software (Fujfilm). Nucleosomal H3 was quantified relative to actin in the corresponding total extracts. Remaining actin protein levels in nucleosomal extracts are very low (***Supplemental Figure 3H).***

ChIP-seq data analysis

Available H3.1 and H3.3 ChIP-seq read data (GSE34840) (Stroud et al., 2012) were aligned to the sequences of interest using Bowtie (default parameters) (Langmead et al., 2009) allowing up to 5 mismatches for the read length of 50 bp in this dataset. Tablet (Milne et al., 2013) was used to visualize the mapped sequences. Finally, a Perl script was developed to count the number of reads mapping to each position of the sequence of interest. The histogram was generated with R software.

Primers

All primer sequences are listed in ***Table S1***.

Acknowledgments

C.D., S.L.G. and A.V.P. were supported by ANR “Dynam'Het” ANR-11 JSV2 009 01; S.C. and A.V.P. by ANR “SINODYN” ANR-12 ISV6 0001. M.B., A.P. and L.S. are supported by stipends from the Region Auvergne (Recherche et Innovation Technologique). M.B. is furthermore supported by an ARC doctoral fellowship. This work was supported by the CNRS, INSERM and Université Blaise Pascal and Université d’Auvergne. We thank Marie-Claude Espagnol and Lucile Borao for

technical assistance, S. Tourmente for stimulating discussion and O. Mittelsten Scheid and Jasmin Bassler for critical comments on the manuscript.

Author contributions

C.D. and A.V.P. designed the research. C.D., M.B., S.L.G., L.S., S.C. and A.V.P performed the experiments and analyzed the data. A.P. contributed analytical methods. C.D., C.T. and A.V.P. wrote the paper.

Conflict of Interest

The authors declare no conflict of interest.

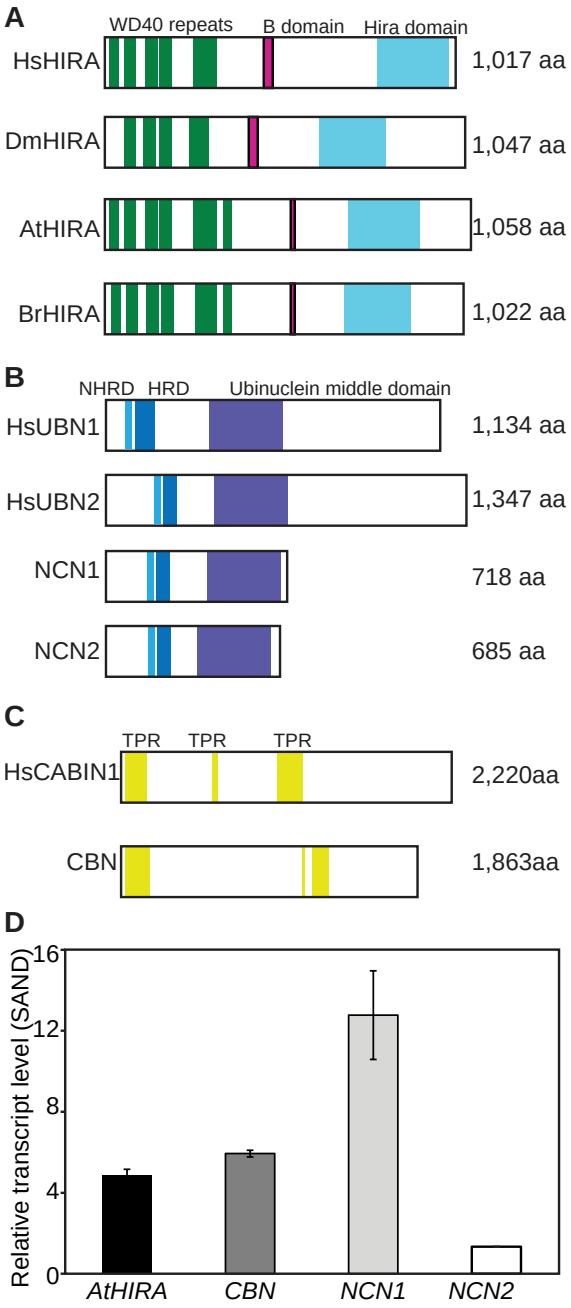

Figure 1: Evolutionary conservation of the HIR complex subunits in plants.

A The mammalian and Drosophila HIRA proteins (respectively 1,017aa and 1,047aa) contain WD40 repeats in their N-terminal region and a Hira domain (also named TUP1-like enhancer of split) at their C-terminus. HIRA proteins also comprise a conserved motif called B domain. A similar protein structure is predicted for Arabidopsis and Brassica rapa HIRA proteins. B The human Ubinucleins (UBN1 and UBN2) and the two Arabidopsis orthologs contain the HRD (Hpc2-related domain) and a putative NHRD (N-terminal to the HRD region) domain as well as a conserved region termed Ubinuclein middle domain at their C-terminus. The two plant proteins miss the large C-terminal domains of the animal counterparts. C The mammalian calcineurin-binding protein 1 (CABIN1) and its Arabidopsis ortholog contain several tetratricopeptide (TPR)-like bi-helical repeats. D RT-qPCR analysis of *AtHIRA*, *NCN1*, *NCN2* and *CABIN* transcript levels in 4-week old plants. Histograms show mean transcript levels ± SEM obtained for two independent PCR amplifications of three biological replicates. The y-axis shows the fold change relative to WT (WT set to 1) after normalization to *SAND* gene expression. *, $p<0.05$; Student's t-test.

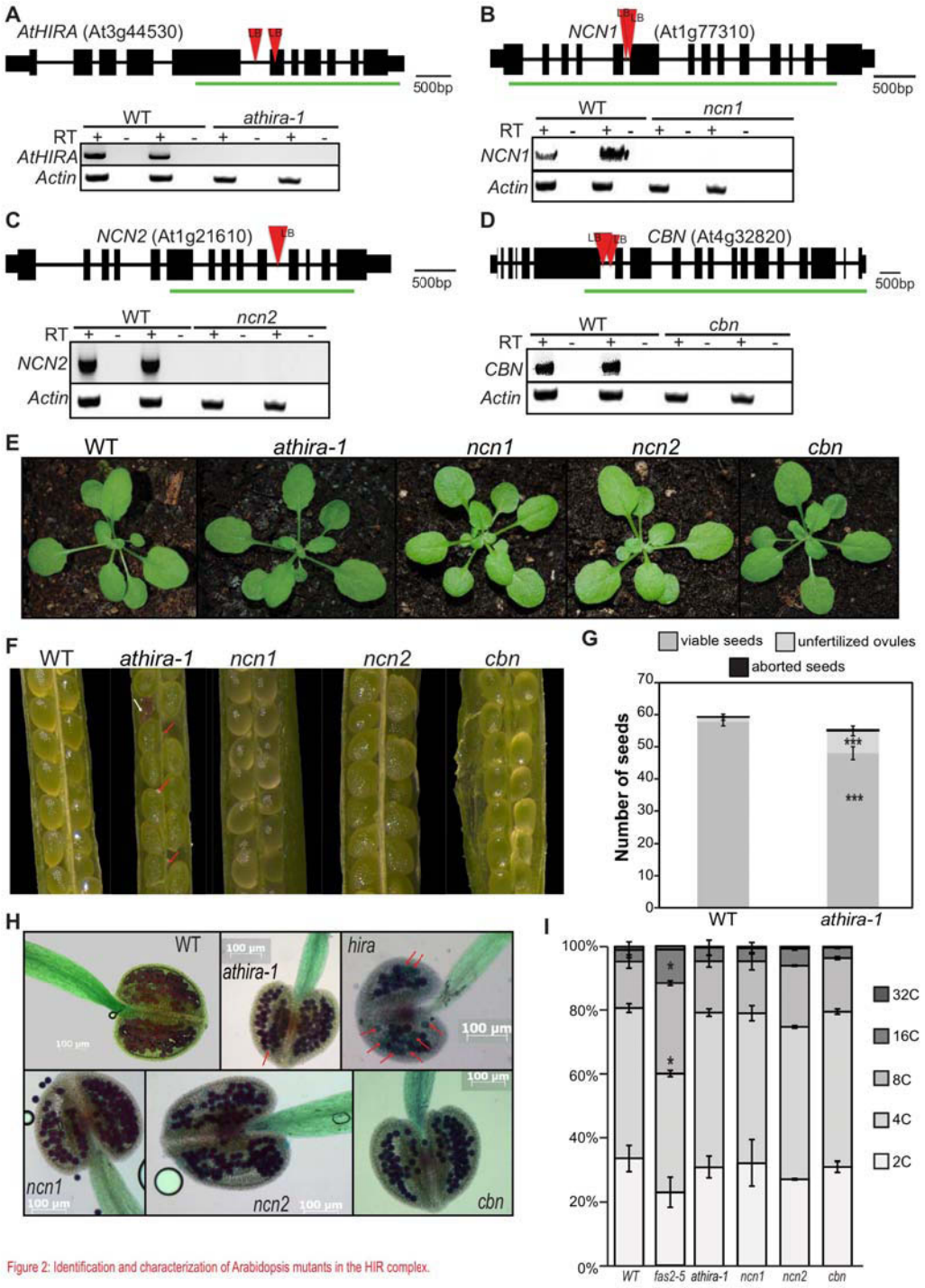

Figure 2: Identification and characterization of Arabidopsis mutants in the HIR complex.

A-D Gene structures and expression of the putative Arabidopsis HIR complex subunits in wild-type (WT) and mutants. Exons are denoted by rectangles, UTRs by adjoining narrower rectangles and introns by lines. T-DNA insertions are displayed as red triangles with the left border (LB) indicated. Absence of full-length transcripts is revealed by RT-PCR on two biological replicates for *athira-1* (A), *ncn1* (B), *ncn2* (C) and *cbn* (D). The amplified region is displayed by a green line. E Representative 25 day-old plantlets of WT, *athira-1*, *ncn1*, *ncn2*, and *cbn* mutants grown on soil. F Representative WT, *athira-1*, *ncn1*, *ncn2*, and *cbn* dissected siliques. Red arrows indicate unfertilized ovules and white arrow aborted seed. G Quantification of seed content in WT and *athira-1* siliques. Histograms show mean of viable seeds, unfertilized ovules and aborted seed content ± SEM. Quantifications were obtained from 23 WT and 37 *athira-1* siliques pooled from, respectively, 4 and 6 plants. ***, p<0.001; Student's t-test. H Pollen viability assessed by Alexander staining. Similar to WT, *cbn*, *ncn1* and *ncn2* mutants show viable pollen (purple-colored cytoplasm). Only *athira-1* mutant anthers contain non-viable pollen (green color) indicated by red arrows. Bar=100 µm. I Ploidy level distribution of WT, *fas2-5*, *athira-1*, *ncn1*, *ncn2* and *cbn* nuclei from 10 day-old plants. For ploidy analysis of each genotype, two independent preparations of pooled shoot material from 15 plants were investigated. A Tukey's HSD (Honest Significant Difference) test was used in conjunction with an ANOVA to determine means that were significantly different from each other (denoted by an asterisk).

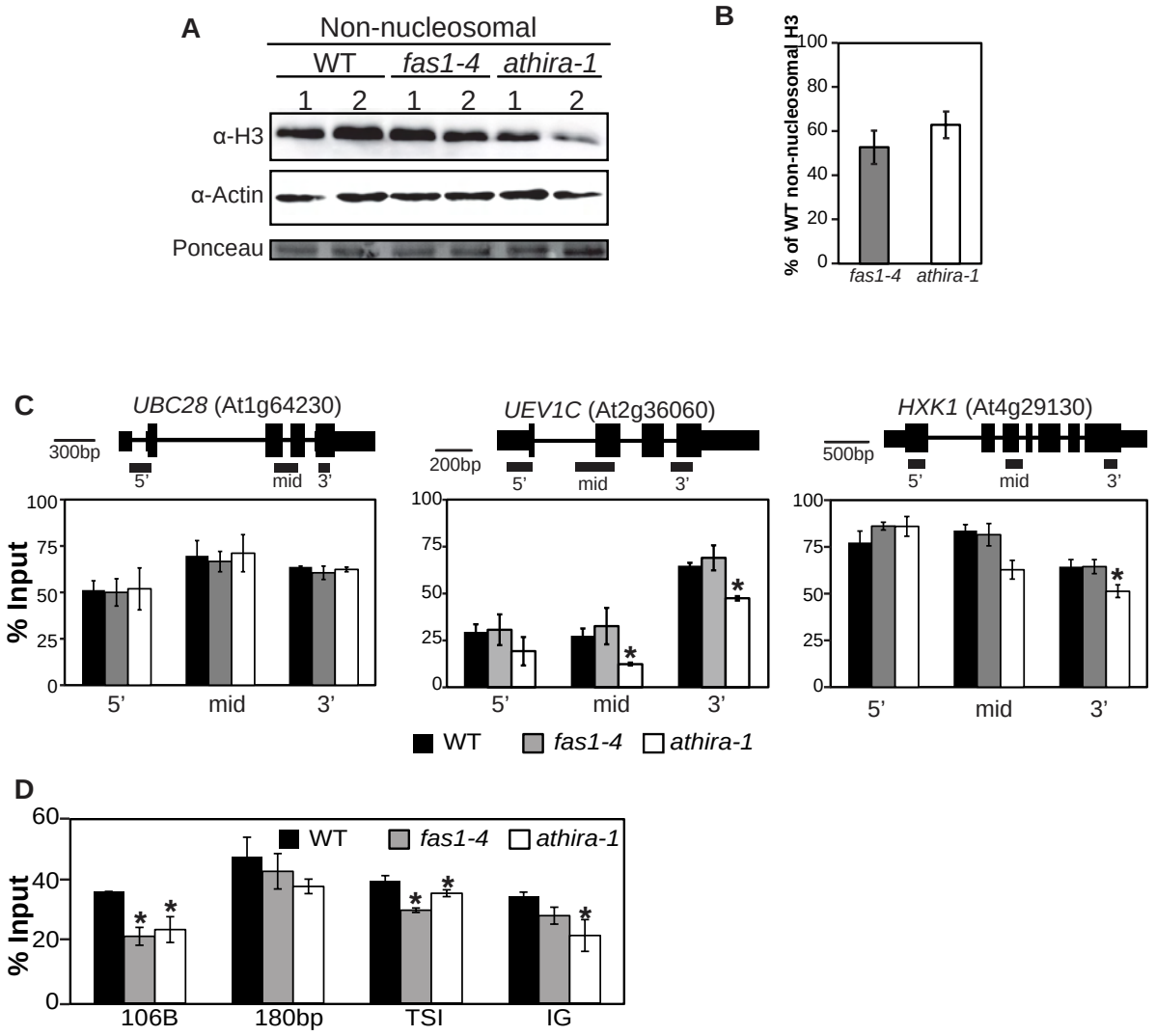

Figure 3: AtHIRA loss affects the non-nucleosomal histone pool and nucleosome occupancy.

A Non-nucleosomal histone H3 protein levels quantified by Western Blot. Twenty micrograms of proteins extracted from two independent biological replicates of WT, *fas1-4* and *athira-1* mutant leaf material were loaded per lane. The upper panel shows the western blot for H3, the central panel the loading control actin and the bottom panel the Ponceau staining.
B Quantification of non-nucleosomal H3 band intensities from 3 independent experiments normalized to actin using Multi Gauge. H3 levels normalized to actin in WT were set to 100%.
C Histone H3 occupancy assessed by H3-ChIP qPCR relative to input in WT, *fas1-4* and *athira-1* mutant plants grown in vitro for 3 weeks at different positions along three active genes (*UBC28, UEV1C* and *HXK1*). Histograms show mean percentage ± SEM of H3-Immunoprecipitation relative to input for three biological replicates. *, p<0.05; Student's t-test.
D Histone H3 occupancy assessed by qPCR H3-ChIP relative to input in WT, *fas1-4* and *athira-1* mutant plants at heterochromatic repeats and at an intergenic region.

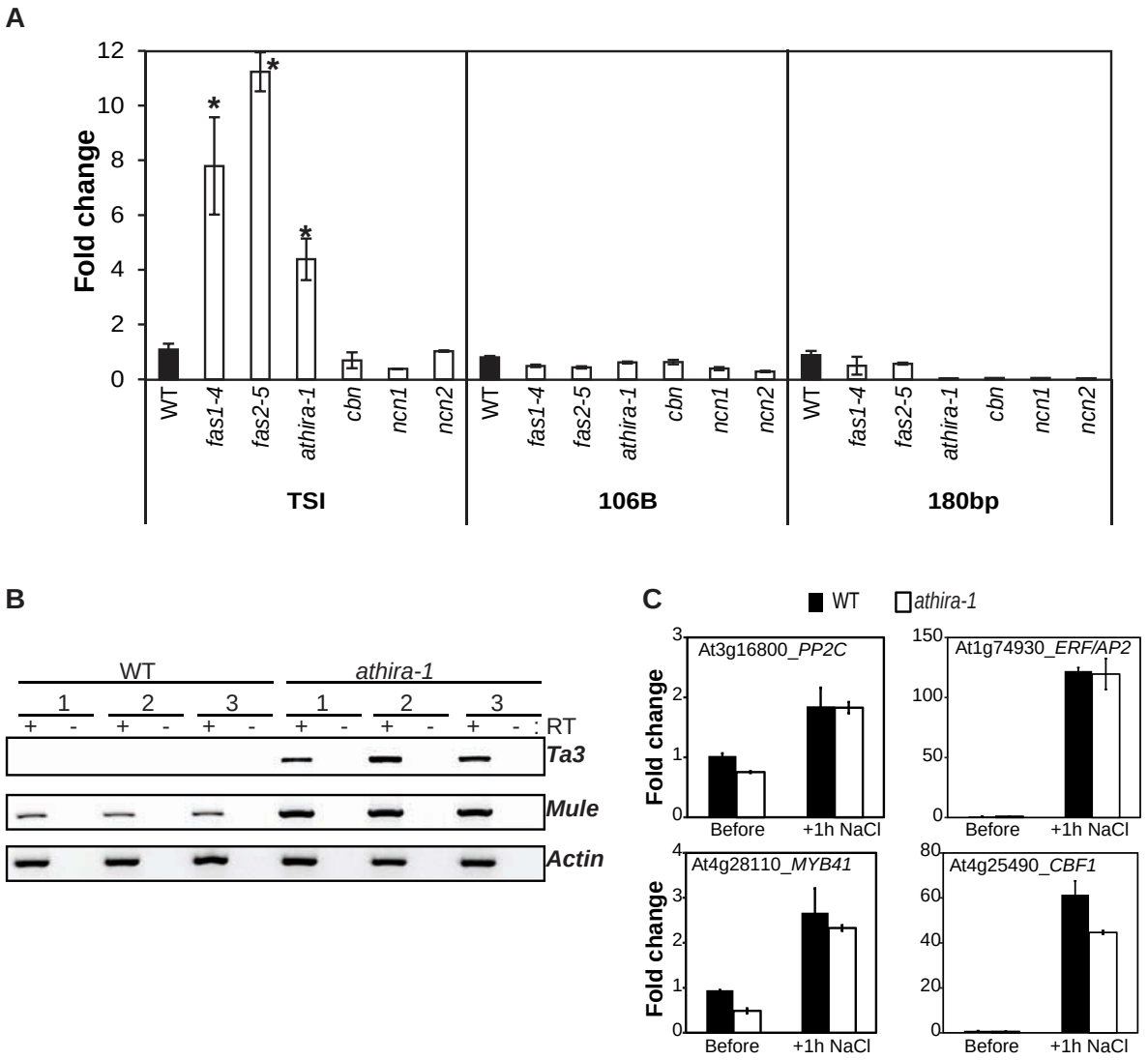

Figure 4: Release of transcriptional gene silencing and induction of gene expression in *athira-1* mutants.

A RT-qPCR analysis of Transcriptional Silent Information (TSI), 106B and 180 bp transcripts in *fasciata* (*fas*) and HIR complex mutants aged of 18d and grown on soil. Histograms show means of transcript levels ± SEM obtained for two independent PCR amplifications of three biological replicates. The y-axis shows the fold change relative to WT (WT set to 1) after normalization to *SAND* expression. *, p<0.05; Student's t-test.
B RT-PCR analysis of *Ta3* and *Mule* (At2g15810) transcripts of three independent biological replicates from WT and *athira-1* plants. *Actin* was used for normalization.
C RT-qPCR analysis of transcript levels of *PP2C* (At3g16800), *ERF/AP2* (At1g74930), *MYB41* (At4g28110) and *CBF1* (At4g25490) before and after 1h exposure to 200mM NaCl (+1h NaCl) of WT and *athira-1* mutant 10-day-old plantlets. Histograms show means of transcript levels ± SEM obtained for two independent PCR amplifications of three biological replicates.

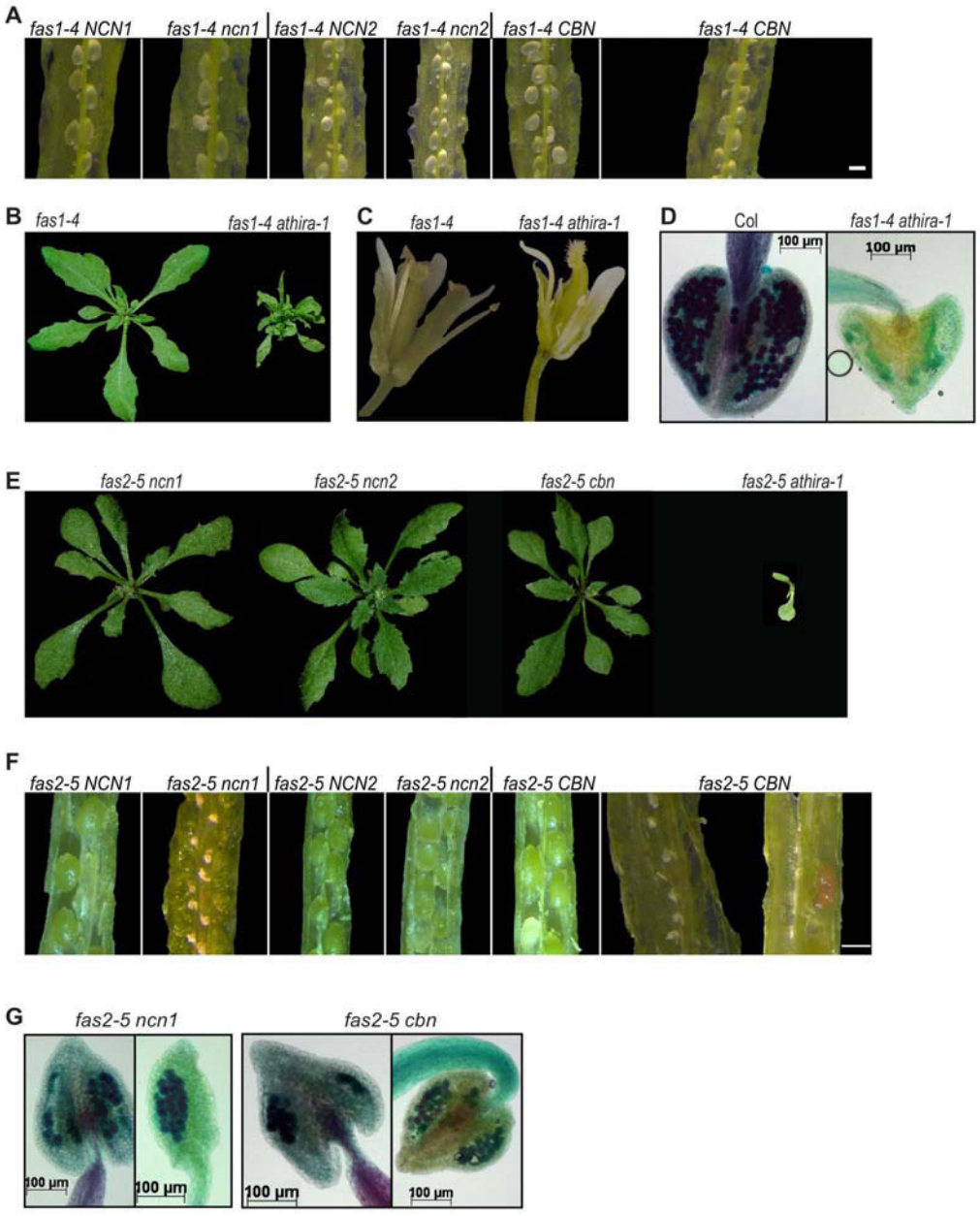

Figure 5: Genetic interactions between members of the CAF-1 and HIR complexes.

A Dissected siliques from F2 progeny of crosses between *fas1-4* and *ncn1*, *ncn2* and *cbn* mutants. For each cross a representative silique from *fas1-4* plants and a double mutant sister plant is shown. Bar, 0.3 mm.
B *fas1-4* and *fas1-4 athira-1* mutant plantlets grown on soil.
C Representative flowers from *fas1-4* and *fas1-4 athira-1* mutants.
D Representative WT and *fas1-4 athira-1* mutant anthers after Alexander staining revealing absence of viable pollen in the double mutant.
E Representative *fas2-5 ncn1, fas2-5 ncn2, fas2-5 cbn* and *fas2-5 athira-1* mutant plants.
F Dissected siliques from F2 progeny of crosses between *fas2-5* and *ncn1, ncn2* and cbn mutants. For each cross a representative silique from *fas2-5* plants and double mutant sister plants is shown. Bar, 0.3 mm
G Pollen viability assessed by Alexander staining of anthers from plants derived from crosses between *fas2-5* and *ncn1* or *cbn*. The respective genotype is indicated. Viable pollen has a purple-colored cytoplasm while non-viable pollen exhibits a green color.

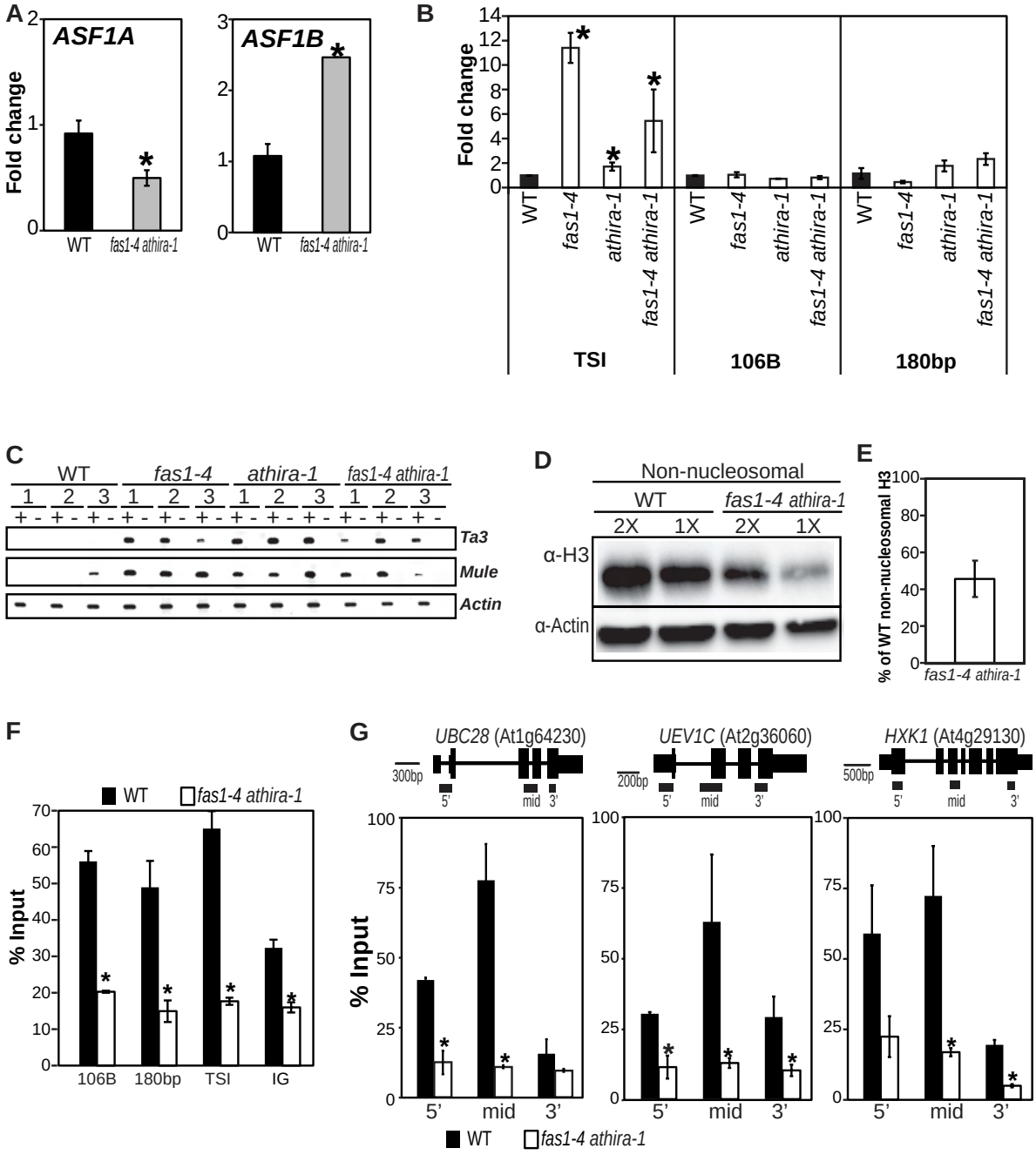

Figure 6: Molecular consequences of simultaneous mutation of CAF and HIR complexes.

A RT-qPCR analysis of *ASF1A* and *ASF1B* expression in WT and *fas1-4 athira-1* 4-week old mutants. Histograms show mean transcript levels ± SEM obtained for two independent PCR amplifications of three biological replicates. The y-axis shows the fold change relative to WT (WT set to 1) after normalization to *SAND* gene expression. *, p<0.05; Student's t-test.
B RT-qPCR analysis of TSI, 106B and 180 bp expression in WT, *fas1-4, athira-1* and *fas1-4 athira-1* 4-week old plants. Histograms show the mean transcript levels ± SEM obtained for two independent PCR amplifications of three biological replicates. The y-axis shows the fold change relative to WT (WT set to 1) after normalization to *SAND* gene expression. *, p<0.05; Student's t-test.
C RT-PCR analysis of *Ta3* and *Mule* (At2g15810) transcript levels. Three independent biological replicates were analyzed. *Actin* was used as control.
D Non-nucleosomal histone H3 protein levels quantified by Western Blot. Twenty and 10µg of non-nucleosomal proteins extracted from WT and *fas1-4 athira-1* mutant leaves were loaded per lane. The upper panel shows the western blot for H3, the middle panel the loading control actin and the bottom panel the Ponceau staining as a second loading control.
E Quantification of non-nucleosomal H3 band intensities from 2 independent experiments normalized to actin using Multi Gauge. H3 levels normalized to actin in WT were set to 100%.
F-G Histone H3 occupancy assessed by H3-ChIP qPCR relative to input in WT and *fas1-4 athira-1* mutant plants at heterochromatic and intergenic regions (G) as well as different positions along three active genes (H). Histograms show mean percentage ± SEM of H3-Immuno-precipitation relative to input for three biological replicates. *, p<0.05; Student's t-test.

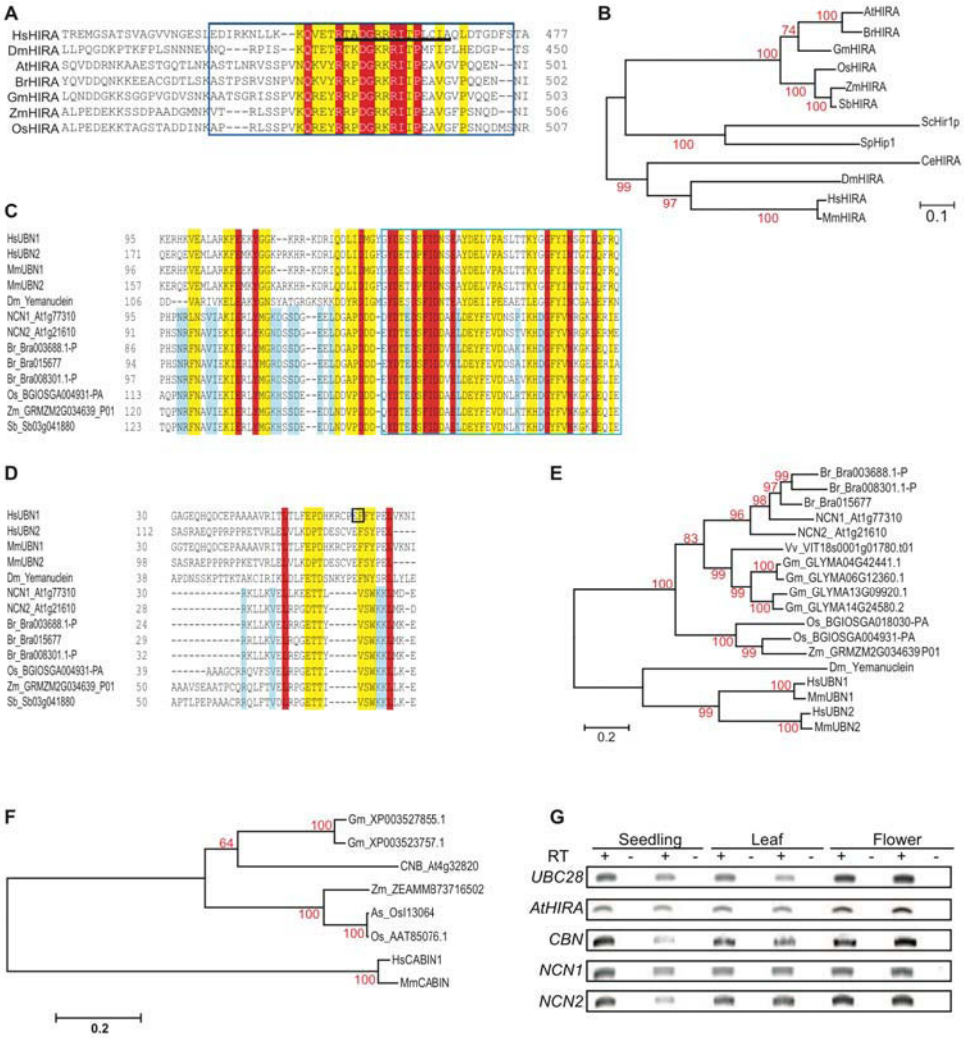

Supplemental Figure 1: Evolutionary conservation and expression of the HIR complex subunits.

A Amino-acid sequence alignment of the B domain of HIRA orthologs. The blue box indicates the core B domain; the minimal peptide required for ASF1 binding is underlined in the mammalian HIRA. Strictly conserved (identical) residues were shaded in red and conserved residues in yellow.
B Phylogenetic tree of HIRA proteins.
C-D Amino-acid sequence alignment of the HRD (C) and NHRD (D) domains in Ubinuclein orthologs. Strictly conserved residues in plants are shaded in blue. The black box indicates HsUBN1 residues that impair HIRA binding when mutated (Tang et al., 2012).
E-F Phylogenetic tree of (E) Ubinuclein and (F) CABIN1 proteins. Mm, Mus musculus; Hs, Homo sapiens; Dm, Drosophila melanogaster; Ce, Caenorhabditis elegans; Sc, Saccharomyces cerevisiae; Sp, Schizosaccharomyces pombe; Sb, Sorghum bicolor; Zm, Zea mays; Os, Oryza sativa; At, Arabidopsis thaliana; Br, Brassica rapa; Gm, Glycin max; Vv, Vitis vinifera. GenBank accession or ChromDB ID numbers are indicated. For all phylogenetic trees, the scale bar indicates the evolutionary distances and bootstrap values are shown along branches.
G Expression of the different subunits of the HIR complex in WT seedlings, leaves and flowers revealed by RT-PCR. *UBC28* was used as control.

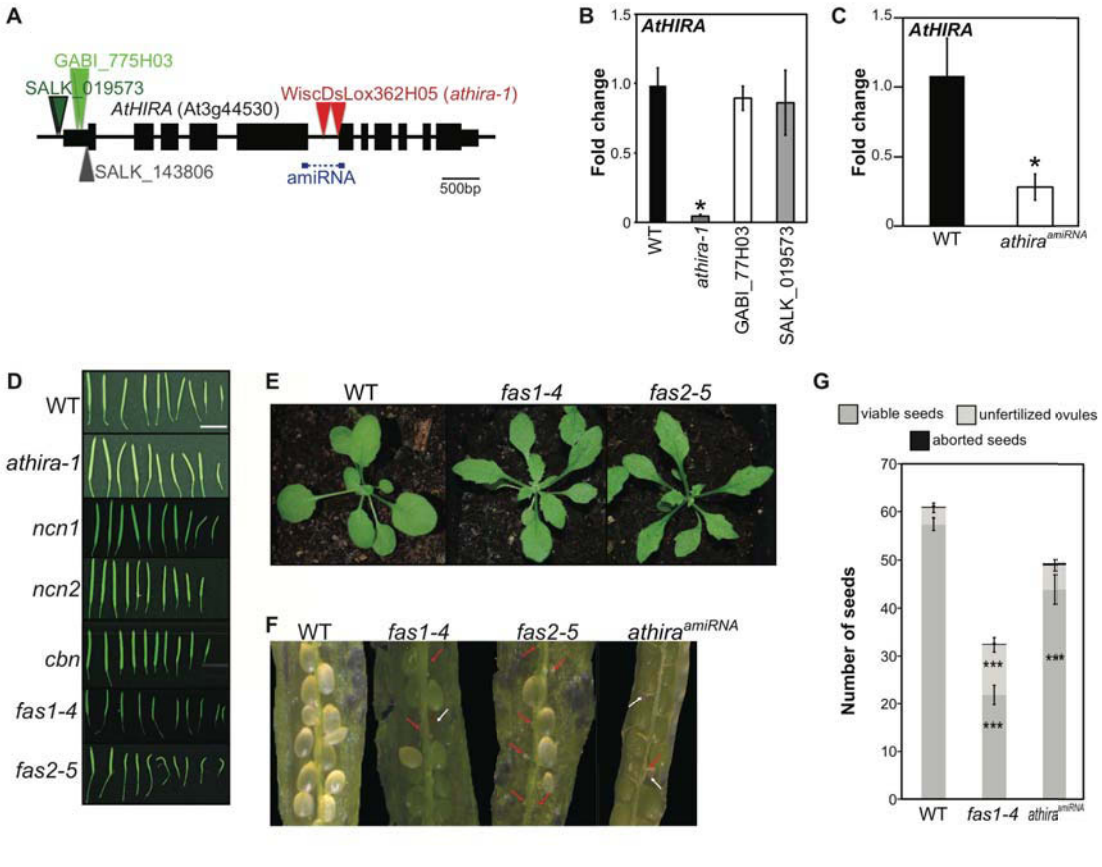

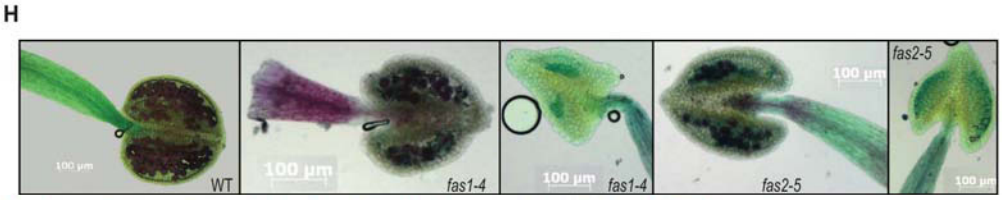

Supplemental Figure 2: Characterization of Arabidopsis mutants in the HIR and CAF-1 complex.

A Structure of *AtHIRA* gene locus. Exons are denoted by rectangles, UTRs by adjoining narrower rectangles and introns by lines. T-DNA insertions are displayed by colored triangles. The blue boxes show the sequence spanning an intron, which is targeted by the artificial microRNA construct.
B RT-qPCR analysis of *AtHIRA* expression in the respective homozygous T-DNA insertion lines. Histograms show mean transcript levels ± SEM obtained for two independent PCR amplifications of three biological replicates. The y-axis shows the fold change relative to WT (WT set to 1) after normalization to *SAND* gene expression. *, p<0.05; Student's t-test.
C RT-qPCR analysis of *AtHIRA* expression in the athiraamiRNA line. Histograms show mean transcript levels ± SEM obtained for two independent PCR amplifications of three biological replicates. The y-axis shows the fold change relative to WT (WT set to 1) after normalization to *SAND* gene expression. *, p<0.05; Student's t-test.
D Representative WT, *athira-1*, *ncn1*, *ncn2*, *cbn*, *fas1-4* and *fas2-5* siliques.
E Representative 25 day-old plantlets of WT, *fas1-4* and *fas2-5* mutants grown on soil.
F Representative WT, *fas1-4*, *fas2-5* and *athira*^{amiRNA} dissected siliques. Red arrows indicate unfertilized ovules, white arrow aborted seeds.
G Quantification of seed content in WT, *fas1-4* and *athira*^{amiRNA} siliques. Histograms show mean of viable seeds, unfertilized ovules and aborted seed content ± SEM. Quantifications were obtained from 16 WT, 19 *fas1-4* and 19 *athira*^{amiRNA} siliques pooled from 4 plants. ***, p<0.001; Student's t-test.
H Pollen viability assessed by Alexander staining of WT, *fas1-4* and *fas2-5* anthers. Viable pollen exhibits a purple-colored, while non-viable pollen displays a green color. Both fas mutants display two kinds of heart-shape anthers: some with a mixture of viable and non-viable pollen and in the same flower anthers lacking viable pollen.

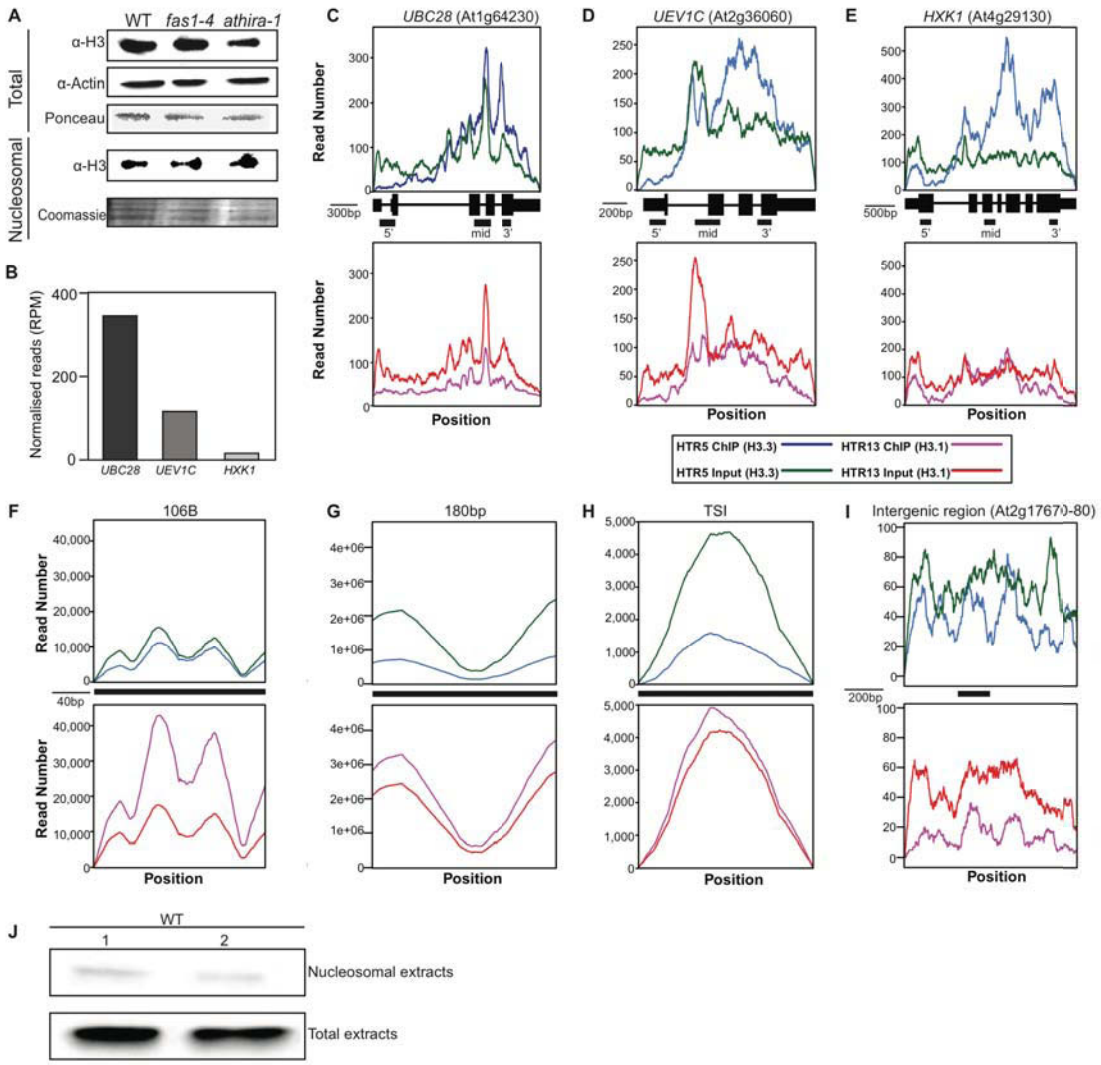

Supplemental Figure 3: Enrichment in H3.1 and H3.3 at targets analyzed in H3-ChIP-Seq assays.

A Total and nucleosomal histone H3 protein levels assayed by Western blot. Ten microliters of total and chromatin extracts isolated from leaves of WT, *fas1-4* and *athira-1* mutant plants were loaded per lane. The upper panel shows the western blot for H3, the central panel the loading control actin (for total extracts) and the bottom panel the Ponceau or Coomassie staining.

B Expression levels of *UBC28, UEV1C* and *HXK1* from Direct RNA Sequencing data of 2 week-old plantlets (Duc et al., 2013).

C-I Distributions of H3.1 (violet) and H3.3 (blue) ChIP-seq reads and corresponding input genomic DNA (red and green respectively) in the ChIP-seq dataset from plants expressing tagged H3.1 or tagged H3.3 (Stroud et al., 2012). For the 3 genes *UBC28, UEV1C* and *HXK1*, the exons are denoted by rectangles, UTRs by adjoining narrower rectangles and introns by lines. The regions amplified by qPCR in H3-ChIP experiments are displayed by black boxes for all targets.

H Total and nucleosomal actin protein levels assayed by Western blot. Ten microliters of total (lower panel) and chromatin (upper panel) extracts isolated from WT plant leaves were loaded per lane. Pictures of bottom and upper panels were taken together and the same exposure time is displayed. Note that actin protein levels are strongly reduced in nucleosomal extracts compared to total extracts.

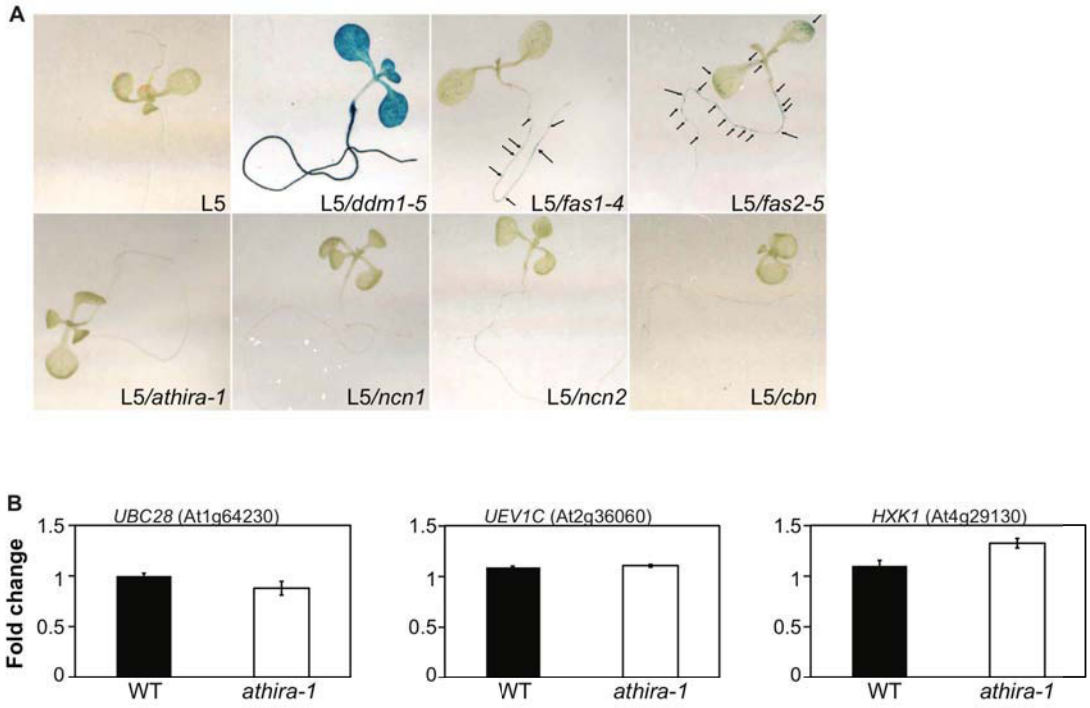

Supplemental Figure 4: Gene expression in athira-1 mutants.

A GUS staining of 7 day-old F3 seedlings derived from crosses of line L5, carrying a multicopy transgenic locus suppressed by transcriptional gene silencing, and *fas1-4*, *fas2-5*, and HIR complex mutants. The positive control L5/*ddm1-5* (Pecinka et al., 2010) turns completely blue indicating GUS gene expression and release of silencing. Only weak staining was observed in fas mutant roots and cotyledons, and none in HIR complex mutants. Arrows indicate blue spots in L5/*fas1-4* and L5/*fas2-5* mutant plants.
B RT-qPCR analysis of *UBC28*, *UEV1C* and *HXK1* expression in athira-1 mutants. Histograms show the mean transcript levels ± SEM obtained for two independent PCR amplifications of three biological replicates. The y-axis shows the fold change relative to WT (WT set to 1) after normalization to *SAND* gene expression. *, $p<0.05$; Student's t-test.

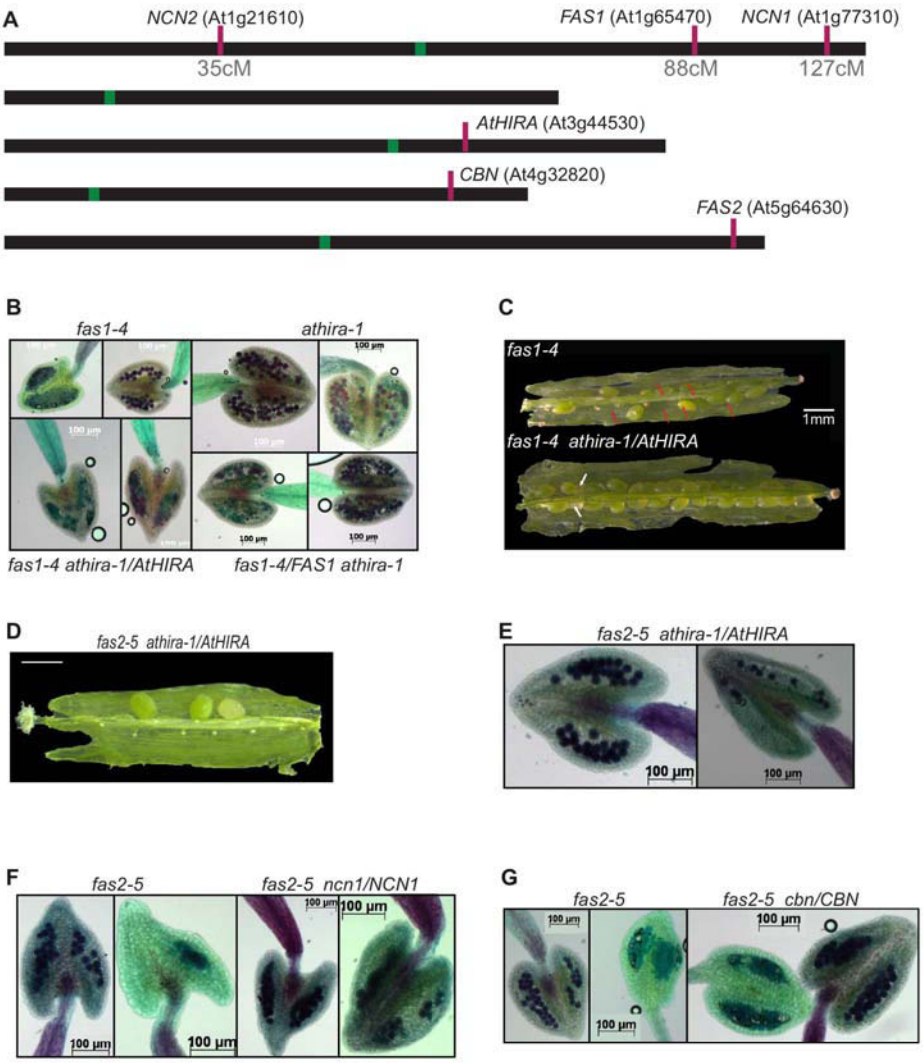

Supplemental Figure 5: Genetic interactions between members of the CAF-1 and HIR complexes.

A Genetic map of the five Arabidopsis chromosomes. Gene locations are marked with vertical purple lines and their location on the genetic map in cM is indicated. Centromere locations are marked with green boxes. Chromosome size is proportional to its sequence length. The map visualization tool was obtained from TAIR (www.arabidopsis.org/jsp/ChromosomeMap/tool.jsp).
B Representative anthers colored by Alexander staining of plants derived from the cross between *fas1-4* and *athira-1* mutants. The respective genotypes are indicated. Note the variable phenotype of fas mutant anthers. In the same flower, anthers with viable and non-viable pollen or immature anthers with only non-viable pollen are observed. In *athira-1* plants heterozygous for *fas1-4* and in *fas1-4* plants heterozygous for *athira-1*, no aggravation of the anther phenotype is observed compared to their sister plants *fas1-4* or *athira-1* mutants.
C Dissected siliques of *fas1-4* plants either WT or heterozygous (*athira-1/AtHIRA*) for the *athira-1* mutant allele. Red arrows indicate unfertilized ovules and white arrows aborted seeds.
D A representative silique from a *fas2-5* homozygous *athira-1* heterozygous (*athira-1/AtHIRA*) plant. Bar, 1 mm.
E-G Representative anthers colored by Alexander staining of plants derived from crosses between *fas2-5* mutants and mutants of the different HIR complex subunits. The respective genotypes are indicated. Note the variable phenotype of fas mutant anthers. In the same flower, anthers with viable and non-viable pollen or immature anthers with only non-viable pollen are observed. Anthers display little viable pollen in *fas2-5 athira-1/AtHIRA* plants. In *fas2-5* mutant plants heterozygous for *ncn1* or *cbn*, no aggravation of the anther phenotype is observed compared to their sister plants that do not carry an *ncn1* or *cbn* mutant allele.

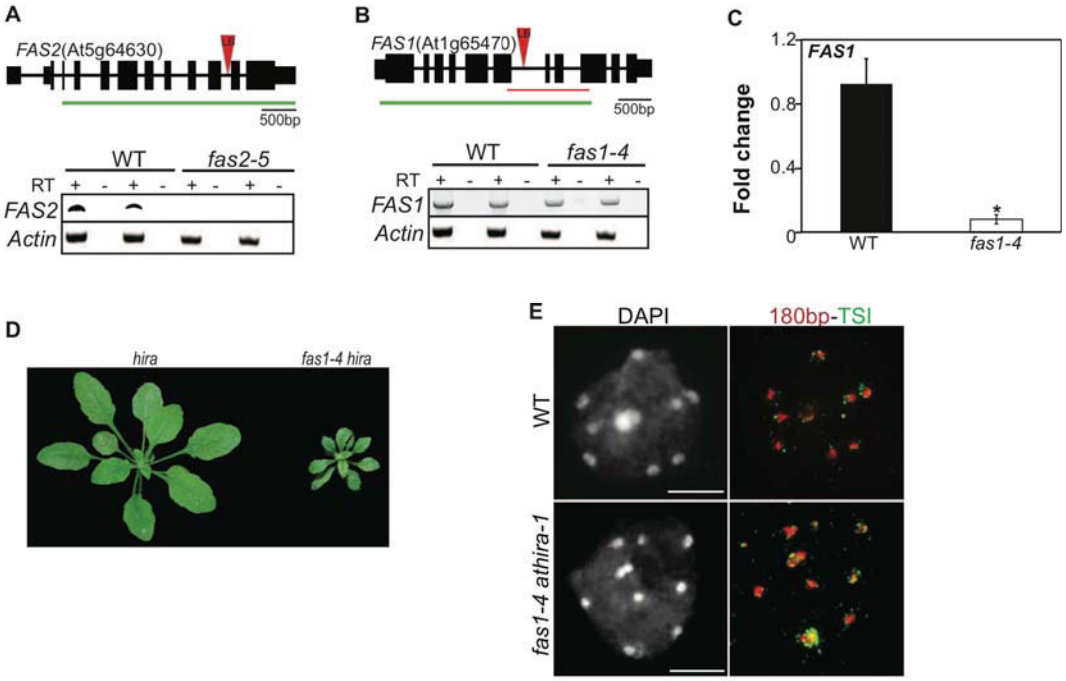

Supplemental Figure 6: Molecular characterization of *fas1-4* and *fas2-5* mutant alleles and generation of *fas1-4 athira-1* double mutant material.

A-B Structures of the genes encoding *FAS2* (A) and *FAS1* (B). Exons are denoted by rectangles, UTRs by adjoining narrower rectangles and introns by lines. T-DNA insertions are displayed by red triangles with the left border (LB) indicated. Presence or absence of full-length transcripts is revealed by RT-PCR performed along the whole RNA (lower panel). *Actin* was used as reference gene. The amplified region is displayed by a green line. No *FAS2* transcript was observed in *fas2-5* mutants (A) and reduced full-length *FAS1* mRNA in *fas1-4* mutants (B).

C Quantification by qPCR of the residual expression of the *FAS1* transcripts in *fas1-4* mutants. The region amplified in quantitative PCR is displayed by a red line and comprises the T-DNA insertion site in B. Histograms show mean transcript levels ± SEM obtained for two independent PCR amplifications of three biological replicates. The y-axis shows the fold change relative to WT (WT set to 1) after normalization to *SAND* gene expression. *, $p<0.05$; Student's t-test.

D Due to the sterility of *fas1-4 athira-1* plants, we derived double mutant plant material from the progeny of F2 plants with the *fas1-4/FAS1 athira-1* genotype. Double mutants plants (right) were selected by visual inspection of their severe growth phenotype compared to plants WT or heterozygous for the *fas1-4* mutant allele (left).

E DNA FISH for 180bp (red) and TSI (green) in leaf nuclei of 4 week-old WT and *fas1-4 athira-1* mutant plants. DAPI staining (grey), left column; merged FISH signals, right column. Bar, 5 µm.

Tables

***Table 1*. Epistatic relationship between CAF-1 and HIR complexes.**

Number of F2 plants with the indicated genotype. F2 plants with *fas* phenotype were selected in the progeny of several independent F1 plants and genotyped for the corresponding HIR complex mutation (+/+, WT; +/-, heterozygous; -/-, homozygous for the studied mutation). For mutations in non-genetically linked genes, we expect a segregation ratio of WT to heterozygous to homozygous of 1:2:1. n = total number of plants analyzed. N = number of independent F1 plants used in this study. The genes *FAS1*, *NCN1* and *NCN2* are positioned on the same chromosome.

Genotype		+/+	+/-	-/-	n	N
fas1-4	***cbn***	**17**	**27**	**19**	**63**	**3**
	ncn1	**28**	**28**	**3**	**59**	**3**
	ncn2	**22**	**27**	**9**	**58**	**3**
	athira-1	**33**	**76**	**3 ***	**112**	**#**
fas2-5	***cbn***	**18**	**68**	**19 ***	**105**	**3**
	ncn1	**27**	**44**	**14**	**85**	**4**
	ncn2	**22**	**73**	**19 ***	**114**	**3**
	athira-1	**10**	**61**	**0 ***	**71**	**4**

Segregation analysis from pool of seeds derived from several independent F1 plants.

* Frequency of double mutants significantly lower than the theoretically expected 25% (X^2 test).

Supplemental Table 1. The *fas athira-1* double mutants are underrepresented in segregating F2 populations

A. Number and percentage of F2 plants with the indicated genotype. 150 F2 plants from one individual F1 plant were genotyped for *fas1-4* and *athira-1* mutations.

Genotype	Number of plants obtained	Observed percentage	Expected percentage
FAS1 AtHIRA	9	6%	6.25%
FAS1 athira-1	12	8%	6.25%
FAS1 athira-1/AtHIRA	25	17%	12.5%
fas1-4 AtHIRA	10	7%	6.25%
fas1-4 athira-1	**0**	**0%**	6.25%
fas1-4 athira-1/AtHIRA	16	11%	12.5%
fas1-4/FAS1 AtHIRA	27	18%	12.5%
fas1-4/FAS1 athira-1	16	11%	12.5%
fas1-4/FAS1athira-1/AtHIRA	35	23%	25%

B. Number and percentage of F2 plants with the indicated genotype. 150 F2 plants from one individual F1 plant were genotyped for *fas2-5* and *athira-1* mutations.

Genotype	Number of plants obtained	Observed percentage	Expected percentage
FAS2 AtHIRA	8	5%	6.25%
FAS2 athira-1	8	5%	6.25%
FAS2 athira-1/AtHIRA	26	17%	12.5%
fas2-5 AtHIRA	11	7%	6.25%
fas2-5 athira-1	**2**	**1%**	6.25%
fas2-5 athira-1/AtHIRA	19	13%	12.5%
fas2-5/FAS2 AtHIRA	20	13%	12.5%
fas2-5/FAS2 athira-1	14	9%	12.5%
fas2-5/FAS2 athira-1/AtHIRA	42	28%	25%

Supplemental Table 2 : List of primers used in the study.

Purpose	Gene	FORWARD (F) and REVERSE (R) PRIMERS (5' to 3')
Genotyping of *fas1-4* (SAIL-662-D10)	At1g65470	Fas1_fw_MI: ATGGTATCTGGCCCAGCCAAA LBR Sail: TAGCATCTGAATTTCATAACCAATCTCGATACAC Fas1_rev_MI: CCTGTTCAGACGGATCAATGTCCA
Genotyping of *fas2-5* (SALK_147693)	At5g64630	FAS2-LP: TTTGCCCTGTTGCATTTAAAC LBb1.3: ATTTTGCCGATTTCGGAAC FAS2-RP: GCCCAATAATGATCCACAATG
Genotyping of *athira-1* (WiscDsLox362H05)	At3g44530	p745_WiscDsLox: AACGTCCGCAATGTGTTATTAAGTTGTC Hira_Wisc_LP: CTACTAAAATTTGAGGCCGGG Hira_Wisc_RP: GAGAGTCACTGTTTTGGCTGG
Genotyping of ncn1 (GABI_018D02)	At1g77310	At1g77310_GK_LP: TTCGCCAATTAAACATGATGG GK_o8409: ATATTGACCATCATACTCATTGC At1g77310_GK_RP: AGGCATGCCATTGTTAACTTG
Genotyping of *ncn2* (GABI_130H01)	At1g21610	At1g21610_GK_LP: TGTGGACCTTGATCTTCATCC GK_o8409: ATATTGACCATCATACTCATTGC At1g21610_GK_RP: AAGCTGATACCTCATCCCAGG
Genotyping of *cbn* (SALK_099927)	At4g32820	Cabin_SALK099927_LP: TGCCAATAAATGCTTAATCGC LBb1.3: ATTTTGCCGATTTCGGAAC Cabin_SALK099927_RP: GCTGTAAAAACGGAAGAAGGG
Genotyping of SALK_019573	At3g44530	LBb1.3: ATTTTGCCGATTTCGGAAC Salk_019573_LP : GTAGGGGATTTGAGCTTCGAC Salk_019573_RP : GCCAGTAGCAAACCTTTCTCC
Genotyping of GABI_775H03	At3g44530	GK_o8409: ATATTGACCATCATACTCATTGC SALK_143806-LP : TTG CAA GAA GCC TCT CTT TTG SALK_143806-RP : CTC CAA AGT CCA AAG GTA GGG
Absence of *FAS1* transcript	At1g65470	FAS1_5UTR_For : CACTCAGCTCGTGTTTCTCG Fas1_rev_MI : CCTGTTCAGACGGATCAATGTCCA
Absence of *FAS2* transcript	At5g64630	FAS2-3_LP : CATTCGTTTTTCTCCATCTGG FAS2-RP : GCC CAA TAA TGA TCC ACA ATG
Absence of *NCN1* transcript	At1g77310	Atnulein1-upstream-F : ACGGCTTCTTAATGCCAAC Atnuclein1_Rev : ACTAAGGACGTGGTGGTTGC
Absence of *NCN2* transcript	At1g21610	Atnuclein2-upstream-F : GAGTCACCTTTGCCTTCTGG Atnuclein2_Rev : TAGTGACCACGGAAGTGCTG
Absence of *CBN* transcript	At4g32820	Cabin_exon6_for : CCGAGCTGTACCATGACTTTG AtCabin_Rev : AACCGAAGGAACCACTGATG
Absence of *AtHIRA* transcript	At3g44530	HIRA_int_For : GTTGGAGTTCCCCAACAGG HIRA qRT R1 : CAAAACATCGAGAGAAGTTCA
Actin (ACTIN2)	At3g18780	Act2d (Act2-7 F) :CTAAGCTCTCAAGATCAAAGGC Act2r (Act2-7 R): AACATTGCAAAGAGTTTCAAGG
qRT-PCR of *FAS1*	At1g65470	Fas1_fw_MI: ATGGTATCTGGCCCAGCCAAA Fas1_rev_MI: CCTGTTCAGACGGATCAATGTCCA
qRT-PCR of *FAS2*	At5g64630	FAS2_qpcr_Forter: AAACCGGTTGTAGTGGTTCG FAS2_qpcr_Revter: TGCAGCATAGTGGAGACCTG
qRT-PCR of *NCN1*	At1g77310	At1g77310_nuclein1_qpcr_Forter : ATCCTGCAGCAGAAGGAAAG At1g77310_nuclein1_qpcr_Revter : TCTTGGCCTTTGGATGTACC
qRT-PCR of *NCN2*	At1g21610	At1g21610_nuclein2_qpcr_Forbis : GCAAAGGAGAGACGAAAAGC At1g21610_nuclein2_qpcr_Revbis : TAGTGACCACGGAAGTGCTG
qRT-PCR of *CBN*	At4g32820	At1g77310_cabin_qpcr_For : CGAACCTGCTCCTAAGGTTG At1g77310_cabin_qpcr_Rev: cctctctgcagaaaatcacc
qRT-PCR of *AtHIRA*	At3g44530	HIRA qRT F2 : AACAAGACCAGAACTCAAGA HIRA qRT R2 : CTTTAACAACGCCTAACTGAG
qRT-PCR of *ASF1A*	At1g66740	At1g66740 RT-For : GTT GGC AAC TAC CGC TTT GT At1g66740 RT-Rev : AAA AGC AAA GCG CAA CAT CT
qRT-PCR of *ASF1B*	At5g38110	ASF1B_qpcr_Forter : TGAATCCATTCCAGTTCGAG ASF1B_qpcr_Revter : AACGGATCTGGAGAGTCAGC
qRT-PCR and ChIP qPCR of 106B	106B	AP394 106Bq-F: TCATTATGCTAGGTGGTTGA AP395 106Bq-R: GACAACAAGTTCATTAACCA
qRT-PCR and ChIP qPCR of 180bp	180bp	180(all)-F: ACCATCAAAGCCTTGAGAAGCA 180(all)-R: CCGTATGAGTCTTTGTCTTTGTATCTTCT
qRT-PCR of At1g74930_*ERF/AP2*	At1g74930	At1g74930_ERF/AP2_qpcr_Forbis: TTACGACACTCCCGAGAAGG At1g74930_ERF/AP2_qpcr_Revbis: CCGGGTACTAAACCCGATTC
qRT-PCR of At3g16800_PP2C	At3g16800	At3g16800_PP2C_qpcr_F : CCGAAAGATAACCGACAAGG At3g16800_PP2C_qpcr_R : TGGCGATGCTTCTTCTCTTC
qRT-PCR of At4g25490_*CBF1*	At4g25490	At4g25490_CBF1_qpcr-F : CGCCAAGGATATCCAAAAAG At4g25490_CBF1_qpcr-R : GGCATCCCAAACATTGTCTC

qRT-PCR of *At4g28110_MYB41*	At4g28110	At4g28110_MYB41_qpcr_Revrter: GACATTGGCGTTGACATGAG At4g28110_MYB41_qpcr_Forter: TTTACCCATCGAACCTCGAC
ChIP qPCR of *HXK1*	At4g29130	At4g29130_ChIP-F: AGGAGCTCGTCTCTCTGCTG At4g29130_ChIP-R: GCTCAAACAATCCACCATCC At4g29130_5-ChIP-F : GTTGGAGCGACTGTTGTTTG At4g29130_5-ChIP-R : TGCATCTCAACGGTCATAGC At4g29130_mid-ChIP-F : TGTTCGCTACAGAATGCGAAG At4g29130_mid-ChIP-R : ggcaaaggcgaaaactaaac
ChIP qPCR of *UEV1C*	At2g36060	At2G36060_ChIP-F: GGTGACTGAAATGTGAATTTGC At2G36060_ChIP-R: ATGCAGCCATCTCTCTTCTTC At2G36060_5-ChIP-F : ttctgctgcaccaatagag At2G36060_5-ChIP-R : ACACTCGATCCTGAGCCAAG At2G36060_mid-ChIP-F : tttcaagctcagtgctttgc At2G36060_mid-ChIP-R : ACCGATGATAGTGCCAGTCC
ChIP qPCR of *UBC28*	At1g64230	At1g64230-ChIP-F: TCATTGTTAACGGACCCAAAC At1g64230-ChIP-R: CCAGCTTCTCGCAGTAGACTC At1g64230_5-ChIP-F : ccgagtttggaggatctgtc At1g64230_5-ChIP-R : GAAGTTGGAGGATCCTTCTGG At1g64230_mid-ChIP-F : GTCCTTATTCAGGCGGTGTC At1g64230_mid-ChIP-R : ATGTCAAGGCAAATGCTCC
ChIP qPCR of *TSI*	TSI	TSIq-F: CTCTACCCTTTGCATTCATGAATCCTT TSIq-R: GATGGGCAAAGCCCTCGGTTTTAAAATG
ChIP qPCR of intergenic region between At2g17670 and At2g17680	Intergenic region between At2g17670 and At2g17680	IG-2g17670-80qF: GGCTACTGTCTAGTTCATATCTTAGA IG-2g17670-80qR: TAGGTTGGCATCCGATCCAGAGT
qRT-PCR of *SAND*	At2g28390	SA-F: AACTCTATGCAGCATTTGATCCACT SA-R: TGATTGCATATCTTTATCGCCATC
semi quantitative RT-PCR of *Ta3*	pericentromeric region of chromosome 1	Ta3 middle-F : GATTCTTACTGTAAAGAACATGGCATTG Ta3 middle-R : TCCAAATTTCCTGAGGTGCTTGTAACC
semi quantitative RT-PCR of *Mule*	At2g15810	MULE-F2 : CTGTCCGCGAGTGTCATCAAGTAGC MULE-R2 : GATACTTGTTGACAAGTGTTTAGCAAGCC
semi quantitative RT-PCR of *UBC28*	At1g64230	UBC28qF : TCCACGAAGGATCCTCCAACTTCCTGCAGT UBC28qR : ATGGTTACGAGAAAAGACACCGCCTGAATA
construction of amiRNA for *AtHIRA*	At3g44530	HIRA I miR-s : gaTTAGTGTAAACCTGACGCTTtctctctttttgtattcc HIRA II miR-a : gaAAGCGTCCAGGTTTACACTAAtcaaagagaatcaatga HIRA III miR*s : gaAAACGTCCAGGTTAACACTATtcacaggtcgtgatatg HIRA IV miR*a : gaATAGTGTTAACCTGGACGTTTctcacatatatattcct

References

Ahmad, K. and Henikoff, S. (2002). The histone variant H3.3 marks active chromatin by replication-independent nucleosome assembly. Mol. Cell **9**: 1191–1200.

Alexander, M. (1969). Differential staining of aborted and nonaborted pollen. Stain Technol. **44**: 117–22.

Amin, A.D., Vishnoi, N., and Prochasson, P. (2011). A global requirement for the HIR complex in the assembly of chromatin. Biochim. Biophys. Acta **1819**: 264–76.

Balaji, S., Iyer, L.M., and Aravind, L. (2009). HPC2 and ubinuclein define a novel family of histone chaperones conserved throughout eukaryotes. Mol. Biosyst. **5**: 269–275.

Banumathy, G., Somaiah, N., Zhang, R., Tang, Y., Hoffmann, J., Andrake, M., Ceulemans, H., Schultz, D., Marmorstein, R., and Adams, P.D. (2009). Human UBN1 is an ortholog of yeast Hpc2p and has an essential role in the HIRA/ASF1a chromatin-remodeling pathway in senescent cells. Mol. Cell. Biol. **29**: 758–70.

Blackwell, C. and Martin, K. (2004). Schizosaccharomyces pombe HIRA-like protein Hip1 is required for the periodic expression of histone genes and contributes to the function of complex centromeres. Mol. Cell. Biol. **24**: 4309–4320.

Bonnefoy, E., Orsi, G. a, Couble, P., and Loppin, B. (2007). The essential role of Drosophila HIRA for de novo assembly of paternal chromatin at fertilization. PLoS Genet. **3**: 1991–2006.

Bowler, C., Benvenuto, G., Laflamme, P., Molino, D., Probst, A. V, Tariq, M., and Paszkowski, J. (2004). Chromatin techniques for plant cells. Plant J. **39**: 776–789.

Campos, E.I., Fillingham, J., Li, G., Zheng, H., Voigt, P., Kuo, W.H., Seepany, H., Gao, Z., Day, L.A., Greenblatt, J.F., and Reinberg, D. (2010). The program for processing newly synthesized histones H3.1 and H4. Nat. Struct. Mol. Biol. **17**: 1343–51.

Cui, B., Liu, Y., and Gorovsky, M. a (2006). Deposition and function of histone H3 variants in Tetrahymena thermophila. Mol. Cell. Biol. **26**: 7719–30.

Czechowski, T., Stitt, M., Altmann, T., Udvardi, M.K., and Scheible, W.R. (2005). Genome-wide identification and testing of superior reference genes for transcript normalization in Arabidopsis. Plant Physiol. **139**: 5–17.

Drané, P., Ouararhni, K., Depaux, A., Shuaib, M., and Hamiche, A. (2010). The death-associated protein DAXX is a novel histone chaperone involved in the replication-independent deposition of H3.3. Genes Dev. **24**: 1253–1265.

Duc, C., Sherstnev, A., Cole, C., Barton, G.J., and Simpson, G.G. (2013). Transcription Termination and Chimeric RNA Formation Controlled by Arabidopsis thaliana FPA. PLoS Genet. **9**: e1003867.

Dunleavy, E.M., Almouzni, G., and Karpen, G.H. (2011). H3.3 is deposited at centromeres in S phase as a placeholder for newly assembled CENP-A in G1 phase. Nucleus **2**: 146–57.

Edgar, R.C. (2004). MUSCLE: multiple sequence alignment with high accuracy and high throughput. Nucleic Acids Res. **32**: 1792–7.

English, C.M., Adkins, M.W., Carson, J.J., Churchill, M.E. a, and Tyler, J.K. (2006). Structural basis for the histone chaperone activity of Asf1. Cell **127**: 495–508.

Exner, V., Taranto, P., Schönrock, N., Gruissem, W., and Hennig, L. (2006). Chromatin assembly factor CAF-1 is required for cellular differentiation during plant development. Development **133**: 4163–4172.

Filipescu, D., Szenker, E., and Almouzni, G. (2013). Developmental roles of histone H3 variants and their chaperones. Trends Genet. **29**: 630–40.

Formosa, T., Ruone, S., and Adams, M. (2002). Defects in SPT16 or POB3 (yFACT) in Saccharomyces cerevisiae cause dependence on the Hir/Hpc pathway: polymerase passage may degrade chromatin structure. Genetics **3**: 1557–1571.

Gaillard, P.H., Martini, E.M., Kaufman, P.D., Stillman, B., Moustacchi, E., and Almouzni, G. (1996). Chromatin assembly coupled to DNA repair: a new role for chromatin assembly factor I. Cell **86**: 887–896.

Galbraith, D.W., Harkins, K.R., Maddox, J.M., Ayres, N.M., Sharma, D.P., and Firoozabady, E. (1983). Rapid flow cytometric analysis of the cell cycle in intact plant tissues. Science **220**: 1049–51.

Goldberg, A.D. et al. (2010). Distinct factors control histone variant H3.3 localization at specific genomic regions. Cell **140**: 678–691.

Groth, A., Corpet, A., Cook, A.J., Roche, D., Bartek, J., Lukas, J., and Almouzni, G. (2007). Regulation of replication fork progression through histone supply and demand. Science (80-.). **318**: 1928–1931.

Hennig, L., Bouveret, R., and Gruissem, W. (2005). MSI1-like proteins: an escort service for chromatin assembly and remodeling complexes. Trends Cell Biol. **15**: 295–302.

Hödl, M. and Basler, K. (2009). Transcription in the absence of histone H3.3. Curr. Biol. **19**: 1221–6.

Houlard, M., Berlivet, S., Probst, A. V, Quivy, J.-P.P., Héry, P., Almouzni, G., and Gérard, M. (2006). CAF-1 is essential for heterochromatin organization in pluripotent embryonic cells. PLoS Genet. **2**: e181.

Ingouff, M. and Berger, F. (2010). Histone3 variants in plants. Chromosoma **119**: 27–33.

Ingouff, M., Hamamura, Y., Gourgues, M., Higashiyama, T., and Berger, F. (2007). Distinct dynamics of HISTONE3 variants between the two fertilization products in plants. Curr. Biol. **17**: 1032–1037.

Ingouff, M., Rademacher, S., Holec, S., Soljić, L., Xin, N., Readshaw, A., Foo, S.H., Lahouze, B., Sprunck, S., and Berger, F. (2010). Zygotic Resetting of the HISTONE 3 Variant Repertoire Participates in Epigenetic Reprogramming in Arabidopsis. Curr. Biol. **20**: 2137–2143.

Jin, C. and Felsenfeld, G. (2007). Nucleosome stability mediated by histone variants H3.3 and H2A.Z. Genes Dev. **21**: 1519–1529.

Jin, C., Zang, C., Wei, G., Cui, K., Peng, W., Zhao, K., and Felsenfeld, G. (2009). H3.3/H2A.Z double variant-containing nucleosomes mark “nucleosome-free regions” of active promoters and other regulatory regions. Nat. Genet. **41**: 941–945.

Kaufman, P.D., Cohen, J.L., and Osley, M. a (1998). Hir proteins are required for position-dependent gene silencing in Saccharomyces cerevisiae in the absence of chromatin assembly factor I. Mol. Cell. Biol. **18**: 4793–806.

Kaya, H., Shibahara, K.I., Taoka, K.I., Iwabuchi, M., Stillman, B., and Araki, T. (2001). FASCIATA genes for chromatin assembly factor-1 in arabidopsis maintain the cellular organization of apical meristems. Cell **104**: 131–142.

Kirik, A., Pecinka, A., Wendeler, E., and Reiss, B. (2006). The chromatin assembly factor subunit FASCIATA1 is involved in homologous recombination in plants. Plant Cell **18**: 2431–2442.

Klapholz, B., Dietrich, B.H., Schaffner, C., Hérédia, F., Quivy, J.-P., Almouzni, G., and Dostatni, N. (2009). CAF-1 is required for efficient replication of euchromatic DNA in Drosophila larval endocycling cells. Chromosoma **118**: 235–48.

De Koning, L., Corpet, A., Haber, J.E., and Almouzni, G. (2007). Histone chaperones: an escort network regulating histone traffic. Nat. Struct. Mol. Biol. **14**: 997–1007.

Langmead, B., Trapnell, C., Pop, M., and Salzberg, S.L. (2009). Ultrafast and memory-efficient alignment of short DNA sequences to the human genome. Genome Biol. **10**: R25.

Lewis, P.W., Elsaesser, S.J., Noh, K.M., Stadler, S.C., and Allis, C.D. (2010). Daxx is an H3.3-specific histone chaperone and cooperates with ATRX in replication-independent chromatin assembly at telomeres. Proc. Natl. Acad. Sci. U. S. A. **107**: 14075–14080.

Loppin, B., Bonnefoy, E., Anselme, C., Laurençon, A., Karr, T.L., and Couble, P. (2005). The histone H3.3 chaperone HIRA is essential for chromatin assembly in the male pronucleus. Nature **437**: 1386–1390.

Milne, I., Stephen, G., Bayer, M., Cock, P.J. a, Pritchard, L., Cardle, L., Shaw, P.D., and Marshall, D. (2013). Using Tablet for visual exploration of second-generation sequencing data. Brief. Bioinform. **14**: 193–202.

Mito, Y., Henikoff, J.G., and Henikoff, S. (2005). Genome-scale profiling of histone H3.3 replacement patterns. Nat. Genet. **37**: 1090–1097.

Morel, J.B., Mourrain, P., Béclin, C., and Vaucheret, H. (2000). DNA methylation and chromatin structure affect transcriptional and post-transcriptional transgene silencing in Arabidopsis. Curr. Biol. **10**: 1591–1594.

Morozov, V., Gavrilova, E., Ogryzko, V., and Ishov, A. (2012). Dualistic function of Daxx at centromeric and pericentromeric heterochromatin in normal and stress conditions. Nucleus **3**: 276–285.

Natsume, R., Eitoku, M., Akai, Y., and Sano, N. (2007). Structure and function of the histone chaperone CIA/ASF1 complexed with histones H3 and H4. Nature **446**: 1–4.

Ono, T., Kaya, H., Takeda, S., Abe, M., Ogawa, Y., Kato, M., Kakutani, T., Mittelsten Scheid, O., Araki, T., and Shibahara, K. (2006). Chromatin assembly factor 1 ensures the stable maintenance of silent chromatin states in Arabidopsis. Genes to Cells **11**: 153–162.

Osley, M. a and Lycan, D. (1987). Trans-acting regulatory mutations that alter transcription of Saccharomyces cerevisiae histone genes. Mol. Cell. Biol. **7**: 4204–10.

Pchelintsev, N.A., Mcbryan, T., Rai, T.S., van Tuyn, J., Ray-Gallet, D., Almouzni, G., and Adams, P.D. (2013). Placing the HIRA Histone Chaperone Complex in the Chromatin Landscape. CellReports **3**: 1012–1019.

Pecinka, A., Dinh, H.Q., Baubec, T., Rosa, M., Lettner, N., and Mittelsten Scheid, O. (2010). Epigenetic regulation of repetitive elements is attenuated by prolonged heat stress in Arabidopsis. Plant Cell **22**: 3118–3129.

Petesch, S. and Lis, J. (2012). Overcoming the nucleosome barrier during transcript elongation. Trends Genet. **28**: 285–94.

Phelps-Durr, T.L., Thomas, J., Vahab, P., and Timmermans, M.C.P. (2005). Maize rough sheath2 and its Arabidopsis orthologue ASYMMETRIC LEAVES1 interact with HIRA, a predicted histone chaperone, to maintain knox gene silencing and determinacy during organogenesis. Plant Cell **17**: 2886–2898.

Probst, A. V, Fransz, P.F., Paszkowski, J., and Mittelsten Scheid, O. (2003). Two means of transcriptional reactivation within heterochromatin. Plant J. **33**: 743–749.

Ramirez-Parra, E. and Gutierrez, C. (2007). E2F regulates FASCIATA1, a chromatin assembly gene whose loss switches on the endocycle and activates gene expression by changing the epigenetic status. Plant Physiol. **144**: 105–20.

Ray-Gallet, D., Quivy, J.P., Scamps, C., Martini, E.M., Lipinski, M., and Almouzni, G. (2002). HIRA is critical for a nucleosome assembly pathway independent of DNA synthesis. Mol. Cell **9**: 1091–1100.

Ray-Gallet, D., Woolfe, A., Vassias, I., Pellentz, C., Lacoste, N., Puri, A., Schultz, D.C., Pchelintsev, N.A., Adams, P.D., Jansen, L.E., and Almouzni, G. (2011). Dynamics of histone H3 deposition in vivo reveal a nucleosome gap-filling mechanism for H3.3 to maintain chromatin integrity. Mol. Cell **44**: 928–941.

Rigal, M. and Mathieu, O. (2011). A “mille-feuille” of silencing: Epigenetic control of transposable elements. Biochim. Biophys. Acta **1809**: 452–8.

Roberts, C., Sutherland, H.F., Farmer, H., Kimber, W., Halford, S., Carey, A., Brickman, J.M., Wynshaw-Boris, A., and Scambler, P.J. (2002). Targeted mutagenesis of the Hira gene results in gastrulation defects and patterning abnormalities of mesoendodermal derivatives prior to early embryonic lethality. Mol. Cell. Biol. **22**: 2318–2328.

Sakai, A., Schwartz, B.E., Goldstein, S., and Ahmad, K. (2009). Transcriptional and developmental functions of the H3.3 histone variant in Drosophila. Curr. Biol. **19**: 1816–1820.

Sawatsubashi, S. et al. (2010). A histone chaperone, DEK, transcriptionally coactivates a nuclear receptor. Genes Dev. **24**: 159–170.

Schneiderman, J.I., Orsi, G.A., Hughes, K.T., Loppin, B., and Ahmad, K. (2012). Nucleosome-depleted chromatin gaps recruit assembly factors for the H3.3 histone variant. Proc. Natl. Acad. Sci. **109**: 19721–19726.

Schönrock, N., Exner, V., Probst, A., Gruissem, W., and Hennig, L. (2006). Functional genomic analysis of CAF-1 mutants in Arabidopsis thaliana. J. Biol. Chem. **281**: 9560–9568.

Schwab, R., Ossowski, S., Riester, M., Warthmann, N., and Weigel, D. (2006). Highly specific gene silencing by artificial microRNAs in Arabidopsis. Plant Cell **18**: 1121–1133.

Schwab, R., Ossowski, S., Warthmann, N., and Weigel, D. (2010). Directed gene silencing with artificial microRNAs. Methods Mol. Biol. (Clifton, NJ) **592**: 71–88.

Schwartz, B.E. and Ahmad, K. (2005). Transcriptional activation triggers deposition and removal of the histone variant H3.3. Genes Dev. **19**: 804–814.

Song, Y., Seol, J.H., Yang, J.H., Kim, H.J., Han, J.W., Youn, H.D., and Cho, E.J. (2013). Dissecting the roles of the histone chaperones reveals the evolutionary conserved mechanism of transcription-coupled deposition of H3.3. Nucleic Acids Res. **41**: 5199–209.

Spector, M., Raff, A., and DeSilva, H. (1997). Hir1p and Hir2p function as transcriptional corepressors to regulate histone gene transcription in the Saccharomyces cerevisiae cell cycle . Mol. Cell. Biol. **17**: 545–552.

Steimer, A., Amedeo, P., Afsar, K., Fransz, P., Mittelsten Scheid, O., and Paszkowski, J. (2000). Endogenous targets of transcriptional gene silencing in Arabidopsis. Plant Cell **12**: 1165–1178.

Stillman, B. (1989). Purification and characterization of CAF-I, a human cell factor required for chromatin assembly during DNA replication in vitro. Cell **58**: 15–25.

Stroud, H., Otero, S., Desvoyes, B., Ramírez-Parra, E., Jacobsen, S.E., and Gutierrez, C. (2012). Genome-wide analysis of histone H3.1 and H3.3 variants in Arabidopsis thaliana. Proc. Natl. Acad. Sci. **109**: 5370–5.

Szenker, E., Lacoste, N., and Almouzni, G. (2012). A developmental requirement for HIRA-dependent H3.3 deposition revealed at gastrulation in Xenopus. Cell Rep. **1**: 730–40.

Tagami, H., Ray-Gallet, D., Almouzni, G., and Nakatani, Y. (2004). Histone H3.1 and H3.3 complexes mediate nucleosome assembly pathways dependent or independent of DNA synthesis. Cell **116**: 51–61.

Takeda, S., Tadele, Z., Hofmann, I., Probst, A. V, Angelis, K.J., Kaya, H., Araki, T., Mengiste, T., Mittelsten Scheid, O., Shibahara, K., Scheel, D., and Paszkowski, J. (2004). BRU1, a novel link between responses to DNA damage and epigenetic gene silencing in Arabidopsis. Genes Dev. **18**: 782–793.

Talbert, P. and Henikoff, S. (2010). Histone variants--ancient wrap artists of the epigenome. Nat. Rev. Mol. cell Biol. **11**: 264–275.

Talbert, P.B. et al. (2012). A unified phylogeny-based nomenclature for histone variants. Epigenetics Chromatin **5**: doi: 10.1186/1756–8935–5–7.

Tamura, K., Peterson, D., Peterson, N., Stecher, G., Nei, M., and Kumar, S. (2011). MEGA5: molecular evolutionary genetics analysis using maximum likelihood, evolutionary distance, and maximum parsimony methods. Mol. Biol. Evol. **28**: 2731–9.

Tang, Y., Poustovoitov, M. V, Zhao, K., Garfinkel, M., Canutescu, A., Dunbrack, R., Adams, P.D., and Marmorstein, R. (2006). Structure of a human ASF1a-HIRA complex and insights into specificity of histone chaperone complex assembly. Nat. Struct. Mol. Biol. **13**: 921–9.

Tang, Y., Puri, A., Ricketts, M.D., Rai, T., Hoffmann, J., Hoi, E., Adams, P., Schultz, D., and Marmorstein, R. (2012). Identification of an Ubinuclein 1 region required for stability of the human HIRA/UBN1/CABIN1/ASF1a histone H3.3 chaperone complex. Biochemistry **51**: 2366–77.

Tyler, J. and Collins, K. (2001). Interaction between the Drosophila CAF-1 and ASF1 Chromatin Assembly Factors. Mol. Cell. Biol. **21**: 6574–6584.

Wollmann, H., Holec, S., Alden, K., Clarke, N., Jacques, P., and Berger, F. (2012). Dynamic deposition of histone variant h3.3 accompanies developmental remodeling of the Arabidopsis transcriptome. PLoS Genet. **8**: e1002658.

Wong, L.H., Ren, H., Williams, E., McGhie, J., Ahn, S., Sim, M., Tam, A., Earle, E., Anderson, M.A., Mann, J., and Choo, K.H. (2009). Histone H3.3 incorporation provides a unique and functionally essential telomeric chromatin in embryonic stem cells. Genome Res. **19**: 404–414.

Yamane, K., Mizuguchi, T., Cui, B., Zofall, M., Noma, K., and Grewal, S.I. (2011). Asf1/HIRA Facilitate Global Histone Deacetylation and Associate with HP1 to Promote Nucleosome Occupancy at Heterochromatic Loci. Mol. Cell **41**: 56–66.

Yang, J.-H., Choi, J.-H., Jang, H., Park, J.-Y., Han, J.-W., Youn, H.-D., and Cho, E.-J. (2011). Histone chaperones cooperate to mediate Mef2-targeted transcriptional regulation during skeletal myogenesis. Biochem. Biophys. Res. Commun. **407**: 541–7.

Ye, X., Franco, A. a, Santos, H., Nelson, D.M., Kaufman, P.D., and Adams, P.D. (2003). Defective S phase chromatin assembly causes DNA damage, activation of the S phase checkpoint, and S phase arrest. Mol. Cell **11**: 341–51.

Zeller, G., Henz, S., Widmer, C., Sachsenberg, T., Rätsch, G., Weigel, D., and Laubinger, S. (2009). Stress-induced changes in the Arabidopsis thalianatranscriptome analyzed using whole-genome tiling arrays. Plant J. **58**: 1068–1082.

Zhu, Y., Dong, A., and Shen, W.H. (2013). Histone variants and chromatin assembly in plant abiotic stress responses. Biochim. Biophys. Acta **1819**: 343–8.

Zhu, Y., Weng, M., Yang, Y., Zhang, C., Li, Z., Shen, W.H., and Dong, A. (2011). Arabidopsis homologues of the histone chaperone ASF1 are crucial for chromatin replication and cell proliferation in plant development. Plant J. **66**: 443–55.

Chapter III: Role of CAF-1 mediated H3.1 deposition in chromocenter formation

Matthias Benoit, Lauriane Simon, Céline Duc, Sylviane Cotterell, Marie-Claude Espagnol, Axel Poulet, Samuel Le Goff, Christophe Tatout and Aline V. Probst.

Submitted to EMBO reports.

In **Chapter II**, we described that the HIR chaperone complex is involved in maintenance of chromatin organization by mediating proper histone dynamics. Moreover, we revealed that genetic interactions between the different nucleosomal assembly pathways, and notably between HIR and the replication-dependent CAF-1 chaperone participate in chromatin maintenance and genome integrity.

Here, we were interested in the role of AtHIRA and CAF-1 in the establishment of the cytological and the molecular features of euchromatic and heterochromatic domains. Previous work from the laboratory showed that chromocenters are established progressively during the early days of post-germination development in cotyledons, but precise kinetics and molecular entities mediating this phenomenon remain unknown. This time window offers an original approach to study how chromatin assembly of specific H3 variants and their relative set of post-translational marks participate in the formation of chromocenters.

Using different mutant lines and the e-H3.1 line characterized in **Chapter I**, we show that deposition of H3K27me1 by ATXR5 and ATXR6, and to a lesser extent H3K9me2 dynamics mediated by SUVH4, SUVH5 and SUVH6, affect the kinetics of chromocenter formation. We reveal that CAF-1, contrary to AtHIRA, participates actively in post-germination clustering of heterochromatic repeats in chromocenters by mediating proper histone H3.1 dynamics. Lack of H3.1 assembly at heterochromatic loci in *fas* mutants interferes with chromatin structure, proper setting of histone post-translational marks and finally chromocenter establishment.

This work describes the importance of proper site-specific deposition of histone variants by chaperones in the setting of local epigenetic features at the

nucleosomal level, to ultimately establish spatial isolation of heterochromatic domains from the euchromatic regions in the nuclear volume.

This research paper is the product of the largest part of my PhD thesis. I generated and validated the e-H3.1 lines and verified the subsequent introgression in the *fas1* background. I led the different molecular analyses presented in this chapter, with exception of the e-H3.1 immunolocalization, which was carried out by Lauriane Simon and Western Blot analysis, which was carried out by Sylviane Cotterell. I carried out the data analysis and participated in the writing of the manuscript.

Abstract

Chromocenter organization compartmentalizes heterochromatin from the rest of the genome and is thought to contribute to transcriptional repression by locally concentrating silencing factors. The question how chromocenters are established during development and subsequently maintained is relevant for eukaryotic genome organization and integrity. Here, we studied heterochromatin organization in Arabidopsis cotyledon nuclei during the first days after germination as paradigm to define factors involved in chromocenter formation. We find that dispersion of centromeric and pericentromeric repeats two days after germination moderately reduces transcriptional silencing at these loci. Repetitive sequence elements, the bulk of chromocenter DNA, are enriched in the repressive post-translational histone modifications H3K9me2 and H3K27me1 as early as two days after germination and the failure to appropriately set these marks affects chromocenter formation. Clustering of repetitive elements in chromocenters correlates with an increase of the canonical histone H3.1 specifically at heterochromatic repeats. The observed H3.1 dynamics at heterochromatin regions require a functional CHROMATIN ASSEMBLY FACTOR-1 (CAF-1) H3 chaperone complex and CAF-1 loss compromises chromocenter formation. Taken together, we suggest that CAF-1 mediated histone deposition and concomitant modification of histone tails is critical for chromocenter formation.

Introduction

In eukaryotes, the genetic information is tightly organized within chromatin, a nucleoprotein structure that compacts the genome to fit into the small compartment of the cell nucleus and functions as carrier of epigenetic information. Different folding of the array of nucleosomes, the basic subunits of chromatin, results in distinct higher-order chromatin structures such as the condensed heterochromatin domains that contain mainly transposable elements and other repetitive sequences. Proper organization of heterochromatin is critical for genome integrity as it prevents illegitimate recombination and transcription of these genetic elements. In certain yeasts, animals and plants, heterochromatin domains cluster in cytologically distinct chromocenters. Chromocenter organization is thought to contribute to heterochromatin function as it physically separates the repetitive elements from the rest of the genome and may so favor the concentration of silencing factors (1). Indeed, heterochromatic repeats in chromocenters are enriched in specific sets of epigenetic marks that repress transcription, including DNA methylation, specific post-translational modifications (PTMs) of histones such as hypoacetylation and methylation of H3K9me2/3 and H3K27me1 (2–5). They further show high nucleosomal density (6) and low DNase I accessibility (7). In addition, histone variants can change the composition of the nucleosomes which profoundly affects stability and ultimately higher-order organization of the chromatin fiber (8, 9). While the H3 variant H3.3 found at actively transcribed genes creates more unstable nucleosomes contributing to accessible chromatin structures (10–12), the canonical H3.1 variant is found in transcriptionally inactive heterochromatin (12–16).

The number and distribution of chromocenters as well as the chromosomes involved in an individual chromocenter can vary in different cell types and during differentiation (17, 18), suggesting that the nuclear organization of heterochromatin has a role beyond transcriptional control of the underlying repeat sequences. Indeed, sequestration or re-localization of certain euchromatic loci close to heterochromatin domains results in altered gene expression (19–21). In Arabidopsis, chromocenters serve as an architectural framework and function as organizing centers for gene-rich euchromatic loops within the chromosome territory (22–24). Interestingly, chromocenter organization is not static. Instead, higher-order chromatin organization can be profoundly affected in response to developmental or environmental cues that

induce important changes in gene expression patterns (25). A transient decondensation of chromocenter structures has been observed upon heat stress or during dedifferentiation (26, 27), but also takes place during developmental phase transitions such the flowering transition or germination (28, 29). Indeed, immediately after germination, centromeric and pericentromeric repeats are dispersed in the nucleus and only small pre-chromocenters are detectable in cotyledon nuclei (29–31). Within a few days, chromocenter organization becomes progressively more pronounced (25, 30, 31). However, the molecular features of centromeric and pericentromeric repeats at the different states of higher-order organization and the mechanisms that drive chromocenter formation are not understood so far.

Here we show that centromeric and pericentromeric repeats change their spatial organization to cluster into chromocenters, in a precise temporal arrangement that coincides with a reinforcement of transcriptional repression of pericentromeric repeats. Early after germination and before conspicuous chromocenter structures are established, repressive histone marks are already enriched at centromeric and pericentromeric repeats. H3K9me2 levels increase during post-germination development and the histone methyltransferases responsible for H3K9 di- or H3K27 monomethylation are required for normal kinetics of repeat clustering. Finally, we show that chromocenter formation correlates with an increase in canonical H3.1 specifically at heterochromatic regions and that H3.1 loading and chromocenter formation require the CAF-1 chaperone. We conclude that chromocenter formation is associated with local enrichments in histone marks and variants and suggest that replication-coupled H3.1 deposition and installation of repressive PTMs play a critical role in this process.

Results

Progressive formation of chromocenters during post-germination development is associated with transcriptional repression

To quantify the centromeric and pericentromeric repeat clustering during chromocenter formation and follow its kinetics, we developed an assay based on 6-diamidino-2-phenylindole (DAPI) staining and Fluorescence *in situ* hybridization (FISH). We used two probes that reveal repetitive sequences present on all five Arabidopsis chromosomes: the centromeric 180 bp satellite repeats (32) and the pericentromeric derivatives of the Athila retrotransposon termed Transcriptionally Silent Information (TSI) (3, 33). We dissected cotyledons from seedlings aged 2 to 5 days after germination (dag), performed FISH and defined two classes of nuclei: either these repeats are clustered within nuclear subdomains termed chromocenters that stain brightly with DAPI, or dispersed into the nucleoplasm (***Figure 1A***). We determined the percentage of nuclei with fully clustered 180 bp and TSI repeats revealing that the majority of cotyledon nuclei at 2 dag exhibit small pre-chromocenters (***Figure 1B***). Indeed, the quantification of clustered nuclei by FISH showed that both repeat types show similar organization kinetics with only about 22% of the nuclei with completely clustered repeats at 2 dag (***Figure 1BC***) compared to ~80% by 5 dag (***Figure 1BC***). Repetitive elements, such as centromeric and pericentromeric repeats, are nearly completely silenced in mature leaf tissue, in which they are known to cluster in chromocenters (3, 33, 34). Therefore, we were interested to know whether chromocenter formation contributes to transcriptional repression of repetitive elements. To this aim, we quantified transcript levels of TSI repeats and the Ta3 retrotransposon located in the pericentromeric region by RT-qPCR from total RNAs isolated from dissected cotyledons aged of 2 to 5 dag. We reproducibly observed higher levels of TSI and Ta3 transcripts in cotyledons aged 2 dag, when these genomic regions are dispersed in the large majority of nuclei (***Figure 1D***). Nevertheless, TSI transcript levels remain low in comparison to *mom1-2* mutants that strongly alleviate TSI silencing (33) (***Supplementary Figure 1***). We conclude that heterochromatic repeats progressively cluster into chromocenter structures from 2 to 5 dag and that chromocenter formation correlates with enhanced transcriptional silencing.

H3K9me2 and H3K27me1 enrichments precede chromocenter formation

We then characterized local chromatin features of these repetitive elements at different states of chromocenter formation and examined if particular PTMs could play a role in the cytologically observed organization process. To obtain sequence-specific and quantitative information, we used a Chromatin Immunoprecipitation (ChIP) approach. We dissected cotyledons from seedlings aged 2 or 5 dag and precipitated chromatin with antibodies directed against H3, H3K4me3, a histone mark associated with transcriptionally active chromatin (35) and two repressive marks H3K9me2 and H3K27me1 enriched at chromocenters in mature leaf tissues (3, 5, 36, 37). Nucleosome occupancy, as reported by the H3 levels, is higher at 180 bp and TSI repeats compared to three euchromatic loci (*HXK1, UEV1C* and *ACTIN2*) (***Figure 2A***), in agreement with observations in mature leaf tissues (6). However, no significant changes in nucleosome occupancy were observed between 2 and 5 dag. Therefore, although organization of repeated sequences such as TSI (pericentromeric) and 180 bp (centromeric) into chromocenters may reflect a different state of higher order chromatin organization, nucleosome occupancy does not seem to be modified during this process. We then analyzed levels of three different PTMs at the same heterochromatic and euchromatic targets. H3K4me3 is one of the signatures of transcription start sites (38) and is thus found enriched at the 5' region of the *ACTIN2* gene as early as 2 dag (***Figure 2B***) but is depleted from the heterochromatic targets both at 2 and 5 dag. Contrary to H3K4me3, the repressive marks H3K27me1 and H3K9me2 are 6- or 10-fold, respectively, enriched at heterochromatin compared to the three euchromatic loci (***Figure 2CD***). This enrichment is observed already at 2 dag when chromocenters are not yet fully formed. While H3K27me1 levels remain rather stable during post-germination development at all targets (***Figure 2C***), H3K9me2 levels increase between 2 and 5 dag (***Figure 2D***). Taken together, these data suggest that while nucleosome occupancy and H3K27me1 levels are not altered during chromocenter formation, H3K9me2 becomes enriched at heterochromatic repeats between 2 and 5 dag. We conclude that centromeric and pericentromeric chromatin domains already show the enrichment in repressive histone marks compared to active genes as early as 2 dag, despite the dispersion of the repetitive elements in the euchromatic compartment of the nucleus and therefore preceding the formation of chromocenters.

Defective setting of H3K27mono and H3K9dimethylation differentially affects kinetics of chromocenter formation

Given that H3K9me2 and H3K27me1 mark centromeric and pericentromeric repeats during early cotyledon development, we examined to what extend the appropriate setting of these repressive marks affects chromocenter formation. The SET domain protein SU(VAR)3-9 HOMOLOG 4/KRYPTONITE (KYP) is the major histone H3K9 dimethyltransferase in Arabidopsis (39), however, SUVH5 and SUVH6 contribute to histone H3K9 dimethylation (40) and all three genes are expressed during this developmental stage (***Supplementary Figure 2A***). H3K27me1 at heterochromatin is set by the histone methyltransferases ARABIDOPSIS TRITHORAX-RELATED PROTEIN 5 (ATXR5) and ATXR6 (37, 41). To evaluate the importance of H3K27me1 and H2K9me2 marks for chromocenter formation, we scored the percentage of nuclei with clustered 180 bp and TSI repeats in *suvh4 suvh5 suvh6* and *atxr5 atxr6* mutant cotyledons aged from 2 to 5 dag. At 2 dag, the percentage of nuclei with complete clustering of centromeric and pericentromeric repeats is significantly lower in *suvh4 suvh5 suvh6* mutants, but reaches levels similar to WT at 3 dag. Clustering then occurs similarly to WT kinetics, and reduced clustering was only observed for the pericentromeric repeats at 5 dag (***Figure 3***, ***Supplementary Figure 2B***). In contrast, in *atxr5 atxr6* cotyledons, the percentage of nuclei with clustered 180 bp and TSI sequences is comparable to WT at 2 dag, but differences appear as early as 3 dag, and only 40% of the nuclei complete chromocenter formation at 4 and 5 dag, compared to 70% and 80%, respectively, in the WT (***Figure 3***, ***Supplementary Figure 2C***).

Taken together, plants largely devoid of H3K9me2 have a higher fraction of nuclei with decondensed chromocenters at 2 dag, suggesting a role for H3K9 dimethylation in preservation of the remaining chromocenter structures during germination. Deficient H3K27 monomethylation in absence of ATXR5 and ATXR6 in contrast severely impairs clustering of 180 bp and TSI repeats into chromocenter structures.

H3.1 becomes enriched at heterochromatin after germination

The enrichment of H3K9me2 and H3K27me1 at the centromeric and pericentromeric domains is known to correlate with the presence of the canonical histone H3.1 (14–16). We were therefore interested to investigate whether there is a

functional link between H3.1 enrichment and clustering of repetitive sequences into chromocenters. To this aim, we first analyzed transcript levels of two H3.1 encoding genes (*HTR1* and *HTR9*) by RT-qPCR from 2 to 5 dag. We found that both genes are expressed in cotyledons during post-germination development and observed the highest expression at 2 dag, which then progressively decreased until 5 dag (***Figure 4A***). Since no antibodies able to distinguish the Arabidopsis canonical H3.1 from its variant counterparts are available, we generated a transgenic line expressing *HTR9*-encoded H3.1 carrying a short FLAG-HA epitope (e-H3.1) under control of the *HTR9* endogenous promoter. We confirmed incorporation of the tagged variant into chromatin by Western Blot of nucleosomal histones (***Supplementary Figure 3A***), its preferential enrichment at heterochromatic versus euchromatic loci by ChIP in mature leaf tissues (***Supplementary Figure 3B***) and controlled the immunoprecipitation specificity with the FLAG-coupled beads in our experimental setup using cotyledon nuclei (Fig. S3D). We then used the line expressing e-H3.1 proteins to carry out immunofluorescence and ChIP experiments on cotyledons aged 2 or 5 dag and determined the enrichment in H3.1 relative to input at the different developmental stages. The e-H3.1 protein is enriched at pre-chromocenters as early as 2 dag (***Figure 4B***). At 5 dag, when chromocenters are fully formed (***Figure 4B***), the e-H3.1 levels at 180 bp and TSI repeats are about 10-fold higher than at the active genes *HXK1* and *UEV1C* (***Figure 4C***). Interestingly, e-H3.1 enrichment increases at all three heterochromatic sequences tested from 2 to 5 dag, but the level is stable at the two active genes or the intergenic region analyzed. This suggests a role for H3.1 dynamics in chromocenter formation during early development. We confirmed the heterochromatin-specific increase in H3.1 between 2 and 5 dag in an independent line expressing *HTR1*-encoded H3.1 fused to CFP (***Supplementary Figure 3E***).

Taken together, our data show different H3.1 dynamics at heterochromatic and euchromatic loci during post-germination development and progressive H3.1 enrichment at centromeric and pericentromeric repeats during chromocenter formation. The establishment of the chromocenters as specialized chromatin domains might therefore require precise and site-specific deposition of the canonical H3.1.

Chromatin assembly mediated by CAF-1 is required for chromocenter formation

Given the observed H3.1 enrichment at repeats during chromocenter formation, we reasoned that proper chromatin assembly is critical for this phenomenon. Histones are deposited by specific, dedicated chaperone complexes at particular genomic domains during different time windows of the cell cycle. In mammals, the canonical H3.1 is deposited by the Chromatin Assembly Complex-1 (CAF-1) that operates in a DNA-synthesis dependent manner, while the HIR complex deposits the replacement variant H3.3 (42, 43). While mutants lacking functional CAF-1 and HIR complexes are embryonic lethal in mammals (44, 45), corresponding Arabidopsis mutants are viable (46, 47), allowing to test the implication of the two assembly complexes in chromocenter dynamics. We first determined transcript levels of the genes *FAS1* and *FAS2*, which encode the two large subunits of the CAF-1 complex, and of *HIRA*, which encodes a subunit of the Arabidopsis HIR complex (47–49). All three genes are expressed during early post-germination development in cotyledons. While expression of *FAS2* and *HIRA* is rather stable, *FAS1* transcript levels decrease from 2 to 5 dag (***Figure 5A***, ***Supplementary Figure 4A***) and mirror the expression patterns of *HTR1* and *HTR9*. To determine whether the different histone assembly complexes are involved in heterochromatin dynamics between 2 and 5 dag, we carried out FISH analysis for 180 bp and TSI repeats with nuclei of WT, *fas1-4* and *hira-1* mutant plants. While at 2 dag around 20% of nuclei show entirely clustered repeats in both WT and *fas1-4* mutants, clustering is observed for only 50% of the *fas1-4* mutant nuclei compared to ~80% in WT at 5 dag (***Figure 5B***, ***Supplementary Figure 4B***). We confirmed impaired chromocenter formation in *fas2-5* mutants lacking the middle subunit of the CAF-1 complex (***Supplementary Figure 4BC***). In contrast, the kinetics of chromocenter formation in *hira-1* mutants is similar to WT (***Figure 5B***). Defects in histone deposition mediated by HIRA therefore do not impact chromocenter formation, while the clustering of centromeric and pericentromeric repeats is clearly affected in CAF-1 mutants.

Given that CAF-1 specifically deposits H3.1 in mammals (43), we wanted to know to what extend H3.1 enrichment and dynamics during post-germination development are altered in CAF-1 mutants. To this aim, we crossed the transgenic line expressing e-H3.1 with the *fas1-4* mutant and analyzed H3.1 occupancy dynamics at heterochromatic and euchromatic regions in absence of CAF-1 in a

quantitative manner. Despite reduced transgene expression in the *fas1-4* mutant background, we observed significant nucleosomal e-H3.1 (***Figure 6A***), which can be explained by the remaining CAF-1 activity in the *fas1-4* mutant that is not a complete loss of function allele (Ramirez-Parra and Gutierrez, 2007). The remnants of nucleosomal e-H3.1 in *fas1-4* cotyledons allowed us to investigate the dynamics of H3.1 enrichment during post-germination development in a situation where chromocenter formation is impaired. We found that, in contrast to WT plants in which e-H3.1 occupancy increased by 5 dag compared to 2 dag, this dynamic is lost in *fas1-4* plants, illustrating that CAF-1 contributes to H3.1 dynamics specifically at heterochromatin. Given the generally reported preferential enrichment of H3.1 in repressive marks (52, 53), we also analyzed the dynamics of H3K27me1 and H3K9me2 enrichment in *fas1-4* mutants. Similar to WT (***Figure 2C***), H3K27me1 levels are stable in *fas1-4* cotyledons at both euchromatic and heterochromatic targets during this developmental time window (***Supplementary Figure 5***). Interestingly, in contrast to WT plants, plants with reduced FAS1 levels do not show increased H3K9me2 at heterochromatic repeats at 5 dag (***Figure 6B***). This suggests that loss of CAF-1 also disturbs H3K9me2 dynamics at 180 bp and TSI repeats.

Taken together, these data show that the CAF-1 complex is a primordial player in H3.1 dynamics at heterochromatic sequences. We conclude that defective chromatin assembly in the absence of a functional CAF-1 complex impairs H3.1 deposition at heterochromatic repeats, the proper setting of epigenetic marks and ultimately chromocenter formation.

Discussion

After nuclear expansion and chromatin decondensation during germination, centromeric and pericentromeric repeats progressively cluster with similar kinetics into chromocenters. We found that, despite dispersion of these repeats at 2 dag, these repetitive elements already display elevated nucleosome occupancy and enrichment in repressive histone modifications compared to euchromatin. While H3K27me1 levels at heterochromatic sequences remain unchanged during the studied developmental time window, H3K9me2 levels increased at heterochromatin regions, which may however result from a more global change of H3K9me2 levels during this developmental stage, since euchromatic sequences are also affected. While loss of H3K9me2 only weakly disturbs heterochromatin organization in leaf tissue (54, 55) and in cotyledons at later stages of seedling growth (this study), we noticed an increased percentage of nuclei with dispersed centromeric and pericentromeric repeats at 2 dag in the absence of the three H3K9 methyltransferases SUVH4, SUVH5 and SUVH6, compared to WT. It might therefore be interesting to explore further the role of H3K9me2 in heterochromatin dynamics during imbibition and germination.

The ratio of canonical histone H3.1 increases specifically at heterochromatic regions between 2 and 5 dag. This process depends on the histone deposition complex CAF-1, and reduced chromocenter structures in *fas* mutant nuclei illustrate a clear role of the CAF-1 complex in formation of higher-order chromatin domains. These observations echo the requirement for CAF-1 in chromocenter formation during early mouse development (44, 56), where lack of CAF-1 results in aberrant organization of pericentromeric domains. The mammalian counterpart of the CAF-1 complex has strong preference for the histone variant H3.1 and operates through interaction with the DNA clamp PCNA in a manner coupled to DNA synthesis (43, 57). While cell proliferation in Arabidopsis is only transiently activated after emergence of the cotyledons from the seed coat (58), cells undergo endoreplication during cotyledon growth (50), likely allowing CAF-1-mediated H3.1 incorporation during this time window. To explain the increase of H3.1 specifically at heterochromatin, we can envision that, in plants, H3.1 is deposited by CAF-1 explicitly at heterochromatic repeats, possibly facilitated by specific timing of heterochromatin replication in S-phase. Alternatively, H3.1 is incorporated in a

genome-wide manner during endoreplication, but actively exchanged for H3.3 at the euchromatic loci analyzed here and leading to the observed differences between heterochromatic and euchromatic regions. Whatever the mechanism, both scenarios suggest that before the studied time-window, heterochromatin was depleted of H3.1, which is then progressively deposited from to 2 to 5 dag. Available expression data (http://bar.utoronto.ca/efp/cgi-bin/efpWeb.cgi) support such a hypothesis, as during seed development transcript levels from four of the five H3.1-encoding genes progressively decrease while those of the three H3.3-encoding genes increase.

Failure to assemble H3.1 at heterochromatin might not be the only explanation for defective chromocenter formation upon loss of CAF-1, as replication-coupled deposition of histone modifications such as the timely H3K27 monomethylation of H3.1 could be affected that takes place in a replication-coupled manner (37, 41). We did not detect differences in H3K27me1 levels in cotyledon nuclei in this study, an observation that might be explained by residual CAF-1 activity in the *fas1-4* mutant or monomethylation by alternative H3K27 methyltransferases. Nevertheless, H3K27me1 is critical for chromocenter formation during this developmental stage, as failure to set proper H3K27me1 levels in heterochromatin in the *atxr5 atxr6* double mutant severely affects the microscopically visible compaction of heterochromatin in chromocenters.

Conspicuous chromocenter structures are found in several organisms. The biological significance of such microscopically visible compaction still remains unclear; however, a role in reinforcing transcriptional repression has been proposed. In line with this working model, we showed here a progressive decrease in repeat-derived transcripts between 2 and 5 dag. While TSI and Ta3 transcript levels are low compared to the levels of non-coding pericentromeric transcripts observed in the mouse embryo, which contribute to chromocenter formation (59), this does not exclude a role for non-coding RNA in chromocenter formation in Arabidopsis, eventually via the RNA-directed DNA Methylation pathway (34, 60). However, we can also conclude from these observations, that transcriptional repression is not the major function of chromocenter formation. Indeed, condensed chromatin domains remain accessible to macromolecules (61) and chromocenters do not prevent accessibility of the transcription factory to DNA (3, 62), suggesting that transcriptional activity is rather determined at the level of local chromatin features. While higher-order chromatin compaction as such does not seem to restrict accessibility to the

underlying DNA, it may still help maintaining other heterochromatin features, such as late replication timing, or contribute to minimizing recombination between sequences by restricting the possibility to interact (63). Another intriguing hypothesis is that heterochromatin reorganization during germination and the subsequent seedling development is essentially driven by the need to reorganize euchromatic chromatin loops to ensure appropriate gene expression during the transition from heterotrophic to autotrophic growth, e.g. by rearranging chromosomal territory or moving expressed loci relative to other nuclear sub-compartments such as the nuclear periphery. Dynamic reorganization of another pericentromeric repetitive array, the 5S rRNA genes, also occurs during this time window (30, 64) and was suggested to contribute to the sequestration and transcriptional repression of mutated 5S genes (30, 65).

While we concentrated here on the aspect of histone H3 variants in chromocenter formation, the contribution of other core histones or the linker histone H1 to characteristics of the nucleosome fiber needs to be considered. Indeed, H1 is thought to promote formation of higher-order chromatin structures at the level of the 30-nm fiber (66) and upon chromatin decondensation associated with reprogramming. Eviction of H1 is one of the first steps associated with heterochromatin decondensation in mammals and plants (67, 68). Furthermore, the plant-specific H2A.W variant that bears similarities to the mammalian macroH2A drives higher order chromatin organization by stimulating fiber-to-fiber interactions at the level of the 10-nm fiber (55) and therefore can be an important candidate besides H3.1 in chromocenter formation during this developmental stage.

Material and Methods

Plant material

All mutants (*fas1-4* (SAIL-662-D10), *fas2-5* (SALK_147693), *hira-1* (WiscDsLox362H05), *htr9-1* (SALK_148171), *atxr5* (SALK_130607) and *atxr6* (SAIL_181_D09), *mom1-2* (SAIL_610_G01) and *suvh4 suvh5 suvh6* (SALK_041474, Gabi_263C05, SAIL_1244_F04)) and transgenic lines are in the Columbia background. Homozygous mutant plants were identified by PCR-based genotyping (***Table S1***). Sterilized seeds were sown on germination medium containing 0.8% w/v agar, 1% w/v sucrose and Murashige & Skoog salts (M0255; Duchefa Biochemie, Netherlands). After 2 days of stratification at 4ºC in the dark, seedlings were grown under 16 h light/8 h dark cycles at 23ºC. Cotyledons were harvested at 78 h, 102 h, 126 h or 150 h after transfer to the growth chamber, corresponding to time points 2, 3, 4 or 5 days after germination (dag), respectively.

Plasmid construction for production of epitope-tagged histones

To generate the transcriptional fusion of H3.1 with the FLAG-HA tag, we cloned the OCS (octopine synthase) terminator, the FLAG-HA tag and the genomic fragment containing the promoter and the coding region of *HTR9* (stop codon excluded) using Gateway technology. T3 monolocus homozygous lines were selected based on segregation of the resistant character.

Antibodies

Anti-H3 (ab1791, Abcam), anti-H3K9me2 (ab1220, Abcam), anti-H3K4me3 (04-745, Millipore), anti-H3K27me1 (pAB-045-50, Diagenode), anti-GFP and anti-HA (ab9110, Abcam) were used.

Protein immunolocalization

For immunofluorescence assays, dissected cotyledons were fixed in 4% formaldehyde (Sigma-Aldrich) in Tris buffer, finely chopped in Lysis Buffer (15 mM Tris-HCl pH 7.5, 80 mM KCl, 2 mM EDTA, 0.5 mM spermidine, 0.5 mM spermine, 20 mM NaCl, 0.1% Triton X-100) and the homogenate filtered through a 30 µm filter prior to centrifugation. The nuclei pellet was resuspended in sorting buffer (100 mM Tris-HCl pH 7.5, 50 mM KCl, 2 mM $MgCl_2$, 0.05% Tween 20 and 5% sucrose) and

deposited onto a microscope slide prior to air-drying. Nuclei preparations were fixed in 2% formaldehyde in PBS, washed with water and air-dried. Slides were incubated with the a-HA antibody (1:200) overnight and the primary antibody revealed with a secondary anti-rabbit antibody coupled to Alexa-488 (Molecular Probes). Slides were mounted in Vectashield (Vector Laboratories) with DAPI (2 µg/mL). For microscopic observation, a fluorescence light microscope DM6000B (Leica) with a Digital CMOS ORCA – Flash4.0 camera (Hamamatsu) was used.

RNA extraction and RT-PCR

Total RNAs were extracted from dissected cotyledon tissues using Tri-Reagent (Euromedex), treated with RQ1 DNase I (Promega) and purified using phenol-chloroform extraction. Reverse transcription was primed either with oligo(dT)15 or with random hexamers supplemented with reverse primers for TSI and Ta3 using M-MLV reverse transcriptase (Promega). The resulting cDNAs were used in quantitative PCR with the LightCycler® 480 SYBR Green I Master kit on the Roche LightCycler® 480. Transcript levels of interest were normalized to *AtSAND* (69) using the comparative threshold cycle method.

Fluorescence in situ hybridization

For Fluorescence in situ hybridization (FISH), *in vitro*-grown cotyledons aged from 2 to 5 dag were fixed in ethanol-acetic acid (3:1 v/v) and FISH was performed essentially as described (3, 70). Slides were analyzed with the Zeiss Axio Imager Z.1 microscope equipped with a Zeiss AxioCam MRm camera system and images processed with ImageJ and Adobe Photoshop. More than 200 nuclei were scored per condition using a double blind experimental setup. Only nuclei in which all 180 bp and TSI repeats are clustered in chromocenters are scored as “clustered”. Differences were compared using the χ^2 test.

ChIP analysis

Formaldehyde-fixed tissue was ground to a fine powder with ceramic beads, chromatin prepared as described (70) and immunoprecipitation carried with the LowCell# ChIP kit (Diagenode). The FLAG-HA tagged H3.1-containing chromatin was precipitated using FLAG-coupled magnetic beads (Sigma). Immunoprecipitated DNA was quantified using qPCR (Roche) and normalized relative to input.

Acknowledgments

M.B., A.P. and L.S. are supported by stipends from the Region Auvergne. M.B. is also supported by an ARC doctoral fellowship. C.D., S.L.G. and A.V.P. were supported by ANR “Dynam'Het” ANR-11 JSV2 009 01; C.D., S.C. and A.V.P. by ANR “SINUDYN” ANR-12 ISV6 0001. CNRS, INSERM and Clermont Universities supported this work. We thank O. Mittelsten Scheid, S. Jacobsen and C. Pikaard for seeds, S. Tourmente for stimulating discussion, A. Eccher, M. Peyny, G. Pompeu and E. Vanrobays for technical help and O. Mittelsten Scheid for critical reading.

Supplementary Methods

Protein extraction and Western analysis

For extracts containing nucleosomal histones, nuclei were prepared from 2 g plant material (3) using HONDA buffer (20 mM Tris-HCl pH 7.4, 10 mM $MgCl_2$, 0.4 M sucrose, 2.5% Ficoll, 5% Dextran 40, 0.5% Triton X-100, 10 mM BSA, 0.5 mM PMSF and protease inhibitors (Complete Mini, Roche)). Nuclei were re-suspended in Laemmli buffer. SDS–PAGE and Western blots were performed according to standard procedures. Western blots were probed with the anti-H3 antibody (1/20,000, Abcam) and the anti-HA antibody (1/4,000, Abcam) to reveal the tagged H3.1. Primary antibodies were revealed by incubation with a horseradish peroxidase-coupled anti-rabbit secondary antibody (1/5,000, Sigma).

Supplementary references

1. Tariq M, Habu Y, Paszkowski J (2002) Depletion of MOM1 in non-dividing cells of Arabidopsis plants releases transcriptional gene silencing. *EMBO Rep* 3:951–955.

2. Koo AJK, Fulda M, Browse J, Ohlrogge JB (2005) Identification of a plastid acyl-acyl carrier protein synthetase in Arabidopsis and its role in the activation and elongation of exogenous fatty acids. *Plant J* 44:620–32.

3. Xia Y, Nikolau BJ, Schnable PS (1997) Developmental and hormonal regulation of the arabidopsis CER2 gene that codes for a nuclear-localized protein required for the normal accumulation of cuticular waxes. *Plant Physiol* 115:925–37.

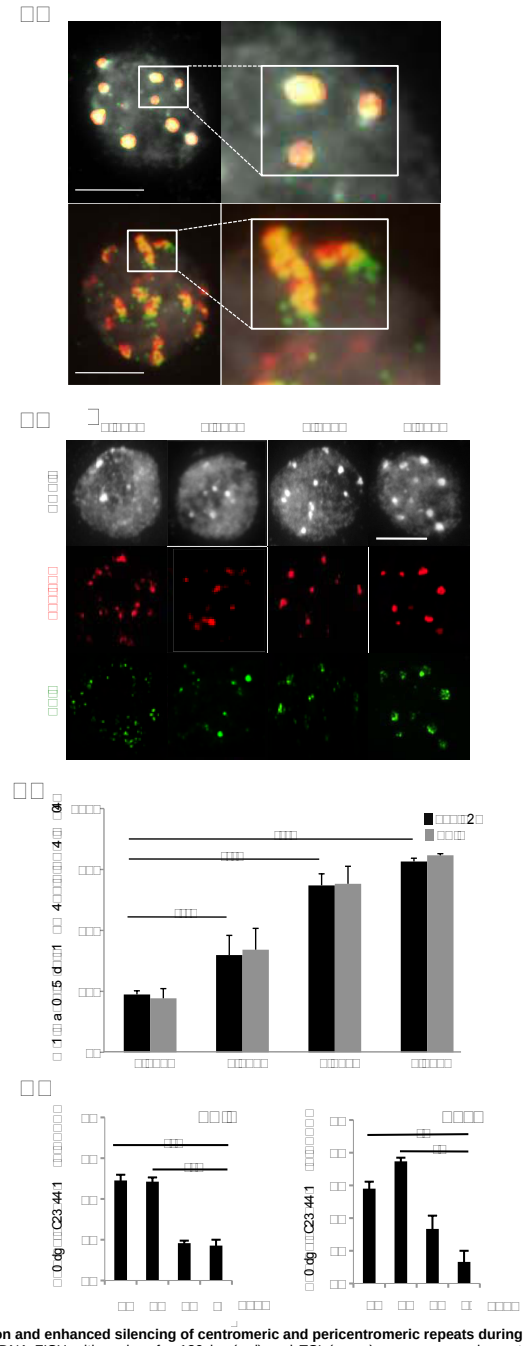

Figure 1: Progressive organization and enhanced silencing of centromeric and pericentromeric repeats during chromocenters formation.
(A-B) Representative nuclei after DNA FISH with probes for 180 bp (red) and TSI (green) sequences and counterstained with DAPI (grey). Scale bars represent 5 µm. (A) Example of a clustered (top) and dispersed (bottom) organization. (B) Nuclei from cotyledons aged 2, 3, 4 or 5 days after germination (dag). (C) Percentage of nuclei with complete clustering of either 180 bp (black) or TSI sequences (grey) in chromocenter structures at 2, 3, 4 or 5 dag ± SEM. Over 200 nuclei were scored at each day for each genotype. *p<0.05; **p<0.01; ***p<0.005; χ^2 test. (D) RT-qPCR analysis of TSI (left) and Ta3 (right) transcripts in WT cotyledons aged 2, 3, 4 or 5 dag. Histograms show mean fold change relative to transcript levels at 5 dag (set to 1) after normalization to *AtSAND* expression ± SEM obtained for two independent PCR amplifications of at least two biological replicates. *p<0.05; **p<0.01; Student's t-test.

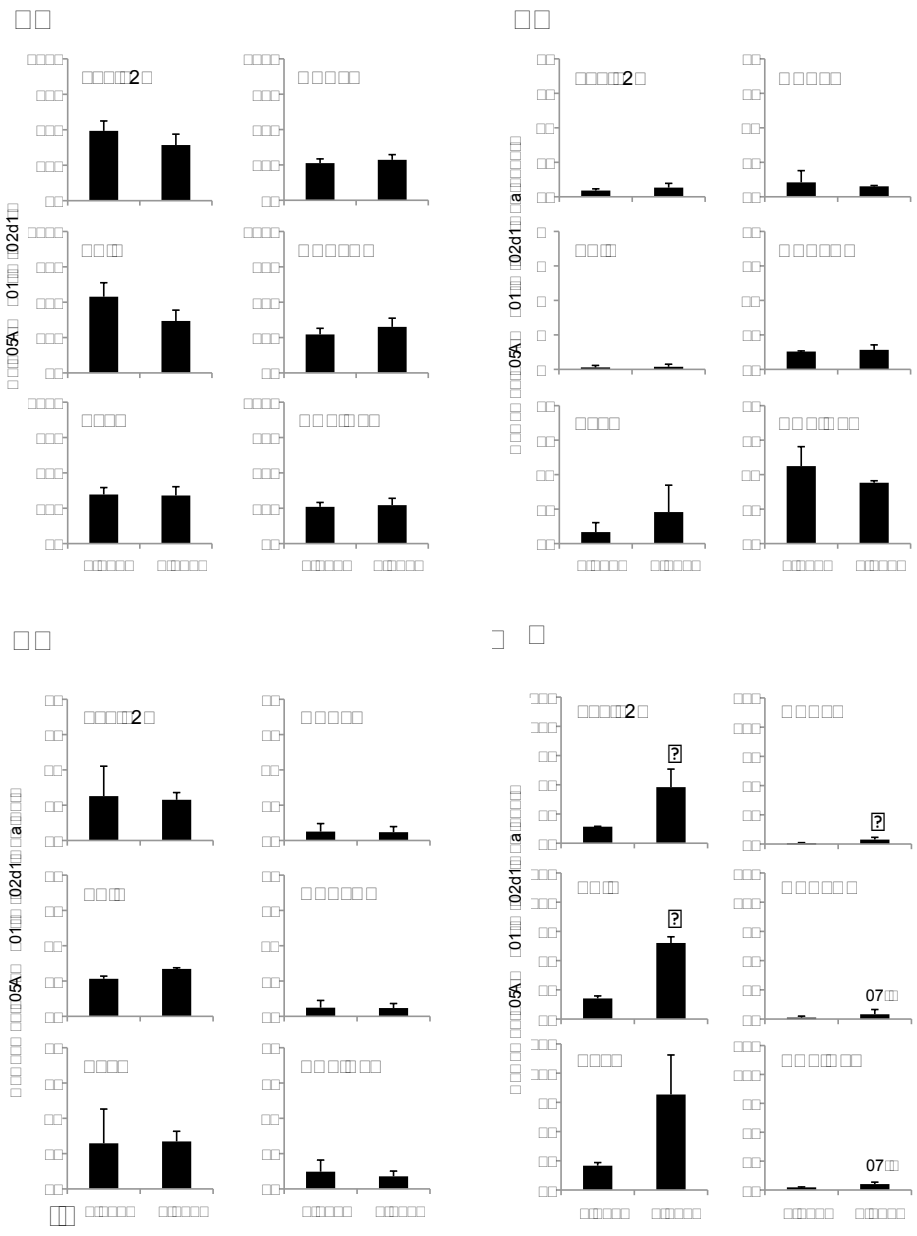

Figure 2: Centromeric and pericentromeric sequences are enriched in repressive marks prior to chromocenter organization.
Histone H3 occupancy assessed by H3-ChIP qPCR relative to input (A) and enrichment of H3K4me3 (B), H3K27me1 (C) and H3K9me2 (D) normalized to H3-levels in WT cotyledons at 2 or 5 dag as assessed by ChIP-qPCR at heterochromatic elements (180 bp, TSI and the Ta3 retrotransposon) and euchromatic loci (*HXK1*, *UEV1C* and *ACTIN2*). Histograms show mean percentage ± SEM for two independent PCR amplifications of three biological replicates. ns. p>0.1; p<0.1; *p<0.05; Student's t-test.

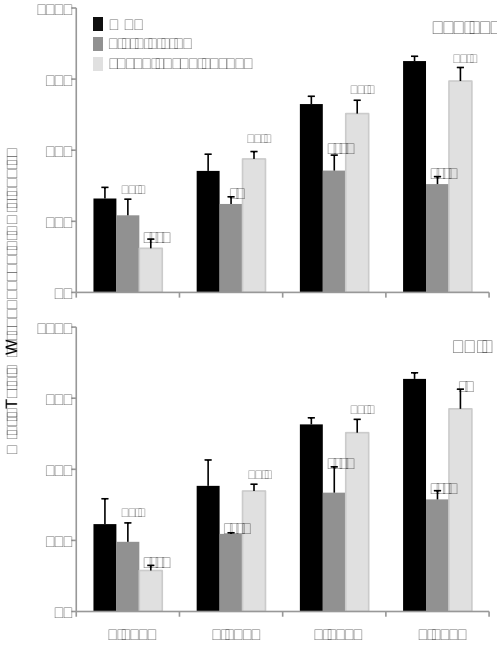

Figure 3: Loss of the H3K9me2 and H3K27me1 histone methyltransferases affects chromocenter formation.
Percentage of nuclei showing clustering of 180 bp (top) and TSI (bottom) repeat sequences into chromocenter structures in WT, *atxr5 atxr6* and *suvh4 suvh5 suvh6* mutants in cotyledons aged 2, 3, 4 or 5 dag. Over 200 nuclei were scored at each day for each genotype. Error bars correspond to ± SEM from two independent biological replicates. *p< 0.05; **p< 0.01; ***p< 0.005; χ^2 test.

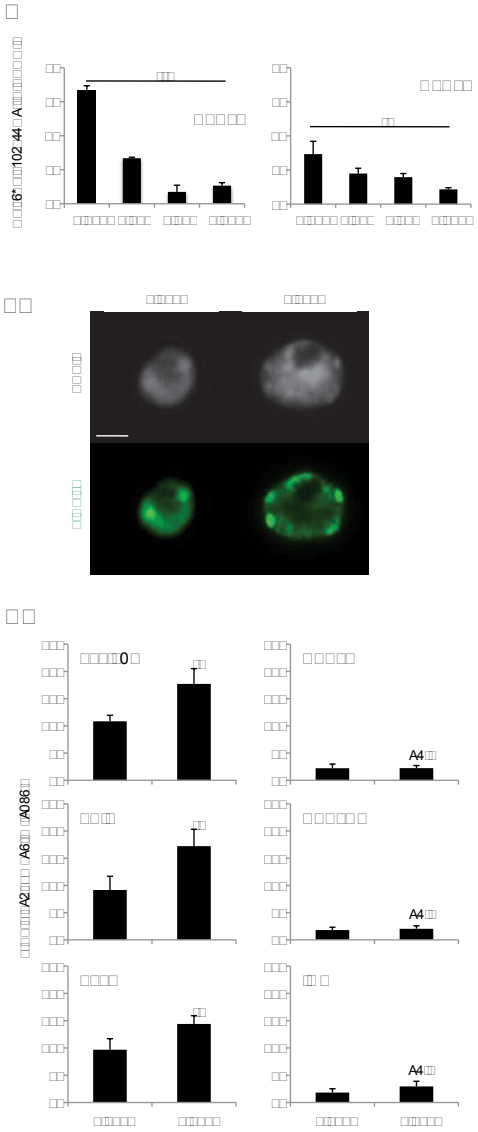

Figure 4: H3.1 levels at heterochromatin increase during post-germination growth.
(A) RT-qPCR analysis of transcript levels of *HTR1* and *HTR9* between 2 and 5 dag. Histograms show means of transcript levels ± SEM obtained in two independent PCR amplifications of three biological replicates. The y-axis shows the fold change relative to transcript levels at 5 dag (set to 1) after normalization to *AtSAND* expression. *p<0.05; **p<0.01; Student's t-test. (B) Subnuclear localization of e-H3.1 revealed by immunostaining (green) in nuclei of cotyledons aged 2 or 5 dag. DNA is counterstained with DAPI (grey). Scale bar represents 5 µm. (C) e-H3.1 enrichment determined by FLAG-ChIP qPCR relative to input in cotyledons from WT plants aged 2 or 5 dag at heterochromatic elements (180 bp, TSI and the Ta3 retrotransposon), two euchromatic loci (*HXK1* and *UEV1C*) and an intergenic region. Histograms show mean percentage ± SEM of FLAG-immunoprecipitation relative to input for two independent PCR amplifications of three biological replicates. p<0.1; *p<0.05; Student's t-test.

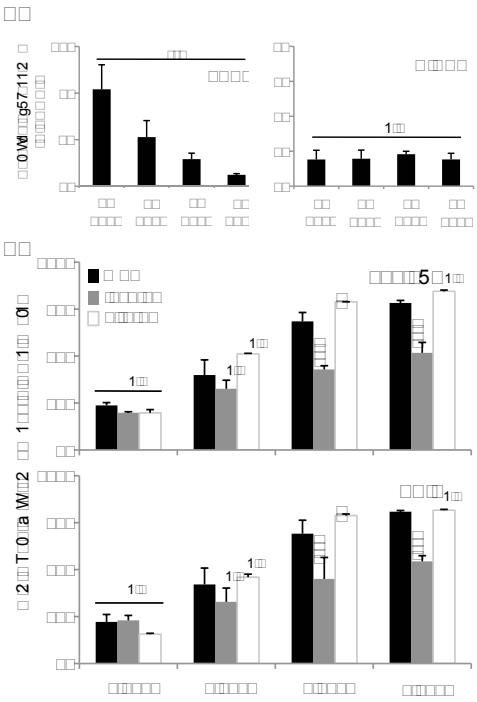

Figure 5: CAF-1, but not HIRA, is critical for chromocenter formation.
(A) RT-qPCR analysis of *FAS1* (left) and *HIRA* (right) transcripts in WT cotyledons aged 2, 3, 4 or 5 dag. Histograms show mean fold change relative to transcript levels at 5 dag (set to 1) after normalization to *AtSAND* expression ± SEM obtained for two independent PCR amplifications of two biological replicates. **p<0.01; Student's t-test. (B) Percentage of nuclei showing clustering of 180 bp (top) and TSI (bottom) repeat sequences into chromocenter structures in *fas1-4* and *hira-1* mutant cotyledon nuclei compared to WT (black) at 2, 3, 4 or 5 dag. Over 200 nuclei were scored at each day for each genotype. Error bars correspond to variation from 2 independent biological replicates. *p<0.05; **p<0.01; ***p<0.005; χ^2 test.

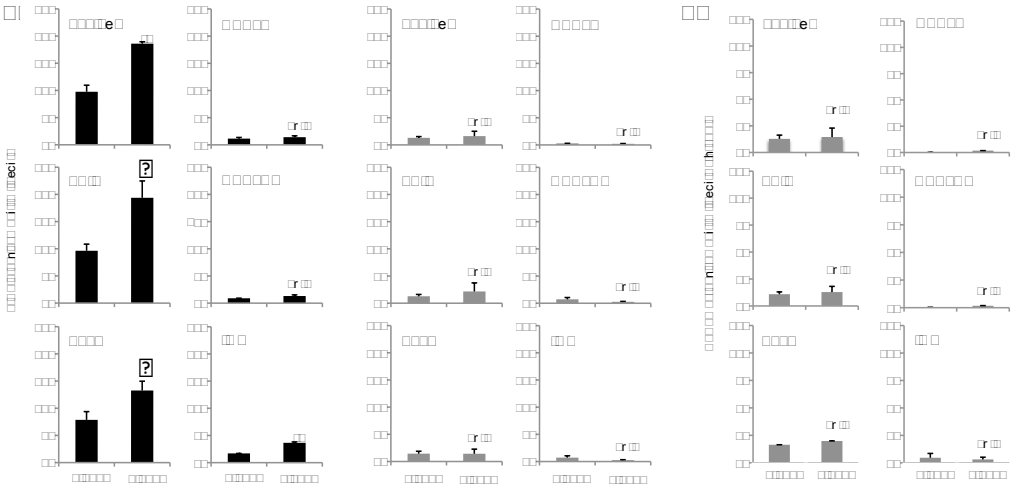

Figure 6: CAF-1 is required for H3.1 and H3K9me2 dynamics at heterochromatin.
(A) e-H3.1 enrichment determined by FLAG-ChIP qPCR relative to input in cotyledons of e-H3.1/WT (black bars, left) and e-H3.1/*fas1-4* plants (grey bars, right) at 2 or 5 dag at heterochromatic elements (180 bp, TSI and the Ta3 retrotransposon), two euchromatic loci (*HXK1* and *UEV1C*) and an intergenic region. The y-axis shows the fold change of FLAG-immunoprecipitation relative to input for two independent PCR amplifications of two biological replicates. p<0.1; *p<0.05; Student's t-test. (B) Enrichment of H3K9me2 assessed by ChIP qPCR at 180 bp, TSI, the Ta3 retrotransposon, as well as *HXK1*, *UEV1C* and *ACTIN2* at day 2 or 5 dag in e-H3.1/*fas1-4* cotyledons. Histograms show mean percentage ± SEM of the respective immunoprecipitation relative to H3 levels for three biological replicates.

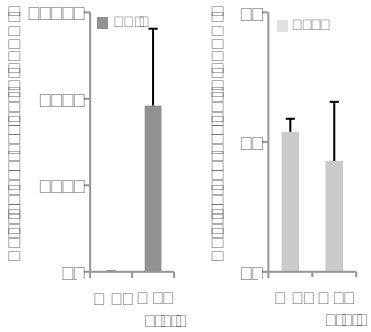

Figure S1 [with Figure 1]
Transcription of TSI and Ta3 in *mom1-2* cotyledons.
RT-qPCR analysis of TSI (left) and Ta3 (right) transcripts in *mom1-2* cotyledons aged 5 dag. Histograms show mean transcript levels relative to transcript levels at 5 dag in WT plants (set to 1) after normalization to *AtSAND* expression ± SEM obtained for two independent PCR amplifications of at least two biological replicates.

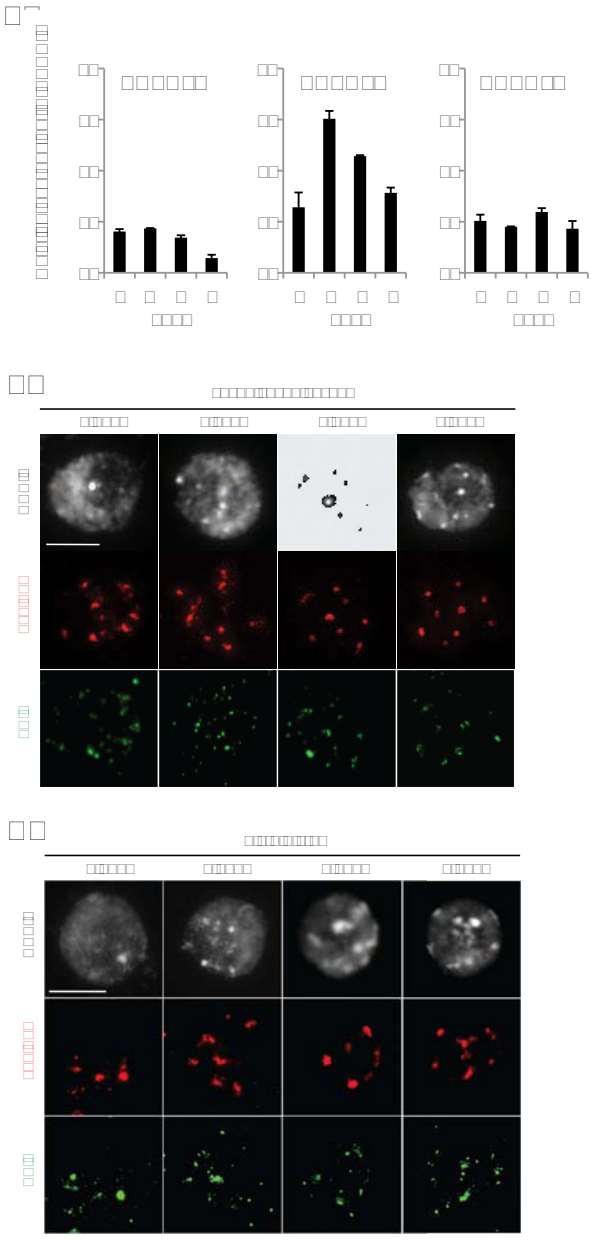

Figure S2 [with Figure 3]
Loss of histone methyltransferases impacts chromocenter formation.
(A) RT-qPCR analysis of *SUVH4, SUVH5* and *SUVH6* transcripts in WT cotyledons aged 2, 3, 4 or 5 dag. Histograms show mean transcript levels relative to 5 dag (set to 1) after normalization to *AtSAND* ± SEM obtained for two independent PCR amplifications of three biological replicates. (B-C) Representative *suvh4 suvh5 suvh6* (B) and *atxr5 atxr6* (C) nuclei, for which 180 bp (red) and TSI (green) were revealed by DNA FISH isolated from cotyledons at 2, 3, 4 or 5 dag. DNA is counterstained with DAPI (grey). Scale bar presents 5 µm.

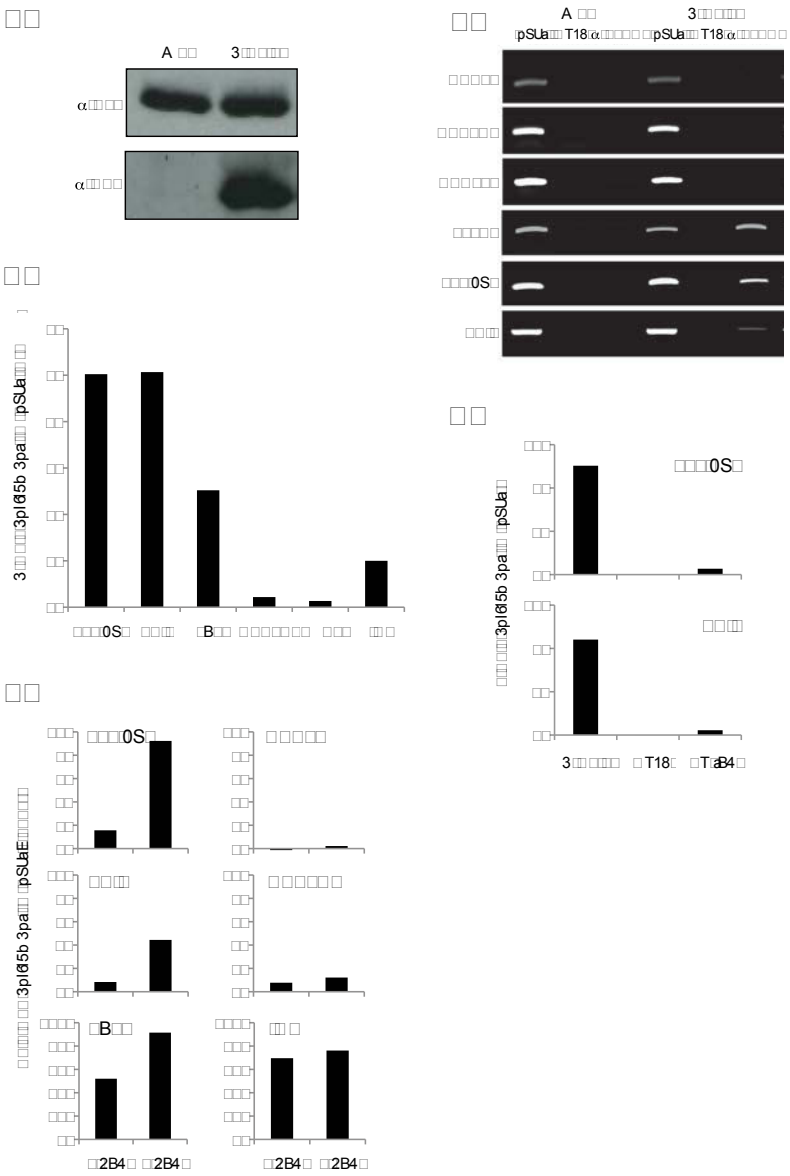

Figure S3 [with Figure 4]
Characterization of e-H3.1 lines.
(A) Western blot of nucleosomal histones showing chromatin incorporation of the tagged histone H3.1 variant. (B) Immunoprecipitation of chromatin isolated from 3-week old plants expressing e-H3.1 with anti-FLAG antibodies reveals enrichment of H3.1 at heterochromatin repeats compared to euchromatic loci. Immunoprecipitated and input DNA were amplified by PCR. (C) Ratio of e-H3.1 enrichment determined by FLAG-ChIP qPCR relative to input and normalized to levels at an intergenic region (IG) in 10-day-old seedlings at heterochromatic elements (180 bp, TSI and the Ta3 retrotransposon) and genes (*HXK1* and *UEV1C*). Histograms show mean percentage of two independent PCR amplifications of 2 independent e-H3.1 lines. (D) e-H3.1 enrichment determined by FLAG-ChIP qPCR relative to input in cotyledons of e-H3.1 expressing and WT plants lacking the e-H3.1 construct. Chromatin was isolated from 5-day-old cotyledon nuclei. Histograms show mean percentage of FLAG-immunoprecipitation relative to input for a representative experiment. (E) H3.1-CFP enrichment determined by anti-GFP-ChIP qPCR relative to input in cotyledons aged 2 and 5 dag of an H3.1-CFP expressing line at heterochromatic elements (180 bp, TSI and the Ta3 retrotransposon), two euchromatic loci (*HXK1* and *UEV1C*) and an intergenic region. Histograms show mean percentage of two independent PCR amplifications.

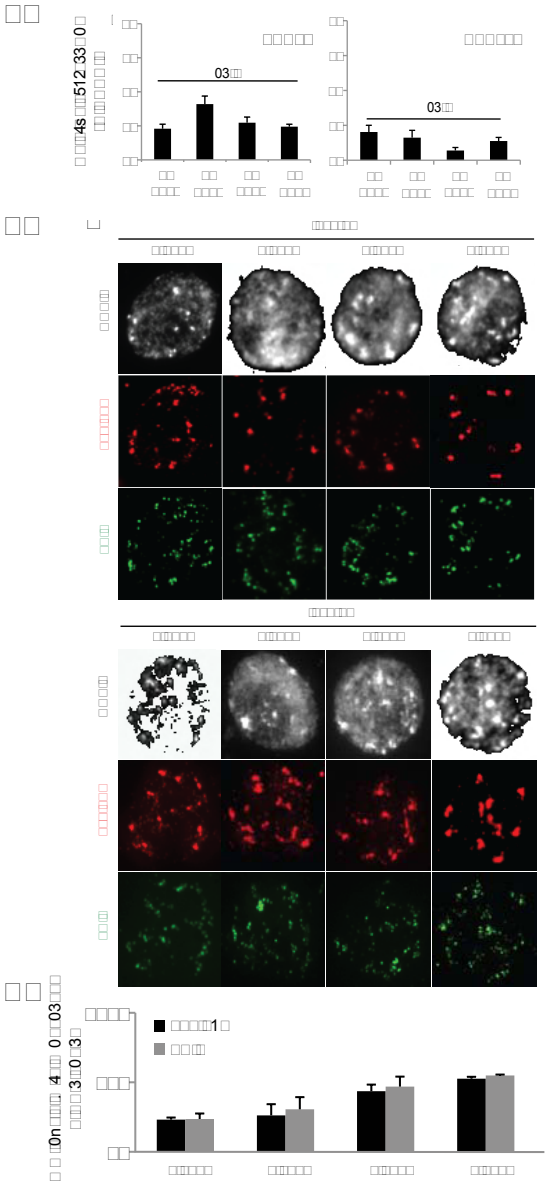

Figure S4 [with Figure 5]
CAF-1 participates in chromocenter formation.
(A) RT-qPCR analysis of transcript levels of *FAS2* and the control gene *AAE15* (2) that is expressed in a stable manner during post-germination development during 2 to 5 dag in cotyledons. Histograms show means of transcript levels ± SEM obtained for two independent PCR amplifications of three biological replicates. The y-axis shows the fold change relative to transcript levels at day 5 (set to 1) after normalization to *AtSAND* expression. Student's t-test. (B) DNA FISH images of representative nuclei from *fas1-4* (top) and *fas2-5* (bottom) cotyledons aged 2, 3, 4 or 5 dag. 180 bp repeats (red) and TSI (green) were revealed by DNA FISH. DNA is counterstained with DAPI. Scale bar represents 5 µm. (C) Percentage of nuclei showing clustering of 180 bp and TSI repeat sequences into chromocenter structures in *fas2-5* mutant cotyledon nuclei at 2, 3, 4 or 5 dag ± SEM from two independent biological replicates. Over 200 nuclei were scored at each timepoint.

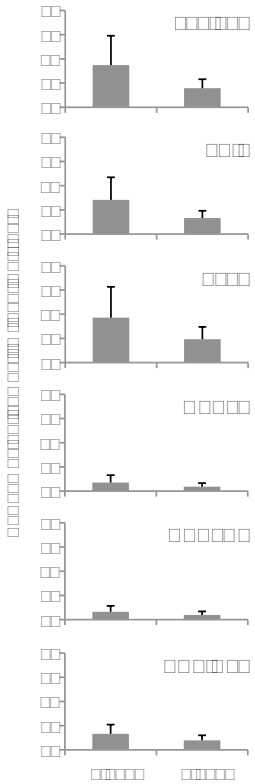

Figure S5 [with Figure 6]
H3K27me1 levels remain stable in *fas1-4* mutants during cotyledon development.
Enrichment of H3K27me1 assessed by ChIP qPCR at 180 bp, TSI, the Ta3 retrotransposon, as well as *HXK1, UEV1C* and *ACTIN2* at day 2 and 5 dag in e-H3.1/*fas1-4* plants. Histograms show mean percentage ± SEM of the respective immunoprecipitation relative to H3 levels for two independent PCR amplifications of three biological replicates.

Experiment	Target	Gene ID	Primer	Sequence 5'-3'
Genotyping	*FAS1*	At1g65470	Fas1_fw_MI	ATGGTATCTGGCCCAGCCAAA
			Fas1_rev_MI	CCTGTTCAGACGGATCAATGTCCA
			LBR Sail	TAGCATCTGAATTTCATAACCAATCTCGATACAC
	FAS2	At5g64630	FAS2-LP	TTTGCCCTGTTGCATTTAAAC
			FAS2-RP	GCCCAATAATGATCCACAATG
			LBb1.3	ATTTTGCCGATTTCGGAAC
	HIRA	At3g44530	Hira_Wisc_LP	CTACTAAAATTTGAGGCCGGG
			Hira_Wisc_RP	GAGAGTCACTGTTTTGGCTGG
			p745_WiscDsLox	AACGTCCGCAATGTGTTATTAAGTTGTC
	HTR9	At5g10400	HTR9_LP	AATAACAACCACACTGCAGCC
			HTR9_RT-R	CGAAAACGAAAAGAGACAGCTT
			LBb1.3	ATTTTGCCGATTTCGGAAC
	ATXR5	At5g09790	ATXR5_LP	TTTCTCTTGTCCGGTGAAATG
			ATXR5_RP	CCTGCAACAATCAGTGTGATG
			LBb1.3	ATTTTGCCGATTTCGGAAC
	ATXR6	At5g24330	ATXR6_LP	TTGAGATGAATCTGGAGACCG
			ATXR6_RP	AAACGACGACGTATTGGAGTG
			LBR Sail	TAGCATCTGAATTTCATAACCAATCTCGATACAC
	SUVH4	At5g13960	KYP_LP	ACTGGTGAACCAGCTGGTATG
			KYP_RP	TGAGGGGTACCTGTTCAATTG
			LBb1.3	ATTTTGCCGATTTCGGAAC
	SUVH5	At2g35160	suvh5 GABI-LP	CTCTTTTTATCCAGGGCAACC
			suvh5 GABI-RP	TCATGGGTTTTGAAGATCTGC
			GK_o8409	ATATTGACCATCATACTCATTGC
	SUVH6	At2g22740	suv6-2 LP	TGCATATTTTGGGAGAAGTGC
			suv6-2 RP	GTCGTTCCCGATTCTTCTTTC
			LBR Sail	TAGCATCTGAATTTCATAACCAATCTCGATACAC
	MOM1	At1g08060	mom1-2_SAIL610_G01_LP	ACAATGCAGGAGCAAACACTC
			mom1-2_SAIL610_G01_RP	GGAAAGGAGATACTTCACCGG
			LBR Sail	TAGCATCTGAATTTCATAACCAATCTCGATACAC
RT-qPCR	*FAS1*	At1g65470	Fas1_fw_M	ATGGTATCTGGCCCAGCCAAA
			Fas1_rev_MI	CCTGTTCAGACGGATCAATGTCCA
	FAS2	At5g64630	FAS2_qpcr_Forter	AAACCGGTTGTAGTGGTTCG
			FAS2_qpcr_Revter	TGCAGCATAGTGGAGACCTG
	HIRA	At3g44530	HIRA qRT F2	AACAAGACCAGAACTCAAGA
			HIRA qRT R2	CTTTAACAACGCCTAACTGAG
	HTR1	At5g65360	At5g65360_HTR1_qpcr_Forbis	AGCGATCTCACGAACCAAAC
			At5g65360_HTR1_qpcr_Revbis	GAAATCCACCGGAGGAAAAG
	HTR9	At5g10400	HTR9_RT-F	TAATCTCTGTGCGATTCATGCT
			HTR9_RT-R	CGAAAACGAAAAGAGACAGCTT
	AtSAND	At2g28390	SAND-F	AACTCTATGCAGCATTTGATCCACT
			SAND-R	TGATTGCATATCTTTATCGCCATC
	AAE15	At1g74960	Acyl-ACP Synthetase qRT F1	TGGACATCAGAATGTTCGTT
			Acyl-ACP Synthetase qRT R1	TTTGTATTTAGCCACGACCA
ChIP-qPCR	TSI	TSI	TSIq-F	CTCTACCCTTTGCATTCATGAATCCTT
			TSIq-R	GATGGGCAAAAGCCCTCGGTTTTAAAATG
	Ta3	At1g37110	QPCR-Ta3-F	AAGAGAGCTGGCAGAAGCAGTTGA
			QPCR-Ta3-R	ACGCCCTTTACCTTGACCTCCTTT
	SUVH4	At5g13960	SUVH4_qRT_F2	AAGATGAGAATGCGCCAGAG
			SUVH4_qRT_R2	ATTGGGGAAATGTTGTCAGC
	SUVH5	At2g35160	SUVH5_qRT_F1	CCCTTGATGTTCAGTTCTGT
			SUVH5_qRT_R1	TGCAGCTAAAACATGACAAC
	SUVH6	At2g22740	SUVH6_qRT_F1	GCAAGTAAGGGTAATGTTGG
			SUVH6_qRT_R1	TTGAAGCGGAGGTATATTGT
	ACTIN2	At3g18780	actin_f	GGTAACATTGTGCTCAGTGGTGG
			actin_r	AACGACCTTAATCTTCATGCTGC
	HXK1	At4g29130	At4g29130_ChIP-F	AGGAGCTCGTCTCTCTGCTG
			At4g29130_ChIP-R	GCTCAAACAATCCACCATCC
	UEV1C	At2g36060	At2g36060_ChIP-F	GGTGACTGAAATGTGAATTTGC
			At2g36060_ChIP-R	ATGCAGCCATCTCCTTCTTC
	UBC28	At1g64230	At1g64230-ChIP-F	TCATTGTTAACGGACCCAAAC
			At1g64230-ChIP-R	CCAGCTTCTCGCAGTAGACTC
	180 bp	180 bp	180(all)-F	ACCATCAAAGCCTTGAGAAGCA
			180(all)-R	CCGTATGAGTCTTTGTCTTTGTATCTTCT
	TSI	TSI	TSIq-F	CTCTACCCTTTGCATTCATGAATCCTT
			TSIq-R	GATGGGCAAAAGCCCTCGGTTTTAAAATG
	Ta3	At1g37110	QPCR-Ta3-F	AAGAGAGCTGGCAGAAGCAGTTGA
			QPCR-Ta3-F	ACGCCCTTTACCTTGACCTCCTTT
	IG	Between At2g17670 and At2g17680	IG-2g17670-80qF	GGCTACTGTCTAGTTCATATCTTAGA
			IG-2g17670-80qR	TAGGTTGGCATCCGATCCAGAGT
Cloning	*HTR9*	At5g10400	NotI_HTR9genomic_ for	ATATATGCGGCCGCTAGACGTCTGCAACGC
			HTR9_NotI_rev	AAATTTGCGGCCGCAGCCCTCTCTCCTCTGATTCTC
	FLAG-HA	FLAG-HA	TAG_NotI_F	ATATATGCGGCCGCTGGAGGAGAC
			TAG_BamHI-R	ATATAGGATCCCTAGGCGTAGTCGGGCACGTC
	OCS Terminator	OCS Terminator	terOCSSalI	TAGAGTCGACCTGCAGGC
			terOCSSalI	GCCGGATCCTGGACAATCAG

Table S1
List of oligonucleotides used in this study.

References

1. Almouzni G, Probst A V (2011) Heterochromatin maintenance and establishment: lessons from the mouse pericentromere. *Nucleus* 2:332–8.

2. Lehnertz B et al. (2003) Suv39h-mediated histone H3 lysine 9 methylation directs DNA methylation to major satellite repeats at pericentric heterochromatin. *Curr Biol* 13:1192–1200.

3. Probst A V, Fransz PF, Paszkowski J, Mittelsten Scheid O (2003) Two means of transcriptional reactivation within heterochromatin. *Plant J* 33:743–749.

4. Martens JH et al. (2005) The profile of repeat-associated histone lysine methylation states in the mouse epigenome. *EMBO J* 24:800–812.

5. Mathieu O, Probst A V, Paszkowski J (2005) Supplemental Information: Distinct regulation of histone H3 methylation at lysines 27 and 9 by CpG methylation in Arabidopsis. *EMBO J* 24:2783–2791.

6. Chodavarapu RK et al. (2010) Relationship between nucleosome positioning and DNA methylation. *Nature* 466:388–392.

7. Shu H, Wildhaber T, Siretskiy A, Gruissem W, Hennig L (2012) Distinct modes of DNA accessibility in plant chromatin. *Nat Commun* 3:1281.

8. Talbert P, Henikoff S (2010) Histone variants--ancient wrap artists of the epigenome. *Nat Rev Mol cell Biol* 11:264–275.

9. Volle C, Dalal Y (2014) Histone variants: the tricksters of the chromatin world. *Curr Opin Genet Dev* 25C:8–14.

10. Jin C, Felsenfeld G (2007) Nucleosome stability mediated by histone variants H3.3 and H2A.Z. *Genes Dev* 21:1519–1529.

11. Mito Y, Henikoff JG, Henikoff S (2005) Genome-scale profiling of histone H3.3 replacement patterns. *Nat Genet* 37:1090–1097.

12. Goldberg AD et al. (2010) Distinct factors control histone variant H3.3 localization at specific genomic regions. *Cell* 140:678–691.

13. Wirbelauer C, Bell O, Schübeler D (2005) Variant histone H3.3 is deposited at sites of nucleosomal displacement throughout transcribed genes while active histone modifications show a promoter-proximal bias. *Genes Dev* 19:1761–6.

14. Stroud H et al. (2012) Genome-wide analysis of histone H3.1 and H3.3 variants in Arabidopsis thaliana. *Proc Natl Acad Sci* 109:5370–5.

15. Wollmann H et al. (2012) Dynamic deposition of histone variant h3.3 accompanies developmental remodeling of the Arabidopsis transcriptome. *PLoS Genet* 8:e1002658.

16. Vaquero-Sedas M, Vega-Palas M (2013) Differential association of Arabidopsis telomeres and centromeres with Histone H3 variants. *Sci Rep* 3:1–3.

17. Mayer R et al. (2005) Common themes and cell type specific variations of higher order chromatin arrangements in the mouse. *BMC Cell Biol* 6.

18. Fransz P, ten Hoopen R, Tessadori F (2006) Composition and formation of heterochromatin in Arabidopsis thaliana. *Chromosome Res* 14:71–82.

19. Csink A, Henikoff S (1996) Genetic modification of heterochromatic association and nuclear organization in Drosophila. *Nature* 381:529–531.

20. Brown KE et al. (1997) Association of transcriptionally silent genes with Ikaros complexes at centromeric heterochromatin. *Cell* 91:845–54.

21. Brown KE et al. (2001) Expression of alpha- and beta-globin genes occurs within different nuclear domains in haemopoietic cells. *Nat Cell Biol* 3:602–6.

22. Fransz P, de Jong JH, Lysak M, Castiglione MR, Schubert I (2002) Interphase chromosomes in Arabidopsis are organized as well defined chromocenters from which euchromatin loops emanate. *Proc Natl Acad Sci U S A* 99:14584–14589.

23. Grob S, Schmid MW, Grossniklaus U (2014) Hi-C Analysis in Arabidopsis Identifies the KNOT, a Structure with Similarities to the flamenco Locus of Drosophila. *Mol Cell*:1–16.

24. Feng S et al. (2014) Genome-wide Hi-C Analyses in Wild-Type and Mutants Reveal High-Resolution Chromatin Interactions in Arabidopsis. *Mol Cell*:1–14.

25. Benoit M, Layat E, Tourmente S, Probst A V (2013) Heterochromatin dynamics during developmental transitions in Arabidopsis - a focus on ribosomal DNA loci. *Gene* 526:39–45.

26. Pecinka A et al. (2010) Epigenetic regulation of repetitive elements is attenuated by prolonged heat stress in Arabidopsis. *Plant Cell* 22:3118–3129.

27. Tessadori F et al. (2007) Large-scale dissociation and sequential reassembly of pericentric heterochromatin in dedifferentiated Arabidopsis cells. *J Cell Sci* 120:1200–1208.

28. Tessadori F, Schulkes RK, van Driel R, Fransz P (2007) Light-regulated large-scale reorganization of chromatin during the floral transition in Arabidopsis. *Plant J* 50:848–857.

29. Van Zanten M et al. (2011) Seed maturation in Arabidopsis thaliana is characterized by nuclear size reduction and increased chromatin condensation. *Proc Natl Acad Sci U S A* 108:20219–24.

30. Mathieu O et al. (2003) Changes in 5S rDNA chromatin organization and transcription during heterochromatin establishment in Arabidopsis. *Plant Cell* 15:2929–2939.

31. Douet J, Blanchard B, Cuvillier C, Tourmente S (2008) Interplay of RNA Pol IV and ROS1 during post-embryonic 5S rDNA chromatin remodeling. *Plant Cell Physiol* 49:1783–1791.

32. Heslop-Harrison JS, Murata M, Ogura Y, Schwarzacher T, Motoyoshi F (1999) Polymorphisms and genomic organization of repetitive DNA from centromeric regions of Arabidopsis chromosomes. *Plant Cell* 11:31–42.

33. Steimer A et al. (2000) Endogenous targets of transcriptional gene silencing in Arabidopsis. *Plant Cell* 12:1165–1178.

34. May BP, Lippman ZB, Fang Y, Spector DL, Martienssen RA (2005) Differential regulation of strand-specific transcripts from Arabidopsis centromeric satellite repeats. *PLoS Genet* 1:e79.

35. Roudier F et al. (2011) Integrative epigenomic mapping defines four main chromatin states in Arabidopsis. *EMBO J* 30:1928–38.

36. Soppe WJ et al. (2002) DNA methylation controls histone H3 lysine 9 methylation and heterochromatin assembly in Arabidopsis. *EMBO J* 21:6549–6559.

37. Jacob Y et al. (2009) ATXR5 and ATXR6 are H3K27 monomethyltransferases required for chromatin structure and gene silencing. *Nat Struct Mol Biol* 16:763–768.

38. Zhang X, Bernatavichute Y, Cokus S, Pellegrini M, Jacobsen SE (2009) Genome-wide analysis of mono-, di- and trimethylation of histone H3 lysine 4 in Arabidopsis thaliana. *Genome Biol* 10:R62.

39. Johnson L, Cao X, Jacobsen S (2002) Interplay between two epigenetic marks. DNA methylation and histone H3 lysine 9 methylation. *Curr Biol* 12:1360–1367.

40. Ebbs M, Bender J (2006) Locus-specific control of DNA methylation by the Arabidopsis SUVH5 histone methyltransferase. *Plant Cell* 18:1166–1176.

41. Jacob Y et al. (2014) Selective Methylation of Histone H3 Variant H3.1 Regulates Heterochromatin Replication. *Science* 343:1249–1253.

42. Stillman B (1989) Purification and characterization of CAF-I, a human cell factor required for chromatin assembly during DNA replication in vitro. *Cell* 58:15–25.

43. Tagami H, Ray-Gallet D, Almouzni G, Nakatani Y (2004) Histone H3.1 and H3.3 complexes mediate nucleosome assembly pathways dependent or independent of DNA synthesis. *Cell* 116:51–61.

44. Houlard M et al. (2006) CAF-1 is essential for heterochromatin organization in pluripotent embryonic cells. *PLoS Genet* 2:e181.

45. Roberts C et al. (2002) Targeted mutagenesis of the Hira gene results in gastrulation defects and patterning abnormalities of mesoendodermal derivatives prior to early embryonic lethality. *Mol Cell Biol* 22:2318–2328.

46. Kaya H et al. (2001) FASCIATA genes for chromatin assembly factor-1 in arabidopsis maintain the cellular organization of apical meristems. *Cell* 104:131–142.

47. Nie X, Wang H, Li J, Holec S, Berger F (2014) The HIRA complex that deposits the histone H3.3 is conserved in Arabidopsis and facilitates transcriptional dynamics. *Biol Open*:1–9.

48. Phelps-Durr TL, Thomas J, Vahab P, Timmermans MCP (2005) Maize rough sheath2 and its Arabidopsis orthologue ASYMMETRIC LEAVES1 interact with HIRA, a predicted histone chaperone, to maintain knox gene silencing and determinacy during organogenesis. *Plant Cell* 17:2886–2898.

49. Ingouff M et al. (2010) Zygotic Resetting of the HISTONE 3 Variant Repertoire Participates in Epigenetic Reprogramming in Arabidopsis. *Curr Biol* 20:2137–2143.

50. Ramirez-Parra E, Gutierrez C (2007) E2F regulates FASCIATA1, a chromatin assembly gene whose loss switches on the endocycle and activates gene expression by changing the epigenetic status. *Plant Physiol* 144:105–20.

51. Duc C et al. The histone chaperone complex HIR controls nucleosome occupancy and tanscriptional silencing in plants. submitted.

52. Loyola A, Bonaldi T, Roche D, Imhof A, Almouzni G (2006) PTMs on H3 variants before chromatin assembly potentiate their final epigenetic state. *Mol Cell* 24:309–316.

53. Johnson L et al. (2004) Mass spectrometry analysis of Arabidopsis histone H3 reveals distinct combinations of post-translational modifications. *Nucleic Acids Res* 32:6511–6518.

54. Jasencakova Z et al. (2003) Histone modifications in Arabidopsis- high methylation of H3 lysine 9 is dispensable for constitutive heterochromatin. *Plant J* 33:471–80.

55. Yelagandula R et al. (2014) The Histone Variant H2A.W Defines Heterochromatin and Promotes Chromatin Condensation in Arabidopsis. *Cell* 158:98–109.

56. Akiyama T, Suzuki O, Matsuda J, Aoki F (2011) Dynamic replacement of histone H3 variants reprograms epigenetic marks in early mouse embryos. *PLoS Genet* 7:e1002279.

57. Shibahara K, Stillman B (1999) Replication-dependent marking of DNA by PCNA facilitates CAF-1-coupled inheritance of chromatin. *Cell* 96:575–85.

58. Masubelele NH et al. (2005) D-type cyclins activate division in the root apex to promote seed germination in Arabidopsis. *Proc Natl Acad Sci U S A* 102:15694–15699.

59. Probst A V et al. (2010) A strand-specific burst in transcription of pericentric satellites is required for chromocenter formation and early mouse development. *Dev Cell* 19:625–638.

60. Verdel A, Vavasseur A, Le Gorrec M, Touat-Todeschini L (2009) Common themes in siRNA-mediated epigenetic silencing pathways. *Int J Dev Biol* 53:245–257.

61. Verschure P, Kraan I Van Der (2003) Condensed chromatin domains in the mammalian nucleus are accessible to large macromolecules. *EMBO Rep* 4:861–66.

62. Vaillant I, Tutois S, Cuvillier C, Schubert I, Tourmente S (2007) Regulation of Arabidopsis thaliana 5S rRNA Genes. *Plant Cell Physiol* 48:745–752.

63. Quivy JP et al. (2004) A CAF-1 dependent pool of HP1 during heterochromatin duplication. *EMBO J* 23:3516–3526.

64. Vaillant I et al. (2008) Hypomethylation and hypermethylation of the tandem repetitive 5S rRNA genes in Arabidopsis. *Plant J* 54:299–309.

65. Layat E, Sáez-Vásquez J, Tourmente S (2012) Regulation of Pol I-transcribed 45S rDNA and Pol III-transcribed 5S rDNA in Arabidopsis. *Plant Cell Physiol* 53:267–276.

66. Robinson PJJ, Rhodes D (2006) Structure of the “30 nm” chromatin fibre: a key role for the linker histone. *Curr Opin Struct Biol* 16:336–43.

67. Hajkova P et al. (2008) Chromatin dynamics during epigenetic reprogramming in the mouse germ line. *Nature* 452:877–881.

68. She W et al. (2013) Chromatin reprogramming during the somatic-to-reproductive cell fate transition in plants. *Development* 140:4008–19.

69. Czechowski T, Stitt M, Altmann T, Udvardi MK, Scheible WR (2005) Genome-wide identification and testing of superior reference genes for transcript normalization in Arabidopsis. *Plant Physiol* 139:5–17.

70. Bowler C et al. (2004) Chromatin techniques for plant cells. *Plant J* 39:776–789.

Discussion and perspectives

My thesis investigated the role of histone H3 variants and the associated histone chaperone network in heterochromatin dynamics. This work was focusing on two different developmental windows: on the one hand vegetative development is suitable for a detailed study of the maintenance of heterochromatin structure, and on the other hand early post-germination development is a privileged time window to monitor heterochromatin reorganization. Our data argue for an independent but not exclusive role of CAF-1 and HIR-dependent assembly pathways in heterochromatin dynamics. We also revealed new and unexpected characteristics of H3 variants, suggesting that the functional distinction between H3.1 and H3.3 should be nuanced.

1. The HIR complex as a major player in maintenance of genome integrity

We identified orthologs of the mammalian HIR complex subunits HIRA, UBINUCLEIN and CABIN1 in Arabidopsis and tested the consequences of their loss on genome function and integrity. Reduced levels of the non-nucleosomal histone pool and decrease in H3 occupancy in the core and 3' region of two euchromatic loci as well as in heterochromatin in *athira-1* mutants argue for a conserved chaperone activity of AtHIRA and interaction with the H3.3 variant, confirmed recently by co-immunoprecipitation assays (Nie et al., 2014). Introgression of e-H3.1 and e-H3.3 transgenes in *athira-1* plants followed by biochemical and genomic analysis will give further insights regarding the specificity of the histone / chaperone interaction. Despite normal growth and vegetative development *athira-1* mutants display defects in male reproductive development under our growth conditions. These phenotypes could be explained by a role of the HIR complex in histone H3 variant dynamics e.g. during gametogenesis. These variant dynamics involve reprogramming of the chromatin histone content by replacing H3.1 by H3.3 and H3.3-like variants and thereby defining particular and distinguishable chromatin properties between parental gametes. Regarding the transmission of the *athira-1* mutant allele, standard segregation rates were observed (Ingouff et al., 2010; Nie et al., 2014), suggesting that the HIR complex does not play an essential role neither in histone variant

exchange prior to fertilization nor immediately following fertilization in contrast to the role of Drosophila HIRA.

Our analysis revealed unexpected roles of AtHIRA in nucleosomal occupancy of heterochromatin and maintenance of transcriptional silencing in plants. While initially surprising these results are consistent with the deposition of e-H3.3 observed at heterochromatic repeats that we revealed in our transgenic lines. The biological significance of H3.3 deposition in heterochromatic regions is unknown, but H3.3 at these sites is susceptible to favor maintenance of nucleosome occupancy upon slow but significant histone turnover at heterochromatin, especially in non-proliferative cells were replication-dependent CAF-1 chromatin assembly activity does not occur anymore (Drané et al., 2010; Lewis et al., 2010). The replacement of H3.1 by H3.3 could lead to a change in post-translational modifications as H3.3 is not modified by the H3K27 monomethyltransferases ATXR5 and ATXR6 (Jacob et al., 2010). The amount of H3.3 at heterochromatic repeats relative to H3.1 as well as the dependence of H3.3 enrichment on AtHIRA are not known to date. Clearly, given the only subtle phenotypes of the *athira-1* mutant, we can expect other H3.3 deposition complexes to exist in plants such as DEK or ATRX, even if plants lack a DAXX ortholog (Zhu et al., 2012), which could also contribute to H3.3 enrichment in heterochromatin.

However, heterochromatin dynamics during post-germination development do not require AtHIRA or the other members of the HIR complex since formation of cytologically distinguishable chromocenters during 2 to 5 dag in cotyledons appeared unchanged in our analysis. This suggests that CAF-1 but not HIR chromatin assembly activity is necessary to establish chromocenters and that deposition of H3.3 occurs afterwards potentially to maintain chromatin structure. On the contrary, mammalian HIRA and UBN1 together with ASF1A are involved in the formation of specialized heterochromatic structures called Senescence-Associated Heterochromatin Foci (SAHF) involved in cellular senescence (Zhang et al., 2005; Banumathy et al., 2009). UBN1 is thought to target the activity of histone methyltransferases to SAHF-localizing DNA for subsequent H3K9me deposition and transcription repression of proliferation-promoting genes that participate in cell cycle arrest (Narita et al., 2003; Banumathy et al., 2009). Whether such a mechanism exists in plants has never been assessed but it suggests that the transition from proliferative to senescent states necessitates replication-independent chromatin

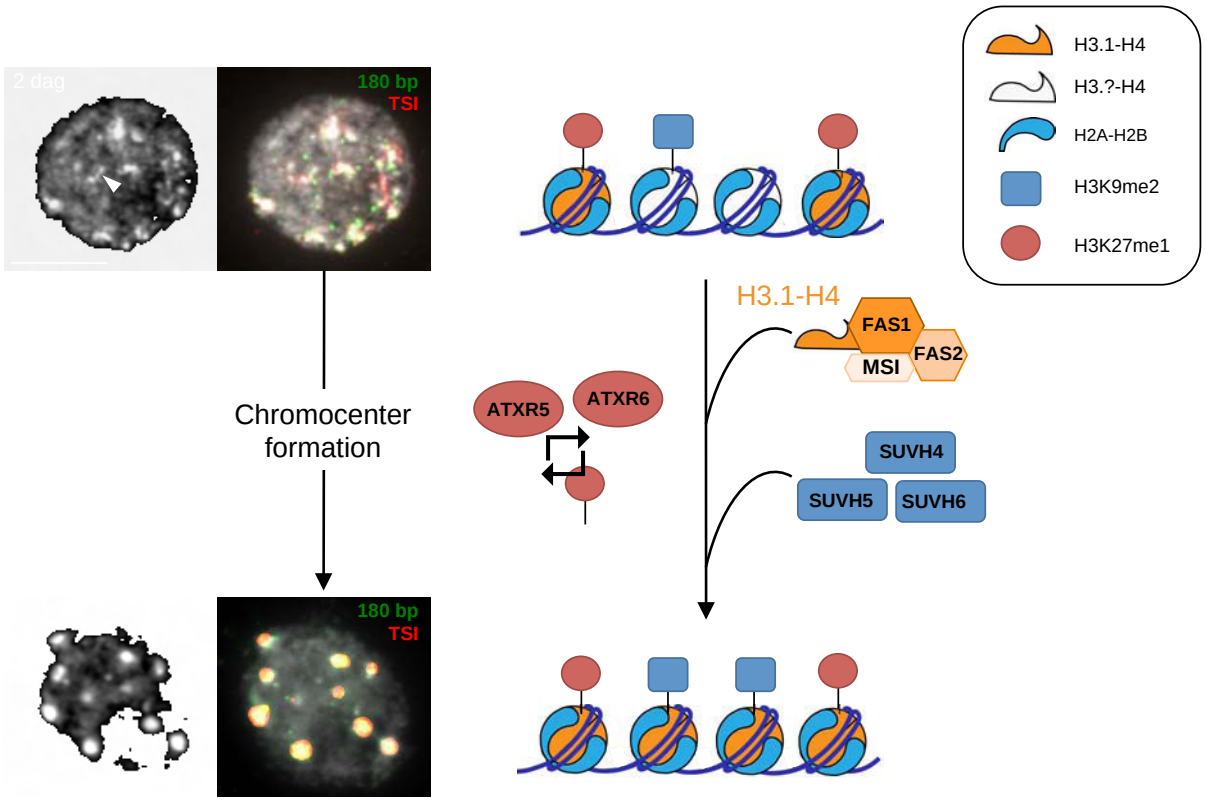

Figure 46: **Model for the interplay between CAF-1, SUVH, ATXR5 and ATXR6 in chromocenter formation during post-germination development in Arabidopsis.**

Chomocenter formation involves site-specific CAF-1-dependent H3.1 enrichment, SUVH-dependent H3K9me2 enrichment and maintenance of H3K27me1 by ATXR5 and ATXR6 at centromeric and pericentromeric repeats. White arrowheads point to a pre-chromocenter (2 dag) and a mature chromocenter (5 dag). Scale bars: 5 µm.

assembly, but also distinct activities of the HIR complex independent from histone chaperoning that may involve interactions with other chromatin modifiers. The exact function of the different subunits of the *Arabidopsis thaliana* HIR complex and their interactions with other proteins remain elusive and their characterization necessitates deeper molecular analysis.

2. CAF-1 links chromatin assembly and epigenetic landscapes

The CAF-1 chaperone complex has been extensively studied from Drosophila to mammals for its replication-dependent H3.1 nucleosome assembly activity, its role in maintenance of epigenetic marks upon nucleosome disruption at the replication fork and in DNA repair (Quivy et al., 2004; Tagami et al., 2004; Gérard et al., 2006; Polo et al., 2006). Plants lacking CAF-1 subunits are viable compared to mammals and Drosophila despite pleiotropic morphological defects. At the chromatin level, nuclei of *fas1* and *fas2* mutants show reduced heterochromatin content associated with transcriptional reactivation of pericentromeric repeats and reduced nucleosome occupancy (Takeda et al., 2004; Exner et al., 2006; Schönrock et al., 2006; Ono et al., 2006 and our study). Chromocenters are transiently disorganized at germination in WT plants, when only pre-chromocenters remain detectable in cotyledon nuclei (Mathieu et al., 2003; Douet et al., 2008; van Zanten et al., 2011). The mechanism by which chromocenters are restructured between 2 and 5 dag was unknown (Mathieu et al., 2003; Douet et al., 2008; Benoit et al., 2013). Here we identified local CAF-1-dependent H3.1 dynamics at repetitive sequences as a driving force favoring clustering into chromocenters. This process concomitantly requires proper setting of the repressive post-translational modifications H3K9me2 and H3K27me1 (***Figure 46***). Plants lacking histone methyltransferases SUVH4, SUVH5 and SUVH6 display increased dispersion of centromeric and pericentromeric repeats at 2 dag, while impaired H3K27me1 deposition in *atxr5 atxr6* mutants prevents chromocenter formation at later developmental stages. This suggests different roles for H3K9me2 and H3K27me1. While H3K27me1 defects can originate from deficiency in higher-order folding or from failure to control heterochromatin over-replication (Jacob et al.,

2010), H3K9me2 might be required for maintenance of transcriptional silencing of centromeric and pericentromeric repeats, even in absence of cytologically visible chromocenters (Malagnac et al., 2002; Jackson et al., 2004; Naumann et al., 2005; Ebbs and Bender, 2006; Johnson et al., 2007). This is in agreement with observations that H3K9me2 together with DNA methylation restricts DNA accessibility at pericentromeric repeats (Shu et al., 2012).

5S rRNA genes were the first repetitive sequences to be studied in the context of post-germination chromatin remodeling (Mathieu et al., 2003; Douet et al., 2008), and it is thus necessary to compare reorganization dynamics of 5S rDNA loci with 180 bp and TSI dynamics described in our study. 5S rDNA loci, despite their localization within pericentromeric heterochromatin, display distinct organizational dynamics. In cotyledon at 2 dag, 5S rDNA chromatin tightly colocalizes with pre-chromocenters, prior to a transient decompaction at 3 dag followed by a recondensation at 5 dag. These particular dynamics have been proposed as critical for the compartmentalization of the silenced, highly mutated 5S rDNA arrays in chromocenters whereas the transcribed fraction forms loops with euchromatic features that emanate from chromocenters (Mathieu et al., 2003). This has been associated with changes in the 5S rDNA methylation pattern, since rapid and active demethylation mediated by the ROS1 demethylase is required for decompaction at 3 dag, while Pol IV, required for *de novo* CHH methylation by the RdDM pathway, is involved in the subsequent recondensation of 5S rDNA chromatin at 5 dag (Douet et al., 2008). Such chromatin dynamics have not been observed for 180 bp repeats and TSI in my study. One explanation is the different techniques used evaluate dispersion *versus* compaction in our different studies. Another explanation is the difference between 180 bp and TSI and the 5S rDNA in the necessity to be transcribed and the co-existence of both euchromatic and heterochromatic marks along the same 5S rDNA locus. Whether the reorganization of 180 bp and TSI sequences involves changes in DNA methylation that might reinforce histone methylation marks such as H3K9me2 and favor clustering remains to be elucidated. A simple relationship between the degree of clustering and the amount of CG and CHG methylation could however not be established (Tariq et al., 2003; Vaillant et al., 2007).

It is interesting to note that global H3 occupancy remains stable between 2 and 5 dag despite enrichment of H3.1 at the repetitive sequences tested, implying replacement of yet uncharacterized histones present at germination by the replicative

H3.1. One exciting hypothesis involves the progressive enrichment of histone H3.3 in the embryonic cotyledon during seed maturation in order to compensate absence of new chromatin assembly coupled to replication and decreased H3.1 incorporation. During imbibition, the H3.3-rich chromatin of seeds is then globally remodeled (van Zanten et al., 2011) and heterochromatin decondensation might be facilitated by H3.3 enrichment. Initiation of the mitotic cycle is observed shortly after emergence of the cotyledons from the seed coat before switching to the endocycle suggesting that H3.3 enrichment is diluted by H3.1 incorporation during DNA synthesis-coupled histone deposition in heterochromatin. In euchromatin, *de novo* deposited H3.1 could be readily exchanged to H3.3 promoting transcriptional permissive landscapes and resulting in the differences observed between euchromatin and heterochromatin in H3.1 enrichment.

Despite the clear role of CAF-1-dependent chromatin assembly in chromocenter formation that we could show in our study, a significant fraction (around 50%) of *fas* cotyledon nuclei at 5 dag are able to cluster efficiently centromeric and pericentromeric repeats into chromocenters. This raises the question concerning the difference between the two nuclei populations. One explanation could be the difference in polyploidy levels between WT and *fas* mutant cotyledons, which switch early to the endocyle (Ramirez-Parra and Gutierrez, 2007a). Indeed, it has been shown that centromeric and pericentromeric repeats organized differently in chromocenters of high ploidy nuclei (Schubert et al., 2012), which could create a bias in our analysis. In an attempt to limit this bias, large nuclei and nuclei with extranumerous well-defined chromocenters (>10) were voluntarily excluded from our quantification. Cell heterogeneity in the tissue analyzed can also partially explain these results. Indeed despite cautious dissection of the cotyledons from the adjacent meristematic tissue, cotyledons still display a large number of different cell types, associated with potential proper chromatin dynamics. This is exemplified by different chromatin dynamics in guard cells *versus* pavement cells in the cotyledon epidermis (Kato and Lam, 2003, Poulet et al., unpublished results). Finally, certain cells may be able to overcome defects caused by deficient replication coupled chromatin assembly by other mechanisms.

Our study focused exclusively on H3 variants, but the nucleosome consists of three other types of histones that may play a critical role. Indeed H2A.W, a recently

characterized H2A variant in Arabidopsis, contributes to global genome organization and condensation of heterochromatin (Yelagandula et al., 2014). H2A.W shares similarities with the vertebrate-specific macroH2A variant found at the X chromosome and associated with transcriptional silencing (Costanzi and Pehrson, 1998; Buschbeck et al., 2009). In light of genome-wide data showing that euchromatin in Arabidopsis and other organisms is tightly correlated with enrichment in both H3.3 and H2A.Z (Zilberman et al., 2008; Stroud et al., 2012; Wollmann et al., 2012), characterization of heterochromatin by a co-enrichment of both H3.1 and H2A.W is a seducing argument in favor of the histone code in defining functional genomic domains in Arabidopsis. The linker histone H1 appears as well as an intriguing player. In line with its role in the compaction of nucleosomal arrays (Robinson and Rhodes, 2006), massive H1 dynamics have been proposed to initiate transient chromatin relaxation required for somatic-to-reproductive cell fate transition in plants (She et al., 2013). Moreover, H1 interacts with the chromatin remodeler DDM1 and modulates access of DNA methyltransferases to the underlying DNA (Zemach et al., 2013), suggesting tight interplay between H1 activity and setting of other chromatin marks. There are three Arabidopsis H1 proteins, including a stress-specific version, suggesting that Arabidopsis H1 may modulate dynamically chromatin compaction and activity as described in mammals and Drosophila (Fan et al., 2005; Lu et al., 2013).

3. Functional independence and interplay between CAF-1 and HIR

The two original research manuscripts presented in this thesis together with data available in the literature define CAF-1 and HIR as important chaperones controlling H3 dynamics and genome integrity in Arabidopsis. However, the signals controlling proper H3.1 and H3.3 recognition and assembly by these chaperones remain elusive. We know that differences in amino acids at position 87 and 90 are necessary to drive H3.1 and H3.3 deposition at the correct genomic domain in Arabidopsis (Shi et al., 2012). A basis for such specific localization would rely on the ability of the histone chaperone to recognize the amino acid signature of the histone to ensure

transport and deposition at the site of assembly. In this view, hybrid e-H3.1 displaying the amino acid signature of H3.3 at position 87 and 90 represent an interesting tool for studying the basis of H3 variant recognition by the different H3 chaperones. We show that plants lacking either the HIR or the CAF-1 complex display defects in chromatin organization and dynamics, improper chromatin assembly and alleviation of transcriptional silencing of heterochromatin, together with various degrees of developmental and reproductive defects. However and contrary to observations made in other eukaryotes, disruption of either DNA synthesis-dependent or DNA-synthesis-independent chromatin assembly pathways does not result in lethality, thereby suggesting that the Arabidopsis model is highly plastic regarding deficiency in nucleosome assembly. We thus asked if a functional compensation in histone deposition occurred between CAF-1 and HIR complexes. Plants lacking both AtHIRA and FAS2 show lethality during early development and *athira-1 fas1* display important defects including aberrant growth and sterility. The phenotypes are intensified compared to the single mutants but double mutants are viable probably because of residual FAS1 transcription. Double *athira-1 fas1* mutants show decrease in nucleosome occupancy compared to single mutants suggesting cooperative but not overlapping roles in histone dynamics and deposition. Surprisingly no aggravated transcriptional silencing release nor disorganized chromocenter structure were observed in the double mutant. This can be explained by the maintenance of other chromatin marks such as DNA methylation, which is of particular importance in Arabidopsis. The weak chromatin defects seen in *athira-1* are suspected to mirror compensation by other H3.3 histone assembly complexes such as DEK and ATRX. It can also be envisaged that CAF-1 deposits H3.3 under certain exceptional conditions. Indeed, in mammalian cells, H3.3 is found chaperoned by CAF-1 upon DAXX disruption in mammalian cells (Drané et al., 2010) and in the early mouse embryo CAF-1 depletion leads to incorporation of H3.3 genome-wide including the DAPI-dense regions potentially corresponding to pericentromeric satellites (Akiyama et al., 2011). Vice versa, HIRA has been shown to fill nucleosome gaps resulting from CAF-1 dysfunction (Ray-Gallet et al., 2011), but to date no evidences suggest that HIRA is able to deposit H3.1 in order to compensate CAF-1 loss. Taken together, the balance of available histone chaperone activity may affect deposition of canonical H3 and its variants and induce changes in its genome localization. Plasticity in histone variant interaction may compensate nucleosome deposition

activity and help maintaining compaction and regulation of DNA even in absence of a particular chaperone complex.

4. Functional diversification of canonical H3.1 and H3.3 variants

Characterization of Arabidopsis histone H3 function and dynamics through mutant studies and tagged lines was challenging regarding the high number of gene copies. Our analysis revealed differences in gene expression levels between H3.1- and H3.3-encoding genes during development and regarding the proliferative status of the tissue. We generated triple *htr1 htr3 htr9* mutants lacking expression of three out of the five H3.1-encoding genes and *htr4 htr8 htr5*^{amiRNA} H3.3 mutants. Preliminary observations revealed no obvious defects in neither vegetative development nor cytological organization of heterochromatin at interphase however these mutants require further molecular characterization, focusing on nucleosomal density, transcriptional silencing and heat stress induced chromatin remodelling. Two hypothesis can thus be proposed on the consequences of the disruption of one or many histone-encoding genes: on the one hand, transcription of the remaining genes (*HTR2* and *HTR13* for H3.1, remaining *HTR5* transcripts for H3.3) could be sufficient to maintain appropriate histone levels, maybe involving compensation at the level of transcription, transcript or protein stability but this remains to be tested. On the other hand, H3.1 and H3.3 assembly pathways might compensate for each other upon impaired histone production or incorporation, as suggested by the viability and the subtle phenotypes defects observed in plants lacking either CAF-1 or AtHIRA. Differences in biochemical properties between histones are nevertheless likely to lead to incomplete compensation, particularly in processes such as fertilization or chromocenters formation that require the specific mobilization of H3.3 and H3.1 respectively. The H3.3 *htr4 htr8 htr5*^{amiRNA} mutant is thus a valuable tool to evaluate consequences of H3.3 loss on vegetative and reproductive development of plants as well as gene expression, but also to study potential compensation by H3.1. The weak phenotypes of plants lacking either H3.1 or H3.3 and their appropriate chaperones, together with evidence of functional compensation observed in Drosophila (Hödl and

Basler, 2009), suggest that the local chromatin context and their post-translational modification, rather than the biochemical differences between H3.1 and H3.3, impact genome organization and expression.

Characterization of Arabidopsis histone H3 variants has further revealed particular expression patterns of H3.3-like H3.6 and H3.14, encoded by *HTR6* and *HTR14* respectively. Our analysis showed absence of transcription of these genes in all vegetative tissues tested, consistent with previous data suggesting time- and cell-specific H3.3-like expression and deposition (Menges et al., 2003; Okada et al., 2005; Ingouff et al., 2007, 2010). Consistently, H3.14 is detected only in vegetative cell and central cell nuclei and is removed rapidly after fertilization. Interestingly, H3.14 incorporation is found in a time window where replication-dependent H3.1 deposition does not occur, suggesting that H3.14 can substitute H3.1 in some particular situations. Interestingly, we observed a transcriptional up-regulation of *HTR14*, and to a lesser extent *HTR6*, in vegetative tissues of plants lacking either *fas1* or *fas2*. Evidences for subsequent incorporation of H3.6 and H3.14 in chromatin are still lacking, but the mobilization of an unknown H3.3-like assembly pathway in order to compensate deficient DNA synthesis-coupled H3.1 assembly by CAF-1, and to limit defects in nucleosome assembly and chromatin organization can be envisaged. Such a hypothesis can be tested using lines displaying ectopic e-H3.14 expression in either WT or *fas* context, allowing new insights in how H3.3-like dynamics are mediated during development and the identification of its dedicated histone chaperone.

Due to the elevated conservation at the level of their amino acid sequence, H3.1 and H3.3 cannot be discriminated by antibodies thus impeding efficient tracking of their respective dynamics. Epitope-tagged H3.1 and H3.3 established during this thesis represent valuable tools to monitor efficiently H3 variant dynamics and deposition in chromatin. However, we have to be aware that these tools allow only an indirect and potentially biased observation of H3 dynamics. We chose one gene out of a multigenic histone family that shows in general coherent expression pattern, assuming identical regulation between the genes. Even if *HTR1*, *HTR2*, *HTR3*, *HTR9*, *HTR13* on the one hand, and *HTR4*, *HTR5*, *HTR8* on the other hand encode identical H3.1 and H3.3 proteins respectively, each gene may be subjected to different transcriptional, co- and post-transcriptional regulation, thereby contributing differently to the resulting H3 pool. Furthermore we included a region up to 2 kb

upstream of the transcription start site of *HTR9* and *HTR5* in our transgenes encoding e-H3 in order to keep both promoter and regulatory regions of the gene. However we cannot exclude the presence of a truncated promoter region and the disruption of short- and long-range regulations upon random insertion of the transgene within the genome, resulting in altered transcriptional regulation of epitope-tagged H3. The transgenes were transformed in plants lacking the functional endogenous copy of either *HTR9* or *HTR5* in order to maintain H3.1/H3.3 protein ratio within the nucleus. Giving that histone biosynthesis and dynamics are finely tuned, this appears important but has never been considered in studies using epitope-tagged histones. Even if we chose the FLAG-HA tag regarding its small size, its potential impact on proper histone assembly is difficult to evaluate. We tagged our histones at the C-terminus as this is done in most studies (Tagami et al., 2004; Ingouff et al., 2007; Santenard et al., 2010; Shi et al., 2011; Stroud et al., 2012; Wollmann et al., 2012) in order to least interfere with the setting of post-translational modifications of the N-terminal tail. However, the position of the tag can also lead to differences in assembly as has been reported for N- or C-terminal tagged H3.1 in mammalian embryos (Akiyama et al., 2011). In order to validate the molecular effects observed based on e-H3, we have to consider using additional transgenes and transgenic lines arising from independent transformation events, but also lines expressing histone fused to different tags, such as H3-Myc or H3-GFP. Ultimately, the CRISPR/Cas9 technology will allow the *in situ* tagging of endogenous genes maintaining native regulation of the tagged gene and avoiding potential bias originating from the use of transgenes.

Nuclear localization and genomic distribution of e-H3.1 revealed preferential association with heterochromatic domains while e-H3.3 enrichment is found at euchromatic loci, but also in the NOR consistent with previous observations (Shi et al., 2011; Nie et al., 2014). It is known that only a small fraction of 45S rRNA genes are transcribed by forming a loop in the nucleolus and protruding from chromocenters where the remaining inactive 45S rRNA fraction is highly condensed (Pontvianne et al., 2007; Durut et al., 2014). A similar organization has been described for 5S rDNA arrays (Cloix et al., 2002; Mathieu et al., 2003; Layat et al., 2012b). An intriguing hypothesis would be that deposition of H3.3 together with its distinctive post-translational marks in rRNA gene arrays would be a framework for subsequent transcription of the correct rDNA repeats, while mutated and silent rDNA arrays

remain depleted from H3.3 and enriched with canonical H3.1, repressive histone marks and DNA methylation. This needs to be tested by high-resolution techniques such as ChIP for e-H3.1 and e-H3.3 during different developmental stages or in different tissues that mobilize different 5S rDNA genes (Mathieu et al., 2003) or 45S rDNA variants (Pontvianne et al., 2010; Durut et al., 2014). Our data revealed as well a reduced but significant enrichment of H3.3 at heterochromatic 180 bp, TSI and Ta3, implying that H3.3 is not limited to euchromatic domains but also deposited at centromeric and pericentromeric regions consistent with the pattern known in mammals (Drané et al., 2010; Szenker et al., 2011). This is in accordance with the decreased nucleosome occupancy at centromeric and pericentromeric repeats together with the transcriptional silencing release of TSI observed in *athira-1*. The role of H3.3 in heterochromatin remains elusive but might participate in the molecular tagging of particular domains subject to stage- or cell-specific chromatin remodeling. One exciting hypothesis would rely on the deposition of H3.3 on a limited subfamily of centromeric and pericentromeric repeats, allowing the limited production of transcripts (May et al., 2005) and thus feeding the RdDM pathway.

5. ASF1, one to rule them all?

Together with CAF-1 and the HIR complex, the small ASF1 chaperones are involved in histone handling and dynamics in eukaryotes. Mammalian ASF1 proteins have been shown to buffer newly synthesized H3-H4 dimers during S phase and to mediate their transport to the sites of CAF-1 and / or HIR chromatin assembly in the nucleus. At the beginning of my thesis, the role of the Arabidopsis orthologs of ASF1 was not known. I revealed that AtASF1A and AtASF1B were ubiquitously expressed and established and characterized plants lacking AtASF1A and AtASF1B. Plants lacking one paralog show WT phenotype while depletion of both AtASF1A and AtASF1B results in impaired plant growth and causes dramatic vegetative and reproductive defects, exemplified by leaf with dentate margins, short roots and limited fertility. This is associated with defects at the chromatin level: *atasf1ab* double mutants, but not *atasf1a* and *atasf1b* single mutants, display impaired chromocenter establishment by 5 dag in cotyledons similar to plants lacking CAF-1. These observations suggest that AtASF1A and AtASF1B share overlapping roles in

chromatin organization but occurrence of gene duplication is susceptible to involve paralog-specific activities. One important question is how newly synthesized H3.1 and H3.3 are targeted and loaded correctly to the appropriate chaperones in plants. One intriguing hypothesis would be that similar to mammals each AtASF1 paralog is preferentially involved in either DNA synthesis-dependent or independent chromatin assembly. Differential timing of AtASF1A and AtASF1B expression during the cell cycle could drive preferential shuttling of either H3.1 and H3.3 to its dedicated assembly complex, thus promoting CAF-1 chromatin assembly during S phase, and HIR chromatin assembly outside S-phase. Such a separation would be important to sustain correct histone flow when needed during development. Biological evidence for sub-functionalization of the ASF1 paralogs in Arabidopsis is still lacking, but the analysis of e-H3.1 and e-H3.3 dynamics in either single *atasf1a* and *atasf1b* or double *atasf1ab* mutants, together with biochemical studies of the HIR or CAF-1 complexes will give insight into this question.

6. Perspectives

As a conclusion, this work contributes to a better global understanding of how eukaryotic genome structure is established and maintained during development. Compartmentalization of heterochromatin away from euchromatin, exemplified by the formation of chromocenters in Arabidopsis and other organisms, is of critical importance in the maintenance of proper genome activity. We show that histone H3 variants and their associated chaperones are involved in such a process. However, clustering of heterochromatin in chromocenters is not a general view regarding genome organization in other eukaryotes. In organisms with large genomes such as wheat, which contains up to 80% of transposable elements, heterochromatin is not concentrated at centromeric and pericentromeric regions as observed for Arabidopsis but dispersed all along chromosomes arms (Choulet et al., 2010). Such genome features necessitate loci-specific mechanisms of silencing without affecting euchromatic genes located nearby and suggest that epigenetic marks have evolved accordingly to fit with the structural challenges that represent complex genomes. Meanwhile, comparison of different eukaryotes revealed conserved features of H3 variant distribution between Arabidopsis, Drosophila and mammals, which was not

expected regarding the independent occurrence and evolution of functionally divergent H3 variants in plants and animals. In striking contrast, high conservation of ASF1, CAF-1 and HIR chaperone complexes suggests that mechanisms of histone assembly are sensibly conserved between species. Regarding the astonishing variety and dynamics of chromatin assembly pathways in eukaryotes, histone chaperones may have played a major role in the diversification of H3 variant structure and activity during evolution.

Material and methods

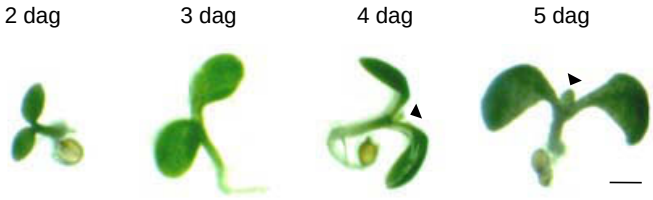

***Figure 47*: Expansion of cotyledons between 2 and 5 dag.**

Representative WT seedlings of the Columbia ecotype aged 2, 3, 4 and 5 dag. Cotyledons are the first aerial tissue to emerge at germination and they expand during early development. Emergence of the first set of leaves (black arrowhead) at 4 dag is a milestone of correct developmental timing. Scale bar: 1 mm.

Plant material

Wild type and mutant Arabidopsis lines used in this study are listed in ***Table 3*** and were obtained from the Nottingham Arabidopsis Stock Center (NASC).

Plant growth conditions

Solid germination medium contains 0.8% w/v agar, 1% w/v sucrose and Murashige & Skoog salts (M0255; Duchefa Biochemie). For *in vitro* culture, seeds were sterilized in 70% ethanol with 0.05% SDS followed by a wash in 95% ethanol, dried and sown on germination medium. Seeds were then stratified for 48h at 4°C in the dark. For *in vitro* culture, plants were grown under long-day conditions (16h light/8h dark cycles, light intensity 150-300 $\mu mol.m^{-2}.s^{-1}$ at 23ºC. For soil culture, seeds were directly sown on soil and stratified for 48h in the cold room. Plants grown in growth chamber under long-day conditions (16h light/8h dark cycles, light intensity 150-300 $\mu mol.m^{-2}.s^{-1}$, 50% humidity at 23°C). Cotyledons were harvested at 50h, 74h, 98h, 122h and 242h after transfer to the growth chamber, corresponding to time points 2, 3, 4 and 5 days after germination (dag) (***Figure 47***). Hygromycin (25 µg/mL, Hygrogold™, Invivogen) and BASTA (150 µg/mL, Bayer) were used for selection of plants containing T-DNA inserts from *Agrobacterium tumefaciens*-mediated transformation.

Crossing of Arabidopsis plants

For most efficient crossings, mother plants with 5-6 inflorescences with large buds and pollen donors that have started to form siliques were selected. Open flowers were removed from the inflorescence and closed flowers with immature pollen were emasculated by removing anthers. The stigmas prepared from the mother plant were covered with pollen grains from an open flower of the pollen donor by tapping the anther. Siliques with mature seeds were harvested after 15-25 days.

Primers

All primers used are listed in ***Table 4***.

Generation of transgenic lines

Plasmids and constructs

Genotyping

Target	Gene ID	Primer	Sequence 5'-3'
		Fas1_fw_MI	ATGGTATCTGGCCCAGCCAAA
FAS1	At1g65470	Fas1_rev_MI	CCTGTTCAGACGGATCAATGTCCA
		LBR Sail	TAGCATCTGAATTTCATAACCAATCTCGATACAC
		FAS2-LP	TTTGCCCTGTTGCATTTAAAC
FAS2	At5g64630	FAS2-RP	GCCCAATAATGATCCACAATG
		LBb1.3	ATTTTGCCGATTTCGGAAC
		Hira_Wisc_LP	CTACTAAAATTTGAGGCCGGG
AtHIRA	At3g44530	Hira_Wisc_RP	GAGAGTCACTGTTTTGGCTGG
		p745_WiscDsLox	AACGTCCGCAATGTGTTATTAAGTTGTC
		At1g77310_GK_LP	TTCGCCAATTAAACATGATGG
NCN1	At1g77310	At1g77310_GK_RP	AGGCATGCCATTGTTAACTTG
		GK_o8409	ATATTGACCATCATACTCATTGC
		At1g21610_GK_LP	TGTGGACCTTGATCTTCATCC
NCN2	At1g21610	At1g21610_GK_RP	AAGCTGATACCTCATCCCAGG
		GK_o8409	ATATTGACCATCATACTCATTGC
		Cabin_SALK099927_LP	TGCCAATAAATGCTTAATCGC
CBN	At4g32820	Cabin_SALK099927_RP	GCTGTAAAAACGGAAGAAGGG
		LBb1.3	ATTTTGCCGATTTCGGAAC
		At1g66740_LP	ATCTTGTTTGGCAACTGTTGG
AtASF1A	At1g66740	At1g66740_RP	ATCTCCTCTTTCTCCTTCCCC
		GK_o8409	ATATTGACCATCATACTCATTGC
		At5g38110 LP	GTGAATCCATTCCAGTTCGAG
AtASF1B	At5g38110	At5g38110 RP	CAAAACCTTGGTAGGAGGCTC
		LBb1.3	ATTTTGCCGATTTCGGAAC
		HTR1_LB	GAGCGATCTCACGAACAAGTC
HTR1	At5g65360	HTR1_RB	AACTTGGGCGCTAAAGAAAAC
		LBb1.3	ATTTTGCCGATTTCGGAAC
		HTR2_LP	TAATCCAACAGTCCAACGTCC
HTR2	At1g09200	HTR2_RT-R	AGCCTCTGGAAAGGGAGTTTACGG
		LBb1.3	ATTTTGCCGATTTCGGAAC
		(HTR2)-SAIL_655_C07-LP	AACAGCAAGCTTGACATCACC
HTR2	At1g09200	(HTR2)-SAIL_655_C07-RP	GAAGCCACACAGATTCAGACC
		LBR Sail	TAGCATCTGAATTTCATAACCAATCTCGATACAC
		HTR3_LP	TCAGGTTAAATTCAACTCTTTTGG
HTR3	At3g27360	HTR3_RP	AAAAGCATCCCAACCTCACTC
		LBb1.3	ATTTTGCCGATTTCGGAAC
		At4g40030-F	TGACTGTTCAATTTCTTGTTAAATGCG
HTR4	At4g40030	At4g40030-R	CTACTTGAACCAAATCTCGGATTCTTG
		LBb1.3	ATTTTGCCGATTTCGGAAC
		HTR5_LP	CCACCCACATTCACATAATCC
HTR5	At4g40040	HTR5_RP	TCGTGAAACTACTGGAATCGC
		LBb1.3	ATTTTGCCGATTTCGGAAC
		At5g10980-F	GCTTATCGAAAAGTCACATCTTTTGGAAG
HTR8	At5g10980	At5g10980-R	ATCATCGTAAAAATCTAAACTTGAATTAGG
		LBb1.3	ATTTTGCCGATTTCGGAAC
		HTR9_LP	AATAACAACCACACTGCAGCC
HTR9	At5g10400	HTR9_RT-R	CGAAAACGAAAAGAGACAGCTT
		LBb1.3	ATTTTGCCGATTTCGGAAC
		(HTR9)-SAIL_305_C12-LP	TAATTTTAGGCGCCAAATCG
HTR9	At5g10400	(HTR9)-SAIL_305_C12-RP	ACATCACTCACTTTCCCATCG
		LBR Sail	TAGCATCTGAATTTCATAACCAATCTCGATACAC
		ATXR5_LP	TTTCTCTTGTCCGGTGAAATG
ATXR5	At5g09790	ATXR5_RP	CCTGCAACAATCAGTGTGATG
		LBb1.3	ATTTTGCCGATTTCGGAAC
		ATXR6_LP	TTGAGATGAATCTGGAGACCG
ATXR6	At5g24330	ATXR6_RP	AAACGACGACGTATTGGAGTG
		LBR Sail	TAGCATCTGAATTTCATAACCAATCTCGATACAC
		KYP_LP	ACTGGTGAACCAGCTGGTATG
SUVH4	At5g13960	KYP_RP	TGAGGGGTACCTGTTCAATTG
		LBb1.3	ATTTTGCCGATTTCGGAAC
		suvh5 GABI-LP	CTCTTTTTATCCAGGGCAACC
SUVH5	At2g35160	suvh5 GABI-RP	TCATGGGTTTTGAAGATCTGC
		GK_o8409	ATATTGACCATCATACTCATTGC
		suv6-2 LP	TGCATATTTTGGGAGAAGTGC
SUVH6	At2g22740	suv6-2 RP	GTCGTTCCCGATTCTTCTTTC
		LBR Sail	TAGCATCTGAATTTCATAACCAATCTCGATACAC
		mom1-2_SAIL610_G01_LP	ACAATGCAGGAGCAAACACTC
MOM1	At1g08060	mom1-2_SAIL610_G01_RP	GGAAAGGAGATACTTCACCGG
		LBR Sail	TAGCATCTGAATTTCATAACCAATCTCGATACAC
		TsGUSF1	TGGATTTTGGCTCGAGATTC
GUS	Chr 3	TsGUSR1	CAATCATGGCAGATCGAGAA
		qPCR-GUS-F	TTAACTATGCCGGAATCCATCGC
		GUS_R_short	CCCGGCTAACGTATCCACGCCGTA

***Table 4*: Primers used in this work (1).**

All plasmids used are listed in ***Table 5*** and corresponding maps are presented in appendices.

Plasmid construction for production of epitope-tagged histones

To generate transcriptional fusion of H3.1 and H3.3 with FLAG-HA tags first the octopine synthase gene OCS terminator sequence was amplified by PCR from pBIN-Hyg-TX plasmid (Gatz et al., 1992) using primers containing BamHI and SalI restriction sites and directionally inserted into the pBluescript SK-derived vector pTP1 that contains the *att*L1 and *att*L2 Gateway recombination sites (kind gift from T. Pélissier) by BamHI/SalI restriction-ligation. A fragment containing the sequence encoding the FLAG-HA epitope was amplified by PCR from the pOZ-FH-C plasmid (Tagami et al., 2004) with primers containing NotI and BamHI restriction sites for directional cloning with the OCS terminator into the pTP1 plasmid by NotI/BamHI restriction-ligation. A genomic fragment containing the promoter and the coding region of *HTR5* and *HTR9* (stop codon excluded) was amplified by PCR using Phusion High-Fidelity DNA Polymerase (Thermo Scientific) with primers containing NotI restriction sites using genomic DNA as template. PCR products containing the promoter and the coding region of *HTR5* or *HTR9* were subsequently cloned in frame with the FLAG-HA tag into pTP1 by NotI restriction-ligation to obtain an entry clone. Directionality of the insert was confirmed either by EcoRV restriction (*HTR5*) or EcoR1/Not1 restriction (*HTR9*) followed by sequencing using the M13 forward primer. After a LR recombination reaction using Gateway technology (Invitrogen) with destination plasmid pTP9, derived from pBIN-Hyg-TX in which the 35S-polylinker-OCS cassette has been replaced by a cassette containing *att*R1-*att*R2 Gateway recombination sites (kind gift from T. Pélissier), an expression clone of either *HTR5* or *HTR9* fused to a FLAG-HA tag was obtained (p*HTR5*::*HTR5*:FLAG-HA and p*HTR9*::*HTR9*:FLAG-HA). Following the same method, full-length cDNA excluding the stop codon of *HTR4*, *HTR9* and *HTR14* were amplified from cDNA by PCR using Phusion High-Fidelity DNA Polymerase (Thermo Scientific) and specific primers containing NotI restriction sites from cDNA. After cloning the cDNA amplicon into the pTP1 plasmid by NotI restriction-ligation in frame with the FLAG-HA/OCS to obtain an entry clone, a LR recombination reaction was performed with destination plasmids (either pUB (Grefen et al., 2010) for *HTR4* and *HTR9* or pMDC32 (Curtis and Grossniklaus, 2003) for *HTR14*) to generate the expression clones

Semi-quantitative RT-PCR

Target	Gene ID	Localization	Primer	Sequence 5'-3'
FAS1	At1g65470	Span T-DNA site	Fas1_fw_M	ATGGTATCTGGCCCAGCCAAA
			Fas1_rev_MI	CCTGTTCAGACGGATCAATGTCCA
FAS2	At5g64630	3'	Fas2 RT F	CGGTCTCAAATAAACCAGCAA
			FAS2-RP	GCCCAATAATGATCCACAATG
AtHIRA	At3g44530	Span T-DNA site	HIRA rt f	GAGAGTCACTGTTTTGGCTGG
			HIRA rt r	CTACTAAAATTTGAGGCCGGG
		3'	HIRA-RT-For	TCTTGGGATCCTTATGTTCT
			HIRA-RT-Rev	AACCCAAACCGGGTCACTA
NCN1	At1g77310	Span T-DNA site	310_TDNAspan_F	CCAGCAGCAACCAAAGAAAAGGCG
			310_TDNAspan_R	TTCGAAGAGGGCCCAGGAGAAGC
		3'	Atnuclein1_For	TGGAAGGAAACATTGGGAAG
			Atnuclein1_Rev	ACTAAGGACGTGGTGGTTGC
NCN2	At1g21610	Span T-DNA site	610_TDNAspan_F	TGGGAGATTCTGCAACCCGAGA
			610_TDNAspan_R	CCTCCAATGCCGCATCCATGACA
		3'	Atnuclein2_For	TATCGTGGGATCAAACATGC
			Atnuclein2_Rev	TAGTGACCACGGAAGTGCTG
CBN	At4g32820	Span T-DNA site	cab-amontExon8-F	TGGGATCACTTGGTGGCGGA
			cab-avalExon8-R	AGCTCCTTCCTCCCCCGCAC
		3'	AtCabin_For	CGGTGACACTCCCTTCTGAT
			AtCabin_Rev	AACCGAAGGAACCACTGATG
AtASF1A	At1g66740	Span T-DNA site	Asf1a_RT-F	TCCTGCTCCTTTTGTTAGCC
			Asf1a_RT-R	GCCAACATTAACAGGCCCTA
		3'	At1g66740 RT-For	GTTGGCAACTACCGCTTTGT
			At1g66740 RT-Rev	AAAAGCAAAGCGCAACATCT
AtASF1B	At5g38110	Span T-DNA site	Asf1b_RT-F	GACAATCCTGCTCCGTTTGT
			Asf1b_RT-R	CCCAACGTTAACAGGACCAA
		3'	At5g38110 RT-For	AACGTTGGGAACTATCGATTTG
			At5g38110 RT-Rev	GGCTGATCAAGCAACGCTAT
HTR1	At5g65360	Span T-DNA site	HTR1 _RT-F	CGTCCTGGAACTGTTGCCCTAAG
			HTR1_RT-R	TTAGCATGAATCGCGCAAAGATTG
HTR2	At1g09200	5'	HTR2_RT-F	CAAGCAGACGGCTAGGAAATCAACC
			HTR2_RT-R	AGCCTCTGGAAAGGGAGTTTACGG
HTR3	At3g27360	3'	HTR3_RT-F	AAGGATATTCAACTTGCGAGGA
			HTR3_RT-R	ATTTTCATTTGGGCATTTCATC
HTR4	At4g40030	3'	At4G40030 RT-F	ATT CAG CTC GCT CGT CGT AT
			At4G40030 RT-R	AAA AAG AGT TCG CAA CAC ACA
HTR5	At4g40040	3'	At4g40040 RT-F	AATGCCCAAAGACATTCAGC
			At4g40040 RT-R	CATTGCCAAAGAAGAAAGCA
HTR6	At1g13370	3'	At1g13370 RT-F	TGTGCCATTCATGCAAAGAG
			At1g13370 RT-R	CGACAAAGCAAAAACAATCG
HTR8	At5g10980	Span T-DNA sites	At5g10980-F	GCTTATCGAAAAGTCACATCTTTTGGAAG
			At5g10980-R	ATCATCGTAAAAATCTAAACTTGAATTAGG
HTR9	At5g10400	3'	HTR9_RT-F	TAATCTCTGTGCGATTCATGCT
			HTR9_RT-R	CGAAAACGAAAAGAGACAGCTT
HTR14	At1g75600	Span T-DNA sites	At1g75600 RT -F	CTTGTTCGTGAAATCGCTCA
			At1g75600 RT -R	CACGAATCCTTCTTGCCAAT
AtSAND	At2g28390	-	SAND-F	AACTCTATGCAGCATTTGATCCACT
			SAND-R	TGATTGCATATCTTTATCGCCATC
ACTIN2	At1g74960	-	Act2d (Act2-7 F)	CTAAGCTCTCAAGATCAAAGGC
			Act2d (Act2-7 R)	AACATTGCAAAGAGTTTCAAGG
UBC28	At1g64230	-	UBC28qF	TCCAGAAGGATCCTCCAACTTCCTGCAGT
			UBC28qR	ATGGTTACGAGAAAGACACCGCCTGAATA
UEV1C	At2g36060	-	At2G36060_F	GGGCTTCTCCATTGTTGGTC
			At2G36060_R	TGAAGTCGTGAGACAGCGTTG
ATXR5	At5g09790	-	ATXR5_P2_RT_F	CCATTGGAACTTGGCTTTGTGTC
			ATXR5_P2_RT_R	AATAGGACCATCTGCTTCAACTGTG
ATXR6	At5g24330	-	ATXR6_P1_RT_F	CATCAGATCCCTAAATCTTTCCCTC
			ATXR6_P1_RT_R	TTCACCGAGGTCCATCATTTTCTTGCA
180 bp	180 bp	-	180(all)-F	ACCATCAAAGCCTTGAGAAGCA
			180(all)-R	CCGTATGAGTCTTTGTCTTTGTATCTTCT
TSI	TSI	-	TSIq-F	CTCTACCCTTTGCATTCATGAATCCTT
			TSIq-R	GATGGGCAAAAGCCCTCGGTTTTAAAATG
106B	106B	-	106Bq-F	TCATTATGCTAGGTGGTTGA
			106Bq-R	GACAACAAGTTCATTAACCA
GUS	Chr 3	-	qPCR GUS-F	TTAACTATGCCGGAATCCATC
			qPCR GUS-R	CACCACCTGCCAGTCAACAGACGC

***Table 4*: Primers used in this work (2).**

p*UBQ10*::*HTR4*:FLAG-HA, p*UBQ10*::*HTR9*:FLAG-HA and p35S::*HTR14*:FLAG-HA. selection of bacterial transformants was based upon Kanamycin (50 µg/mL) (pTP9) or Ampicillin (50 µg/mL)) (pTP1) resistance encoded by the plasmids.

Plasmid construction for production of artificial miRNA

The artificial microRNA sequence was chosen using the artificial miRNA designer WMD (http://wmd3.weigelworld.org) (Schwab et al., 2006; Ossowski et al., 2008): 4 sequence-specific oligonucleotides were used to engineer the artificial miRNA targeting the gene of interest into the endogenous miR319a precursor. The plasmid pRS300, which contains the miR319a precursor in the pBSK plasmid cloned *via* a SmaI site was used as a template to generate the artificial miRNA containing precursor by overlapping PCR using primers containing sequences specific for the gene to be targeted (Ossowski et al., 2008). The amiRNA-containing precursor was then recombined through the BP reaction (Invitrogen) with pDONR221 (Invitrogen). After a LR recombination reaction (Invitrogen) with pMDC32 (Curtis and Grossniklaus, 2003), an expression clone with the amiRNA-containing precursor under control of the 35S promoter was obtained. DH5α or One Shot® TOP10 Competent *Escherichia coli* were used for cloning. selection of transformants was based upon Kanamycin resistance encoded by the plasmids.

Site-directed mutagenesis

Entry clones containing full-length *HTR9* in frame with the FLAG-HA tag were used to perform site-directed mutagenesis to convert lysine residues in position 9 and 27 to argenine residues according to the manufacturer's instructions with the QuikChange® Lightning Site-Directed Mutagenesis Kit (Agilent). After sequencing, the mutated plasmids were subsequently recombined with the appropriate destination plasmid to generate expression clones as described before.

Ligation and bacterial transformation

Ligation of the PCR product to the appropriate vector was done using T4 DNA Ligase (Invitrogen) following the manufacturer's protocol. DH5α or One Shot® TOP10 Competent Escherichia coli (Invitrogen) were transformed with plasmid DNA or ligated plasmid products using the heat shock transformation protocol. After thawing

qRT-PCR

Target	Gene ID	Primer	Sequence 5'-3'
FAS1	At1g65470	Fas1_fw_M	ATGGTATCTGGCCCAGCCAAA
		Fas1_rev_MI	CCTGTTCAGACGGATCAATGTCCA
FAS2	At5g64630	FAS2_qpcr_Forter	AAACCGGTTGTAGTGGTTCG
		FAS2_qpcr_Revter	TGCAGCATAGTGGAGACCTG
AtHIRA	At3g44530	HIRA qRT F2	AACAAGACCAGAACTCAAGA
		HIRA qRT R2	CTTTAACAACGCCTAACTGAG
NCN1	At1g77310	At1g77310_nuclein1_qpcr_Forter	ATCCTGCAGCAGAAGGAAAG
		At1g77310_nuclein1_qpcr_Revter	TCTTGGCCTTTGGATGTACC
NCN2	At1g21610	At1g21610_nuclein2_qpcr_Forbis	GCAAAGGAGAGACGAAAAGC
		At1g21610_nuclein2_qpcr_Revbis	TAGTGACCACGGAAGTGCTG
CBN	At4g32820	At1g77310_cabin_qpcr_For	CGAACCTGCTCCTAAGGTTG
		At1g77310_cabin_qpcr_Rev	CCTCTCTGCAGAAATTCACC
AtASF1A	At1g66740	At1g66740 RT-For	GTTGGCAACTACCGCTTTGT
		At1g66740 RT-Rev	AAAAGCAAAGCGCAACATCT
AtASF1B	At5g38110	Asf1b_RT-F	GACAATCCTGCTCCGTTTGT
		Asf1b_RT-R	CCCAACGTTAACAGGACCAA
HTR1	At5g65360	At5g65360_HTR1_qpcr_Forbis	AGCGATCTCACGAACCAAAC
		At5g65360_HTR1_qpcr_Revbis	GAAATCCACCGGAGGAAAAG
HTR5	At4g40040	At4g40040 RT-F	AATGCCCAAAGACATTCAGC
		At4g40040 RT-R	CATTGCCAAAGAAGAAAGCA
HTR8	At5g10980	At5g10980_HTR8_qpcr_Forbis	AAGAGCTAACACCGCGTGAC
		At5g10980_HTR8_qpcr_Revbis	AGGAAATCAGCACCAACCAC
HTR9	At5g10400	HTR9_RT-F	TAATCTCTGTGCGATTCATGCT
		HTR9_RT-R	CGAAAACGAAAAGAGACAGCTT
AtSAND	At2g28390	SAND-F	AACTCTATGCAGCATTTGATCCACT
		SAND-R	TGATTGCATATCTTTATCGCCATC
AAE15	At1g74960	Acyl-ACP Synthetase qRT F1	TGGACATCAGAATGTTCGTT
		Acyl-ACP Synthetase qRT R1	TTTGTATTTAGCCACGACCA
180 bp	180 bp	180(all)-F	ACCATCAAAGCCTTGAGAAGCA
		180(all)-R	CCGTATGAGTCTTTGTCTTTGTATCTTCT
TSI	TSI	TSIq-F	CTCTACCCTTTGCATTCATGAATCCTT
		TSIq-R	GATGGGCAAAAGCCCTCGGTTTTAAAATG
106B	106B	106Bq-F	TCATTATGCTAGGTGGTTGA
		106Bq-R	GACAACAAGTTCATTAACCA
GUS	Chr 3	qPCR GUS-F	TTAACTATGCCGGAATCCATC
		qPCR GUS-R	CACCACCTGCCAGTCAACAGACGC

ChIP-qPCR

Target	Gene ID	Primer	Sequence 5'-3'
ACTIN2	At3g18780	actin_f	GGTAACATTGTGCTCAGTGGTGG
		actin_r	AACGACCTTAATCTTCATGCTGC
HXK1	At4g29130	At4g29130_ChIP-F	AGGAGCTCGTCTCTCTGCTG
		At4g29130_ChIP-R	GCTCAAACAATCCACCATCC
UEV1C	At2g36060	At2g36060_ChIP-F	GGTGACTGAAATGTGAATTTGC
		At2g36060_ChIP-R	ATGCAGCCATCTCCTTCTTC
UBC28	At1g64230	At1g64230-ChIP-F	TCATTGTTAACGGACCCAAAC
		At1g64230-ChIP-R	CCAGCTTCTCGCAGTAGACTC
TUB8	At1g74960	TUB8-F	ATAACCGTTTCAAATTCTCTCTCTC
		TUB8-R	TGCAAATCGTTCTCTCCTTG
180 bp	180 bp	180(all)-F	ACCATCAAAGCCTTGAGAAGCA
		180(all)-R	CCGTATGAGTCTTTGTCTTTGTATCTTCT
TSI	TSI	TSIq-F	CTCTACCCTTTGCATTCATGAATCCTT
		TSIq-R	GATGGGCAAAAGCCCTCGGTTTTAAAATG
106B	106B	106Bq-F	TCATTATGCTAGGTGGTTGA
		106Bq-R	GACAACAAGTTCATTAACCA
Ta3	Pericentric region of chromosome 1	QPCR-Ta3-F	AAGAGAGCTGGCAGAAGCAGTTGA
		QPCR-Ta3-F	ACGCCCTTTACCTTGACCTCCTTT
IG	Between At2g17670 and At2g17680	IG-2g17670-80qF	GGCTACTGTCTAGTTCATATCTTAGA
		IG-2g17670-80qR	TAGGTTGGCATCCGATCCAGAGT

***Table 4*: Primers used in this work (3).**

competent cells on ice and incubation with plasmid DNA for 15 min on ice, cells were heat-shocked at 42°C for 90 sec, then transferred to ice for 2 min. 800 µL of LB medium was added to the cells prior to 1 h incubation at 37°C followed by plating on appropriate selection medium. Competent Agrobacterium tumefaciens C58C1 were transformed using the E. coli pulser (BioRad) at a voltage of 1,8 kV according to the manufacturer's recommendations.

Agrobacterium tumefaciens-mediated plant transformation

Agrobacterium tumefaciens strain C58C1 cultures were prepared by inoculation of 15 mL LB medium supplemented with Rifampicin (10 µg/mL), Gentamycin (25 µg/mL) and Kanamycin (50 µg/mL) for prior selection of the bacteria containing the plasmids. After 48 h at 28°C, the culture (0.6 OD_{600nm}) were inoculated into 500 mL LB media containing Kanamycin (50 µg/mL) and grown to an OD_{600nm} of 1.8/2.0. The bacteria were pelleted by centrifugation (20 min, 400 rpm) prior to resuspension in 500 mL infiltration medium (5% sucrose, 100 mM $MgCl_2$ and 0,05% Silwet L-77). Three-week-old appropriate *Arabidopsis thaliana* plants were transformed according to the germline transformation protocol using the floral dip method (Clough and Bent, 1998): plants with early flowering stage inflorescences were dipped into the bacterial suspension for 30 sec. After infiltration, plants were kept within hermetic plastic bags for 24h in the greenhouse and then grown to produce seeds. To select transformants, T1 progeny were selected either on plates supplemented with Hygromycin (25 µg/mL) or grown on soil and selected by BASTA treatments (150 µg/mL, Bayer). T2 monolocus lines and T3 homozygous monolocus lines were selected based on segregation of the resistant character.

DNA extraction and genotyping of Arabidopsis mutants

Arabidopsis thaliana tissues were harvested, ground with stainless steel beads (Qiagen) in 300 µL Extraction Buffer (200 mM Tris-HCl pH 7.5, 250 mM NaCl, 0.5% SDS, 25 mM EDTA pH 8.0) using a Tissue Lyser (Qiagen) and incubated 15 min at 65°C prior to centrifugation (5 min, 13000 rpm). An equal volume of isopropanol was added to the supernatant and the DNA precipitated by centrifugation (5 min, 13000 rpm). The DNA pellet was washed in 70% ethanol, dried and resuspended in 50 µL water. Two microliters were used in a standard PCR reaction with 25 µL final volume

Cloning

Target	Gene ID	Type	Primer	Sequence 5'-3'
HTR4	At4g40030	cDNA	NotI_HTR4cDNA_for	ATATATGCGGCCGCCCCTATTACTGCTTTTGTTACG
			HTR4_NotI rev	tttaaaGCGGCCGCAGCGCGTTCACCTCTGATACG
HTR5	At4g40040	Genomic	NotI_HTR5_for	atatatGCGGCCGCCATCCTTGTCGCTGCTC
			HTR5_g_MI_rev	tttaaaGCGGCCGCAGCACGTTCTCCTCTGATCCTG
HTR9	At5g10400	cDNA	NotI_HTR9 for	ATATATgcggccgCGATCGCATTCTCACCGAAT
			HTR9_NotI_rev	AAATTTgcggccgcAGCCCTCTCTCCTCTGATTCTC
HTR9	At5g10400	Genomic	NotI_HTR9genomic_ for	ATATATGCGGCCGCTAGACGTCTGCAACGC
			HTR9_NotI_rev	AAATTTgcggccgcAGCCCTCTCTCCTCTGATTCTC
HTR14	At1g75600	cDNA	HTR14_cDNA_F	TTTAAAgcggccgCTCTCAAGTTCTTGACGAAGCAA
			HTR14_cDNA_R	ATATATGCGGCCGAGCACGCTCTCCACGAATCC
FLAG-HA	FLAG-HA	Plasmid	TAG_NotI_F	ATATATGCGGCCGCTGGAGGAGAC
			TAG_BamHI-R	ATATAGGATCCCTAGGCGTAGTCGGGCACGTC
OCS Terminator	OCS Terminator	Plasmid	terOCSSalI	TAGAGTCGACCTGCAGGC
			terOCSSalI	GCCGGATCCTGGACAATCAG

Artificial miRNA synthesis

Target	Gene ID	Primer	Sequence 5'-3'
Plasmid	pRS300	Oligo A	CTGCAAGGCGATTAAGTTGGGTAAC
		Oligo B	GCGGATAACAATTTCACACAGGAAACAG
AtHIRA	At3g44530	HIRA I miR-s	gaTTAGTGTAAACCTGGACGCTTtctctcttttgtattcc
		HIRA II miR-a	gaAAGCGTCCAGGTTTACACTAAtcaaagagaatcaatga
		HIRA III miR*s	gaAAACGTCCAGGTTAACACTATtcacaggtcgtgatatg
		HIRA IV miR*a	gaATAGTGTTAACCTGGACGTTTtctacatatatattcct
AtASF1A	At1g66740	SGA2 I miR-s	gaTAAAACCTTAGTTGGACGCTCtctctcttttgtattcc
		SGA2 II miR-a	gaGAGCGTCCAACTAAGGTTTTAtcaaagagaatcaatga
		SGA2 III miR*s	gaGAACGTCCAACTATGGTTTTTtcacaggtcgtgatatg
		SGA2 IV miR*a	gaAAAAACCATAGTTGGACGTTCtctacatatatattcct
AtASF1B / AtASF1B	At1g66740 / At5g38110	SGA1+2 I miR-s	gaTTCGTAAGAAATCGCGAACTTtctctcttttgtattcc
		SGA1+2 II miR-a	gaAAGTTCGCGATTTCTTACGAAtcaaagagaatcaatga
		SGA1+2 III miR*s	gaAAATTCGCGATTTGTTACGATtcacaggtcgtgatatg
		SGA1+2 IV miR*a	gaATCGTAACAAATCGCGAATTTtctacatatatattcct
HTR5	At4g40040	HTR5_1_miR-s	gaTATCTATTTAGAAAACCGCCCtctctcttttgtattcc
		HTR5_1_miR-a	gaGGGCGGTTTTCTAAATAGATAtcaaagagaatcaatga
		HTR5_1_miR*s	gaGGACGGTTTTCTATATAGATTtcacaggtcgtgatatg
		HTR5_1_miR*a	gaAATCTATATAGAAAACCGTCCtctacatatatattcct
	At4g40040	HTR5_6_miR-s	gaTTCCAGTAGACTTACGCGCTGtctctcttttgtattcc
		HTR5_6_miR-a	gaCAGCGCGTAAGTCTACTGGAAtcaaagagaatcaatga
		HTR5_6_miR*s	gaCAACGCGTAAGTCAACTGGATtcacaggtcgtgatatg
		HTR5_6_miR*a	gaATCCAGTTGACTTACGCGTTGtctacatatatattcct

Mutagenesis

Target	Gene ID	Type	Substitution	Primer	Sequence 5'-3'
HTR9	At5g10400	cDNA	K9 to R9	HTR9K9R_F	ccaagcaaacagctcgtagatccaccggaggaaag
				HTR9K9R_R	ctttcctccggtggatctacgagctgtttgcttgg
			K9 to R27	HTR9K27R_F	ccaaagctgcgaggagatcagctccagccac
				HTR9K27R_R	gtggctggagctgatctcctcgcagctttgg

***Table 4*: Primers used in this work (4).**

(***Table 6***). Homozygous *Arabidopsis thaliana* mutant plants used in this study were identified with the primers listed in ***Table 4***.

DNA extraction for cloning

Genomic DNA for cloning was prepared from 100 mg of *Arabidopsis thaliana* tissues frozen in liquid nitrogen and ground to fine powder with stainless steel beads (Qiagen) using a Tissue Lyser (Qiagen). After adding 1.5 mL of Cetyltrimethyl Ammonium Bromide (CTAB) 2X buffer (100 mM Tris HCl pH 8.0, 1.4 M NaCl, 20 mM EDTA, 2% (w/v) cetyltrimethyl ammonium bromide, 2% (w/v) polyvinylpyrrolidone, (PVP), 2% (v/v) 2-mercaptoethanol), samples were homogenized with a vortex. After incubation for 3 h at 65°C, 500 µL from each sample were transferred to new tubes and complemented with 1 volume of phenol-chloroform-isoamylic alcohol (25:24:1) prior to homogenisation on a rotating wheel for 10 min. After centrifugation (10 min, 5000 g), the aqueous phase was transferred to a new tube and the DNA precipitated with 0.7 volume of isopropanol for 1h at -20°C prior to centrifugation (30 min, 6000 g). The DNA pellet was washed once with 70% ethanol, air-dried, then resuspended in 100 µL of 10 µg/mL RNase A in water (Sigma-Aldrich) and incubated 1h at 37°C. DNA concentration was evaluated by spectophotometry.

RNA isolation

RNA was extracted using Tri-Reagent (Euromedex) following manufacturer's instructions. In brief, *Arabidopsis thaliana* tissues, frozen in liquid nitrogen, were ground to fine powder with stainless steel beads (Qiagen) using a a Tissue Lyser (Qiagen). After adding 1 mL of Tri-Reagent, samples were homogenized with a vortex and incubated for 5 min. Chloroform (200 µL) was added to each sample prior to homogenisation with a vortex for 15 sec. After centrifugation (5 min, 12000 rpm, 4°C), the aqueous phase was transferred to a new tube and the RNA precipitated with 500 µL isopropanol for 10 min at RT prior to centrifugation (10 min, 12000 rpm, 4°C). The RNA pellet was washed once with 70% ethanol, air-dried, and then resuspended in 50 µL Rnase Free H_20 (Sigma-Aldrich).

Name	Aim	Reference
pBIN-Hyg-TX	Amplification of OCS Terminator	Gatz et al., 1992
pTP1	Subcloning of histone genes	-
pOZ-FH-C	Amplification of FLAG-HA tag	Tagami et al., 2004
pTP9	*HTR5*- and *HTR9*-FLAG-HA (genomic) native expression	-
pUB	p*UBQ10* for *HTR5*- and *HTR9*-FLAG-HA (cDNA) ectopic expression	Grefen et al., 2010
pMDC32	p35S for amiRNA and *HTR14*-FLAG-HA (cDNA) ectopic expression	Curtis and Grossniklaus, 2003
pRS300	Artificial miRNA synthesis	Ossowski et al., 2008
pDONR221	Subcloning of artificial miRNA	Magnani et al., 2006

Name	Type	Aim
p*HTR9*:*HTR9*:FLAG-HA	Genomic	Monitoring of native H3.1 dynamics
p*HTR5*:*HTR5*:FLAG-HA	Genomic	Monitoring of native H3.3 dynamics
p*UBQ10*:*HTR9*:FLAG-HA	cDNA	Monitoring of ectopic H3.1 dynamics
p*UBQ10*:*HTR5*:FLAG-HA	cDNA	Monitoring of ectopic H3.1 dynamics
p35S:*HTR14*:FLAG-HA	cDNA	Monitoring of ectopic H3.14 dynamics
p*UBQ10*:*HTR9*_K9R:FLAG-HA	cDNA	Monitoring of H3.1 dynamics with mutated K9
p*UBQ10*:*HTR9*_K27R:FLAG-HA	cDNA	Monitoring of H3.1 dynamics with mutated K27
p*UBQ10*:*HTR9*_K9RK27R:FLAG-HA	cDNA	Monitoring of H3.1 dynamics with mutated K9 and K27
p*UBQ10*:*HTR9*_S87HA90L:FLAG-HA	cDNA	Monitoring of H3.1 dynamics displaying H3.3 signature at residues 87 and 90

***Table 5*: Plasmids used for cloning (top) and expression of e-H3 (bottom).**

Reverse-Transcription (RT-PCR)

RNA (50 µg) was treated with 4 µL of RQ1 RNase-Free DNase (Promega) for 30 min at 37°C in 1X RQ1 buffer in a total volume of 60 µL. After addition of 140 µL Rnase Free H_20 (Sigma-Aldrich), 200 µL of phenol-chloroform-isoamylic alcohol (25:24:1) were added to the DNAse-treated RNA and centrifuged (10 min, 13200 rpm, 4°C). In new tubes, the supernatant was added to 200 µL chloroform-isoamylic alcohol (24:1) and centrifuged (5 min, 13200 rpm, 4°C). The RNA containing supernatant was precipitated with 1/10 volume NaAc and 2.5 volumes of ethanol overnight at -20°C. Samples were centrifuged (30 min, 13200 rpm, 4°C) and the pellet washed in 70% ethanol. The RNA pellet was resuspended in 50 µL of Rnase Free H_2O (Sigma-Aldrich). RNA concentration and purity were checked with a Nanodrop (Thermo Scientific). One microgram RNA was divided into 2 PCR tubes and incubated either with or without 200 U of M-MLV reverse transcriptase (Promega) (respectively for RT+ and RT- reactions) in 1X M-MLV buffer with 400 µM dNTPS and 0,5 µg of either Oligo(dT) or Random Hexamers (Promega) and 25 U of Recombinant RNasin® Ribonuclease Inhibitor in a final volume of 25 µL for reverse transcription during 1 h. For Random Hexamers reverse transcription was performed at 37°C, and at 42°C for Oligo(dT). The resulting cDNAs were used in semi-quantitative PCR (Promega Flexi) (***Table 7***) and analyzed using the Quantity One software (Bio-Rad Laboratories) after acquisition with a Versadoc imager (Bio-Rad Laboratories), or in quantitative PCR with the LightCycler® 480 SYBR Green I Master kit on the Roche LightCycler® 480 (***Table 8***). Transcript levels were normalized to (Czechowski et al., 2005) using the comparative threshold cycle method.

Fluorescent In Situ Hybridization (FISH)

The Fluorescent *In Situ* Hybridization (FISH) method was adapted from (Fransz et al., 2001). Cotyledons from 2-day- to 10-day-old plantlets were dissected and fixed in ice-cold 3:1 ethanol-acetic acid and stored at 4°C until use. After two washes in water and 1X citrate buffer (10 mM $C_6H_8O_7$ and 10 mM $Na_3C_6H_5O_7$ pH 4.8), tissues were digested by a cellulase and pectolyase enzyme mix (0.3% w/v each) in 1X citrate buffer. The digested tissue was transferred onto a clean microscope slide and the tissue tapped to form a fine milky suspension. After addition of 10 µL of 50% acetic acid, the suspension was spread on a slide and incubated for 1 min on a heating

Genotyping PCR Mix	Volume (µL)	Final Concentration
Green GoTaq® Reaction Buffer	5	1X
$MgCl_2$	2	2mM
dNTPs	0.8	0.2 mM
Forward Primer	1	0,4 µM
Reverse Primer	1	0,4 µM
GoTaq® DNA Polymerase	0.06	0,012 U/µL
gDNA Template	2	2
H_20 PCR Grade	13.94 µL	Up to 25 µL

	Temperature (°C)	Time	Cycles
Activation	95	5 min	1
PCR	95	1 min	30
	Tm primers	1 min	
	72	1 min	
	72	5 min	1

***Table 6*: PCR mix and program used for genotyping.**

block at 45°C. After a second addition of 10 µL of 50% acetic acid and subsequent 1 min spreading of the suspension, the spread nuclei were fixed in 3:1 ethanol-acetic acid. After 5 min of post-fixation in 2% formaldehyde (Sigma-Aldrich) in 1X PBS (11.9 mM phosphate buffer, 137 mM NaCl, 2.7 mM KCl, pH 7.4, Fisher), the slides were air-dried followed by a RNase A treatment (100 µg/mL in 2X SSC (30 mM $Na_3C_6H_5O_7$ pH 7.0, 300 mM NaCl, Fisher) at 37°C for 1 h. After 3 washes in 2X SSC, the slides were post-fixed in 1% formaldehyde (Sigma-Aldrich) in 1X PBS, washed once again in 2X SSC followed by dehydration using an ethanol series (70%, 90% and 100%, 1 min each). The slides were then air-dried.

Biotin labelled probes complementary to the 180 bp repeats region were generated by PCR from the pSK180bp plasmid (Douet et al., 2008), containing a cloned tandem repeat in pBluescript, using T3 and T7 standard primers and 0.1 mM dATP, 0.1 mM dCTP, 0.1 mM dGTP, 0.065 mM dTTP and 0.035 mM Biotin-dUTP (Roche). TSI probes were produced by PCR from plasmids containing either a 1.5 kb fragment of TSI A2 or A15 (Steimer et al., 2000), using a Nick translation kit (Roche) with Digoxygenin-11-dUTP (Roche). Probes were precipitated with 1/10 volume NaAc and 2.5 volumes of ethanol overnight at -20°C. Samples were centrifuged (30 min, 13200 rpm, 4°C) and the pellet washed in 70% ethanol. The probe pellet was resuspended in 50% deionized formamide (product code 10011430838, Sigma-Aldrich), 2X SSC and 50 mM sodium phosphate pH 7.0.

For hybridization, 1 µL of the 180 bp probe and 2.5 µL of the TSI probe were used per slide in a total volume of 20 µL hybridization mix (50% deionized formamide, 2X SSC, 50 mM sodium phosphate pH 7.0, 10% dextran sulfate (Sigma-Aldrich). Both probe and nuclear DNA were denatured for 2 min at 80°C prior to overnight incubation in a wet chamber at 37°C. Slides were then washed at 42°C for 5 min in 2X SSC, 5 min in 0,1X SSC, 3 min in 2X SSC and at RT for 5 min in 2X SSC/0.1% Tween 20.

The Biotin labelled probe was detected with Texas Red-conjugated Avidin (5 µg/mL, Vector Laboratories) followed by a biotinylated goat anti-Avidin antibody (5 µg/mL, Vector Laboratories) and once again Texas Red-conjugated Avidin. The Digoxygenin probe was detected with a mouse anti-Digoxygenin antibody (0.2 µg/mL, Roche), followed by a fluorescein isothiocyanate (FITC)-conjugated rabbit anti-mouse antibody (5 µg/mL, Sigma-Aldrich) and finally a goat anti-rabbit antibody coupled to

RT-PCR Mix	Volume (µL)	Final Concentration
Green GoTaq® Reaction Buffer	5	1X
$MgCl_2$	2	2mM
dNTPs	0.8	0.2 mM
Forward Primer	1	0,4 µM
Reverse Primer	1	0,4 µM
GoTaq® DNA Polymerase	0.06	0,012 U/µL
cDNA Template	2	2
H_20 PCR Grade	Up to 25 µL	Up to 25 µL

	Temperature (°C)	Time (min)	Cycles
Activation	95	5 min	1
PCR	95	30 sec	22-35
	Tm primers	30 sec	
	72	30 sec	
	72	3 min	1

***Table 7*: Mix and program used for RT-PCR.**

Alexa 488 (10 µg/mL, Invitrogen). The antibody incubations were performed for 30 min at 37°C in a wet chamber and followed by 3 washes of 5 min in 4T buffer (4X SSC, 0.05% (v/v) Tween 20) or TNT buffer (100mM Tris-HCL pH 7.5, 150mM NaCl, 0.05% (v/v) Tween 20), with subsequent dehydration using ethanol series (70%, 90% and 100%, 1 min each). The slides were then air-dried and DNA was counterstained with DAPI (2 µg/mL) in Vectashield Mounting Medium (Vector Laboratories). More than 200 nuclei were scored in double-blind per condition using an epifluorescence Imager Z1 microscope (Zeiss) with an Axiocam MRm camera (Zeiss) was used. Fluorescence images for each fluorochrome were captured separately through the appropriate excitation and emission filters. The images were pseudocolored, merged and processed with Adobe Photoshop (Adobe Systems).

Chromatin Immunoprecipitation (ChIP)

Chromatin of *Arabidopsis thaliana* was prepared as previously described (Mathieu et al, 2005). In brief, 1.5 g of leaf tissue from 3-week-old plants grown in soil, or cotyledons from *in vitro* grown plantlets at 2 and 5 dag were vacuum-infiltrated with 1% formaldehyde for 10 min. The reaction was stopped by the addition of glycine to a final concentration of 125 mM followed by vacuum infiltration for 5 additional minutes. The tissues were rinsed in cold water, dried briefly, ground to fine powder in liquid nitrogen with ceramic beads or with pestle and mortar and resuspended in ice-cold Extraction Buffer 1 (0.4 M sucrose, 10 mM Tris-HCl pH 8.0, 10 mM $MgCl_2$, 5 mM β-mercaptoethanol, 0.1 mM PMSF and protease inhibitors (Complete Mini, Roche) prior to filtration and centrifugation (10 min, 4000 rpm, 4°C). The pellet was resuspended in Extraction Buffer 2 (0.25 M sucrose, 10 mM Tris-HCl pH 8.0, 10 mM $MgCl_2$, 1% Triton X-100, 5 mM β-mercaptoethanol, 0.1 mM PMSF and protease inhibitors) and transferred to a fresh 1.5 mL tube. After centrifugation (10 min, 16000 g, 4°C), the nuclear pellet was dissolved in Extraction Buffer 3 and layered on top of an equal volume of Extraction Buffer 3 (1.7 M sucrose, 10 mM Tris-HCl pH 8.0, 2 mM $MgCl_2$, 0.15% Triton X-100, 5 mM β-mercaptoethanol, 0.1 mM PMSF and protease inhibitors) prior to centrifugation (1h, 16000 g, 4°C). At this stage, leaf and cotyledons tissues were treated differently. Regarding the low amount of tissue obtained for cotyledons, ChIP on cotyledons was performed using the LowCell# ChIP kit (Diagenode) following the manufacturer's protocol, while leaf tissues were processed

RT-qPCR Mix	Volume (µL)	Final Concentration
LightCycler® 480 SYBR Green I Master	5	1X
Forward Primer	0.5	1 µM
Reverse Primer	0.5	1 µM
cDNA Template	4	-

ChIP-qPCR Mix	Volume (µL)	Final Concentration
LightCycler® 480 SYBR Green I Master	5	1X
Forward Primer	0.5	1 µM
Reverse Primer	0.5	1 µM
gDNA Template	2	-
H_20 PCR Grade	Up to 10 µL	-

	Temperature (°C)	Time	Ramp Rate (°C/s)	Cycles
Activation	95	3 min	4.4	1
PCR	95	15 sec	4.4	45
	Tm primers	15 sec	2.2	
	72	20 sec	4.4	
Melting Curve	72	15 sec	2.2	1
	95	Hold	0.19	

***Table 8*: Mix used for RT-qPCR, ChIP-qPCR and qPCR program.**

following the classical ChIP protocol: the nuclear pellet of leaf tissue was resuspended in Nuclei Lysis Buffer (50 mM Tris-HCl pH 8.0, 10 mM EDTA, 1% SDS), incubated for 20 min on ice, sonicated 10 times for 30 sec ON, 1min 30 sec OFF using the Bioruptor (Diagenode) and diluted with ChIP Dilution Buffer (1.1% Triton X-100, 1.2 mM EDTA, 16.7 mM Tris-HCl pH 8.0, 167 mM NaCl) to 0.1% SDS final concentration. After removal of cellular fragments by centrifugation (10 min, 4500 g, 4°C), the sheared chromatin was pre-cleared for 3 h in presence of protein A-coupled Dynabeads (Invitrogen) before immunoprecipitation with anti-H3 antibody (Abcam, ab1791), anti-H3K4me3 (Millipore, 04-745), anti-H3K9me2 (Abcam, ab1220) and anti-H3K27me1 (Diagenode, pAB-045-050) with gentle agitation at 4°C overnight. Anti-FLAG M2 antibody-conjugated magnetic beads (Sigma-Aldrich) were used to immunoprecipitate e-H3/DNA complexes. The immunocomplexes were then collected with protein A-coupled magnetic beads (Diagenode) pre-coated overnight with glycogen, BSA and yeast t-RNA at 0.2 mg/mL each in ChIP Dilution buffer (16.7 mM Tris-HCl pH 8.0, 1.2 mM EDTA, 1.1% Triton X-100, 167 mM NaCl) for 4h at 4°C. The beads with the immunoprecipitated material were then washed 7 times: twice in Wash Buffer 1 (50 mM Tris-HCl pH 7.4, 150 mM NaCl, 1% (v/v) Igepal, 1 mM EDTA, 0.25% deoxycholic acid), twice in Wash Buffer 2 (100 mM Tris-HCl pH 8.0, 500 mM LiCl, 1% (v/v) Igepal, 1% deoxycholic acid), once in Wash Buffer 3 (100 mM Tris-HCl pH 8.0, 500 mM LiCl, 1% (v/v) Igepal, 1% deoxycholic acid, 150 mM NaCl) and twice in TE buffer, for 2 min each. Between each wash the beads were collected with a magnetic rack (Diagenode). Finally the immunoprecipitated chromatin was eluted in 10% Chelex and cross-linking was reversed at 99°C for 10 min. Samples were then treated with proteinase K (33 µg/mL) at 43°C for 1 h before inactivation by incubation at 95°C for 10 min. Immunoprecipitated DNA was quantified by semi-quantitative PCR (Promega Flexi) (***Table 6***) or in quantitative PCR with the LightCycler® 480 SYBR Green I Master kit on the Roche LightCycler® 480 (***Table 8***) using appropriate primers and normalized to the input.

Protein immunolocalization

For protein immunofluorescence detection assay, *Arabidopsis thaliana* tissues were fixed in 4% formaldehyde (Sigma-Aldrich) in Tris buffer (10 mM Tris HCl pH 7.5, 10 mM EDTA, 100 mM NaCl) for 20 min under vacuum. Tissues were finely chopped in 500 µL of LB01 buffer (15 mM Tris-HCl pH 7.5, 80 mM KCl, 2mM EDTA, 0.5 mM

spermidine, 0.5 mM spermine, 20mM NaCl, 0.1% Triton X-100). The homogenate was filtered through a 30 µm filter prior to centrifugation (3 min, 5000 rpm, 4°C) and the nuclei pellet was resuspended in 50 µL of sorting buffer (100 mM Tris-HCl pH 7.5, 50 mM KCL, 2 mM $MgCl_2$, 0.05% Tween 20 and 5% sucrose). Twenty microliters of the nuclei suspension were deposited as a thin layer onto a clean microscope slide prior to air-drying. Nuclei preparations were fixed in 2% formaldehyde in PBS for 50 min, washed with water and air-dried. The slides were incubated in 1X PBS, 0.5% Triton X-100 for 15 min and then washed three times in 1X PBS for 5 min. The primary α-HA antibody (ab9110, Abcam - 1:200 dilution in 1X PBS, 3% BSA and 0.05% Tween 20) was layered onto the slide and incubated in a wet chamber at 4°C overnight. Three washes in 1X PBS were done prior to incubation with a goat anti-rabbit antibody coupled to Alexa 488 (Invitrogen, 1:800 dilution in 1X PBS, 3% BSA and 0.05% Tween 20) for 2 h at 37°C. After 3 washes in 1X PBS, the slides were mounted in Vectashield Mounting Medium (Vector Laboratories) with DAPI (2 µg/mL). For microscopic observation, a Light microscope DM6000B (Leica) with a Digital CMOS ORCA – Flash4.0 camera (Hamamatsu) were used.

Histochemical detection of GUS expression

For histochemical GUS activity assays, *Arabidopsis thaliana* tissues were vacuum infiltrated for 15 min in GUS staining solution (50 mM $NaPO_4$ buffer pH 7.2, 2 mM Potassium-Ferocyanide (K_4FeCN_6), 2 mM Potassium-Ferricyanide (K_3FeCN_6), 0.2% Triton X-100 and 2 mM 5-bromo-4-chloro-3-indolyl-3β-d-glucuronide (X-Gluc)) and incubated overnight at 37°C. Tissues were gradually dehydrated by ethanol series at 80°C. Pictures of seedlings were taken using a Leica MZ FL III Fluorescence Stereomicroscope with a Leica DFC420 camera.

Ploidy analysis

Nuclei were prepared using a variant of the original method of Galbraith (Galbraith et al., 1983). For ploidy analysis of nuclei, *Arabidopsis thaliana* tissues were chopped in ice-cold Galbraith buffer (45 mM $MgCl_2$, 30 mM $NaHCO_3$, 20 mM MOPS pH 7.0, 0.1% (w/v) Triton X-100, and 1% BSA). After filtration and 2% formaldehyde complementation, the nuclear suspension was layered in fresh tubes over 100 µL of ice-cold 2 M sucrose and 100 µL of ice-cold Galbraith Sucrose buffer (45 mM $MgCl_2$,

30 mM $NaHCO_3$, 20 mM MOPS pH 7.0, 0.1% (w/v) Triton X-100, 1 M sucrose and 10% BSA). After centrifugation (4 min, 800g at 4°C with slow brake), the Galbraith Sucrose buffer layer containing nuclei was collected in new tubes and mixed to 1 mL of ice-cold Galbraith buffer together with 12 ng/mL DAPI. Cytometric analysis was then performed using the *Attune*® *Acoustic* Focusing cytometer and data analysed using the *Attune*® Cytometer Software.

Protein extraction and Western analysis

For extracts containing non-nucleosomal histones, 100 mg *Arabidopsis thaliana* tissues were frozen in liquid nitrogen and ground to a fine powder. Proteins were extracted in 50 mM Tris-HCl pH 8.0, 150 mM NaCl, 10 mM EDTA, 50 mM NaF, 1% NP40, 0.45% desoxycholate, 1% SDS and proteinase inhibitors (Roche). The supernatant of a first centrifugation step (20 min, 15000 g) was centrifuged again with the same parameters and the protein concentration of the second supernatant was quantified using a Bicinchoninic Acid assay (Sigma-Aldrich) with BSA as the reference standard. For extracts containing nucleosomal histones, nuclei were prepared from 2 g plant material according to an adapted ChIP protocol using HONDA buffer (10 mM $MgCl_2$, 0.4 M sucrose, 2.5% Ficoll, 5% Dextran 40, 25 mM Tris-HCl pH 7.4, 5 mM DTT, 0.5 mM PMSF, 1% protease inhibitors). Briefly, tissue was ground to powder in liquid nitrogen and re-suspended in HONDA buffer and filtrated; an aliquot was recovered for total extract. After incubation with 0.5% Triton X-100 samples were centrifuged (5 min, 1500 g). Nuclei were washed successively in HONDA buffer with 0.1% Triton X-100 then without Triton X-100 and finally re-suspended in Laemli buffer. SDS–PAGE and Western blots were performed according to standard procedures. Western blots were probed with an anti-H3 (ab1791, Abcam – from 1:5,000 to 1:20,000) or anti-HA (ab9110, Abcam – 1:4,000). Equal loading of proteins was confirmed with a mouse monoclonal anti-Actin antibody (Sigma-Aldrich – 1:1,000), anti-H4 (ab10158, Abcam – 1:2,000), Ponceau or Coomassie staining. Primary antibodies were revealed by incubation with a horseradish peroxidase-coupled anti-rabbit secondary antibody (Sigma-Aldrich, 1:25,000) or a horseradish peroxidase-coupled anti-mouse secondary antibody (Sigma-Aldrich, 1:5000). Chemiluminescence of the immunoblots were developed using ECL Western blotting detection reagents (GE Healthcare Bio-Sciences). Densitometric analysis of the immunoreactive protein bands obtained in Western

blots was performed on non-saturated signals using Multi Gauge software (Fujfilm). Nucleosomal H3 was quantified relative to actin in the corresponding total extracts. Remaining actin protein levels in nucleosomal extracts are very low.

References

Adam, S., Polo, S.E., and Almouzni, G. (2013). Transcription recovery after DNA damage requires chromatin priming by the H3.3 histone chaperone HIRA. Cell **155**: 94–106.

Adkins, M.W. and Tyler, J.K. (2004). The histone chaperone Asf1p mediates global chromatin disassembly in vivo. J. Biol. Chem. **279**: 52069–74.

Adrian, J., Torti, S., and Turck, F. (2009). From decision to commitment: the molecular memory of flowering. Mol. Plant **2**: 628–642.

Ahmad, K. and Henikoff, S. (2002a). Histone H3 variants specify modes of chromatin assembly. Proc. Natl. Acad. Sci. U. S. A. **99 Suppl 4**: 16477–84.

Ahmad, K. and Henikoff, S. (2002b). The histone variant H3. 3 marks active chromatin by replication-independent nucleosome assembly. Mol. Cell **9**: 1191–1200.

Aho, S., Buisson, M., Pajunen, T., Ryoo, Y.W., Giot, J.F., Gruffat, H., Sergeant, A., and Uitto, J. (2000). Ubinuclein, a novel nuclear protein interacting with cellular and viral transcription factors. J. Cell Biol. **148**: 1165–76.

Akiyama, T., Suzuki, O., Matsuda, J., and Aoki, F. (2011). Dynamic replacement of histone H3 variants reprograms epigenetic marks in early mouse embryos. PLoS Genet. **7**: e1002279.

Allshire, R.C. and Karpen, G.H. (2008). Epigenetic regulation of centromeric chromatin: old dogs, new tricks? Nat. Rev. Genet. **9**: 923–37.

Almouzni, G. and Probst, A. V (2011). Heterochromatin maintenance and establishment: lessons from the mouse pericentromere. Nucleus **2**: 332–8.

Amasino, R. (2010). Seasonal and developmental timing of flowering. Plant J. **61**: 1001–13.

Amedeo, P., Habu, Y., Afsar, K., Mittelsten Scheid, O., and Paszkowski, J. (2000). Disruption of the plant gene MOM releases transcriptional silencing of methylated genes. Nature **405**: 203–206.

Amin, A.D., Vishnoi, N., and Prochasson, P. (2012). A global requirement for the HIR complex in the assembly of chromatin. BBA - Gene Regul. Mech. **1819**: 264–276.

Arents, G. and Moudrianakis, E.N. (1995). The histone fold: a ubiquitous architectural motif utilized in DNA compaction and protein dimerization. Proc. Natl. Acad. Sci. U. S. A. **92**: 11170–4.

Arya, G., Maitra, A., and Grigoryev, S.A. (2010). A structural perspective on the where, how, why, and what of nucleosome positioning. J. Biomol. Struct. Dyn. **27**: 803–20.

Ausín, I., Alonso-Blanco, C., Jarillo, J.A., Ruiz-García, L., and Martínez-Zapater, J.M. (2004). Regulation of flowering time by FVE, a retinoblastoma-associated protein. Nat. Genet. **36**: 162–6.

Autran, D. et al. (2011). Maternal epigenetic pathways control parental contributions to Arabidopsis early embryogenesis. Cell **145**: 707–19.

Avivi, Y., Morad, V., Ben-Meir, H., Zhao, J., Kashkush, K., Tzfira, T., Citovsky, V., and Grafi, G. (2004). Reorganization of specific chromosomal domains and activation of silent genes in plant cells acquiring pluripotentiality. Dev. Dyn. **230**: 12–22.

Balaji, S., Iyer, L.M., and Aravind, L. (2009). HPC2 and ubinuclein define a novel family of histone chaperones conserved throughout eukaryotes. Mol. Biosyst. **5**: 269–75.

Bannister, A.J., Zegerman, P., Partridge, J.F., Miska, E.A., Thomas, J.O., Allshire, R.C., and Kouzarides, T. (2001). Selective recognition of methylated lysine 9 on histone H3 by the HP1 chromo domain. Nature **410**: 120–4.

Banumathy, G., Somaiah, N., Zhang, R., Tang, Y., Hoffmann, J., Andrake, M., Ceulemans, H., Schultz, D., Marmorstein, R., and Adams, P.D. (2009). Human UBN1 is an ortholog of yeast Hpc2p and has an essential role in the HIRA/ASF1a chromatin-remodeling pathway in senescent cells. Mol. Cell. Biol. **29**: 758–70.

Barah, P., Jayavelu, N.D., Mundy, J., and Bones, A.M. (2013). Genome scale transcriptional response diversity among ten ecotypes of Arabidopsis thaliana during heat stress. Front. Plant Sci. **4**: 532.

Benoit, M., Layat, E., Tourmente, S., and Probst, A. V (2013). Heterochromatin dynamics during developmental transitions in Arabidopsis - a focus on ribosomal DNA loci. Gene **526**: 39–45.

Benson, L.J., Gu, Y., Yakovleva, T., Tong, K., Barrows, C., Strack, C.L., Cook, R.G., Mizzen, C.A., and Annunziato, A.T. (2006). Modifications of H3 and H4 during chromatin replication, nucleosome assembly, and histone exchange. J. Biol. Chem. **281**: 9287–96.

Bernatavichute, Y. V, Zhang, X., Cokus, S., Pellegrini, M., and Jacobsen, S.E. (2008). Genome-wide association of histone H3 lysine nine methylation with CHG DNA methylation in Arabidopsis thaliana. PLoS One **3**: e3156.

Berr, A. and Schubert, I. (2007). Interphase chromosome arrangement in Arabidopsis thaliana is similar in differentiated and meristematic tissues and shows a transient mirror symmetry after nuclear division. Genetics **176**: 853–63.

Blasco, M.A. (2007). The epigenetic regulation of mammalian telomeres. Nat. Rev. Genet. **8**: 299–309.

Blower, M., Sullivan, B., and Karpen, G. (2002). Conserved organization of centromeric chromatin in flies and humans. Dev. Cell **2**: 319–330.

Bonnefoy, E., Orsi, G.A., Couble, P., and Loppin, B. (2007). The essential role of Drosophila HIRA for de novo assembly of paternal chromatin at fertilization. PLoS Genet. **3**: 1991–2006.

Bouveret, R., Schönrock, N., Gruissem, W., and Hennig, L. (2006). Regulation of flowering time by Arabidopsis MSI1. Development **133**: 1693–702.

Bowler, C., Benvenuto, G., Laflamme, P., Molino, D., Probst, A. V, Tariq, M., and Paszkowski, J. (2004). Chromatin techniques for plant cells. Plant J. **39**: 776–89.

Boyle, S., Gilchrist, S., Bridger, J.M., Mahy, N.L., Ellis, J.A., and Bickmore, W.A. (2001). The spatial organization of human chromosomes within the nuclei of normal and emerin-mutant cells. Hum. Mol. Genet. **10**: 211–9.

Brooks, W. and Jackson, V. (1994). The rapid transfer and selective association of histones H2A and H2B onto negatively coiled DNA at physiological ionic strength. J. Biol. Chem. **269**: 18155–66.

Brown, J.M., Leach, J., Reittie, J.E., Atzberger, A., Lee-Prudhoe, J., Wood, W.G., Higgs, D.R., Iborra, F.J., and Buckle, V.J. (2006). Coregulated human globin genes are frequently in spatial proximity when active. J. Cell Biol. **172**: 177–87.

Brownfield, L., Hafidh, S., Borg, M., Sidorova, A., Mori, T., and Twell, D. (2009). A plant germline-specific integrator of sperm specification and cell cycle progression. PLoS Genet. **5**: e1000430.

Buschbeck, M., Uribesalgo, I., Wibowo, I., Rué, P., Martin, D., Gutierrez, A., Morey, L., Guigó, R., López-Schier, H., and Di Croce, L. (2009). The histone

variant macroH2A is an epigenetic regulator of key developmental genes. Nat. Struct. Mol. Biol. **16**: 1074–9.

Caikovski, M., Yokthongwattana, C., Habu, Y., Nishimura, T., Mathieu, O., and Paszkowski, J. (2008). Divergent evolution of CHD3 proteins resulted in MOM1 refining epigenetic control in vascular plants. PLoS Genet. **4**: e1000165.

Campell, B.R., Song, Y., Posch, T.E., Cullis, C.A., and Town, C.D. (1992). Sequence and organization of 5S ribosomal RNA-encoding genes of Arabidopsis thaliana. Gene **112**: 225–228.

Campos, E.I. and Reinberg, D. (2010). New chaps in the histone chaperone arena. Genes Dev. **24**: 1334–1338.

Cavrak, V. V, Lettner, N., Jamge, S., Kosarewicz, A., Bayer, L.M., and Mittelsten Scheid, O. (2014). How a retrotransposon exploits the plant's heat stress response for its activation. PLoS Genet. **10**: e1004115.

Chakravarthy, S. and Luger, K. (2006). The histone variant macro-H2A preferentially forms "hybrid nucleosomes". J. Biol. Chem. **281**: 25522–31.

Chambeyron, S. and Bickmore, W. (2004). Chromatin decondensation and nuclear reorganization of the HoxB locus upon induction of transcription. Genes Dev.: 1119–1130.

Chan, S.W.-L., Zilberman, D., Xie, Z., Johansen, L.K., Carrington, J.C., and Jacobsen, S.E. (2004). RNA silencing genes control de novo DNA methylation. Science **303**: 1336.

Chandler, J. (2008). Cotyledon organogenesis. J. Exp. Bot. **59**: 2917–31.

Chaubet-Gigot, N., Kapros, T., Flenet, M., Kahn, K., Gigot, C., and Waterborg, J.H. (2001). Tissue-dependent enhancement of transgene expression by introns of replacement histone H3 genes of Arabidopsis. Plant Mol. Biol. **45**: 17–30.

Chen, C.-C., Carson, J.J., Feser, J., Tamburini, B., Zabaronick, S., Linger, J., and Tyler, J.K. (2008). Acetylated lysine 56 on histone H3 drives chromatin assembly after repair and signals for the completion of repair. Cell **134**: 231–43.

Chen, T., Ueda, Y., Dodge, J.E., Wang, Z., and Li, E. (2003). Establishment and maintenance of genomic methylation patterns in mouse embryonic stem cells by Dnmt3a and Dnmt3b. Mol. Cell. Biol. **23**: 5594–605.

Chodavarapu, R.K. et al. (2010). Relationship between nucleosome positioning and DNA methylation. Nature **466**: 388–92.

Choo, K. (1997). Centromere DNA dynamics: latent centromeres and neocentromere formation. Am. J. Hum. Genet.: 1225–1233.

Choulet, F. et al. (2010). Megabase level sequencing reveals contrasted organization and evolution patterns of the wheat gene and transposable element spaces. Plant Cell **22**: 1686–701.

Cloix, C., Tutois, S., Mathieu, O., Cuvillier, C., Espagnol, M.C., Picard, G., and Tourmente, S. (2000). Analysis of 5S rDNA arrays in Arabidopsis thaliana: physical mapping and chromosome-specific polymorphisms. Genome Res. **10**: 679–90.

Cloix, C., Tutois, S., Yukawa, Y., Mathieu, O., Cuvillier, C., Espagnol, M.-C., Picard, G., and Tourmente, S. (2002). Analysis of the 5S RNA pool in Arabidopsis thaliana: RNAs are heterogeneous and only two of the genomic 5S loci produce mature 5S RNA. Genome Res. **12**: 132–44.

Cloix, C., Yukawa, Y., Tutois, S., Sugiura, M., and Tourmente, S. (2003). In vitro analysis of the sequences required for transcription of the Arabidopsis thaliana 5S rRNA genes. Plant J. **35**: 251–61.

Clough, S.J. and Bent, A.F. (1998). Floral dip: a simplified method for Agrobacterium-mediated transformation of Arabidopsis thaliana. Plant J. **16**: 735–43.

Cokus, S.J., Feng, S., Zhang, X., Chen, Z., Merriman, B., Haudenschild, C.D., Pradhan, S., Nelson, S.F., Pellegrini, M., and Jacobsen, S.E. (2008). Shotgun bisulphite sequencing of the Arabidopsis genome reveals DNA methylation patterning. Nature **452**: 215–9.

Cooper, J.L. and Henikoff, S. (2004). Adaptive evolution of the histone fold domain in centromeric histones. Mol. Biol. Evol. **21**: 1712–8.

Copenhaver, G.P. et al. (1999). Genetic definition and sequence analysis of Arabidopsis centromeres. Science **286**: 2468–74.

Copenhaver, G.P., Doelling, J.H., Gens, S., and Pikaard, C.S. (1995). Use of RFLPs larger than 100 kbp to map the position and internal organization of the nucleolus organizer region on chromosome 2 in Arabidopsis thaliana. Plant J. **7**: 273–86.

Copenhaver, G.P. and Pikaard, C.S. (1996). RFLP and physical mapping with an rDNA-specific endonuclease reveals that nucleolus organizer regions of Arabidopsis thaliana adjoin the telomeres on chromosomes 2 and 4. Plant J. **9**: 259–72.

Corpet, A., De Koning, L., Toedling, J., Savignoni, A., Berger, F., Lemaître, C., O'Sullivan, R.J., Karlseder, J., Barillot, E., Asselain, B., Sastre-Garau, X., and Almouzni, G. (2011). Asf1b, the necessary Asf1 isoform for proliferation, is predictive of outcome in breast cancer. EMBO J. **30**: 480–93.

Costanzi, C. and Pehrson, J. (1998). Histone macroH2A1 is concentrated in the inactive X chromosome of female mammals. Nature **628**: 1997–1999.

Cremer, T. and Cremer, C. (2001). Chromosome territories, nuclear architecture and gene regulation in mammalian cells. Nat. Rev. Genet. **2**: 292–301.

Cremer, T. and Cremer, M. (2010). Chromosome territories. Cold Spring Harb. Perspect. Biol. **2**: a003889.

Croft, J.A., Bridger, J.M., Boyle, S., Perry, P., Teague, P., and Bickmore, W.A. (1999). Differences in the localization and morphology of chromosomes in the human nucleus. J. Cell Biol. **145**: 1119–31.

Curtis, M. and Grossniklaus, U. (2003). A Gateway Cloning Vector Set for High-Throughput Functional Analysis of Genes in Planta. Plant Physiol. **133**: 462–469.

Czechowski, T., Stitt, M., Altmann, T., Udvardi, M.K., and Scheible, W.-R.R. (2005). Genome-wide identification and testing of superior reference genes for transcript normalization in Arabidopsis. Plant Physiol. **139**: 5–17.

Czermin, B., Melfi, R., McCabe, D., Seitz, V., Imhof, A., and Pirrotta, V. (2002). Drosophila enhancer of Zeste/ESC complexes have a histone H3 methyltransferase activity that marks chromosomal Polycomb sites. Cell **111**: 185–96.

Daganzo, S.M., Erzberger, J.P., Lam, W.M., Skordalakes, E., Zhang, R., Franco, A.A., Brill, S.J., Adams, P.D., Berger, J.M., and Kaufman, P.D. (2003). Structure and Function of the Conserved Core of Histone Deposition Protein Asf1. Curr. Biol. **13**: 2148–2158.

Davie, J.R. and Chadee, D.N. (1998). Regulation and regulatory parameters of histone modifications. J. Cell. Biochem. Suppl. **30-31**: 203–13.

Deal, R.B., Henikoff, J.G., and Henikoff, S. (2010). Genome-wide kinetics of nucleosome turnover determined by metabolic labeling of histones. Science **328**: 1161–4.

Dittmer, T.A., Stacey, N.J., Sugimoto-Shirasu, K., and Richards, E.J. (2007). LITTLE NUCLEI genes affecting nuclear morphology in Arabidopsis thaliana. Plant Cell **19**: 2793–803.

Dominski, Z. and Marzluff, W.F. (2007). Formation of the 3' end of histone mRNA: getting closer to the end. Gene **396**: 373–90.

Dorigo, B., Schalch, T., Bystricky, K., and Richmond, T.J. (2003). Chromatin Fiber Folding: Requirement for the Histone H4 N-terminal Tail. J. Mol. Biol. **327**: 85–96.

Douet, J., Blanchard, B., Cuvillier, C., and Tourmente, S. (2008). Interplay of RNA Pol IV and ROS1 during post-embryonic 5S rDNA chromatin remodeling. Plant Cell Physiol. **49**: 1783–1791.

Drané, P., Ouararhni, K., Depaux, A., Shuaib, M., and Hamiche, A. (2010). The death-associated protein DAXX is a novel histone chaperone involved in the replication-independent deposition of H3.3. Genes Dev. **24**: 1253–65.

Du, J. et al. (2012). Dual binding of chromomethylase domains to H3K9me2-containing nucleosomes directs DNA methylation in plants. Cell **151**: 167–80.

Dunleavy, E., Pidoux, A., and Allshire, R. (2005). Centromeric chromatin makes its mark. Trends Biochem. Sci. **30**: 172–5.

Dunleavy, E.M., Almouzni, G., and Karpen, G.H. (2011). H3.3 is deposited at centromeres in S phase as a placeholder for newly assembled CENP-A in G1 phase. Nucleus **2**: 146–57.

Durut, N. et al. (2014). A duplicated NUCLEOLIN gene with antagonistic activity is required for chromatin organization of silent 45S rDNA in Arabidopsis. Plant Cell **26**: 1330–44.

Ebbs, M. and Bender, J. (2006). Locus-specific control of DNA methylation by the Arabidopsis SUVH5 histone methyltransferase. Plant Cell Online **18**: 1166–1176.

Ebbs, M.L., Bartee, L., and Bender, J. (2005). H3 lysine 9 methylation is maintained on a transcribed inverted repeat by combined action of SUVH6 and SUVH4 methyltransferases. Mol. Cell. Biol. **25**: 10507–15.

Eberl, D., Duyf, B., and Hilliker, A. (1993). The Role of Heterochromatin in the Expression of a Heterochromatic Gene, the rolled Locus of Drosophila melanogaster. Genetics **292**: 277–292.

Ebert, A., Schotta, G., Lein, S., Kubicek, S., Krauss, V., Jenuwein, T., and Reuter, G. (2004). Su(var) genes regulate the balance between euchromatin and heterochromatin in Drosophila. Genes Dev. **18**: 2973–83.

Edgar, B.A. and Orr-Weaver, T.L. (2001). Endoreplication cell cycles: more for less. Cell **105**: 297–306.

Edgar, B.A., Zielke, N., and Gutierrez, C. (2014). Endocycles: a recurrent evolutionary innovation for post-mitotic cell growth. Nat. Rev. Mol. Cell Biol. **15**: 197–210.

Eickbush, T.H. and Moudrianakis, E.N. (1978). The histone core complex: an octamer assembled by two sets of protein-protein interactions. Biochemistry **17**: 4955–4964.

Elmayan, T., Proux, F., and Vaucheret, H. (2005). Arabidopsis RPA2: a genetic link among transcriptional gene silencing, DNA repair, and DNA replication. Curr. Biol. **15**: 1919–25.

Elsaesser, S.J., Goldberg, A.D., and Allis, C.D. (2010). New functions for an old variant: no substitute for histone H3.3. Curr. Opin. Genet. Dev. **20**: 110–7.

Elsässer, S.J., Huang, H., Lewis, P.W., Chin, J.W., Allis, C.D., and Patel, D.J. (2012). DAXX envelops a histone H3.3-H4 dimer for H3.3-specific recognition. Nature **491**: 560–5.

Endo, M., Ishikawa, Y., Osakabe, K., Nakayama, S., Kaya, H., Araki, T., Shibahara, K., Abe, K., Ichikawa, H., Valentine, L., Hohn, B., and Toki, S. (2006). Increased frequency of homologous recombination and T-DNA integration in Arabidopsis CAF-1 mutants. EMBO J. **25**: 5579–90.

English, C.M., Adkins, M.W., Carson, J.J., Churchill, M.E.A., and Tyler, J.K. (2006). Structural basis for the histone chaperone activity of Asf1. Cell **127**: 495–508.

Enomoto, S. and Berman, J. (1998). Chromatin assembly factor I contributes to the maintenance, but not the re-establishment, of silencing at the yeast silent mating loci. Genes Dev. **12**: 219–232.

Estève, P.-O., Chin, H.G., Smallwood, A., Feehery, G.R., Gangisetty, O., Karpf, A.R., Carey, M.F., and Pradhan, S. (2006). Direct interaction between DNMT1 and G9a coordinates DNA and histone methylation during replication. Genes Dev. **20**: 3089–103.

Exner, V., Gruissem, W., and Hennig, L. (2008). Control of trichome branching by chromatin assembly factor-1. BMC Plant Biol. **8**: 54.

Exner, V. and Hennig, L. (2008). Chromatin rearrangements in development. Curr. Opin. Plant Biol. **11**: 64–9.

Exner, V., Taranto, P., Schönrock, N., Gruissem, W., and Hennig, L. (2006). Chromatin assembly factor CAF-1 is required for cellular differentiation during plant development. Development **133**: 4163–72.

Fan, Y., Nikitina, T., Zhao, J., Fleury, T.J., Bhattacharyya, R., Bouhassira, E.E., Stein, A., Woodcock, C.L., and Skoultchi, A.I. (2005). Histone H1 depletion in mammals alters global chromatin structure but causes specific changes in gene regulation. Cell **123**: 1199–212.

Fang, Y. and Spector, D.L. (2005). Centromere positioning and dynamics in living Arabidopsis plants. Mol. Biol. Cell **16**: 5710–8.

Feng, S., Jacobsen, S.E., and Reik, W. (2010). Epigenetic reprogramming in plant and animal development. Science **330**: 622–7.

Filion, G.J., van Bemmel, J.G., Braunschweig, U., Talhout, W., Kind, J., Ward, L.D., Brugman, W., de Castro, I.J., Kerkhoven, R.M., Bussemaker, H.J., and van Steensel, B. (2010). Systematic protein location mapping reveals five principal chromatin types in Drosophila cells. Cell **143**: 212–24.

Filipescu, D., Szenker, E., and Almouzni, G. (2013). Developmental roles of histone H3 variants and their chaperones. Trends Genet. **29**: 1–11.

Folco, H.D., Pidoux, A.L., Urano, T., and Allshire, R.C. (2008). Heterochromatin and RNAi are required to establish CENP-A chromatin at centromeres. Science **319**: 94–7.

Franco, A.A., Lam, W.M., Burgers, P.M., and Kaufman, P.D. (2005). Histone deposition protein Asf1 maintains DNA replisome integrity and interacts with replication factor C. Genes Dev. **19**: 1365–75.

Franklin, S.G. and Zweidler, A. (1977). Non-allelic variants of histones 2a, 2b and 3 in mammals. Nature **266**: 273–5.

Fransz, P. and de Jong, H. (2011). From nucleosome to chromosome: a dynamic organization of genetic information. Plant J. **66**: 4–17.

Fransz, P., De Jong, J.H., Lysak, M., Castiglione, M.R., and Schubert, I. (2002). Interphase chromosomes in Arabidopsis are organized as well defined chromocenters from which euchromatin loops emanate. Proc. Natl. Acad. Sci. U. S. A. **99**: 14584–9.

Fuks, F., Hurd, P.J., Deplus, R., and Kouzarides, T. (2003). The DNA methyltransferases associate with HP1 and the SUV39H1 histone methyltransferase. Nucleic Acids Res. **31**: 2305–12.

Gaillard, P.H., Martini, E.M., Kaufman, P.D., Stillman, B., Moustacchi, E., and Almouzni, G. (1996). Chromatin assembly coupled to DNA repair: a new role for chromatin assembly factor I. Cell **86**: 887–96.

Galbraith, D.W., Harkins, K.R., Maddox, J.M., Ayres, N.M., Sharma, D.P., and Firoozabady, E. (1983). Rapid flow cytometric analysis of the cell cycle in intact plant tissues. Science **220**: 1049–51.

Garrick, D., Sharpe, J.A., Arkell, R., Dobbie, L., Smith, A.J.H., Wood, W.G., Higgs, D.R., and Gibbons, R.J. (2006). Loss of Atrx affects trophoblast development and the pattern of X-inactivation in extraembryonic tissues. PLoS Genet. **2**: e58.

Gatz, C., Frohberg, C., and Wendenburg, R. (1992). Stringent repression and homogeneous de-repression by tetracycline of a modified CaMV 35S promoter in intact transgenic tobacco plants. Plant J. **2**: 397–404.

Gaudin, V., Libault, M., Pouteau, S., Juul, T., Zhao, G., Lefebvre, D., and Grandjean, O. (2001). Mutations in LIKE HETEROCHROMATIN PROTEIN 1 affect flowering time and plant architecture in Arabidopsis. Development **128**: 4847–4858.

Gauthier, N.P., Jensen, L.J., Wernersson, R., Brunak, S., and Jensen, T.S. (2010). Cyclebase.org: version 2.0, an updated comprehensive, multi-species repository of cell cycle experiments and derived analysis results. Nucleic Acids Res. **38**: D699–702.

Gehring, M., Bubb, K.L., and Henikoff, S. (2009). Extensive demethylation of repetitive elements during seed development underlies gene imprinting. Science **324**: 1447–51.

Gendrel, A.-V., Lippman, Z., Yordan, C., Colot, V., and Martienssen, R.A. (2002). Dependence of heterochromatic histone H3 methylation patterns on the Arabidopsis gene DDM1. Science **297**: 1871–3.

Gérard, A., Koundrioukoff, S., Ramillon, V., Sergère, J.-C., Mailand, N., Quivy, J.-P., and Almouzni, G. (2006). The replication kinase Cdc7-Dbf4 promotes the interaction of the p150 subunit of chromatin assembly factor 1 with proliferating cell nuclear antigen. EMBO Rep. **7**: 817–23.

Gerlich, D., Beaudouin, J., Kalbfuss, B., and Daigle, N. (2003). Global chromosome positions are transmitted through mitosis in mammalian cells. Cell **112**: 751–764.

Goldberg, A.D. et al. (2010). Distinct factors control histone variant H3.3 localization at specific genomic regions. Cell **140**: 678–91.

Goodfellow, H., Krejcí, A., Moshkin, Y., Verrijzer, C.P., Karch, F., and Bray, S.J. (2007). Gene-specific targeting of the histone chaperone asf1 to mediate silencing. Dev. Cell **13**: 593–600.

Green, C.M. and Almouzni, G. (2003). Local action of the chromatin assembly factor CAF-1 at sites of nucleotide excision repair in vivo. EMBO J. **22**: 5163–74.

Green, E.M., Antczak, A.J., Bailey, A.O., Franco, A.A., Wu, K.J., Yates, J.R., and Kaufman, P.D. (2005). Replication-independent histone deposition by the HIR complex and Asf1. Curr. Biol. **15**: 2044–9.

Grefen, C., Donald, N., Hashimoto, K., Kudla, J., Schumacher, K., and Blatt, M.R. (2010). A ubiquitin-10 promoter-based vector set for fluorescent protein tagging facilitates temporal stability and native protein distribution in transient and stable expression studies. Plant J. **64**: 355–65.

Grigoryev, S.A., Arya, G., Correll, S., Woodcock, C.L., and Schlick, T. (2009). Evidence for heteromorphic chromatin fibers from analysis of nucleosome interactions. Proc. Natl. Acad. Sci. U. S. A. **106**: 13317–22.

Grob, S., Schmid, M.W., Luedtke, N.W., Wicker, T., and Grossniklaus, U. (2013). Characterization of chromosomal architecture in Arabidopsis by chromosome conformation capture. Genome Biol. **14**: R129.

Groth, A., Corpet, A., Cook, A.J.L., Roche, D., Bartek, J., Lukas, J., and Almouzni, G. (2007). Regulation of replication fork progression through histone supply and demand. Science **318**: 1928–1931.

Groth, A., Ray-Gallet, D., Quivy, J.-P., Lukas, J., Bartek, J., and Almouzni, G. (2005). Human Asf1 regulates the flow of S phase histones during replicational stress. Mol. Cell **17**: 301–11.

Guenatri, M., Bailly, D., Maison, C., and Almouzni, G. (2004). Mouse centric and pericentric satellite repeats form distinct functional heterochromatin. J. Cell Biol. **166**: 493–505.

Guo, M., Thomas, J., Collins, G., and Timmermans, M.C.P. (2008). Direct repression of KNOX loci by the ASYMMETRIC LEAVES1 complex of Arabidopsis. Plant Cell **20**: 48–58.

Gurard-Levin, Z.A., Quivy, J.-P., and Almouzni, G. (2014). Histone chaperones: assisting histone traffic and nucleosome dynamics. Annu. Rev. Biochem. **83**: 487–517.

Gutierrez, C. (2005). Coupling cell proliferation and development in plants. Nat. Cell Biol. **7**: 535–41.

Habu, Y., Mathieu, O., Tariq, M., Probst, A. V, Smathajitt, C., Zhu, T., and Paszkowski, J. (2006). Epigenetic regulation of transcription in intermediate heterochromatin. EMBO Rep. **7**: 1279–1284.

Hake, S.B. and Allis, C.D. (2006). Histone H3 variants and their potential role in indexing mammalian genomes: the “H3 barcode hypothesis”. Proc. Natl. Acad. Sci. U. S. A. **103**: 6428–35.

Hake, S.B., Garcia, B.A., Duncan, E.M., Kauer, M., Dellaire, G., Shabanowitz, J., Bazett-Jones, D.P., Allis, C.D., and Hunt, D.F. (2006). Expression patterns and post-translational modifications associated with mammalian histone H3 variants. J. Biol. Chem. **281**: 559–68.

Hall, I.M., Shankaranarayana, G.D., Noma, K.-I., Ayoub, N., Cohen, A., and Grewal, S.I.S. (2002). Establishment and maintenance of a heterochromatin domain. Science **297**: 2232–7.

Hall, S.E., Kettler, G., and Preuss, D. (2003). Centromere satellites from Arabidopsis populations: maintenance of conserved and variable domains. Genome Res. **13**: 195–205.

Han, J., Zhou, H., Li, Z., Xu, R.-M., and Zhang, Z. (2007). Acetylation of lysine 56 of histone H3 catalyzed by RTT109 and regulated by ASF1 is required for replisome integrity. J. Biol. Chem. **282**: 28587–96.

Hartford, S.A., Luo, Y., Southard, T.L., Min, I.M., Lis, J.T., and Schimenti, J.C. (2011). Minichromosome maintenance helicase paralog MCM9 is dispensible for DNA replication but functions in germ-line stem cells and tumor suppression. Proc. Natl. Acad. Sci. U. S. A. **108**: 17702–7.

Haupt, W., Fischer, T.C., Winderl, S., Fransz, P., and Torres-Ruiz, R.A. (2001). The centromere1 (CEN1) region of Arabidopsis thaliana: architecture and functional impact of chromatin. Plant J. **27**: 285–96.

Havecker, E.R., Wallbridge, L.M., Hardcastle, T.J., Bush, M.S., Kelly, K.A., Dunn, R.M., Schwach, F., Doonan, J.H., and Baulcombe, D.C. (2010). The Arabidopsis RNA-directed DNA methylation argonautes functionally diverge based on their expression and interaction with target loci. Plant Cell **22**: 321–34.

Hayes, J.J., Clark, D.J., and Wolffe, A.P. (1991). Histone contributions to the structure of DNA in the nucleosome. Proc. Natl. Acad. Sci. U. S. A. **88**: 6829–33.

Hayes, J.J., Tullius, T.D., and Wolffe, A.P. (1990). The structure of DNA in a nucleosome. Proc. Natl. Acad. Sci. U. S. A. **87**: 7405–9.

He, Y. (2009). Control of the transition to flowering by chromatin modifications. Mol. Plant **2**: 554–64.

Van der Heijden, G.W., Derijck, A.A.H.A., Pósfai, E., Giele, M., Pelczar, P., Ramos, L., Wansink, D.G., van der Vlag, J., Peters, A.H.F.M., and de Boer, P. (2007). Chromosome-wide nucleosome replacement and H3.3 incorporation during mammalian meiotic sex chromosome inactivation. Nat. Genet. **39**: 251–8.

Heitz, E. (1928). Das Heterochromatin der Moose. Jahrb Wiss Bot. **69**: 762–818.

Henikoff, S. (2000). Heterochromatin function in complex genomes. Biochim. Biophys. Acta **1470**: O1–8.

Henikoff, S., McKittrick, E., and Ahmad, K. (2004). Epigenetics, histone H3 variants, and the inheritance of chromatin states. Cold Spring Harb. Symp. Quant. Biol. **69**: 235–43.

Hennig, L. (2003). Arabidopsis MSI1 is required for epigenetic maintenance of reproductive development. Development **130**: 2555–2565.

Hennig, W. (1999). Heterochromatin. Chromosoma **108**: 1–9.

Herr, A.J., Jensen, M.B., Dalmay, T., and Baulcombe, D.C. (2005). RNA polymerase IV directs silencing of endogenous DNA. Science **308**: 118–20.

Heslop-Harrison, J.S., Murata, M., Ogura, Y., Schwarzacher, T., and Motoyoshi, F. (1999). Polymorphisms and genomic organization of repetitive DNA from centromeric regions of Arabidopsis chromosomes. Plant Cell **11**: 31–42.

Hödl, M. and Basler, K. (2009). Transcription in the absence of histone H3.3. Curr. Biol. **19**: 1221–6.

Hoek, M. and Stillman, B. (2003). Chromatin assembly factor 1 is essential and couples chromatin assembly to DNA replication in vivo. Proc. Natl. Acad. Sci. U. S. A. **100**: 12183–8.

Holdsworth, M.J., Finch-Savage, W.E., Grappin, P., and Job, D. (2008). Post-genomics dissection of seed dormancy and germination. Trends Plant Sci. **13**: 7–13.

Horn, P.J. and Peterson, C.L. (2002). Molecular biology. Chromatin higher order folding--wrapping up transcription. Science **297**: 1824–7.

Hosouchi, T., Kumekawa, N., Tsuruoka, H., and Kotani, H. (2002). Physical map-based sizes of the centromeric regions of Arabidopsis thaliana chromosomes 1, 2, and 3. DNA Res. **9**: 117–21.

Houlard, M., Berlivet, S., Probst, A. V, Quivy, J.-P., Héry, P., Almouzni, G., and Gérard, M. (2006). CAF-1 is essential for heterochromatin organization in pluripotent embryonic cells. PLoS Genet. **2**: e181.

Hsieh, T.-F., Ibarra, C.A., Silva, P., Zemach, A., Eshed-Williams, L., Fischer, R.L., and Zilberman, D. (2009). Genome-wide demethylation of Arabidopsis endosperm. Science **324**: 1451–4.

Hsu, T.C., Cooper, J.E., Mace, M.L., and Brinkley, B.R. (1971). Arrangement of centromeres in mouse cells. Chromosoma **34**: 73–87.

Huijser, P. and Schmid, M. (2011). The control of developmental phase transitions in plants. Development **138**: 4117–29.

Ibarra, C.A. et al. (2012). Active DNA demethylation in plant companion cells reinforces transposon methylation in gametes. Science **337**: 1360–4.

Ingouff, M. and Berger, F. (2010). Histone3 variants in plants. Chromosoma **119**: 27–33.

Ingouff, M., Hamamura, Y., Gourgues, M., Higashiyama, T., and Berger, F. (2007). Distinct dynamics of HISTONE3 variants between the two fertilization products in plants. Curr. Biol. **17**: 1032–7.

Ingouff, M., Rademacher, S., Holec, S., Soljić, L., Xin, N., Readshaw, A., Foo, S.H., Lahouze, B., Sprunck, S., and Berger, F. (2010). Zygotic resetting of the HISTONE 3 variant repertoire participates in epigenetic reprogramming in Arabidopsis. Curr. Biol. **20**: 2137–43.

Ishii, T. and Houben, A. (2014). How to eliminate a partner for good. Cell Cycle **13**: 1368–9.

Ito, H., Gaubert, H., Bucher, E., Mirouze, M., Vaillant, I., and Paszkowski, J. (2011). An siRNA pathway prevents transgenerational retrotransposition in plants subjected to stress. Nature **472**: 115–9.

Iwasaki, M. and Paszkowski, J. (2014). Identification of genes preventing transgenerational transmission of stress-induced epigenetic states. Proc. Natl. Acad. Sci. U. S. A. **111**: 8547–52.

Jackson, J.P., Johnson, L., Jasencakova, Z., Zhang, X., PerezBurgos, L., Singh, P.B., Cheng, X., Schubert, I., Jenuwein, T., and Jacobsen, S.E. (2004). Dimethylation of histone H3 lysine 9 is a critical mark for DNA methylation and gene silencing in Arabidopsis thaliana. Chromosoma **112**: 308–15.

Jackson, J.P., Lindroth, A.M., Cao, X., and Jacobsen, S.E. (2002). Control of CpNpG DNA methylation by the KRYPTONITE histone H3 methyltransferase. Nature **416**: 556–60.

Jackson, V. (1990). In vivo studies on the dynamics of histone-DNA interaction: evidence for nucleosome dissolution during replication and transcription and a low level of dissolution independent of both. Biochemistry **29**: 719–31.

Jacob, Y., Bergamin, E., Donoghue, M.T.A., Mongeon, V., LeBlanc, C., Voigt, P., Underwood, C.J., Brunzelle, J.S., Michaels, S.D., Reinberg, D., Couture, J.-F., and Martienssen, R.A. (2014). Selective methylation of histone H3 variant H3.1 regulates heterochromatin replication. Science **343**: 1249–53.

Jacob, Y., Feng, S., LeBlanc, C.A., Bernatavichute, Y. V, Stroud, H., Cokus, S., Johnson, L.M., Pellegrini, M., Jacobsen, S.E., and Michaels, S.D. (2009). ATXR5 and ATXR6 are H3K27 monomethyltransferases required for chromatin structure and gene silencing. Nat. Struct. Mol. Biol. **16**: 763–8.

Jacob, Y., Stroud, H., Leblanc, C., Feng, S., Zhuo, L., Caro, E., Hassel, C., Gutierrez, C., Michaels, S.D., and Jacobsen, S.E. (2010). Regulation of

heterochromatic DNA replication by histone H3 lysine 27 methyltransferases. Nature **466**: 987–91.

Jansen, L.E.T., Black, B.E., Foltz, D.R., and Cleveland, D.W. (2007). Propagation of centromeric chromatin requires exit from mitosis. J. Cell Biol. **176**: 795–805.

Jarillo, J.A., Piñeiro, M., Cubas, P., and Martínez-Zapater, J.M. (2009). Chromatin remodeling in plant development. Int. J. Dev. Biol. **53**: 1581–96.

Jasencakova, Z., Scharf, A.N.D., Ask, K., Corpet, A., Imhof, A., Almouzni, G., and Groth, A. (2010). Replication stress interferes with histone recycling and predeposition marking of new histones. Mol. Cell **37**: 736–43.

Jasencakova, Z., Soppe, W.J.J., Meister, A., Gernand, D., Turner, B.M., and Schubert, I. (2003). Histone modifications in Arabidopsis- high methylation of H3 lysine 9 is dispensable for constitutive heterochromatin. Plant J. **33**: 471–480.

Jeddeloh, J.A., Stokes, T.L., and Richards, E.J. (1999). Maintenance of genomic methylation requires a SWI2/SNF2-like protein. Nat. Genet. **22**: 94–7.

Jeppesen, P., Mitchell, A., Turner, B., and Perry, P. (1992). Antibodies to defined histone epitopes reveal variations in chromatin conformation and underacetylation of centric heterochromatin in human metaphase chromosomes. Chromosoma **101**: 322–332.

Jin, C. and Felsenfeld, G. (2007). Nucleosome stability mediated by histone variants H3.3 and H2A.Z. Genes Dev. **21**: 1519–29.

Jin, C., Zang, C., Wei, G., Cui, K., Peng, W., Zhao, K., and Felsenfeld, G. (2009). H3.3/H2A.Z double variant-containing nucleosomes mark “nucleosome-free regions” of active promoters and other regulatory regions. Nat. Genet. **41**: 941–5.

Johnson, L., Mollah, S., Garcia, B.A., Muratore, T.L., Shabanowitz, J., Hunt, D.F., and Jacobsen, S.E. (2004). Mass spectrometry analysis of Arabidopsis histone H3 reveals distinct combinations of post-translational modifications. Nucleic Acids Res. **32**: 6511–8.

Johnson, L.L.M., Bostick, M., Zhang, X., Kraft, E., Henderson, I., Callis, J., and Jacobsen, S.E. (2007). The SRA methyl-cytosine-binding domain links DNA and histone methylation. Curr. Biol. **17**: 379–384.

Joseph, A., Mitchell, A.R., and Miller, O.J. (1989). The organization of the mouse satellite DNA at centromeres. Exp. Cell Res. **183**: 494–500.

Joti, Y., Hikima, T., Nishino, Y., Kamada, F., Hihara, S., Takata, H., Ishikawa, T., and Maeshima, K. (2012). Chromosomes without a 30-nm chromatin fiber. Nucleus **3**: 404–10.

Kalmárová, M., Smirnov, E., Kovácik, L., Popov, A., and Raska, I. (2008). Positioning of the NOR-bearing chromosomes in relation to nucleoli in daughter cells after mitosis. Physiol. Res. **57**: 421–5.

Kanellopoulou, C., Muljo, S.A., Kung, A.L., Ganesan, S., Drapkin, R., Jenuwein, T., Livingston, D.M., and Rajewsky, K. (2005). Dicer-deficient mouse embryonic stem cells are defective in differentiation and centromeric silencing. Genes Dev. **19**: 489–501.

Kanno, T., Huettel, B., Mette, M.F., Aufsatz, W., Jaligot, E., Daxinger, L., Kreil, D.P., Matzke, M., and Matzke, A.J.M. (2005). Atypical RNA polymerase subunits required for RNA-directed DNA methylation. Nat. Genet. **37**: 761–5.

Kanno, T., Mette, M., Kreil, D., and Aufsatz, W. (2004). Involvement of putative SNF2 chromatin remodeling protein DRD1 in RNA-directed DNA methylation. Curr. Biol. **14**: 801–805.

Kappes, F., Burger, K., Baack, M., Fackelmayer, F.O., and Gruss, C. (2001). Subcellular localization of the human proto-oncogene protein DEK. J. Biol. Chem. **276**: 26317–23.

Kappes, F., Waldmann, T., Mathew, V., Yu, J., Zhang, L., Khodadoust, M.S., Chinnaiyan, A.M., Luger, K., Erhardt, S., Schneider, R., and Markovitz, D.M. (2011). The DEK oncoprotein is a Su(var) that is essential to heterochromatin integrity. Genes Dev. **25**: 673–8.

Karachentsev, D., Sarma, K., Reinberg, D., and Steward, R. (2005). PR-Set7-dependent methylation of histone H4 Lys 20 functions in repression of gene expression and is essential for mitosis. Genes Dev. **19**: 431–5.

Karpen, G.H. and Allshire, R.C. (1997). The case for epigenetic effects on centromere identity and function. Trends Genet. **13**: 489–96.

Kato, N. and Lam, E. (2003). Chromatin of endoreduplicated pavement cells has greater range of movement than that of diploid guard cells in Arabidopsis thaliana. J. Cell Sci. **116**: 2195–201.

Kaufman, P., Cohen, J., and Osley, M. (1998). Hir Proteins Are Required for Position-Dependent Gene Silencing in Saccharomyces cerevisiae in the Absence of Chromatin Assembly Factor I. Mol. Cell. Biol. **18**: 4793–806.

Kaufman, P.D., Kobayashi, R., Kessler, N., and Stillman, B. (1995). The p150 and p60 subunits of chromatin assembly factor I: a molecular link between newly synthesized histones and DNA replication. Cell **81**: 1105–14.

Kaufman, P.D., Kobayashi, R., and Stillman, B. (1997). Ultraviolet radiation sensitivity and reduction of telomeric silencing in Saccharomyces cerevisiae cells lacking chromatin assembly factor-I. Genes Dev. **11**: 345–357.

Kaya, H., Shibahara, K., Taoka, K., and Iwabuchi, M. (2001). FASCIATA Genes for Chromatin Assembly Factor-1 in Arabidopsis Maintain the Cellular Organization of Apical Meristems. Cell **104**: 131–142.

Kharchenko, P. V et al. (2011). Comprehensive analysis of the chromatin landscape in Drosophila melanogaster. Nature **471**: 480–5.

Kimura, H. and Cook, P.R. (2001). Kinetics of core histones in living human cells: little exchange of H3 and H4 and some rapid exchange of H2B. J. Cell Biol. **153**: 1341–53.

Kirik, A., Pecinka, A., Wendeler, E., and Reiss, B. (2006). The chromatin assembly factor subunit FASCIATA1 is involved in homologous recombination in plants. Plant Cell **18**: 2431–2442.

Klapholz, B., Dietrich, B.H., Schaffner, C., Hérédia, F., Quivy, J.-P., Almouzni, G., and Dostatni, N. (2009). CAF-1 is required for efficient replication of euchromatic DNA in Drosophila larval endocycling cells. Chromosoma **118**: 235–48.

Köhler, C., Hennig, L., Bouveret, R., Gheyselinck, J., Grossniklaus, U., and Gruissem, W. (2003). Arabidopsis MSI1 is a component of the MEA/FIE Polycomb group complex and required for seed development. EMBO J. **22**: 4804–14.

Kondorosi, E., Roudier, F., and Gendreau, E. (2000). Plant cell-size control: growing by ploidy? Curr. Opin. Plant Biol. **3**: 488–92.

De Koning, L., Corpet, A., Haber, J.E., and Almouzni, G. (2007). Histone chaperones: an escort network regulating histone traffic. Nat. Struct. Mol. Biol. **14**: 997–1007.

Koukalova, B., Fojtova, M., Lim, K.Y., Fulnecek, J., Leitch, A.R., and Kovarik, A. (2005). Dedifferentiation of tobacco cells is associated with ribosomal RNA gene

hypomethylation, increased transcription, and chromatin alterations. Plant Physiol. **139**: 275–86.

Kouzarides, T. (2007). Chromatin modifications and their function. Cell **128**: 693–705.

Kozubek, S., Lukásová, E., Jirsová, P., Koutná, I., Kozubek, M., Ganová, A., Bártová, E., Falk, M., and Paseková, R. (2002). 3D Structure of the human genome: order in randomness. Chromosoma **111**: 321–31.

Kraushaar, D.C., Jin, W., Maunakea, A., Abraham, B., Ha, M., and Zhao, K. (2013). Genome-wide incorporation dynamics reveal distinct categories of turnover for the histone variant H3.3. Genome Biol. **14**: R121.

Krawitz, D., Kama, T., and Kaufman, P. (2002). Chromatin Assembly Factor I Mutants Defective for PCNA Binding Require Asf1 / Hir Proteins for Silencing. Mol. Cell. Biol. **22**.

Krouwels, I.M., Wiesmeijer, K., Abraham, T.E., Molenaar, C., Verwoerd, N.P., Tanke, H.J., and Dirks, R.W. (2005). A glue for heterochromatin maintenance: stable SUV39H1 binding to heterochromatin is reinforced by the SET domain. J. Cell Biol. **170**: 537–49.

Krude, T. (1999). Chromatin assembly during DNA replication in somatic cells. Eur. J. Biochem. **263**: 1–5.

Kumekawa, N., Hosouchi, T., Tsuruoka, H., and Kotani, H. (2000). The size and sequence organization of the centromeric region of arabidopsis thaliana chromosome 5. DNA Res. **7**: 315–321.

Küpper, K., Kölbl, A., Biener, D., Dittrich, S., von Hase, J., Thormeyer, T., Fiegler, H., Carter, N.P., Speicher, M.R., Cremer, T., and Cremer, M. (2007). Radial chromatin positioning is shaped by local gene density, not by gene expression. Chromosoma **116**: 285–306.

Kuzmichev, A., Nishioka, K., Erdjument-Bromage, H., Tempst, P., and Reinberg, D. (2002). Histone methyltransferase activity associated with a human multiprotein complex containing the Enhancer of Zeste protein. Genes Dev. **16**: 2893–905.

Kuznetsova, I., Podgornaya, O., and Ferguson-Smith, M.A. (2006). High-resolution organization of mouse centromeric and pericentromeric DNA. Cytogenet. Genome Res. **112**: 248–55.

Lang-Mladek, C., Popova, O., Kiok, K., Berlinger, M., Rakic, B., Aufsatz, W., Jonak, C., Hauser, M.-T., and Luschnig, C. (2010). Transgenerational inheritance and resetting of stress-induced loss of epigenetic gene silencing in Arabidopsis. Mol. Plant **3**: 594–602.

Lario, L.D., Ramirez-Parra, E., Gutierrez, C., Spampinato, C.P., and Casati, P. (2013). ANTI-SILENCING FUNCTION1 proteins are involved in ultraviolet-induced DNA damage repair and are cell cycle regulated by E2F transcription factors in Arabidopsis. Plant Physiol. **162**: 1164–77.

Larkins, B.A., Dilkes, B.P., Dante, R.A., Coelho, C.M., Woo, Y.M., and Liu, Y. (2001). Investigating the hows and whys of DNA endoreduplication. J. Exp. Bot. **52**: 183–92.

Law, J.A., Du, J., Hale, C.J., Feng, S., Krajewski, K., Palanca, A.M.S., Strahl, B.D., Patel, D.J., and Jacobsen, S.E. (2013). Polymerase IV occupancy at RNA-directed DNA methylation sites requires SHH1. Nature **498**: 385–9.

Law, J.A. and Jacobsen, S.E. (2010). Establishing, maintaining and modifying DNA methylation patterns in plants and animals. Nat. Rev. Genet. **11**: 204–20.

Layat, E., Cotterell, S., Vaillant, I., Yukawa, Y., Tutois, S., and Tourmente, S. (2012a). Transcript levels, alternative splicing and proteolytic cleavage of TFIIIA control 5S rRNA accumulation during Arabidopsis thaliana development. Plant J. **71**: 35–44.

Layat, E., Saez-Vasquez, J., and Tourmente, S. (2012b). Regulation of Pol I-Transcribed 45S rDNA and Pol III-Transcribed 5S rDNA in Arabidopsis. Plant Cell Physiol. **53**: 267–276.

Le, S., Davis, C., Konopka, J.B., and Sternglanz, R. (1997). Two new S-phase-specific genes from Saccharomyces cerevisiae. Yeast **13**: 1029–42.

Lehnertz, B., Ueda, Y., Derijck, A.A.H.A., Braunschweig, U., Perez-Burgos, L., Kubicek, S., Chen, T., Li, E., Jenuwein, T., and Peters, A.H.F.M. (2003). Suv39h-mediated histone H3 lysine 9 methylation directs DNA methylation to major satellite repeats at pericentric heterochromatin. Curr. Biol. **13**: 1192–200.

Lermontova, I., Koroleva, O., Rutten, T., Fuchs, J., Schubert, V., Moraes, I., Koszegi, D., and Schubert, I. (2011). Knockdown of CENH3 in Arabidopsis reduces mitotic divisions and causes sterility by disturbed meiotic chromosome segregation. Plant J. **68**: 40–50.

Lermontova, I., Schubert, V., Fuchs, J., Klatte, S., Macas, J., and Schubert, I. (2006). Loading of Arabidopsis centromeric histone CENH3 occurs mainly during G2 and requires the presence of the histone fold domain. Plant Cell **18**: 2443–51.

Lewis, P.W., Elsaesser, S.J., Noh, K.-M.M., Stadler, S.C., and Allis, C.D. (2010). Daxx is an H3.3-specific histone chaperone and cooperates with ATRX in replication-independent chromatin assembly at telomeres. Proc. Natl. Acad. Sci. U. S. A. **107**: 14075–14080.

Leyser, H. and Furner, I. (1992). Characterisation of three shoot apical meristem mutants of Arabidopsis thaliana. Development **403**: 397–403.

Libault, M., Tessadori, F., Germann, S., Snijder, B., Fransz, P., and Gaudin, V. (2005). The Arabidopsis LHP1 protein is a component of euchromatin. Planta **222**: 910–925.

Lieberman-Aiden, E. et al. (2009). Comprehensive mapping of long-range interactions reveals folding principles of the human genome. Science **326**: 289–93.

Lim, C.Y., Reversade, B., Knowles, B.B., and Solter, D. (2013). Optimal histone H3 to linker histone H1 chromatin ratio is vital for mesodermal competence in Xenopus. Development **140**: 853–60.

Lindroth, A.M. et al. (2004). Dual histone H3 methylation marks at lysines 9 and 27 required for interaction with CHROMOMETHYLASE3. EMBO J. **23**: 4286–96.

Lindroth, A.M., Cao, X., Jackson, J.P., Zilberman, D., McCallum, C.M., Henikoff, S., and Jacobsen, S.E. (2001). Requirement of CHROMOMETHYLASE3 for maintenance of CpXpG methylation. Science **292**: 2077–80.

Lippman, Z. et al. (2004). Role of transposable elements in heterochromatin and epigenetic control. Nature **430**: 471–6.

Lippman, Z. and Martienssen, R. (2004). The role of RNA interference in heterochromatic silencing. Nature **431**: 364–70.

Lister, R. et al. (2009). Human DNA methylomes at base resolution show widespread epigenomic differences. Nature **462**: 315–22.

Lister, R., O'Malley, R.C., Tonti-Filippini, J., Gregory, B.D., Berry, C.C., Millar, A.H., and Ecker, J.R. (2008). Highly integrated single-base resolution maps of the epigenome in Arabidopsis. Cell **133**: 523–36.

Liu, C., Thong, Z., and Yu, H. (2009). Coming into bloom: the specification of floral meristems. Development **136**: 3379–91.

Lohe, A., Hilliker, A., and Roberts, P. (1993). Mapping simple repeated DNA sequences in heterochromatin of Drosophila melanogaster. Trends Genet. **9**: 379.

López-Fernández, L.A., López-Alañón, D.M., Castañeda, V., Krimer, D.B., and del Mazo, J. (1997). Developmental expression of H3.3A variant histone mRNA in mouse. Int. J. Dev. Biol. **41**: 699–703.

Loppin, B., Bonnefoy, E., Anselme, C., Laurençon, A., Karr, T.L., and Couble, P. (2005). The histone H3.3 chaperone HIRA is essential for chromatin assembly in the male pronucleus. Nature **437**: 1386–1390.

Loyola, A. and Almouzni, G. (2007). Marking histone H3 variants: how, when and why? Trends Biochem. Sci. **32**: 425–433.

Loyola, A., Bonaldi, T., Roche, D., Imhof, A., and Almouzni, G. (2006). PTMs on H3 variants before chromatin assembly potentiate their final epigenetic state. Mol. Cell **24**: 309–316.

Loyola, A., Tagami, H., Bonaldi, T., Roche, D., Quivy, J.P., Imhof, A., Nakatani, Y., Dent, S.Y.R., and Almouzni, G. (2009). The HP1alpha-CAF1-SetDB1-containing complex provides H3K9me1 for Suv39-mediated K9me3 in pericentric heterochromatin. EMBO Rep. **10**: 769–75.

Lu, X., Wontakal, S.N., Kavi, H., Kim, B.J., Guzzardo, P.M., Emelyanov, A. V, Xu, N., Hannon, G.J., Zavadil, J., Fyodorov, D. V, and Skoultchi, A.I. (2013). Drosophila H1 regulates the genetic activity of heterochromatin by recruitment of Su(var)3-9. Science **340**: 78–81.

Luger, K. (2001). Nucleosomes: Structure and Function. eLS: 1–8.

Luger, K., Mäder, A., and Richmond, R. (1997). Crystal structure of the nucleosome core particle at 2 . 8 A resolution. Nature **7**: 251–260.

Lyko, F., Ramsahoye, B., and Jaenisch, R. (1999). DNA methylation in Drosophila melanogaster. Dev. Dyn. **216**: 1.

MacAlpine, H.K., Gordân, R., Powell, S.K., Hartemink, A.J., and MacAlpine, D.M. (2010). Drosophila ORC localizes to open chromatin and marks sites of cohesin complex loading. Genome Res. **20**: 201–11.

Maeshima, K., Hihara, S., and Eltsov, M. (2010). Chromatin structure: does the 30-nm fibre exist in vivo? Curr. Opin. Cell Biol. **22**: 291–7.

Maeshima, K., Imai, R., Tamura, S., and Nozaki, T. (2014). Chromatin as dynamic 10-nm fibers. Chromosoma **123**: 225–37.

Magnani, E., Bartling, L., and Hake, S. (2006). From Gateway to MultiSite Gateway in one recombination event. BMC Mol. Biol. **7**: 46.

Maison, C. and Almouzni, G. (2004). HP1 and the dynamics of heterochromatin maintenance. Nat. Rev. Mol. Cell Biol. **5**: 296–304.

Maison, C., Bailly, D., Peters, A.H.F.M., Quivy, J.-P., Roche, D., Taddei, A., Lachner, M., Jenuwein, T., and Almouzni, G. (2002). Higher-order structure in pericentric heterochromatin involves a distinct pattern of histone modification and an RNA component. Nat. Genet. **30**: 329–34.

Malagnac, F., Bartee, L., and Bender, J. (2002). An Arabidopsis SET domain protein required for maintenance but not establishment of DNA methylation. EMBO J. **21**: 6842–52.

Malay, A.D., Umehara, T., Matsubara-Malay, K., Padmanabhan, B., and Yokoyama, S. (2008). Crystal structures of fission yeast histone chaperone Asf1

complexed with the Hip1 B-domain or the Cac2 C terminus. J. Biol. Chem. **283**: 14022–31.

Malik, H.S. and Henikoff, S. (2001). Adaptive evolution of Cid, a centromere-specific histone in Drosophila. Genetics **157**: 1293–8.

Malik, H.S. and Henikoff, S. (2003). Phylogenomics of the nucleosome. Nat. Struct. Biol. **10**: 882–91.

Martens, J.H.A., O'Sullivan, R.J., Braunschweig, U., Opravil, S., Radolf, M., Steinlein, P., and Jenuwein, T. (2005). The profile of repeat-associated histone lysine methylation states in the mouse epigenome. EMBO J. **24**: 800–12.

Martínez-Balbás, M.A., Tsukiyama, T., Gdula, D., and Wu, C. (1998). Drosophila NURF-55, a WD repeat protein involved in histone metabolism. Proc. Natl. Acad. Sci. U. S. A. **95**: 132–7.

Martini, E., Roche, D.M., Marheineke, K., Verreault, A., and Almouzni, G. (1998). Recruitment of phosphorylated chromatin assembly factor 1 to chromatin after UV irradiation of human cells. J. Cell Biol. **143**: 563–75.

Marzluff, W.F., Gongidi, P., Woods, K.R., Jin, J., and Maltais, L.J. (2002). The Human and Mouse Replication-Dependent Histone Genes. Genomics **80**: 487–498.

Mathieu, O., Jasencakova, Z., Vaillant, I., Gendrel, A.V.A.-V., Colot, V., Schubert, I., and Tourmente, S. (2003). Changes in 5S rDNA chromatin organization and transcription during heterochromatin establishment in Arabidopsis. Plant Cell **15**: 2929–2939.

Mathieu, O., Probst, A. V, and Paszkowski, J. (2005). Distinct regulation of histone H3 methylation at lysines 27 and 9 by CpG methylation in Arabidopsis. EMBO J. **24**: 2783–2791.

May, B.P., Lippman, Z.B., Fang, Y., Spector, D.L., and Martienssen, R.A. (2005). Differential regulation of strand-specific transcripts from Arabidopsis centromeric satellite repeats. PLoS Genet. **1**: e79.

McDowell, T.L. et al. (1999). Localization of a putative transcriptional regulator (ATRX) at pericentromeric heterochromatin and the short arms of acrocentric chromosomes. Proc. Natl. Acad. Sci. U. S. A. **96**: 13983–8.

McKittrick, E., Gafken, P.R., Ahmad, K., and Henikoff, S. (2004). Histone H3.3 is enriched in covalent modifications associated with active chromatin. Proc. Natl. Acad. Sci. U. S. A. **101**: 1525–30.

Mello, J.A., Silljé, H.H.W., Roche, D.M.J., Kirschner, D.B., Nigg, E.A., and Almouzni, G. (2002). Human Asf1 and CAF-1 interact and synergize in a repair-coupled nucleosome assembly pathway. EMBO Rep. **3**: 329–34.

Menges, M., Hennig, L., Gruissem, W., and Murray, J. (2003). Genome-wide gene expression in an Arabidopsis cell suspension. Plant Mol. Biol.: 423–442.

Meshi, T., Taoka, K.I., and Iwabuchi, M. (2000). Regulation of histone gene expression during the cell cycle. Plant Mol. Biol. **43**: 643–57.

Michaelson, J.S., Bader, D., Kuo, F., Kozak, C., and Leder, P. (1999). Loss of Daxx, a promiscuously interacting protein, results in extensive apoptosis in early mouse development. Genes Dev. **13**: 1918–23.

Miklos, G.L. and Cotsell, J.N. (1990). Chromosome structure at interfaces between major chromatin types: alpha- and beta-heterochromatin. Bioessays **12**: 1–6.

Mito, Y., Henikoff, J.G., and Henikoff, S. (2005). Genome-scale profiling of histone H3.3 replacement patterns. Nat. Genet. **37**: 1090–7.

Mittelsten Scheid, O., Probst, A. V, Afsar, K., and Paszkowski, J. (2002). Two regulatory levels of transcriptional gene silencing in Arabidopsis. Proc. Natl. Acad. Sci. U. S. A. **99**: 13659–13662.

Moggs, J.G., Grandi, P., Quivy, J.-P., Jonsson, Z.O., Hubscher, U., Becker, P.B., and Almouzni, G. (2000). A CAF-1-PCNA-Mediated Chromatin Assembly Pathway Triggered by Sensing DNA Damage. Mol. Cell. Biol. **20**: 1206–1218.

Mohd-Sarip, A. and Verrijzer, C.P. (2004). Molecular biology. A higher order of silence. Science **306**: 1484–5.

Moissiard, G. et al. (2012). MORC family ATPases required for heterochromatin condensation and gene silencing. Science **336**: 1448–51.

Moissiard, G., Bischof, S., Husmann, D., Pastor, W.A., Hale, C.J., Yen, L., Stroud, H., Papikian, A., Vashisht, A.A., Wohlschlegel, J.A., and Jacobsen, S.E. (2014). Transcriptional gene silencing by Arabidopsis microrchidia homologues involves the formation of heteromers. Proc. Natl. Acad. Sci. U. S. A. **111**: 7474–9.

Monson, E.K., de Bruin, D., and Zakian, V.A. (1997). The yeast Cac1 protein is required for the stable inheritance of transcriptionally repressed chromatin at telomeres. Proc. Natl. Acad. Sci. U. S. A. **94**: 13081–6.

Morales, V., Giamarchi, C., Chailleux, C., Moro, F., Marsaud, V., Le Ricousse, S., and Richard-Foy, H. (2001). Chromatin structure and dynamics: functional implications. Biochimie **83**: 1029–39.

Moshkin, Y.M., Armstrong, J.A., Maeda, R.K., Tamkun, J.W., Verrijzer, P., Kennison, J.A., and Karch, F. (2002). Histone chaperone ASF1 cooperates with the Brahma chromatin-remodelling machinery. Genes Dev. **16**: 2621–6.

Mousson, F., Lautrette, A., Thuret, J.-Y., Agez, M., Courbeyrette, R., Amigues, B., Becker, E., Neumann, J.-M., Guerois, R., Mann, C., and Ochsenbein, F. (2005). Structural basis for the interaction of Asf1 with histone H3 and its functional implications. Proc. Natl. Acad. Sci. U. S. A. **102**: 5975–80.

Mousson, F., Ochsenbein, F., and Mann, C. (2007). The histone chaperone Asf1 at the crossroads of chromatin and DNA checkpoint pathways. Chromosoma **116**: 79–93.

Munakata, T., Adachi, N., Yokoyama, N., Kuzuhara, T., and Horikoshi, M. (2000). A human homologue of yeast anti-silencing factor has histone chaperone activity. Genes Cells **5**: 221–33.

Murzina, N., Verreault, A., Laue, E., and Stillman, B. (1999). Heterochromatin dynamics in mouse cells: interaction between chromatin assembly factor 1 and HP1 proteins. Mol. Cell **4**: 529–40.

Myung, K., Pennaneach, V., Kats, E.S., and Kolodner, R.D. (2003). Saccharomyces cerevisiae chromatin-assembly factors that act during DNA replication function in the maintenance of genome stability. Proc. Natl. Acad. Sci. U. S. A. **100**: 6640–5.

Nabatiyan, A. and Krude, T. (2004). Silencing of chromatin assembly factor 1 in human cells leads to cell death and loss of chromatin assembly during DNA synthesis. Mol. Cell. Biol. **24**: 2853–62.

Nagaki, K., Talbert, P.B., Zhong, C.X., Dawe, R.K., Henikoff, S., and Jiang, J. (2003). Chromatin immunoprecipitation reveals that the 180-bp satellite repeat is the key functional DNA element of Arabidopsis thaliana centromeres. Genetics **163**: 1221–1225.

Nakano, S., Stillman, B., and Horvitz, H. (2011). Replication-Coupled Chromatin Assembly Generates a Neuronal Bilateral Asymmetry in C. elegans. Cell **147**: 1525–1536.

Nakayama, J., Rice, J.C., Strahl, B.D., Allis, C.D., and Grewal, S.I. (2001). Role of histone H3 lysine 9 methylation in epigenetic control of heterochromatin assembly. Science **292**: 110–3.

Nakayama, T., Nishioka, K., Dong, Y.-X., Shimojima, T., and Hirose, S. (2007). Drosophila GAGA factor directs histone H3.3 replacement that prevents the heterochromatin spreading. Genes Dev. **21**: 552–61.

Narita, M., Nuñez, S., and Heard, E. (2003). Rb-Mediated Heterochromatin Formation and Silencing of E2F Target Genes during Cellular Senescence. Cell **113**: 703–716.

Natsume, R., Eitoku, M., Akai, Y., Sano, N., Horikoshi, M., and Senda, T. (2007). Structure and function of the histone chaperone CIA/ASF1 complexed with histones H3 and H4. Nature **446**: 338–41.

Naumann, K., Fischer, A., Hofmann, I., Krauss, V., Phalke, S., Irmler, K., Hause, G., Aurich, A.-C., Dorn, R., Jenuwein, T., and Reuter, G. (2005). Pivotal role of AtSUVH2 in heterochromatic histone methylation and gene silencing in Arabidopsis. EMBO J. **24**: 1418–29.

Naumann, U., Daxinger, L., Kanno, T., Eun, C., Long, Q., Lorkovic, Z.J., Matzke, M., and Matzke, A.J.M. (2011). Genetic evidence that DNA methyltransferase DRM2 has a direct catalytic role in RNA-directed DNA methylation in Arabidopsis thaliana. Genetics **187**: 977–9.

Nicolas, E., Ait-Si-Ali, S., and Trouche, D. (2001). The histone deacetylase HDAC3 targets RbAp48 to the retinoblastoma protein. Nucleic Acids Res. **29**: 3131–6.

Nie, X., Wang, H., Li, J., Holec, S., and Berger, F. (2014). The HIRA complex that deposits the histone H3.3 is conserved in Arabidopsis and facilitates transcriptional dynamics. Biol. Open: 1–9.

Numa, H. et al. (2010). Transduction of RNA-directed DNA methylation signals to repressive histone marks in Arabidopsis thaliana. EMBO J. **29**: 352–62.

Okada, T., Endo, M., Singh, M.B., and Bhalla, P.L. (2005). Analysis of the histone H3 gene family in Arabidopsis and identification of the male-gamete-specific variant AtMGH3. Plant J. **44**: 557–568.

Ondrej, V., Kitner, M., Dolezalová, I., Nádvorník, P., Navrátilová, B., and Lebeda, A. (2009). Chromatin structural rearrangement during dedifferentiation of protoplasts of Cucumis sativus L. Mol. Cells **27**: 443–7.

Ono, T., Kaya, H., Takeda, S., Abe, M., Ogawa, Y., Kato, M., Kakutani, T., Mittelsten Scheid, O., Araki, T., and Shibahara, K. (2006). Chromatin assembly factor 1 ensures the stable maintenance of silent chromatin states in Arabidopsis. Genes Cells **11**: 153–62.

Onodera, Y., Haag, J.R., Ream, T., Costa Nunes, P., Pontes, O., and Pikaard, C.S. (2005). Plant nuclear RNA polymerase IV mediates siRNA and DNA methylation-dependent heterochromatin formation. Cell **120**: 613–22.

Ooi, S.L., Henikoff, J.G., and Henikoff, S. (2010). A native chromatin purification system for epigenomic profiling in Caenorhabditis elegans. Nucleic Acids Res. **38**: e26.

Orsi, G.A., Algazeery, A., Meyer, R.E., Capri, M., Sapey-Triomphe, L.M., Horard, B., Gruffat, H., Couble, P., Aït-Ahmed, O., and Loppin, B. (2013). Drosophila Yemanuclein and HIRA cooperate for de novo assembly of H3.3-containing nucleosomes in the male pronucleus. PLoS Genet. **9**: e1003285.

Orsi, G.A., Couble, P., and Loppin, B. (2009). Epigenetic and replacement roles of histone variant H3.3 in reproduction and development. Int. J. Dev. Biol. **53**: 231–43.

Osley, M.A. and Lycan, D. (1987). Trans-acting regulatory mutations that alter transcription of Saccharomyces cerevisiae histone genes. Mol. Cell. Biol. **7**: 4204–10.

Ossowski, S., Schwab, R., and Weigel, D. (2008). Gene silencing in plants using artificial microRNAs and other small RNAs. Plant J. **53**: 674.

Palmer, D.K., O'Day, K., Trong, H.L., Charbonneau, H., and Margolis, R.L. (1991). Purification of the centromere-specific protein CENP-A and demonstration that it is a distinctive histone. Proc. Natl. Acad. Sci. U. S. A. **88**: 3734–8.

Palmer, D.K., O'Day, K., Wener, M.H., Andrews, B.S., and Margolis, R.L. (1987). A 17-kD centromere protein (CENP-A) copurifies with nucleosome core particles and with histones. J. Cell Biol. **104**: 805–15.

Pecinka, A., Dinh, H.Q., Baubec, T., Rosa, M., Lettner, N., and Mittelsten Scheid, O. (2010). Epigenetic regulation of repetitive elements is attenuated by prolonged heat stress in Arabidopsis. Plant Cell **22**: 3118–29.

Pecinka, A., Schubert, V., Meister, A., Kreth, G., Klatte, M., Lysak, M.A., Fuchs, J., and Schubert, I. (2004). Chromosome territory arrangement and homologous pairing in nuclei of Arabidopsis thaliana are predominantly random except for NOR-bearing chromosomes. Chromosoma **113**: 258–69.

Pélissier, T., Tutois, S., Tourmente, S., Deragon, J.M., and Picard, G. (1996). DNA regions flanking the major Arabidopsis thaliana satellite are principally enriched in Athila retroelement sequences. Genetica **97**: 141–51.

Penterman, J., Zilberman, D., Huh, J.H., Ballinger, T., Henikoff, S., and Fischer, R.L. (2007). DNA demethylation in the Arabidopsis genome. Proc. Natl. Acad. Sci. U. S. A. **104**: 6752–7.

Peters, A.H. et al. (2001). Loss of the Suv39h histone methyltransferases impairs mammalian heterochromatin and genome stability. Cell **107**: 323–37.

Phelps-Durr, T.L., Thomas, J., Vahab, P., and Timmermans, M.C.P. (2005). Maize rough sheath2 and its Arabidopsis orthologue ASYMMETRIC LEAVES1 interact with HIRA, a predicted histone chaperone, to maintain knox gene silencing and determinacy during organogenesis. Plant Cell **17**: 2886–2898.

Pidoux, A.L. and Allshire, R.C. (2005). The role of heterochromatin in centromere function. Philos. Trans. R. Soc. Lond. B. Biol. Sci. **360**: 569–79.

Pillot, M., Baroux, C., Vazquez, M.A., Autran, D., Leblanc, O., Vielle-Calzada, J.P., Grossniklaus, U., and Grimanelli, D. (2010). Embryo and endosperm inherit distinct chromatin and transcriptional states from the female gametes in Arabidopsis. Plant Cell **22**: 307–20.

Polo, S.E., Roche, D., and Almouzni, G. (2006). New histone incorporation marks sites of UV repair in human cells. Cell **127**: 481–93.

Pontier, D., Yahubyan, G., Vega, D., Bulski, A., Saez-Vasquez, J., Hakimi, M.-A., Lerbs-Mache, S., Colot, V., and Lagrange, T. (2005). Reinforcement of silencing at transposons and highly repeated sequences requires the concerted action of two distinct RNA polymerases IV in Arabidopsis. Genes Dev. **19**: 2030–40.

Pontvianne, F. et al. (2010). Nucleolin is required for DNA methylation state and the expression of rRNA gene variants in Arabidopsis thaliana. PLoS Genet. **6**: e1001225.

Pontvianne, F., Matía, I., Douet, J., Tourmente, S., Medina, F.J., Echeverria, M., and Sáez-Vásquez, J. (2007). Characterization of AtNUC-L1 reveals a central role of nucleolin in nucleolus organization and silencing of AtNUC-L2 gene in Arabidopsis. Mol. Biol. Cell **18**: 369–79.

Prado, F., Cortés-Ledesma, F., and Aguilera, A. (2004). The absence of the yeast chromatin assembly factor Asf1 increases genomic instability and sister chromatid exchange. EMBO Rep. **5**: 497–502.

Probst, A. V, Dunleavy, E., and Almouzni, G. (2009). Epigenetic inheritance during the cell cycle. Nat. Rev. Mol. Cell Biol. **10**: 192–206.

Probst, A. V, Fagard, M., Proux, F., Mourrain, P., Boutet, S., Earley, K., Lawrence, R.J., Pikaard, C.S., Murfett, J., Furner, I., Vaucheret, H., and Mittelsten Scheid, O. (2004). Arabidopsis histone deacetylase HDA6 is required for maintenance of transcriptional gene silencing and determines nuclear organization of rDNA repeats. Plant Cell **16**: 1021–34.

Probst, A. V, Fransz, P.F., Paszkowski, J., and Mittelsten Scheid, O. (2003). Two means of transcriptional reactivation within heterochromatin. Plant J. **33**: 743–749.

Qi, Y., He, X., Wang, X.-J., Kohany, O., Jurka, J., and Hannon, G.J. (2006). Distinct catalytic and non-catalytic roles of ARGONAUTE4 in RNA-directed DNA methylation. Nature **443**: 1008–12.

Qian, Y.-W. and Lee, E.Y.-H.P. (1995). Dual Retinoblastoma-binding Proteins with Properties Related to a Negative Regulator of Ras in Yeast. J. Biol. Chem. **270**: 25507–25513.

Quivy, J.-P., Gérard, A., Cook, A.J.L., Roche, D., and Almouzni, G. (2008). The HP1–p150/CAF-1 interaction is required for pericentric heterochromatin replication and S-phase progression in mouse cells. Nat. Struct. Mol. Biol. **15**: 972–979.

Quivy, J.-P., Roche, D., Kirschner, D., Tagami, H., Nakatani, Y., and Almouzni, G. (2004). A CAF-1 dependent pool of HP1 during heterochromatin duplication. EMBO J. **23**: 3516–26.

Quivy, J.P., Grandi, P., and Almouzni, G. (2001). Dimerization of the largest subunit of chromatin assembly factor 1: importance in vitro and during Xenopus early development. EMBO J. **20**: 2015–27.

Rai, T.S. and Adams, P.D. (2012). Lessons from senescence: Chromatin maintenance in non-proliferating cells. Biochim. Biophys. Acta **1819**: 322–31.

Raissig, M.T., Baroux, C., and Grossniklaus, U. (2011). Regulation and flexibility of genomic imprinting during seed development. Plant Cell **23**: 16–26.

Ramey, C.J., Howar, S., Adkins, M., Linger, J., Spicer, J., and Tyler, J.K. (2004). Activation of the DNA damage checkpoint in yeast lacking the histone chaperone anti-silencing function 1. Mol. Cell. Biol. **24**: 10313–27.

Ramirez-Parra, E. and Gutierrez, C. (2007a). E2F regulates FASCIATA1, a chromatin assembly gene whose loss switches on the endocycle and activates gene expression by changing the epigenetic status. Plant Physiol. **144**: 105–120.

Ramirez-Parra, E. and Gutierrez, C. (2007b). The many faces of chromatin assembly factor 1. Trends Plant Sci. **12**: 570–576.

Ramsahoye, B.H., Biniszkiewicz, D., Lyko, F., Clark, V., Bird, A.P., and Jaenisch, R. (2000). Non-CpG methylation is prevalent in embryonic stem cells and may be mediated by DNA methyltransferase 3a. Proc. Natl. Acad. Sci. U. S. A. **97**: 5237–42.

Ravi, M., Shibata, F., Ramahi, J.S., Nagaki, K., Chen, C., Murata, M., and Chan, S.W.L. (2011). Meiosis-specific loading of the centromere-specific histone CENH3 in Arabidopsis thaliana. PLoS Genet. **7**: e1002121.

Ray-Gallet, D., Quivy, J.-P., Silljé, H.W.W., Nigg, E.A., and Almouzni, G. (2007). The histone chaperone Asf1 is dispensable for direct de novo histone deposition in Xenopus egg extracts. Chromosoma **116**: 487–96.

Ray-Gallet, D., Quivy, J.-P.P., Scamps, C., Martini, E.M.-D., Lipinski, M., and Almouzni, G. (2002). HIRA is critical for a nucleosome assembly pathway independent of DNA synthesis. Mol. Cell **9**: 1091–100.

Ray-Gallet, D., Woolfe, A., Vassias, I., Pellentz, C., Lacoste, N., Puri, A., Schultz, D.C., Pchelintsev, N.A., Adams, P.D., Jansen, L.E.T., and Almouzni, G. (2011). Dynamics of histone H3 deposition in vivo reveal a nucleosome gap-filling mechanism for H3.3 to maintain chromatin integrity. Mol. Cell **44**: 928–41.

Reese, B.E., Bachman, K.E., Baylin, S.B., and Rountree, M.R. (2003). The methyl-CpG binding protein MBD1 interacts with the p150 subunit of chromatin assembly factor 1. Mol. Cell. Biol. **23**: 3226–36.

Reichheld, J.-P., Sonobe, S., Clement, B., Chaubet, N., and Gigot, C. (1995). Cell cycle-regulated histone gene expression in synchronized plant cells. Plant J. **7**: 245–252.

Reichheld, J.P., Gigot, C., and Chaubet-Gigot, N. (1998). Multilevel regulation of histone gene expression during the cell cycle in tobacco cells. Nucleic Acids Res. **26**: 3255–62.

Richards, E. (1991). The centromere region of Arabidopsis thaliana chromosome 1 contains telomere-similar sequences. Nucleic Acids Res. **19**: 3351–3357.

Riddle, N.C. et al. (2011). Plasticity in patterns of histone modifications and chromosomal proteins in Drosophila heterochromatin. Genome Res. **21**: 147–63.

Ridgway, P. and Almouzni, G. (2000). CAF-1 and the inheritance of chromatin states: at the crossroads of DNA replication and repair. J. Cell Sci. **113 (Pt 1**: 2647–58.

Riggs, A., Russo, V., and Martienssen, R. (1996). Epigenetic mechanisms of gene regulation. In Epigenetic Mechanisms of Gene Regulation, V.E.A. Russo, R.A. Martienssen, and A.D. Riggs, eds (Cold Spring Harbor Laboratory Press: New York), pp. 29–54.

Roberts, C., Sutherland, H.F., Farmer, H., Kimber, W., Halford, S., Carey, A., Brickman, J.M., Wynshaw-Boris, A., and Scambler, P.J. (2002). Targeted Mutagenesis of the Hira Gene Results in Gastrulation Defects and Patterning Abnormalities of Mesoendodermal Derivatives Prior to Early Embryonic Lethality. Mol. Cell. Biol. **22**: 2318–2328.

Robinson, P.J.J. and Rhodes, D. (2006). Structure of the “30 nm” chromatin fibre: a key role for the linker histone. Curr. Opin. Struct. Biol. **16**: 336–43.

Rogakou, E.P., Pilch, D.R., Orr, A.H., Ivanova, V.S., and Bonner, W.M. (1998). DNA Double-stranded Breaks Induce Histone H2AX Phosphorylation on Serine 139. J. Biol. Chem. **273**: 5858–5868.

Rogers, R.S., Inselman, A., Handel, M.A., and Matunis, M.J. (2004). SUMO modified proteins localize to the XY body of pachytene spermatocytes. Chromosoma **113**: 233–43.

Roudier, F. et al. (2011). Integrative epigenomic mapping defines four main chromatin states in Arabidopsis. EMBO J. **30**: 1928–38.

Roy, S. et al. (2010). Identification of functional elements and regulatory circuits by Drosophila modENCODE. Science **330**: 1787–97.

Saez-Vasquez, J. and Gadal, O. (2010). Genome Organization and Function: A View from Yeast and Arabidopsis. Mol. Plant **3**: 678–690.

Sakai, A., Schwartz, B.E., Goldstein, S., and Ahmad, K. (2009). Transcriptional and developmental functions of the H3.3 histone variant in Drosophila. Curr. Biol. **19**: 1816–20.

Salomoni, P. and Khelifi, A.F. (2006). Daxx: death or survival protein? Trends Cell Biol. **16**: 97–104.

Sanematsu, F., Takami, Y., Barman, H.K., Fukagawa, T., Ono, T., Shibahara, K.-I., and Nakayama, T. (2006). Asf1 is required for viability and chromatin assembly during DNA replication in vertebrate cells. J. Biol. Chem. **281**: 13817–27.

Santenard, A., Ziegler-Birling, C., Koch, M., Tora, L., Bannister, A.J., and Torres-Padilla, M.-E. (2010). Heterochromatin formation in the mouse embryo requires critical residues of the histone variant H3.3. Nat. Cell Biol. **12**: 853–62.

Santos, A.P. and Shaw, P. (2004). Interphase chromosomes and the Rabl configuration: does genome size matter? J. Microsc. **214**: 201–6.

Sarraf, S.A. and Stancheva, I. (2004). Methyl-CpG binding protein MBD1 couples histone H3 methylation at lysine 9 by SETDB1 to DNA replication and chromatin assembly. Mol. Cell **15**: 595–605.

Sawatsubashi, S. et al. (2010). A histone chaperone, DEK, transcriptionally coactivates a nuclear receptor. Genes Dev. **24**: 159–70.

Saze, H., Mittelsten Scheid, O., and Paszkowski, J. (2003). Maintenance of CpG methylation is essential for epigenetic inheritance during plant gametogenesis. Nat. Genet. **34**: 65–9.

Scheuermann, M.O., Tajbakhsh, J., Kurz, A., Saracoglu, K., Eils, R., and Lichter, P. (2004). Topology of genes and nontranscribed sequences in human interphase nuclei. Exp. Cell Res. **301**: 266–79.

Schmid, M., Uhlenhaut, N.H., Godard, F., Demar, M., Bressan, R., Weigel, D., and Lohmann, J.U. (2003). Dissection of floral induction pathways using global expression analysis. Development **130**: 6001–6012.

Schneiderman, J.I., Orsi, G.A., Hughes, K.T., Loppin, B., and Ahmad, K. (2012). Nucleosome-depleted chromatin gaps recruit assembly factors for the H3 . 3 histone variant. Proc. Natl. Acad. Sci. U. S. A. **109**: 19721–6.

Schoeftner, S. and Blasco, M.A. (2009). A “higher order” of telomere regulation: telomere heterochromatin and telomeric RNAs. EMBO J. **28**: 2323–36.

Schönrock, N., Exner, V., Probst, A., Gruissem, W., and Hennig, L. (2006). Functional genomic analysis of CAF-1 mutants in Arabidopsis thaliana. J. Biol. Chem. **281**: 9560–9568.

Schotta, G., Ebert, A., Krauss, V., Fischer, A., Hoffmann, J., Rea, S., Jenuwein, T., Dorn, R., and Reuter, G. (2002). Central role of Drosophila SU(VAR)3-9 in histone H3-K9 methylation and heterochromatic gene silencing. EMBO J. **21**: 1121–31.

Schotta, G., Lachner, M., Sarma, K., Ebert, A., Sengupta, R., Reuter, G., Reinberg, D., and Jenuwein, T. (2004). A silencing pathway to induce H3-K9 and H4-K20 trimethylation at constitutive heterochromatin. Genes Dev. **18**: 1251–62.

Schubert, V., Berr, A., and Meister, A. (2012). Interphase chromatin organisation in Arabidopsis nuclei: constraints versus randomness. Chromosoma **121**: 369–87.

Schueler, M.G. and Sullivan, B.A. (2006). Structural and functional dynamics of human centromeric chromatin. Annu. Rev. Genomics Hum. Genet. **7**: 301–13.

Schulz, L.L. and Tyler, J.K. (2006). The histone chaperone ASF1 localizes to active DNA replication forks to mediate efficient DNA replication. FASEB J. **20**: 488–90.

Schümperli, D. (1986). Cell-cycle regulation of histone gene expression. Cell **45**: 471–472.

Schwab, R., Ossowski, S., Riester, M., Warthmann, N., and Weigel, D. (2006). Highly specific gene silencing by artificial microRNAs in Arabidopsis. Plant Cell **18**: 1121–33.

Seiler-Tuyns, A. and Paterson, B. (1986). A chimeric mouse histone H4 gene contaning either an intron or poly(A) addition signal behaves like a basal histone. Nucleic Acids Res. **14**: 8845–8862.

Seisenberger, S., Peat, J.R., Hore, T.A., Santos, F., Dean, W., and Reik, W. (2013). Reprogramming DNA methylation in the mammalian life cycle: building and breaking epigenetic barriers. Philos. Trans. R. Soc. Lond. B. Biol. Sci. **368**: 20110330.

Sequeira-Mendes, J., Aragüez, I., Peiró, R., Mendez-Giraldez, R., Zhang, X., Jacobsen, S.E., Bastolla, U., and Gutierrez, C. (2014). The Functional Topography of the Arabidopsis Genome Is Organized in a Reduced Number of Linear Motifs of Chromatin States. Plant Cell **26**: 2351–2366.

Sharp, J.A., Fouts, E.T., Krawitz, D.C., and Kaufman, P.D. (2001). Yeast histone deposition protein Asf1p requires Hir proteins and PCNA for heterochromatic silencing. Curr. Biol. **11**: 463–73.

She, W., Grimanelli, D., Rutowicz, K., Whitehead, M.W.J., Puzio, M., Kotlinski, M., Jerzmanowski, A., and Baroux, C. (2013). Chromatin reprogramming during the somatic-to-reproductive cell fate transition in plants. Development **140**: 4008–19.

Shelby, R.D., Monier, K., and Sullivan, K.F. (2000). Chromatin assembly at kinetochores is uncoupled from DNA replication. J. Cell Biol. **151**: 1113–8.

Shelby, R.D., Vafa, O., and Sullivan, K.F. (1997). Assembly of CENP-A into centromeric chromatin requires a cooperative array of nucleosomal DNA contact sites. J. Cell Biol. **136**: 501–13.

Sherstnev, A., Duc, C., Cole, C., Zacharaki, V., Hornyik, C., Ozsolak, F., Milos, P.M., Barton, G.J., and Simpson, G.G. (2012). Direct sequencing of Arabidopsis thaliana RNA reveals patterns of cleavage and polyadenylation. Nat. Struct. Mol. Biol. **19**: 845–52.

Shi, L., Wang, J., Hong, F., Spector, D.L., and Fang, Y. (2011). Four amino acids guide the assembly or disassembly of Arabidopsis histone H3.3-containing nucleosomes. Proc. Natl. Acad. Sci. **108**: 10574–10578.

Shibahara, K. and Stillman, B. (1999). Replication-dependent marking of DNA by PCNA facilitates CAF-1-coupled inheritance of chromatin. Cell **96**: 575–85.

Shu, H., Gruissem, W., and Hennig, L. (2013). Measuring Arabidopsis chromatin accessibility using DNase I-polymerase chain reaction and DNase I-chip assays. Plant Physiol. **162**: 1794–801.

Shu, H., Nakamura, M., Siretskiy, A., Borghi, L., Moraes, I., Wildhaber, T., Gruissem, W., and Hennig, L. (2014). Arabidopsis replacement histone variant H3.3 occupies promoters of regulated genes. Genome Biol. **15**: R62.

Shu, H., Wildhaber, T., Siretskiy, A., Gruissem, W., and Hennig, L. (2012). Distinct modes of DNA accessibility in plant chromatin. Nat. Commun. **3**: 1281.

Sidorenko, L., Dorweiler, J.E., Cigan, A.M., Arteaga-Vazquez, M., Vyas, M., Kermicle, J., Jurcin, D., Brzeski, J., Cai, Y., and Chandler, V.L. (2009). A dominant mutation in mediator of paramutation2, one of three second-largest

subunits of a plant-specific RNA polymerase, disrupts multiple siRNA silencing processes. PLoS Genet. **5**: e1000725.

Simpson, V., Johnson, T., and Hammen, R. (1986). Caenorhabditis elegans DNA does not contain 5-methylcytosine at any time during development or aging. Nucleic Acids Res. **14**: 6711–6719.

Slotkin, R.K. (2010). The epigenetic control of the Athila family of retrotransposons in Arabidopsis. Epigenetics **5**: 483–490.

Slotkin, R.K. and Martienssen, R. (2007). Transposable elements and the epigenetic regulation of the genome. Nat. Rev. Genet. **8**: 272–85.

Solovei, I., Kreysing, M., Lanctôt, C., Kösem, S., Peichl, L., Cremer, T., Guck, J., and Joffe, B. (2009). Nuclear architecture of rod photoreceptor cells adapts to vision in mammalian evolution. Cell **137**: 356–68.

Solovei, I., Schermelleh, L., Düring, K., Engelhardt, A., Stein, S., Cremer, C., and Cremer, T. (2004). Differences in centromere positioning of cycling and postmitotic human cell types. Chromosoma **112**: 410–23.

Soppe, W.J.J., Jasencakova, Z., Houben, A., Kakutani, T., Meister, A., Huang, M.S., Jacobsen, S.E., Schubert, I., and Fransz, P.F. (2002). DNA methylation controls histone H3 lysine 9 methylation and heterochromatin assembly in Arabidopsis. EMBO J. **21**: 6549–59.

Steimer, A., Amedeo, P., Afsar, K., Fransz, P., Mittelsten Scheid, O., and Paszkowski, J. (2000). Endogenous targets of transcriptional gene silencing in Arabidopsis. Plant Cell **12**: 1165–78.

Stillman, B. and Smith, S. (1989). Purification and characterization of CAF-I, a human cell factor required for chromatin assembly during DNA replication in vitro. Cell **58**: 15–25.

Stroud, H., Do, T., Du, J., Zhong, X., Feng, S., Johnson, L., Patel, D.J., and Jacobsen, S.E. (2014). Non-CG methylation patterns shape the epigenetic landscape in Arabidopsis. Nat. Struct. Mol. Biol. **21**: 64–72.

Stroud, H., Otero, S., Desvoyes, B., Ramírez-Parra, E., Jacobsen, S.E., and Gutierrez, C. (2012). Genome-wide analysis of histone H3.1 and H3.3 variants in Arabidopsis thaliana. Proc. Natl. Acad. Sci. U. S. A. **109**: 5370–5.

Sullivan, B.A. and Karpen, G.H. (2004). Centromeric chromatin exhibits a histone modification pattern that is distinct from both euchromatin and heterochromatin. Nat. Struct. Mol. Biol. **11**: 1076–83.

Sun, L., Youn, H.D., Loh, C., Stolow, M., He, W., and Liu, J.O. (1998). Cabin 1, a negative regulator for calcineurin signaling in T lymphocytes. Immunity **8**: 703–11.

Szenker, E., Lacoste, N., and Almouzni, G. (2012). A developmental requirement for HIRA-dependent H3.3 deposition revealed at gastrulation in Xenopus. Cell Rep. **1**: 730–740.

Szenker, E., Ray-Gallet, D., and Almouzni, G. (2011). The double face of the histone variant H3.3. Cell Res. **21**: 421–34.

Tachiwana, H., Osakabe, A., Kimura, H., and Kurumizaka, H. (2008). Nucleosome formation with the testis-specific histone H3 variant, H3t, by human nucleosome assembly proteins in vitro. Nucleic Acids Res. **36**: 2208–18.

Tagami, H., Ray-Gallet, D., Almouzni, G., and Nakatani, Y. (2004). Histone H3.1 and H3.3 complexes mediate nucleosome assembly pathways dependent or independent of DNA synthesis. Cell **116**: 51–61.

Takeda, S., Tadele, Z., Hofmann, I., Probst, A. V, Angelis, K.J., Kaya, H., Araki, T., Mengiste, T., Mittelsten Scheid, O., Shibahara, K., Scheel, D., and

Paszkowski, J. (2004). BRU1, a novel link between responses to DNA damage and epigenetic gene silencing in Arabidopsis. Genes Dev. **18**: 782–793.

Talbert, P.B. et al. (2012). A unified phylogeny-based nomenclature for histone variants. Epigenetics Chromatin **5**: 7.

Talbert, P.B. and Henikoff, S. (2010). Histone variants--ancient wrap artists of the epigenome. Nat. Rev. Mol. Cell Biol. **11**: 264–75.

Talbert, P.B., Masuelli, R., Tyagi, A.P., Comai, L., and Henikoff, S. (2002). Centromeric localization and adaptive evolution of an Arabidopsis histone H3 variant. Plant Cell **14**: 1053–66.

Tamburini, B.A., Carson, J.J., Adkins, M.W., and Tyler, J.K. (2005). Functional conservation and specialization among eukaryotic anti-silencing function 1 histone chaperones. Eukaryot. Cell **4**: 1583–90.

Tamburini, B.A., Carson, J.J., Linger, J.G., and Tyler, J.K. (2006). Dominant mutants of the Saccharomyces cerevisiae ASF1 histone chaperone bypass the need for CAF-1 in transcriptional silencing by altering histone and Sir protein recruitment. Genetics **173**: 599–610.

Tang, M.C.W., Jacobs, S.A., Wong, L.H., and Mann, J.R. (2013). Conditional allelic replacement applied to genes encoding the histone variant H3.3 in the mouse. Genesis **51**: 142–6.

Tang, Y., Gao, X.-D., Wang, Y., Yuan, B.-F., and Feng, Y.-Q. (2012). Widespread existence of cytosine methylation in yeast DNA measured by gas chromatography/mass spectrometry. Anal. Chem. **84**: 7249–55.

Tang, Y., Poustovoitov, M. V, Zhao, K., Garfinkel, M., Canutescu, A., Dunbrack, R., Adams, P.D., and Marmorstein, R. (2006). Structure of a human ASF1a-HIRA complex and insights into specificity of histone chaperone complex assembly. Nat. Struct. Mol. Biol. **13**: 921–929.

Tariq, M., Saze, H., Probst, A. V, Lichota, J., Habu, Y., and Paszkowski, J. (2003). Erasure of CpG methylation in Arabidopsis alters patterns of histone H3 methylation in heterochromatin. Proc. Natl. Acad. Sci. U. S. A. **100**: 8823–8827.

Terranova, R., Sauer, S., Merkenschlager, M., and Fisher, A.G. (2005). The reorganisation of constitutive heterochromatin in differentiating muscle requires HDAC activity. Exp. Cell Res. **310**: 344–56.

Tessadori, F., Chupeau, M.-C., Chupeau, Y., Knip, M., Germann, S., van Driel, R., Fransz, P., and Gaudin, V. (2007a). Large-scale dissociation and sequential reassembly of pericentric heterochromatin in dedifferentiated Arabidopsis cells. J. Cell Sci. **120**: 1200–1208.

Tessadori, F., van Driel, R., and Fransz, P. (2004). Cytogenetics as a tool to study gene regulation. Trends Plant Sci. **9**: 147–53.

Tessadori, F., Schulkes, R.K., van Driel, R., and Fransz, P. (2007b). Light-regulated large-scale reorganization of chromatin during the floral transition in Arabidopsis. Plant J. **50**: 848–857.

Thakar, A., Gupta, P., Ishibashi, T., Finn, R., Silva-Moreno, B., Uchiyama, S., Fukui, K., Tomschik, M., Ausio, J., and Zlatanova, J. (2009). H2A.Z and H3.3 histone variants affect nucleosome structure: biochemical and biophysical studies. Biochemistry **48**: 10852–7.

The Arabidopsis Genome Initiative (2000). Analysis of the genome sequence of the flowering plant Arabidopsis thaliana. Nature **408**: 796–815.

Thomas, J. (1999). Histone H1 : location and role. Curr. Opin. Cell Biol.: 312–317.

Thompson, H.L., Schmidt, R., and Dean, C. (1996). Identification and distribution of seven classes of middle-repetitive DNA in the Arabidopsis thaliana genome. Nucleic Acids Res. **24**: 3017–3022.

Tittel-Elmer, M., Bucher, E., Broger, L., Mathieu, O., Paszkowski, J., and Vaillant, I. (2010). Stress-induced activation of heterochromatic transcription. PLoS Genet. **6**: e1001175.

Turck, F., Roudier, F., Farrona, S., Martin-Magniette, M.-L., Guillaume, E., Buisine, N., Gagnot, S., Martienssen, R.A., Coupland, G., and Colot, V. (2007). Arabidopsis TFL2/LHP1 specifically associates with genes marked by trimethylation of histone H3 lysine 27. PLoS Genet. **3**: e86.

Turner, J.M.A. (2007). Meiotic sex chromosome inactivation. Development **134**: 1823–31.

Tyler, J.K., Adams, C.R., Chen, S.R., Kobayashi, R., Kamakaka, R.T., and Kadonaga, J.T. (1999). The RCAF complex mediates chromatin assembly during DNA replication and repair. Nature **402**: 555–60.

Tyler, J.K., Collins, K.A., Prasad-Sinha, J., Amiott, E., Bulger, M., Harte, P.J., Kobayashi, R., and Kadonaga, J.T. (2001). Interaction between the Drosophila CAF-1 and ASF1 chromatin assembly factors. Mol. Cell. Biol. **21**: 6574–84.

Vaillant, I., Schubert, I., Tourmente, S., and Mathieu, O. (2006). MOM1 mediates DNA-methylation-independent silencing of repetitive sequences in Arabidopsis. EMBO Rep. **7**: 1273–8.

Vaillant, I., Tutois, S., Cuvillier, C., Schubert, I., and Tourmente, S. (2007). Regulation of Arabidopsis thaliana 5S rRNA Genes. Plant Cell Physiol. **48**: 745–52.

Vaillant, I., Tutois, S., Jasencakova, Z., Douet, J., Schubert, I., and Tourmente, S. (2008). Hypomethylation and hypermethylation of the tandem repetitive 5S rRNA genes in Arabidopsis. Plant J. **54**: 299–309.

Vaquero-Sedas, M.I. and Vega-Palas, M.A. (2013). Differential association of Arabidopsis telomeres and centromeres with histone H3 variants. Sci. Rep. **3**: 1202.

Vaughn, M.W. et al. (2007). Epigenetic natural variation in Arabidopsis thaliana. PLoS Biol. **5**: e174.

Verdel, A., Jia, S., Gerber, S., Sugiyama, T., Gygi, S., Grewal, S.I.S., and Moazed, D. (2004). RNAi-mediated targeting of heterochromatin by the RITS complex. Science **303**: 672–6.

Vermaak, D., Wade, P.A., Jones, P.L., Shi, Y.B., and Wolffe, A.P. (1999). Functional analysis of the SIN3-histone deacetylase RPD3-RbAp48-histone H4 connection in the Xenopus oocyte. Mol. Cell. Biol. **19**: 5847–60.

Verreault, A., Kaufman, P.D., Kobayashi, R., and Stillman, B. (1996). Nucleosome assembly by a complex of CAF-1 and acetylated histones H3/H4. Cell **87**: 95–104.

De Veylder, L., Larkin, J.C., and Schnittger, A. (2011). Molecular control and function of endoreplication in development and physiology. Trends Plant Sci. **16**: 624–34.

Vissel, B. and Choo, K.H. (1989). Mouse major (gamma) satellite DNA is highly conserved and organized into extremely long tandem arrays: implications for recombination between nonhomologous chromosomes. Genomics **5**: 407–14.

Volle, C. and Dalal, Y. (2014). Histone variants: the tricksters of the chromatin world. Curr. Opin. Genet. Dev. **25**: 8–14,138.

Volpe, T. and Martienssen, R.A. (2011). RNA interference and heterochromatin assembly. Cold Spring Harb. Perspect. Biol. **3**: a003731.

Volpe, T.A., Kidner, C., Hall, I.M., Teng, G., Grewal, S.I.S., and Martienssen, R.A. (2002). Regulation of heterochromatic silencing and histone H3 lysine-9 methylation by RNAi. Science **297**: 1833–7.

Waterborg, J.H. (1990). Sequence analysis of acetylation and methylation in two histone H3 variants of alfalfa. J. Biol. Chem. **265**: 17157–61.

Wellman, S., Casano, P., and Pilch, D. (1987). Characterization of mouse H3.3-like histone genes. Gene **59**: 29–39.

Wells, D., Hoffman, D., and Kedes, L. (1987). Unusual structure, evolutionary conservation of non-coding sequences and numerous pseudogenes characterize the human H3.3 histone multigene family. Nucleic Acids Res. **15**: 2871–2889.

Weng, M., Yang, Y., Feng, H., Pan, Z., Shen, W.-H., Zhu, Y., and Dong, A. (2014). Histone chaperone ASF1 is involved in gene transcription activation in response to heat stress in Arabidopsis thaliana. Plant. Cell Environ. **37**: 2128–38.

Wierzbicki, A.T., Cocklin, R., Mayampurath, A., Lister, R., Rowley, M.J., Gregory, B.D., Ecker, J.R., Tang, H., and Pikaard, C.S. (2012). Spatial and functional relationships among Pol V-associated loci, Pol IV-dependent siRNAs, and cytosine methylation in the Arabidopsis epigenome. Genes Dev. **26**: 1825–36.

Wierzbicki, A.T., Haag, J.R., and Pikaard, C.S. (2008). Noncoding transcription by RNA polymerase Pol IVb/Pol V mediates transcriptional silencing of overlapping and adjacent genes. Cell **135**: 635–48.

Wierzbicki, A.T., Ream, T.S., Haag, J.R., and Pikaard, C.S. (2009). RNA polymerase V transcription guides ARGONAUTE4 to chromatin. Nat. Genet. **41**: 630–4.

Wollmann, H. and Berger, F. (2012). Epigenetic reprogramming during plant reproduction and seed development. Curr. Opin. Plant Biol. **15**: 63–9.

Wollmann, H., Holec, S., Alden, K., Clarke, N.D., Jacques, P.-É., and Berger, F. (2012). Dynamic deposition of histone variant H3.3 accompanies developmental remodeling of the Arabidopsis transcriptome. PLoS Genet. **8**: e1002658.

Wong, A. and Rattner, J. (1988). Sequence organization and cytological localization of the minor satellite of mouse. Nucleic Acids Res. **16**: 11645–11661.

Wong, L.H., Ren, H., Williams, E., McGhie, J., Ahn, S., Sim, M., Tam, A., Earle, E., Anderson, M.A., Mann, J., and Choo, K.H.A. (2009). Histone H3.3 incorporation provides a unique and functionally essential telomeric chromatin in embryonic stem cells. Genome Res. **19**: 404–14.

Wu, C., Bassett, A., and Travers, A. (2007). A variable topology for the 30-nm chromatin fibre. EMBO Rep. **8**: 1129–34.

Wu, S., Gyorgyey, J., and Dudits, D. (1989). Polyadenylated H3 histone transcripts and H3 histone variants in alfalfa. Nuc **17**: 3057–3063.

Xie, Z., Johansen, L.K., Gustafson, A.M., Kasschau, K.D., Lellis, A.D., Zilberman, D., Jacobsen, S.E., and Carrington, J.C. (2004). Genetic and functional diversification of small RNA pathways in plants. PLoS Biol. **2**: E104.

Xue, Y., Gibbons, R., Yan, Z., Yang, D., McDowell, T.L., Sechi, S., Qin, J., Zhou, S., Higgs, D., and Wang, W. (2003). The ATRX syndrome protein forms a chromatin-remodeling complex with Daxx and localizes in promyelocytic leukemia nuclear bodies. Proc. Natl. Acad. Sci. U. S. A. **100**: 10635–40.

Yamane, K., Mizuguchi, T., Cui, B., Zofall, M., Noma, K., and Grewal, S.I.S. (2011). Asf1/HIRA facilitate global histone deacetylation and associate with HP1 to promote nucleosome occupancy at heterochromatic loci. Mol. Cell **41**: 56–66.

Yang, J.-H., Choi, J.-H., Jang, H., Park, J.-Y., Han, J.-W., Youn, H.-D., and Cho, E.-J. (2011). Histone chaperones cooperate to mediate Mef2-targeted transcriptional regulation during skeletal myogenesis. Biochem. Biophys. Res. Commun. **407**: 541–7.

Ye, R., Wang, W., Iki, T., Liu, C., Wu, Y., Ishikawa, M., Zhou, X., and Qi, Y. (2012). Cytoplasmic assembly and selective nuclear import of Arabidopsis Argonaute4/siRNA complexes. Mol. Cell **46**: 859–70.

Ye, X., Franco, A.A., Santos, H., Nelson, D.M., Kaufman, P.D., and Adams, P.D. (2003). Defective S phase chromatin assembly causes DNA damage, activation of the S phase checkpoint, and S phase arrest. Mol. Cell **11**: 341–51.

Yelagandula, R. et al. (2014). The Histone Variant H2A.W Defines Heterochromatin and Promotes Chromatin Condensation in Arabidopsis. Cell **158**: 98–109.

Yoda, K., Ando, S., Morishita, S., Houmura, K., Hashimoto, K., Takeyasu, K., and Okazaki, T. (2000). Human centromere protein A (CENP-A) can replace histone H3 in nucleosome reconstitution in vitro. Proc. Natl. Acad. Sci. U. S. A. **97**: 7266–71.

Youn, H.D., Sun, L., Prywes, R., and Liu, J.O. (1999). Apoptosis of T cells mediated by Ca2+-induced release of the transcription factor MEF2. Science **286**: 790–3.

Yu, A., Lepère, G., Jay, F., Wang, J., Bapaume, L., Wang, Y., Abraham, A.-L., Penterman, J., Fischer, R.L., Voinnet, O., and Navarro, L. (2013). Dynamics and biological relevance of DNA demethylation in Arabidopsis antibacterial defense. Proc. Natl. Acad. Sci. U. S. A. **110**: 2389–94.

Van Zanten, M., Carles, A., Li, Y., and Soppe, W.J.J. (2012). Control and consequences of chromatin compaction during seed maturation in Arabidopsis thaliana. Plant Signal. Behav. **7**: 338–41.

Van Zanten, M., Koini, M.A., Geyer, R., Liu, Y., Brambilla, V., Bartels, D., Koornneef, M., Fransz, P., and Soppe, W.J.J. (2011). Seed maturation in Arabidopsis thaliana is characterized by nuclear size reduction and increased chromatin condensation. Proc. Natl. Acad. Sci. U. S. A. **108**: 20219–24.

Van Zanten, M., Tessadori, F., Bossen, L., Peeters, A.J.M., and Fransz, P. (2010). Large-scale chromatin de-compaction induced by low light is not accompanied by nucleosomal displacement. Plant Signal. Behav. **5**: 1677–8.

Zemach, A., Kim, M.Y., Hsieh, P., Coleman-Derr, D., Eshed-Williams, L., Thao, K., Harmer, S.L., and Zilberman, D. (2013). The Arabidopsis nucleosome remodeler DDM1 allows DNA methyltransferases to access H1-containing heterochromatin. Cell **153**: 193–205.

Zhang, R. et al. (2005). Formation of MacroH2A-containing senescence-associated heterochromatin foci and senescence driven by ASF1a and HIRA. Dev. Cell **8**: 19–30.

Zhang, X., Henderson, I.R., Lu, C., Green, P.J., and Jacobsen, S.E. (2007). Role of RNA polymerase IV in plant small RNA metabolism. Proc. Natl. Acad. Sci. U. S. A. **104**: 4536–41.

Zhang, X., Yazaki, J., Sundaresan, A., Cokus, S., Chan, S.W.-L., Chen, H., Henderson, I.R., Shinn, P., Pellegrini, M., Jacobsen, S.E., and Ecker, J.R. (2006). Genome-wide high-resolution mapping and functional analysis of DNA methylation in arabidopsis. Cell **126**: 1189–201.

Zhao, J., Morozova, N., Williams, L., Libs, L., Avivi, Y., and Grafi, G. (2001). Two phases of chromatin decondensation during dedifferentiation of plant cells: distinction between competence for cell fate switch and a commitment for S phase. J. Biol. Chem. **276**: 22772–8.

Zheng, C. and Hayes, J.J. (2003). Structures and interactions of the core histone tail domains. Biopolymers **68**: 539–46.

Zhong, C.X., Marshall, J.B., Topp, C., Mroczek, R., Kato, A., Nagaki, K., Birchler, J.A., Jiang, J., and Dawe, R.K. (2002). Centromeric retroelements and satellites interact with maize kinetochore protein CENH3. Plant Cell **14**: 2825–36.

Zhu, J.-K. (2009). Active DNA demethylation mediated by DNA glycosylases. Annu. Rev. Genet. **43**: 143–66.

Zhu, Y., Dong, A., and Shen, W.-H.H. (2012). Histone variants and chromatin assembly in plant abiotic stress responses. Biochim. Biophys. Acta **1819**: 343–8.

Zhu, Y., Weng, M., Yang, Y., Zhang, C., Li, Z., Shen, W.-H., and Dong, A. (2011). Arabidopsis homologues of the histone chaperone ASF1 are crucial for chromatin replication and cell proliferation in plant development. Plant J. **66**: 443–55.

Zilberman, D., Coleman-Derr, D., Ballinger, T., and Henikoff, S. (2008). Histone H2A.Z and DNA methylation are mutually antagonistic chromatin marks. Nature **456**: 125–9.

Zilberman, D., Gehring, M., Tran, R.K., Ballinger, T., and Henikoff, S. (2007). Genome-wide analysis of Arabidopsis thaliana DNA methylation uncovers an interdependence between methylation and transcription. Nat. Genet. **39**: 61–9.

Zlatanova, J., Bishop, T.C., Victor, J.-M., Jackson, V., and van Holde, K. (2009). The nucleosome family: dynamic and growing. Structure **17**: 160–71.

Zweidler, A. (1984). Core histone variants of the mouse: primary structure and expression. In Histone Genes: Structure, Organization and Regulation, G. Stein, J. Stein, and W. Marzluff, eds (New York), pp. 373–395.

Appendices

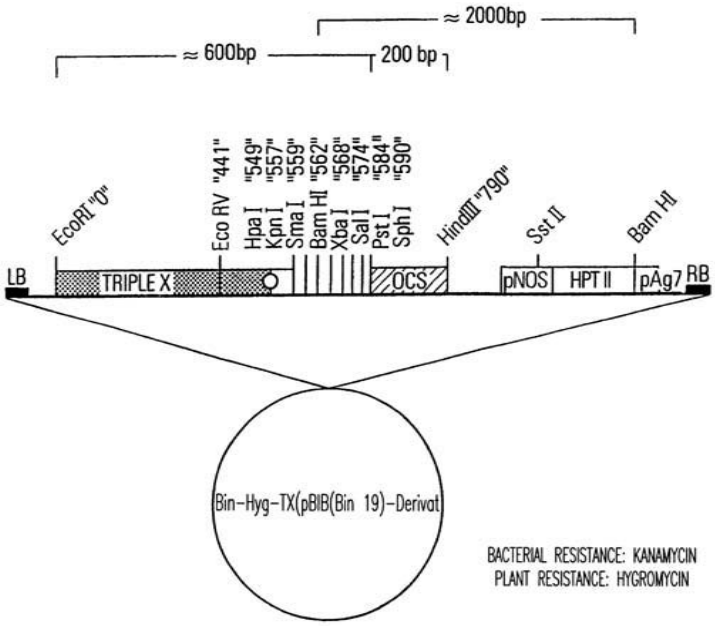

Appendix 1: Restriction map of the pBIN-Hyg-TX plasmid (Gatz et al., 1992).

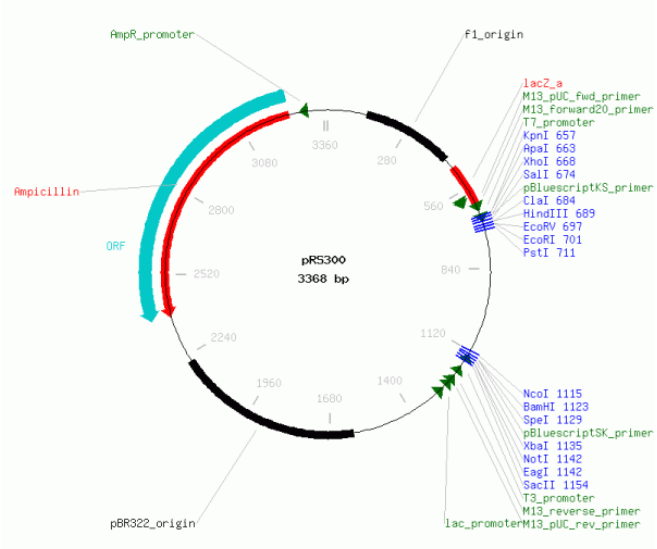

Appendix 2: Restriction map of the pRS300 plasmid (Ossowski et al., 2008).

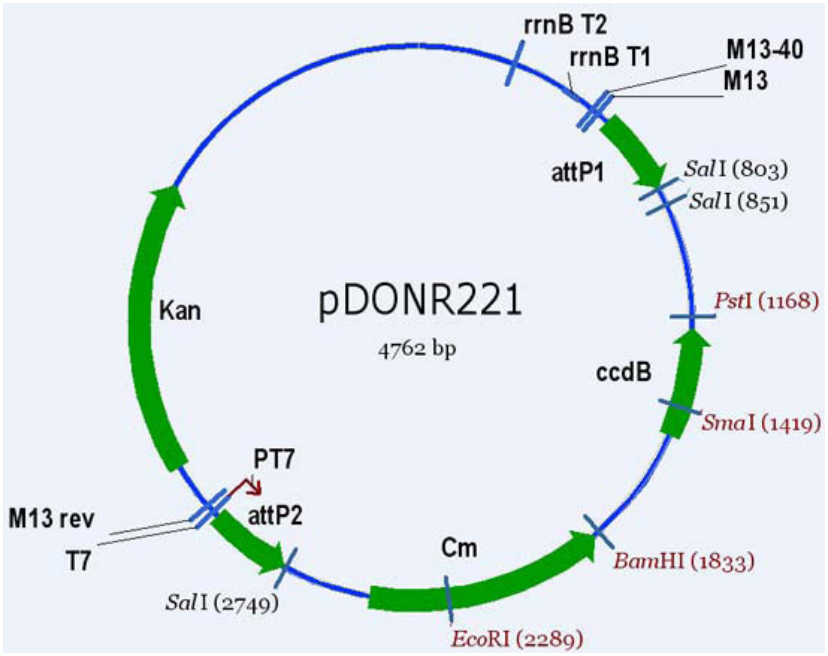

Appendix 3: Restriction map of the pDONR221 plasmid (Magnani et al., 2006).

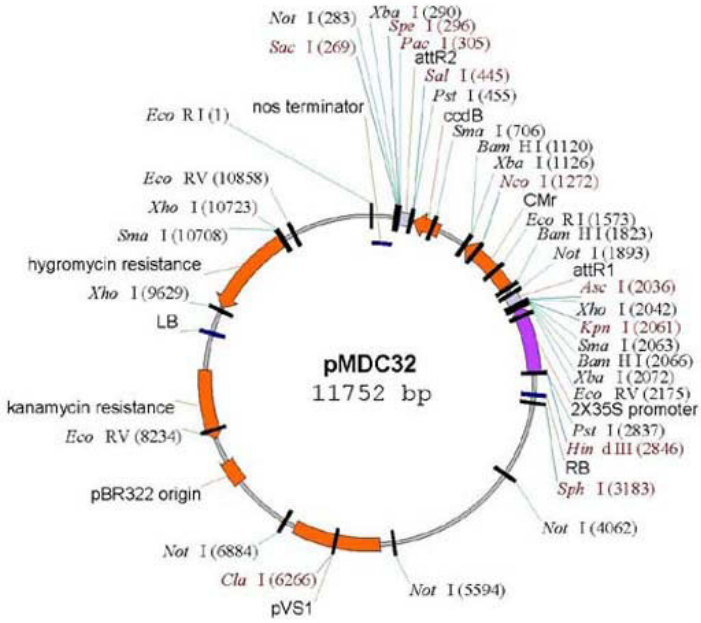

Appendix 4: Restriction map of the pMDC32 plasmid (Curtis and Grossniklaus, 2003).

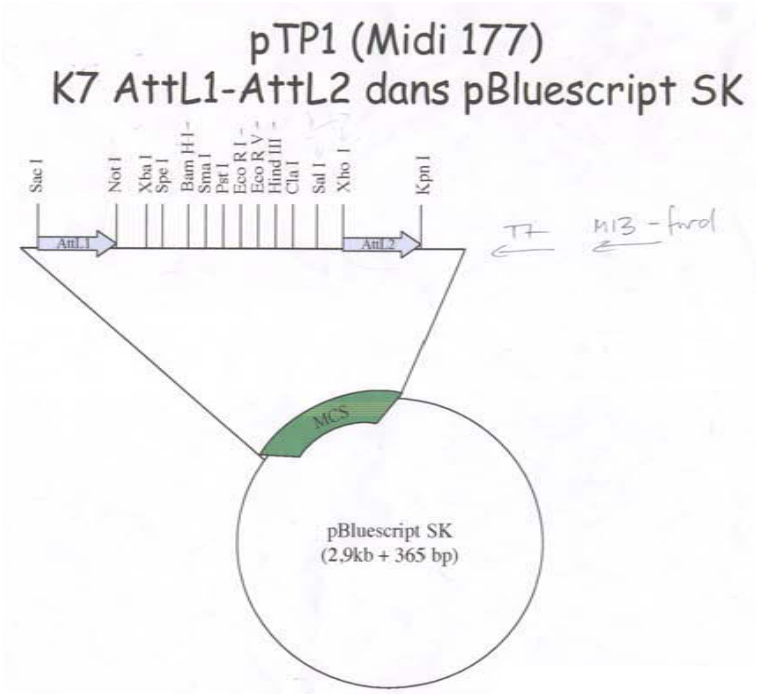

Appendix 5: Restriction map of the multiple cloning site of pTP1 (gift from T. Pélissier).

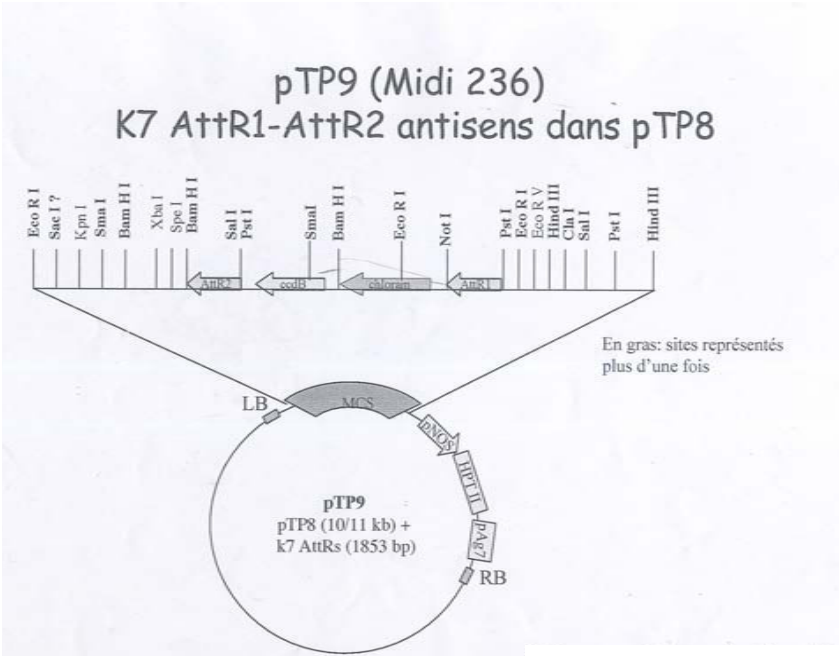

Appendix 6: Restriction map of the multiple cloning site of pTP9 (gift from T. Pélissier).

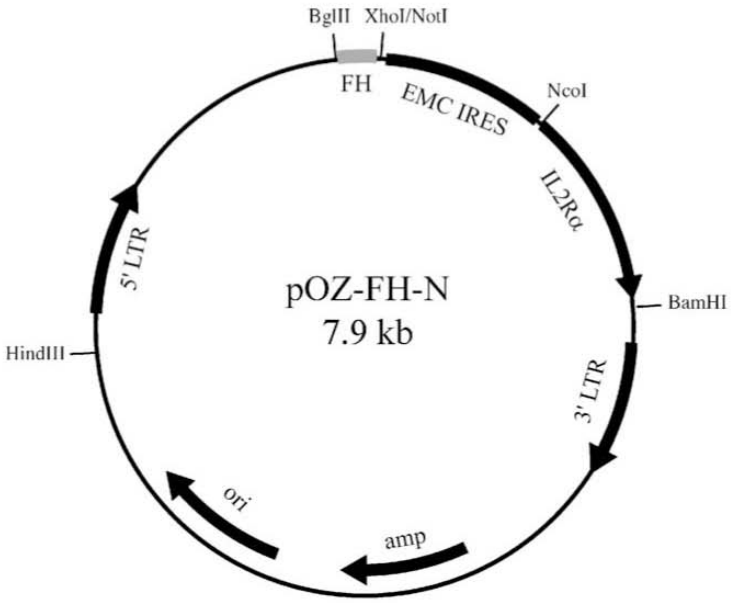

pOZ-FH-N

BglII
AGATCTTCCGCTCGATGAACCATGGACTACAAGGACGACGATGACAAGCTCGATGGAGGATACCCCTACGACGTGCCCGACTAC
M D Y K D D D D K L D G G Y P Y D V P D Y
FLAG HA

XhoI NotI
GCCGGAGGACTCGAGAATTCGCGGCCGCT
A G G L E N S R P L

pOZ-FH-C

BglII XhoI NotI
AGATCTTCCGCTCGAGGAATTCGCGGCCGCTGGAGGAGACTACAAGGACGACGATGACAAGTCGGCCGCTGGAGGATACCCC
D L P L E E F A A A G G D Y K D D D D K S A A G G Y P
FLAG

TACGACGTGCCCGACTACGCCTAG
Y D V P D Y A *
HA

Appendix 7: Restriction map of the pOZ-FH-N plasmid (Top).
Cloning sites of pOZ-FH-N and pOZ-FH-C (bottom) (Tagami et al., 2004).

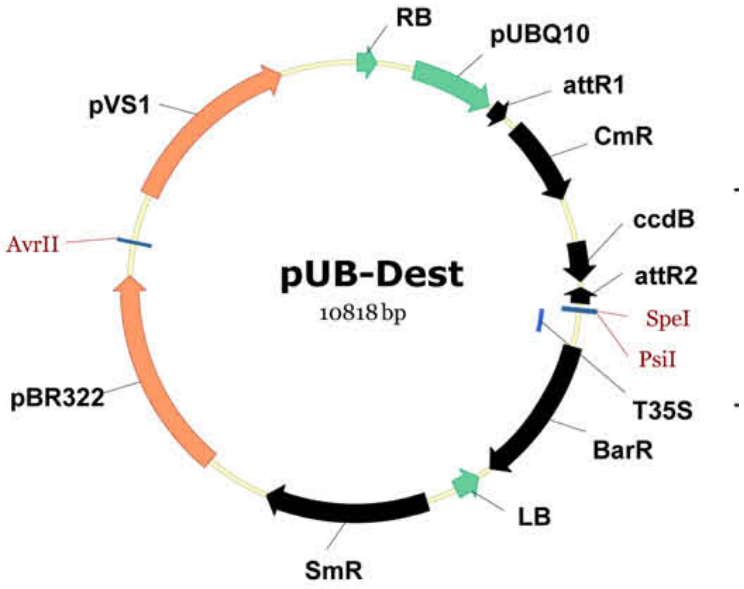

Appendix 8: Restriction map of the pUB plasmid (Grefen et al., 2010).

Gene 526 (2013) 39–45

Contents lists available at SciVerse ScienceDirect

Gene

journal homepage: www.elsevier.com/locate/gene

Heterochromatin dynamics during developmental transitions in *Arabidopsis* — a focus on ribosomal DNA loci

Matthias Benoit [a], Elodie Layat [b], Sylvette Tourmente [a], Aline V. Probst [a,*]

[a] Génétique, Reproduction et Développement, UMR CNRS 6293, Clermont Université, INSERM U1103, 24 Avenue des Landais, BP 80026, 63171 Aubière Cedex, France
[b] UR5 UAC7180 CNRS Université Pierre et Marie Curie-Paris 6, Bat C, 4 place Jussieu, 75252 Paris cedex 05, France

ARTICLE INFO

Article history:
Accepted 23 January 2013
Available online 12 February 2013

Keywords:
Ribosomal DNA
Heterochromatin
Development
Cotyledon
Arabidopsis thaliana
Phase transition

ABSTRACT

The *Arabidopsis* chromosomes contain conspicuous heterochromatin domains comprising the repetitive 45S and 5S ribosomal DNA loci as well as centromeric and pericentromeric repeats that organize into chromocenters during interphase. During developmental phase transitions such as seed maturation, germination, seedling growth and flowering that require large-scale reprogramming of gene expression patterns, the organization of repetitive sequences into chromocenters dynamically changes. Here we illustrate recent studies that shed light on the heterochromatin dynamics in cotyledons, the first aerial tissues preformed in the embryo, and in true leaves. We will summarize available data for the 5S rDNA repeat loci, in particular their chromatin organization and expression dynamics during the first days of post-germination development, and discuss how the plant accommodates 5S rRNA transcription during large-scale chromatin reorganization events.

1. Introduction

To ensure successful reproduction, annual plants need to tightly time their major developmental phase transitions such as germination and flowering with environmental stimuli. The switch from a developmental phase to the next requires changes in the spatial and temporal patterns of gene expression. Many signaling cascades and receptors have been described (reviewed in Amasino, 2010; Huijser and Schmid, 2011), as well as specific sets of genes undergoing selective activation or repression through different phase changes (Holdsworth et al., 2008; Schmid et al., 2003). Transcriptional reprogramming of these genes involves active modification of their chromatin structure (Adrian et al., 2009; Exner and Hennig, 2008; He, 2009; Jarillo et al., 2009; Wollmann and Berger, 2012). Interestingly, studies in the model plant *Arabidopsis thaliana* have revealed certain environmental conditions and developmental transitions not only to locally affect chromatin structure of the genes undergoing activation or repression but to profoundly impact higher-order chromatin organization (Mathieu et al., 2003a; Pecinka et al., 2010; Tessadori et al., 2004, 2007a, 2007b; Tittel-Elmer et al., 2010; van Zanten et al., 2011). In a leaf mesophyll nucleus of *Arabidopsis*, two major chromatin states, initially defined by their distinct compaction levels in interphase (Heitz, 1928), can be distinguished: euchromatin, mainly decondensed, contains the majority of genes, and heterochromatin, highly condensed, is composed of silent repetitive sequences and transposable elements. The *Arabidopsis* genome comprises several repeat families including direct centromeric and interspersed pericentromeric repeats that are transcriptionally repressed. Furthermore, the 5S and 45S rDNA repeat arrays that express the ribosomal RNAs, integral components of the ribosome, are partly heterochromatic (Fig. 1A, left). The different heterochromatic repeat loci cluster together into discrete structures, termed chromocenters (Fransz and de Jong, 2011; Fransz et al., 2002) (Fig. 1A), from which gene-rich euchromatin loops emanate thereby building the distinct chromosome territories (Fransz et al., 2002; Pecinka et al., 2004). Cytologically, chromocenters can be revealed as 6–10 intensely 4′,6′-diamidino-2-phenylindole (DAPI)-stained chromatin domains (Fig. 1A, middle) (Dittmer et al., 2007; Fransz et al., 2002), which are highly enriched in DNA methylation and repressive histone modifications such as dimethylation of lysine 9 (K9me2) and monomethylation of lysine 27 (K27me1) of histone 3 (Mathieu et al., 2005; Probst et al., 2003; Soppe et al., 2002). Several studies in the last 10 years have however revealed that this chromatin organization is not static but dynamic and that chromatin undergoes reorganization in certain mutants (Probst et al., 2003; Soppe et al., 2002), specific cell types (e.g. vegetative nucleus of the pollen or the central cell, Slotkin et al., 2009; Ingouff et al., 2010; Pillot et al., 2010) or upon developmental and environmental stimuli in aerial tissues. Indeed, numerous signals, ranging from biotic (e.g. pathogen infections, Pavet et al., 2006) to abiotic (e.g. shade, heat stress, Tessadori

Abbreviations: DAPI, 4′,6′-diamidino-2-phenylindole; FISH, fluorescence *in situ* hybridization; 5mC, 5 methylcytosine; rDNA/rRNA, ribosomal DNA/RNA; RHF, relative heterochromatin fraction; ROS, repressor of silencing 1; RdDM, RNA-directed DNA methylation; si-RNA, small interfering RNA; TFIIIA, transcription factor IIIA.

* Corresponding author at: Génétique, Reproduction et Développement, UMR CNRS 6293, Clermont Université, INSERM U1103, 24 Avenue des Landais, BP 80026, 63171 Aubière Cedex, France. Tel.: +33 4 73 40 53 04; fax: +33 4 73 40 77 77.
E-mail addresses: matthias.benoit@univ-bpclermont.fr (M. Benoit), elodie.layat@upmc.fr (E. Layat), sylvette.tourmente@univ-bpclermont.fr (S. Tourmente), aline.probst@univ-bpclermont.fr (A.V. Probst).

0378-1119/$ – see front matter © 2013 Elsevier B.V. All rights reserved.
http://dx.doi.org/10.1016/j.gene.2013.01.060

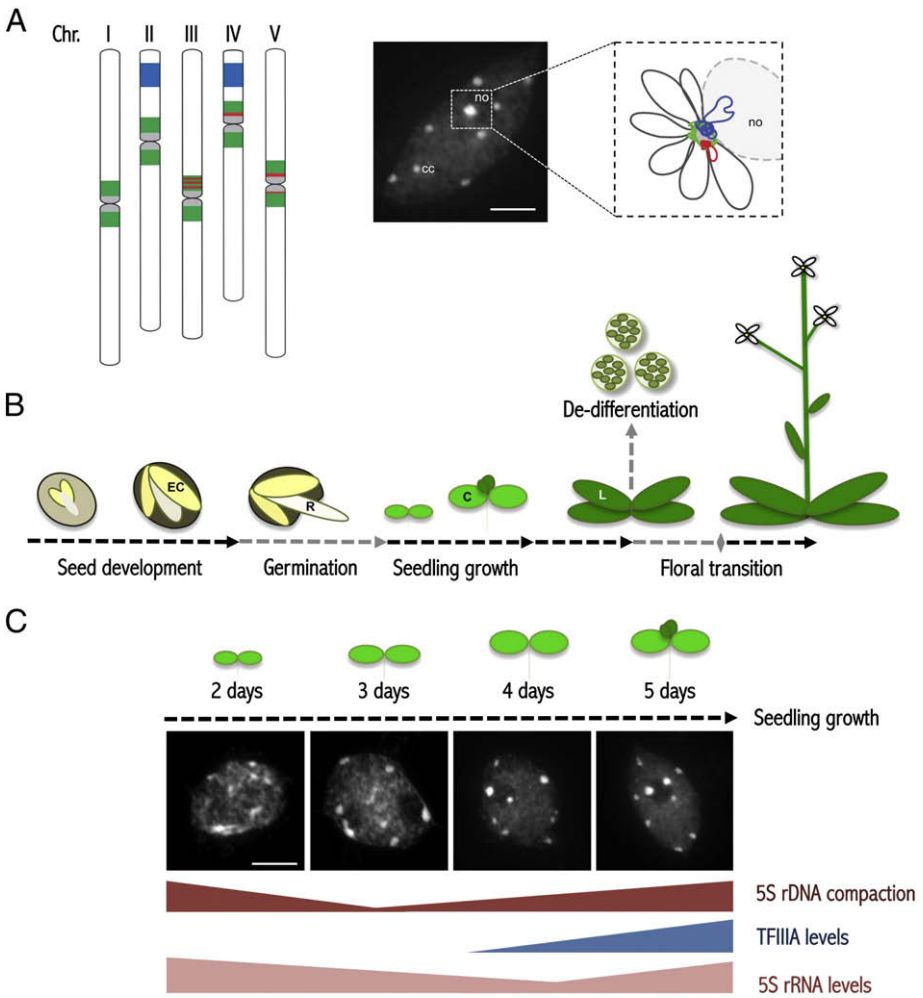

Fig. 1. Chromocenter organization and heterochromatin dynamics during developmental phase transitions. A. Left: Schematic representation of the 5 *Arabidopsis* chromosomes (2n = 10) in the Columbia accession. Chromosome II and IV carry the 45S rDNA loci (blue). The 5S rDNA loci (red) are present on chromosomes III, IV and V, in close proximity to centromeric repeats (180 bp repeats, gray) and inside the pericentromeric domains (green) (AGI, 2000; Fransz et al., 2000; Tabata et al., 2000; Tutois et al., 1999). Middle: Spread of an *Arabidopsis* leaf mesophyll nucleus stained with 4′,6′-diamidino-2-phenylindole (DAPI). Note the euchromatin in light gray and the nine brightly stained chromocenters (cc). The nucleolus (no) appears as DAPI-unstained region. Scale bar represents 5 μm. Right: Model of an *Arabidopsis* chromocenter of chromosome IV adjacent to the nucleolus (no). The chromocenter of chromosome IV comprises the 45S (blue), the 5S (red), centromeric (light gray) and pericentromeric (green) repeats from which euchromatic loops (dark gray) emanate (modified from Fransz et al., 2002). Parts of the ribosomal DNA repeats which are actively transcribed are represented as 45S rDNA sequences (blue) that loop out from the chromocenter into the nucleolus (Probst et al., 2004) and 5S rDNA (red) loops within the euchromatin compartment (Mathieu et al., 2003a) respectively. B. Overview of developmental phase transitions that implicate important chromatin dynamics. Large-scale chromatin dynamics take place in embryonic cotyledons (EC, yellow) during seed development and germination, in cotyledons (C, light green) during seedling growth from 2 to 5 days post-germination and in leaves (L, dark green) upon de-differentiation into protoplasts or during the floral transition. Developmental transitions globally associated with heterochromatin decondensation are marked with gray, those implicating predominantly heterochromatin condensation with black arrows. The radicle (R) is shown in white in the developing and germinating seed. C. DAPI-stained nuclear spreads of cotyledon nuclei at 2, 3, 4 and 5 days after germination. Note the presence of small pre-chromocenters at day 2 and the progressive formation of chromocenters that reach a mature organization at days 4 to 5. Bars below indicate 5S rDNA chromatin compaction (red), presence of functional 5S-specific transcription factor III A (TFIIIA, blue) and amounts of 5S rRNA (pink) during this developmental time window.

et al., 2009; Pecinka et al., 2010; van Zanten et al., 2010) environmental stimuli but also cellular de-differentiation (Tessadori et al., 2007a) or developmental transitions such as seed maturation and germination (van Zanten et al., 2011), seedling growth (Douet et al., 2008; Mathieu et al., 2003a) and floral transition (Tessadori et al., 2007b) have been shown to result in large-scale reorganization of chromatin (Fig. 1B). The chromatin dynamics can affect both euchromatic and heterochromatic regions (reviewed in van Zanten et al., 2012b), but most studies have concentrated on the fate of the heterochromatic sequences as they can be easily visualized using fluorescence *in situ* hybridization (FISH) and their organization into chromocenters monitored by chromocenter size and fluorescence intensity (Soppe et al., 2002; van Zanten et al., 2012b). Upon most phase transitions studied, heterochromatin undergoes decondensation, a change that seems to be of transient nature, as the initial organization of chromocenters is restored in most cases (Tessadori et al., 2007a and reviewed in van Zanten et al., 2012b). However, while certain similarities between the different chromatin reorganization events have been described, their timing can vary from hours to days and each situation appears to reveal its specific characteristics and may implicate different mechanisms depending on developmental context and tissue.

In this review, we will concentrate on the fate of the heterochromatic sequences organized in chromocenters during developmental phase transitions, as those have been investigated in most studies and will allow comparisons to be drawn between the different analyses discussed. We will first illustrate the characteristics of heterochromatin decondensation during floral transition and de-differentiation of leaf cells into protoplasts and then discuss in detail the chromatin dynamics during germination and early post-germination development that take place in the cotyledon. We will particularly emphasize the chromatin dynamics of a specific set of repetitive sequences, the 5S rDNA repeats, during the first days of post-germination growth

and discuss possible links between heterochromatin dynamics and transcription.

2. Heterochromatin dynamics during floral transition and de-differentiation

When the plant is exposed to favorable environmental conditions including photoperiod and temperature, which are crucial for the timing of developmental phase transitions, it can initiate flowering and the reprogramming from vegetative to reproductive growth (Huijser and Schmid, 2011; Liu et al., 2009). This transition requires external and endogenous triggers to be sensed by the leaves of the plant and to be transmitted to the apical meristem, the meristematic tissue at the tip of the plant shoot, which will then undertake fate change. During the reproductive phase transition, *Arabidopsis* leaf chromatin undergoes a subtle and slow global reorganization (Fig. 1B). Indeed, decondensation of chromocenters in the nuclei of leaves was noted 4 days before emergence of the floral stem, under both short day and floral-inductive long day photoperiods (Tessadori et al., 2007b). To quantify compaction of repetitive sequences into chromocenters during the floral transition, the relative heterochromatin fraction (RHF), which is defined by the area and fluorescence intensities of the chromocenters relative to the fluorescence intensity of the entire nucleus (Soppe et al., 2002), was assessed. A strong reduction to about half of the values usually observed in leaf tissues was scored, which resulted essentially from the dispersion of 5S rDNA and other pericentromeric repeats, while centromeric 180 bp repeats and 45S rDNA sequences remained highly condensed (Tessadori et al., 2007b). Therefore, the different tandem repeats of the *Arabidopsis* genome are unequally affected by the chromatin dynamics during floral transition. In addition, decondensation was not restricted to heterochromatic sequences, but affected also euchromatic domains as exemplified by the decondensation observed for a gene-rich domain on the long arm of chromosome IV (Tessadori et al., 2007b). After elongation of the floral stem, the chromocenters reform, endorsing the reversibility of the global chromatin decondensation process in this circumstance.

Other studies (Koukalova et al., 2005; Ondrej et al., 2009; Tessadori et al., 2007a; Zhao et al., 2001) reported decondensation of heterochromatin to occur upon de-differentiation of *Arabidopsis*, cucumber and tobacco leaf cells into protoplasts, plant cells devoid of cell walls (Fig. 1B), or upon callus formation. Indeed, during the de-differentiation of *Arabidopsis* mesophyll cells, the relative heterochromatin fraction decreased to less than one third compared to the leaf tissue from which the protoplasts were isolated (Tessadori et al., 2007a). Furthermore, DAPI-staining revealed the prevalence of only a few chromocenters in de-differentiated cells. FISH analysis allowed the authors to determine that those contain the only partially condensed 45S rDNA sequences, while pericentromeric repeats, 5S rDNA repeats and even the centromeric 180 bp repeats underwent complete decondensation. This decondensation occurs rapidly in less than a day but could be partially reversed during further protoplast culturing (Tessadori et al., 2007a). Interestingly, a sequential reformation of chromocenters was observed starting from the 45S rDNA, which form the longest repeat arrays, and 180 bp centromeric sequences to the tandemly repeated 5S rDNA sequences, while the interspersed pericentromeric repeats remained largely dispersed, suggesting specific dynamics for the distinct repeat families in *Arabidopsis* and a potential correlation between length of the repeat array and the temporal order of condensation (Tessadori et al., 2007a).

During floral transition heterochromatin decondensation was suggested not to involve major changes in epigenetic marks (Tessadori et al., 2007b) as repetitive sequences remain highly DNA methylated. Only the nuclear distribution of 5-methylcytosines (5mC), as revealed by an antibody, which recognizes methylated cytosines indifferent of their sequence context (symmetric CG, CHG or asymmetric CHH methylation), changes to a more dispersed pattern mirroring the decondensation of the highly methylated repeats (Tessadori et al., 2007b).

Similarly, during de-differentiation of *Arabidopsis* leaf cells into protoplasts, the nuclear distribution of 5mC changes, while DNA methylation at repetitive sequences was globally unaltered and no differences in the total amount of repressive histone modifications such as H3K9 methylation were observed (Tessadori et al., 2007a). Other studies however revealed localized subtle changes in DNA methylation of an Athila retroelement (Avivi et al., 2004) or certain promoters (Berdasco et al., 2008) during *Arabidopsis* protoplast generation or in cell suspensions, respectively. Furthermore, global changes in histone H3 post-translational modifications (Williams et al., 2003) and DNA methylation at the 35S rDNA loci (Koukalova et al., 2005) during tobacco protoplast or callus generation were monitored. Interestingly, mutants in the H3K9 methyltransferase KYP show reduced dedifferentiation and re-entry into the cell cycle (Grafi et al., 2007), suggesting that changes in chromatin modifications take place during de-differentiation, those might however be rather localized to certain loci or chromosomal regions.

Developmental phase transitions involve gene expression changes in large sets of genes located in euchromatin (Avivi et al., 2004; Schmid et al., 2003). Whether the expression of heterochromatic sequences is affected during floral transition and de-differentiation concomitant with their reorganization has not been intensively studied and was limited to the Athila retroelement undergoing demethylation (Avivi et al., 2004) and a repetitive transgenic locus (Tessadori et al., 2007a). For both loci no release of transcriptional silencing was observed.

3. Heterochromatin dynamics in cotyledons

3.1. Cotyledons: a unique plant tissue

While the above discussed chromatin dynamics have been reported to occur in mature leaf tissues, other major reorganization events of heterochromatin structure have been observed in *Arabidopsis* cotyledons (Douet et al., 2008; Mathieu et al., 2003a; van Zanten et al., 2011). Cotyledons are the first aerial tissues present at germination. They are formed during embryogenesis and then expand after germination, become photosynthetic, and are maintained throughout the vegetative life of the plant (Chandler, 2008). Cotyledons and leaves are often considered as homologous organs, due to their apical positioning on the shoot, similar organ expansion programs and mature morphology (Kaplan and Cooke, 1997). But despite the similarity between cotyledon and leaf development, the two tissues have different features in terms of storage and photosynthesis and structural differences at the level of trichomes and stipules, which are only present in leaves. In contrast to the true leaves, cotyledons might not arise from the shoot apical meristem since most cotyledon cells have never expressed *STEMLESS*, which is an efficient marker of meristem identity (Long and Barton, 1998). Some mutants that completely fail to develop cotyledons, but correctly initiate leaf primordia are available (Chandler et al., 2007). Other mutations display phenotypes that either demonstrate partial transformation of leaves into cotyledons or cotyledons into leaves in the case of the *LEAFY COTYLEDON* class of genes. In mutants of this class of genes, cotyledons show features usually found in vegetative leaves, such as trichomes, storage products, desiccation tolerance and more developed vasculature (Lotan et al., 1998; Stone et al., 2001; West et al., 1994). This genetic cleavage of cotyledon and leaf development (Fransz and de Jong, 2002) shows that these two aerial structures are distinct tissues with at least partially independent developmental programs and suggests that they might exhibit discrete ways of gene expression control and different dynamics in chromatin organization.

3.2. Heterochromatin dynamics in embryonic cotyledons during seed development

Seed development is initiated at fertilization and comprises a phase of embryogenesis, followed by the maturation of the seed and finally the acquisition of dormancy and desiccation tolerance. Like other phase changes, the phase transition from embryogenesis to dry seed requires adjustment of the gene expression program. Recent data now provide evidence for the occurrence of major modifications in chromatin compaction in embryonic cotyledons during seed maturation (Fig. 1B) (van Zanten et al., 2012a). In *Arabidopsis*, seed development takes approximately 20 days after pollination. Embryo development is completed during the first 8–10 days, and the seeds mature during the remainder of the period (van Zanten et al., 2012a). Van Zanten et al. (2012a) determined chromatin condensation into chromocenters during seed maturation by quantification of the RHF as an indicator of heterochromatin compaction. While nuclei of embryonic cotyledons at 8 days after pollination show RHF values comparable to those observed in leaf tissue (van Zanten et al., 2010), chromatin further condensates during seed maturation, the RHF reaching maximum levels in the dry seed. At the same time a progressive reduction in nuclear size was observed; however, given the different dynamics of changes in nuclear size and chromatin compaction the two processes were suggested not to be interdependent (van Zanten et al., 2012a). FISH experiments analyzing the distribution of centromeric, pericentromeric, and 45S rDNA sequences in cotyledons during seed development confirmed the high condensation of repetitive sequences in chromocenters in dry seeds (van Zanten et al., 2011). While 45S rDNA and 180 bp repeats were always structured into chromocenters, pericentromeric sequences progressively condensed during seed maturation. This condensation is reflected by changes in the nuclear 5mC distribution from early to late seed maturation. Mirroring the localization of pericentromeric sequences, the 5mC signals are moderately dispersed at 8 and 10 days after pollination, but significantly condensed at the DAPI-bright chromocenters in dry seeds.

While most phase transitions are associated with transient chromatin decondensation, the transition from embryo to dry seeds involves increased chromatin compaction and reduced nuclear volume (van Zanten et al., 2011). Seed maturation therefore differs from the phase transitions discussed above, likely because the aspired chromatin state in the mature seed does not need to support high levels of transcription, but in turn needs to contribute to desiccation tolerance. Consistently with the negative correlation between chromatin compaction and expression (Exner and Hennig, 2008; Fransz and de Jong, 2011; Tessadori et al., 2004), transcription in mature seeds is very low. At germination, in turn, the nuclear volume increases and heterochromatin decondenses concomitantly with important changes in the transcriptome (Holdsworth et al., 2008).

3.3. Heterochromatin decondensation during germination

Once the plant seed encounters favorable environmental conditions, dormancy is alleviated and the seed will initiate germination. During seed imbibition and the following germination process heterochromatin strongly decondenses as reflected by an important decrease in the RHF in the embryonic cotyledon nuclei (van Zanten et al., 2011). FISH experiments with heterochromatic probes revealed that while the 45S rDNA sequences remained condensed during the transition from dry seed to seedling, the centromeric and pericentromeric sequences dispersed in imbibed seeds. These heterochromatin dynamics were again reflected by changes in the distribution of 5mC signals on nuclear spreads (van Zanten et al., 2011). Accordingly, other studies showed reduced chromocenter size and the presence of small pre-chromocenters in cotyledon nuclei of *Arabidopsis* following germination (Douet et al., 2008; Mathieu et al., 2003a). Consequently, heterochromatin in embryonic cotyledons undergoes decondensation when the dry seed, in which chromatin is highly condensed and nuclear size reduced, initiates germination (Fig. 1B).

3.4. Heterochromatin dynamics during seedling growth

After seed germination, which is associated with heterochromatin decompaction, the cotyledons, formed during embryogenesis, start to expand and the seedling undergoes the transition from heterotrophic to photoautotrophic growth. During seedling growth a chromocenter organization is established that resembles the one in mesophyll leaf tissues (compare Figs. 1A, middle and C). During this time window, the dynamics of one repeat family, the 5S rDNA, has been analyzed in depth, both at the level of chromatin organization and transcription during the first days of seedling development (Douet et al., 2008; Mathieu et al., 2003a). The *Arabidopsis* genome contains at least 1 000 copies of 5S rRNA genes, arranged in tandem arrays and located in the pericentromeric regions of chromosomes III, IV and V (AGI, 2000; Campell et al., 1992; Fransz et al., 2000; Tabata et al., 2000; Tutois et al., 1999) (Fig. 1A, left). Each 0.5 kb 5S rDNA unit comprises the transcribed sequence (120-bp) carrying the internal promoter and an intergenic spacer region. At the DNA level, “major” copies can be distinguished from “minor” copies, which carry one or several base pair substitutions within the transcribed region. However predominantly those genes without mutations contribute to the 5S rRNA pool transcribed by Pol III in leaf tissues (Cloix et al., 2002; Layat et al., 2011). In mesophyll nuclei part of the 5S rDNA array is comprised in chromocenters. Other parts of the array however, which are thought to contain the actively transcribed genes (Mathieu et al., 2003a), are arranged in 5S rDNA loops (Fig. 1A, right). This functional organization of the 5S rDNA arrays is altered during floral transition and de-differentiation (Tessadori et al., 2007a, 2007b).

Between days 2 and 5 post-germination, 5S rDNA repeat arrays undergo large-scale reorganization (Douet et al., 2008). At 2 days post-germination, despite the absence of a mature chromocenter organization and reduced RHF values (van Zanten et al., 2011) (Fig. 1C) and dispersion of 45S rDNA repeats (Pontvianne et al., 2010; van Zanten et al., 2011), 5S rDNA loci are rather condensed and co-localize with the pre-chromocenters. At 3 days, they undergo decondensation and then adopt the mature organization in which part of the 5S rDNA locus forms loop structures (Douet et al., 2008; Mathieu et al., 2003a) (Fig. 1A, right). The dynamics by which the other repeat families acquire a mature organization during seedling development and whether they undergo similar condensation/decondensation cycles has not been addressed to date. It would be interesting to investigate whether the reformation of chromocenters occurs in sequential steps depending on the size of the repeat blocks as suggested for the heterochromatin condensation in protoplasts (Tessadori et al., 2007a). Furthermore, in contrast to centromeric and pericentromeric repeats that will likely be maintained transcriptionally repressed, ribosomal DNA arrays have to adopt a structure that ensures appropriate transcription. It would therefore be interesting to investigate further whether the mature chromatin organization of the rDNA loci acquired in a particular cell type or at a specific developmental stage reflects the respective requirement for ribosomal RNAs.

In contrast to the chromatin decondensation during floral transition that seems not to implicate important changes in DNA methylation (Tessadori et al., 2007b), 5S rDNA repeats gain symmetric (CG, CHG) (Mathieu et al., 2003a) and loose asymmetric (CHH) DNA methylation (Douet et al., 2008) during seedling growth. The loss of asymmetric DNA methylation at 5S rDNA repeats during the first days post-germination development is an active process catalyzed by the DNA demethylase Repressor of Silencing (ROS1) (Douet et al., 2008; Gong et al., 2002). ROS1 is required for 5S rDNA decondensation, suggesting a link between DNA methylation reprogramming and chromatin reorganization in this context.

In addition, the same study (Douet et al., 2008) reported that 5S rDNA chromatin fails to recondense during days 4 and 5 post-germination in mutants of a common subunit of the two RNA polymerases PolIV and PolV. These plant-specific polymerases are involved in RNA-directed DNA methylation (RdDM) at heterochromatic targets including 5S rDNA (Herr et al., 2005; Kanno et al., 2005; Onodera et al., 2005; Pontier et al., 2005; Zhang et al., 2007). The RdDM pathway further controls the quality of 5S rRNA transcripts (Douet et al., 2009), more precisely the repression of minor rRNA gene copies and of an atypical 5S rRNA transcript (5S-210) that comprises the transcribed region and part of the adjacent intergenic region. The 5S-210 transcript is a marker for silencing release within the 5S loci and likely a precursor for small interfering RNA (siRNA) production (Blevins et al., 2009; Douet et al., 2009; Vaillant et al., 2006). Furthermore, in leaves of RdDM mutants, the quantities of 24nt 5S siRNAs are reduced and 5S rDNA appears decondensed (Blevins et al., 2009; Herr et al., 2005; Onodera et al., 2005; Pontier et al., 2005), which implies that 5S rDNA array expression and chromatin compaction require siRNAs and components of the RdDM pathway. Whether the 5S-210 transcript and 5S siRNA levels vary during the first days post-germination development concomitantly with the dynamic rearrangement of 5S rDNA chromatin remains to be addressed.

The important chromatin re-organization observed for the 5S rDNA loci opened the possibility to investigate the link between chromatin dynamics and transcriptional regulation at this developmental stage — information missing for the other repetitive sequences. The transcription of 5S rRNA genes is controlled by the expression and availability of the transcription factor IIIA (TFIIIA), a 5S rDNA-specific transcription factor (Layat et al., in press; Mathieu et al., 2003b). To gain insight into the regulation of 5S rRNA transcription in cotyledons, the correlation between levels of 5S rRNA and TFIIIA expression was addressed (Layat et al., 2012). During the first days post-germination development, during which 5S rDNA chromatin is reorganized, TFIIIA expression is modulated both at transcriptional and post-translational levels. TFIIIA transcript levels were found to be low, and the small amounts of proteins produced are proteolytically cleaved resulting in the absence of the functional full-length TFIIIA protein at days 2 and 3 after germination (Fig. 1C) (Layat et al., 2012). This suggests that 5S rRNA genes are not actively transcribed during this developmental stage. Indeed, 5S rRNA quantities decrease during the first days of post-germination growth (Fig. 1C) during which the seedling uses the 5S rRNA previously accumulated throughout embryonic development (Layat et al., 2012; Rajjou et al., 2004). The complete proteolytic cleavage of the TFIIIA protein at a moment when 5S rDNA is largely decompacted (Douet et al., 2008), can be considered as a way to prevent undesirable transcription of highly mutated 5S rRNA genes. Transcripts derived from these genes could be deleterious for the cell and are silenced later on during development through a compact chromatin organization. Concomitant with a mature 5S rDNA chromatin structure comparable to leaf tissues established at day 4 after germination, full-length and transcriptionally functional TFIIIA protein is *de novo* detected and 5S rRNA transcription resumes (Fig. 1C). One can therefore suggest that the reorganization of 5S rDNA arrays allows the acquisition of an organization considered as mature, which supports expression of an appropriate amount and quality of 5S rRNA transcripts. This organization could be distinct from the one during seed development, which permits expression of high amounts of 5S rRNA transcripts including some copies, carrying a single base-pair substitution and which are normally repressed (Mathieu et al., 2003a). The case of 5S rDNA discussed here therefore illustrates a correlation between chromatin reorganization and transcriptional reprogramming.

Transcriptional reprogramming during seedling growth is however not restricted to 5S rRNA gene copies: 45S rDNA loci were also found to be decondensed at day 2 following germination (Pontvianne et al., 2010; van Zanten et al., 2011). Here, the decondensed state of rDNA loci clearly correlates with the presence of certain 45S rRNA variants that are not expressed in leaf tissue (Earley et al., 2010; Pontvianne et al., 2010) suggesting likewise transcriptional reprogramming of 45S rDNA repeats during seedling growth. Other studies in *Arabidopsis suecica* plants, an allotetraploid hybrid of *A. thaliana* and *Arabidopsis arenosa*, further imply that transcriptional reprogramming of the repetitive 45S rDNA loci might also occur further on during the vegetative growth phase. In *A. suecica*, the 45S rDNA repeats from the *A thaliana* progenitor are transcriptionally repressed, a phenomenon termed nucleolar dominance (Tucker et al., 2010). Nucleolar dominance was not observed in cotyledons, where the 45S rDNA loci are decondensed, but later on in true leaves where the under-dominant rDNA species is condensed and has lost active histone modifications (Pontes et al., 2007).

4. Heterochromatin dynamics at the crossroad of major developmental switches?

Developmental transitions are associated with important alterations in gene expression patterns. Those take place concomitantly with large-scale reorganization of heterochromatic sequences in different aerial plant tissues (Mathieu et al., 2003a; Pecinka et al., 2010; Tessadori et al., 2004, 2007a, 2007b; Tittel-Elmer et al., 2010; van Zanten et al., 2011), demonstrating that plants display a remarkable dynamic in chromatin organization upon major developmental switches. This phenomenon is not restricted to the plant kingdom, as in mammals reprogramming of gene expression during key developmental transitions, such as the generation of totipotency in the zygote (Martin et al., 2006; Probst et al., 2007) or in primordial germ cells (Hajkova et al., 2008) and fate changes from a differentiated cell to an induced pluripotent stem cell (Mattout et al., 2011) involves major changes in heterochromatin organization.

To explain the reason for such large-scale chromatin rearrangements, it has been hypothesized that chromatin decondensation increases the accessibility to DNA necessary for the activation of genes involved in cell fate switch (Tessadori et al., 2007a; Zhao et al., 2001). Considering the organization of *Arabidopsis* chromosomes in interphase as euchromatic loops that emanate from the heterochromatic chromocenters (Fransz et al., 2002) (Fig. 1A, right), heterochromatin dynamics might be necessary to rearrange the euchromatic domains and to allocate new contact points with the chromocenter. This rearrangement could allow changing the position of genes in the nuclear volume, relative to the border of a chromosome territory, a transcription factory or the nuclear periphery, which in turn will impact positively or negatively on gene expression (Fransz and de Jong, 2011; Tessadori et al., 2004). Whether expression of these heterochromatic sequences is affected by its large-scale decondensation has been addressed for a selection of targets: no transcriptional reactivation of a silent transgenic locus (Tessadori et al., 2007a) or an Athila retroelement (Avivi et al., 2004) was observed during de-differentiation. However normally repressed 45S rRNA gene variants are activated after germination when 45S rDNA loci are decondensed (Earley et al., 2010; Pontvianne et al., 2010). Furthermore, heat stress induces reactivation of silent transposons and repeats (Pecinka et al., 2010; Tittel-Elmer et al., 2010) concomitantly with heterochromatin decondensation. However, re-silencing occurs without recompaction of the analyzed repetitive elements into chromocenters (Pecinka et al., 2010). Taken together, these observations do not support a simple causal relationship between chromatin higher-order structure and gene expression and suggest that chromatin compaction and transcriptional activity can be at least partly uncoupled.

While the changes in nuclear organization of heterochromatic domains have now been well characterized, we still know little about the changes taking place at the level of the chromatin fiber or about the triggers or the mechanisms involved. The tentative to find common principles for the different heterochromatin reorganization processes has been hindered by the distinct experimental setups, the differences in reorganization timings, the different tissues affected

as well as the presence of several cell types within a tissue. It is suggestive that changes in epigenetic marks play a role in these large-scale heterochromatin dynamics. However, heterochromatin decondensation during floral transition seems not to involve changes in DNA methylation. This is comparable to the situation upon dedifferentiation or prolonged heat stress, during which global DNA methylation levels were preserved, despite the decondensation of repetitive elements (Pecinka et al., 2010; Tessadori et al., 2007a; Tittel-Elmer et al., 2010). In contrast, 5S rRNA genes that are dynamically rearranged during seedling growth are subject to DNA methylation changes. While the presence of histone post-translational modifications has been assessed globally in some studies, quantitative approaches to compute enrichments in histone modifications at the repetitive loci during developmental transitions are still missing. Those approaches allowed revealing that prolonged heat stress has only a subtle impact on histone modifications, however transiently reduces nucleosomal density (Pecinka et al., 2010; Tittel-Elmer et al., 2010). Much remains to be explored concerning nucleosome composition, structure, modification and positioning till we understand the mechanisms and molecular players responsible for heterochromatin dynamics during developmental transitions.

Acknowledgments

We apologize for not having been able to quote all colleagues for their contribution due to space limitation and thank S. Desset and C. Tatout for critical reading of the article. M.B. is financed by a doctoral stipend from the Region Auvergne (Recherche et Innovation Technologique, program 1130). A.V.P and S.T. are supported by ANR “Dynam'Het” ANR-11 JSV2 009 01.

References

Adrian, J., Torti, S., Turck, F., 2009. From decision to commitment: the molecular memory of flowering. Mol. Plant 2, 628–642.
AGI, 2000. Analysis of the genome sequence of the flowering plant *Arabidopsis thaliana*. Nature 408, 796–815.
Amasino, R., 2010. Seasonal and developmental timing of flowering. Plant J. 61, 1001–1013.
Avivi, Y., et al., 2004. Reorganization of specific chromosomal domains and activation of silent genes in plant cells acquiring pluripotentiality. Dev. Dyn. 230, 12–22.
Berdasco, M., et al., 2008. Promoter DNA hypermethylation and gene repression in undifferentiated *Arabidopsis* cells. PLoS One 3, e3306.
Blevins, T., Pontes, O., Pikaard, C.S., Meins Jr., F., 2009. Heterochromatic siRNAs and DDM1 independently silence aberrant 5S rDNA transcripts in *Arabidopsis*. PLoS One 4, e5932.
Campell, B.R., Song, Y., Posch, T.E., Cullis, C.A., Town, C.D., 1992. Sequence and organization of 5S ribosomal RNA-encoding genes of *Arabidopsis thaliana*. Gene 112, 225–228.
Chandler, J.W., 2008. Cotyledon organogenesis. J. Exp. Bot. 59, 2917–2931.
Chandler, J.W., Cole, M., Flier, A., Grewe, B., Werr, W., 2007. The AP2 transcription factors DORNROSCHEN and DORNROSCHEN-LIKE redundantly control *Arabidopsis* embryo patterning via interaction with PHAVOLUTA. Development 134, 1653–1662.
Cloix, C., et al., 2002. Analysis of the 5S RNA pool in *Arabidopsis thaliana*: RNAs are heterogeneous and only two of the genomic 5S loci produce mature 5S RNA. Genome Res. 12, 132–144.
Dittmer, T.A., Stacey, N.J., Sugimoto-Shirasu, K., Richards, E.J., 2007. LITTLE NUCLEI genes affecting nuclear morphology in *Arabidopsis thaliana*. Plant Cell 19, 2793–2803.
Douet, J., Blanchard, B., Cuvillier, C., Tourmente, S., 2008. Interplay of RNA Pol IV and ROS1 during post-embryonic 5S rDNA chromatin remodeling. Plant Cell Physiol. 49, 1783–1791.
Douet, J., Tutois, S., Tourmente, S., 2009. A Pol V-mediated silencing, independent of RNA-directed DNA methylation, applies to 5S rDNA. PLoS Genet. 5, e1000690.
Earley, K.W., et al., 2010. Mechanisms of HDA6-mediated rRNA gene silencing: suppression of intergenic Pol II transcription and differential effects on maintenance versus siRNA-directed cytosine methylation. Genes Dev. 24, 1119–1132.
Exner, V., Hennig, L., 2008. Chromatin rearrangements in development. Curr. Opin. Plant Biol. 11, 64–69.
Fransz, P.F., de Jong, J.H., 2002. Chromatin dynamics in plants. Curr. Opin. Plant Biol. 5, 560–567.
Fransz, P., de Jong, H., 2011. From nucleosome to chromosome: a dynamic organization of genetic information. Plant J. 66, 4–17.
Fransz, P.F., et al., 2000. Integrated cytogenetic map of chromosome arm 4S of *A. thaliana*: structural organization of heterochromatic knob and centromere region. Cell 100, 367–376.
Fransz, P., De Jong, J.H., Lysak, M., Castiglione, M.R., Schubert, I., 2002. Interphase chromosomes in *Arabidopsis* are organized as well defined chromocenters from which euchromatin loops emanate. Proc. Natl. Acad. Sci. U. S. A. 99, 14584–14589.
Gong, Z., Morales-Ruiz, T., Ariza, R.R., Roldan-Arjona, T., David, L., Zhu, J.K., 2002. ROS1, a repressor of transcriptional gene silencing in *Arabidopsis*, encodes a DNA glycosylase/lyase. Cell 111, 803–814.
Grafi, G., Ben-Meir, H., Avivi, Y., Moshe, M., Dahan, Y., Zemach, A., 2007. Histone methylation controls telomerase-independent telomere lengthening in cells undergoing dedifferentiation. Dev. Biol. 306, 838–846.
Hajkova, P., et al., 2008. Chromatin dynamics during epigenetic reprogramming in the mouse germ line. Nature 452, 877–881.
He, Y., 2009. Control of the transition to flowering by chromatin modifications. Mol. Plant 2, 554–564.
Heitz, E., 1928. Das Heterochromatin der Moose. Jahrb. Wiss. Bot. 762–818.
Herr, A.J., Jensen, M.B., Dalmay, T., Baulcombe, D.C., 2005. RNA polymerase IV directs silencing of endogenous DNA. Science 308, 118–120.
Holdsworth, M.J., Finch-Savage, W.E., Grappin, P., Job, D., 2008. Post-genomics dissection of seed dormancy and germination. Trends Plant Sci. 13, 7–13.
Huijser, P., Schmid, M., 2011. The control of developmental phase transitions in plants. Development 138, 4117–4129.
Ingouff, M., et al., 2010. Zygotic resetting of the HISTONE 3 variant repertoire participates in epigenetic reprogramming in *Arabidopsis*. Curr. Biol. 20, 2137–2143.
Jarillo, J.A., Pineiro, M., Cubas, P., Martinez-Zapater, J.M., 2009. Chromatin remodeling in plant development. Int. J. Dev. Biol. 53, 1581–1596.
Kanno, T., et al., 2005. Atypical RNA polymerase subunits required for RNA-directed DNA methylation. Nat. Genet. 37, 761–765.
Kaplan, D.R., Cooke, T.J., 1997. Fundamental concepts in the embryogenesis of dicotyledons: a morphological interpretation of embryo mutants. Plant Cell 9, 1903–1919.
Koukalova, B., Fojtova, M., Lim, K.Y., Fulnecek, J., Leitch, A.R., Kovarik, A., 2005. Dedifferentiation of tobacco cells is associated with ribosomal RNA gene hypomethylation, increased transcription, and chromatin alterations. Plant Physiol. 139, 275–286.
Layat, E., Saez-Vasquez, J., Tourmente, S., 2011. Regulation of Pol I-transcribed 45S rDNA and Pol III-transcribed 5S rDNA in *Arabidopsis*. Plant Cell Physiol. 53, 267–276.
Layat, E., Cotterell, S., Vaillant, I., Yukawa, Y., Tutois, S., Tourmente, S., 2012. Transcript levels, alternative splicing and proteolytic cleavage of TFIIIA control 5S rRNA accumulation during *Arabidopsis thaliana* development. Plant J. 71, 35–44.
Layat, E., Probst, A.V., Tourmente, S., in press. Structure, function and regulation of Transcription Factor IIIA: from Xenopus to Arabidopsis. Biochim. Biophys. Acta. http://dx.doi.org/10.1016/j.bbagrm.2012.10.013.
Liu, C., Thong, Z., Yu, H., 2009. Coming into bloom: the specification of floral meristems. Development 136, 3379–3391.
Long, J.A., Barton, M.K., 1998. The development of apical embryonic pattern in *Arabidopsis*. Development 125, 3027–3035.
Lotan, T., et al., 1998. *Arabidopsis* LEAFY COTYLEDON1 is sufficient to induce embryo development in vegetative cells. Cell 93, 1195–1205.
Martin, C., Beaujean, N., Brochard, V., Audouard, C., Zink, D., Debey, P., 2006. Genome restructuring in mouse embryos during reprogramming and early development. Dev. Biol. 292, 317–332.
Mathieu, O., et al., 2003a. Changes in 5S rDNA chromatin organization and transcription during heterochromatin establishment in *Arabidopsis*. Plant Cell 15, 2929–2939.
Mathieu, O., Yukawa, Y., Prieto, J.L., Vaillant, I., Sugiura, M., Tourmente, S., 2003b. Identification and characterization of transcription factor IIIA and ribosomal protein L5 from *Arabidopsis thaliana*. Nucleic Acids Res. 31, 2424–2433.
Mathieu, O., Probst, A.V., Paszkowski, J., 2005. Distinct regulation of histone H3 methylation at lysines 27 and 9 by CpG methylation in *Arabidopsis*. EMBO J. 24, 2783–2791.
Mattout, A., Biran, A., Meshorer, E., 2011. Global epigenetic changes during somatic cell reprogramming to iPS cells. J. Mol. Cell Biol. 3, 341–350.
Ondrej, V., Kitner, M., Dolezalova, I., Nadvornik, P., Navratilova, B., Lebeda, A., 2009. Chromatin structural rearrangement during dedifferentiation of protoplasts of *Cucumis sativus* L. Mol. Cell 27, 443–447.
Onodera, Y., Haag, J.R., Ream, T., Costa Nunes, P., Pontes, O., Pikaard, C.S., 2005. Plant nuclear RNA polymerase IV mediates siRNA and DNA methylation-dependent heterochromatin formation. Cell 120, 613–622.
Pavet, V., Quintero, C., Cecchini, N.M., Rosa, A.L., Alvarez, M.E., 2006. *Arabidopsis* displays centromeric DNA hypomethylation and cytological alterations of heterochromatin upon attack by pseudomonas syringae. Mol. Plant Microbe Interact. 19, 577–587.
Pecinka, A., et al., 2004. Chromosome territory arrangement and homologous pairing in nuclei of *Arabidopsis thaliana* are predominantly random except for NOR-bearing chromosomes. Chromosoma 113, 258–269.
Pecinka, A., Dinh, H.Q., Baubec, T., Rosa, M., Lettner, N., Mittelsten Scheid, O., 2010. Epigenetic regulation of repetitive elements is attenuated by prolonged heat stress in *Arabidopsis*. Plant Cell 22, 3118–3129.
Pillot, M., et al., 2010. Embryo and endosperm inherit distinct chromatin and transcriptional states from the female gametes in *Arabidopsis*. Plant Cell 22, 307–320.
Pontes, O., et al., 2007. Postembryonic establishment of megabase-scale gene silencing in nucleolar dominance. PLoS One 2, e1157.
Pontier, D., et al., 2005. Reinforcement of silencing at transposons and highly repeated sequences requires the concerted action of two distinct RNA polymerases IV in *Arabidopsis*. Genes Dev. 19, 2030–2040.
Pontvianne, F., et al., 2010. Nucleolin is required for DNA methylation state and the expression of rRNA gene variants in *Arabidopsis thaliana*. PLoS Genet. 6, e1001225.
Probst, A.V., Fransz, P.F., Paszkowski, J., Mittelsten Scheid, O., 2003. Two means of transcriptional reactivation within heterochromatin. Plant J. 33, 743–749.
Probst, A.V., et al., 2004. *Arabidopsis* histone deacetylase HDA6 is required for maintenance of transcriptional gene silencing and determines nuclear organization of rDNA repeats. Plant Cell 16, 1021–1034.

Probst, A.V., Santos, F., Reik, W., Almouzni, G., Dean, W., 2007. Structural differences in centromeric heterochromatin are spatially reconciled on fertilisation in the mouse zygote. Chromosoma 116, 403–415.
Rajjou, L., Gallardo, K., Debeaujon, I., Vandekerckhove, J., Job, C., Job, D., 2004. The effect of alpha-amanitin on the *Arabidopsis* seed proteome highlights the distinct roles of stored and neosynthesized mRNAs during germination. Plant Physiol. 134, 1598–1613.
Schmid, M., et al., 2003. Dissection of floral induction pathways using global expression analysis. Development 130, 6001–6012.
Slotkin, R.K., et al., 2009. Epigenetic reprogramming and small RNA silencing of transposable elements in pollen. Cell 136, 461–472.
Soppe, W.J., et al., 2002. DNA methylation controls histone H3 lysine 9 methylation and heterochromatin assembly in *Arabidopsis*. EMBO J. 21, 6549–6559.
Stone, S.L., et al., 2001. LEAFY COTYLEDON2 encodes a B3 domain transcription factor that induces embryo development. Proc. Natl. Acad. Sci. U. S. A. 98, 11806–11811.
Tabata, S., et al., 2000. Sequence and analysis of chromosome 5 of the plant *Arabidopsis thaliana*. Nature 408, 823–826.
Tessadori, F., van Driel, R., Fransz, P., 2004. Cytogenetics as a tool to study gene regulation. Trends Plant Sci. 9, 147–153.
Tessadori, F., et al., 2007a. Large-scale dissociation and sequential reassembly of pericentric heterochromatin in dedifferentiated *Arabidopsis* cells. J. Cell Sci. 120, 1200–1208.
Tessadori, F., Schulkes, R.K., van Driel, R., Fransz, P., 2007b. Light-regulated large-scale reorganization of chromatin during the floral transition in *Arabidopsis*. Plant J. 50, 848–857.
Tessadori, F., et al., 2009. Phytochrome B and histone deacetylase 6 control light-induced chromatin compaction in *Arabidopsis thaliana*. PLoS Genet. 5, e1000638.
Tittel-Elmer, M., Bucher, E., Broger, L., Mathieu, O., Paszkowski, J., Vaillant, I., 2010. Stress-induced activation of heterochromatic transcription. PLoS Genet. 6, e1001175.
Tucker, S., Vitins, A., Pikaard, C.S., 2010. Nucleolar dominance and ribosomal RNA gene silencing. Curr. Opin. Cell Biol. 22, 351–356.
Tutois, S., et al., 1999. Structural analysis and physical mapping of a pericentromeric region of chromosome 5 of *Arabidopsis thaliana*. Chromosom. Res. 7, 143–156.
Vaillant, I., Schubert, I., Tourmente, S., Mathieu, O., 2006. MOM1 mediates DNA-methylation-independent silencing of repetitive sequences in *Arabidopsis*. EMBO Rep. 7, 1273–1278.
van Zanten, M., et al., 2010. Photoreceptors CRYTOCHROME2 and phytochrome B control chromatin compaction in *Arabidopsis*. Plant Physiol. 154, 1686–1696.
van Zanten, M., et al., 2011. Seed maturation in *Arabidopsis thaliana* is characterized by nuclear size reduction and increased chromatin condensation. Proc. Natl. Acad. Sci. U. S. A. 108, 20219–20224.
van Zanten, M., Carles, A., Li, Y., Soppe, W.J., 2012a. Control and consequences of chromatin compaction during seed maturation in *Arabidopsis thaliana*. Plant Signal. Behav. 7, 338–341.
van Zanten, M., Tessadori, F., Peeters, A.J., Fransz, P., 2012b. Shedding light on large-scale chromatin reorganization in *Arabidopsis thaliana*. Mol. Plant 5, 583–590.
West, M., et al., 1994. LEAFY COTYLEDON1 is an essential regulator of late embryogenesis and cotyledon identity in *Arabidopsis*. Plant Cell 6, 1731–1745.
Williams, L., Zhao, J., Morozova, N., Li, Y., Avivi, Y., Grafi, G., 2003. Chromatin reorganization accompanying cellular dedifferentiation is associated with modifications of histone H3, redistribution of HP1, and activation of E2F-target genes. Dev. Dyn. 228, 113–120.
Wollmann, H., Berger, F., 2012. Epigenetic reprogramming during plant reproduction and seed development. Curr. Opin. Plant Biol. 15, 63–69.
Zhang, X., Henderson, I.R., Lu, C., Green, P.J., Jacobsen, S.E., 2007. Role of RNA polymerase IV in plant small RNA metabolism. Proc. Natl. Acad. Sci. U. S. A. 104, 4536–4541.
Zhao, J., Morozova, N., Williams, L., Libs, L., Avivi, Y., Grafi, G., 2001. Two phases of chromatin decondensation during dedifferentiation of plant cells: distinction between competence for cell fate switch and a commitment for S phase. J. Biol. Chem. 276, 22772–22778.

Abstract

To understand how histones H3 are handled and how histone dynamics impact higher-order chromatin organization such as chromocenter formation in Arabidopsis, a comprehensive analysis of the different histone chaperone complexes is required. We identified and characterized the different subunits of the Arabidopsis HIR complex. AtHIRA is the central subunit and its loss affects non-nucleosomal histone levels, reduces nucleosomal occupancy not only at euchromatic but also at heterochromatic targets and alleviates transcriptional gene silencing. While the HIR complex-mediated histone deposition is dispensable for higher-order organization of Arabidopsis heterochromatin, I show that CAF-1 plays a central role in chromocenter formation. During post-germination development in cotyledons when centromeric and pericentromeric repeats cluster progressively into chromocenter structures, these repetitive elements but not euchromatic loci become enriched in H3.1 in a CAF-1-dependent manner. This enrichment, together with the appropriate setting of repressive histone post-translational marks, contributes to chromocenter formation, identifying chromatin assembly by CAF-1 as driving force in formation and maintenance of genome structure. Finally, while absence of HIR or CAF-1 complexes sustains viability, only the simultaneous loss of both severely impairs nucleosomal occupancy and plant development, suggesting a limited functional compensation between the different histone chaperone complexes and plasticity in histone variant interaction and deposition in plants.

Keywords: Heterochromatin dynamics, chromocenter, histone H3, histone chaperone, *Arabidopsis thaliana*

Afin d'étudier la prise en charge des histones H3 jusqu'à l'ADN et pour comprendre l'influence de leur dynamique dans l'organisation d'ordre supérieur de la chromatine, une analyse des chaperonnes d'histones a été menée. Nous avons identifié et caractérisé les sous-unités du complexe HIR, impliqué dans l'assemblage de la chromatine réplication-indépendante chez Arabidopsis. La perte d'AtHIRA, la sous-unité centrale du complexe, affecte le niveau d'histone soluble, l'occupation nucléosomale des régions euchromatiniennes et héterochromatiniennes ainsi que la mise sous silence transcriptionnel des séquences d'ADN répétées. Alors que le complexe HIR ne participe pas à l'organisation d'ordre supérieur de la chromatine, j'ai montré que CAF-1, impliqué dans l'assemblage de la chromatine au cours de la réplication, joue un rôle central dans la formation des chromocentres. Lors du développement post-germinatif des cotylédons, les séquences d'ADN répétées centromériques et péricentromériques se concentrent dans les chromocentres et s'enrichissent en histone H3.1 de manière CAF-1 dépendante. Cet enrichissement, associé à des modifications post-traductionnelles d'histones associées à un état répressif de la transcription, participe à la formation des chromocentres et met en évidence l'importance de l'assemblage de la chromatine par CAF-1 dans la structure et le maintien du génome. Alors que la perte individuelle de HIR ou de CAF-1 n'affecte pas la viabilité, l'absence des deux complexes altère fortement l'occupation nucléosomale et le développement des plantes. Ceci suggère que la compensation fonctionnelle entre ces complexes de chaperonnes ainsi que la plasticité des voies de dépôt des histones restent limitées.

Mots-clés: Dynamique de l'heterochromatine, chromocentre, histone H3, chaperonne d'histone, *Arabidopsis thaliana*